

NASA Technical Memorandum 81182

USAAVRADCOM TR 80-A-5

AD A 090513

LEVEL



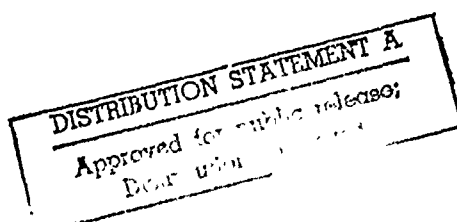
A Comprehensive Analytical Model of Rotorcraft Aerodynamics and Dynamics

Part I: Analysis Development

Wayne Johnson

OCT 14 1980

June 1980



DOC FILE COPY

NASA

National Aeronautics and
Space Administration

United States Army
Aviation Research
and Development
Command



80 10 3 058

DISCLAIMER NOTICE

**THIS DOCUMENT IS BEST QUALITY
PRACTICABLE. THE COPY FURNISHED
TO DTIC CONTAINED A SIGNIFICANT
NUMBER OF PAGES WHICH DO NOT
REPRODUCE LEGIBLY.**

A Comprehensive Analytical Model of Rotorcraft Aerodynamics and Dynamics

Part I: Analysis Development

Wayne Johnson, Aeromechanics Laboratory, AVRADCOM
Research and Technology Laboratories
Moffett Field, California



National Aeronautics and
Space Administration

Ames Research Center
Moffett Field, California 94035

United States Army
Aviation Research and
Development Command
St. Louis, Missouri, 63166



CONTENTS

1. INTRODUCTION	1
2. ROTOR MODEL	4
2.1 Structural Analysis	4
2.1.1 Geometry	6
2.1.2 Description of the bending	7
2.1.3 Analysis of strain	9
2.1.4 Section moments	12
2.1.5 Vector formulation	15
2.2 Inertia Analysis	17
2.2.1 Rotor geometry	17
2.2.2 Rotor motion	25
2.2.3 Coordinate frames	29
2.2.4 Blade acceleration	30
2.2.5 Aerodynamic forces	37
2.2.6 Force and moment equilibrium	37
2.2.7 Bending equation	40
2.2.8 Elastic torsion equation	44
2.2.9 Rigid pitch equation	48
2.2.10 Root force	51
2.2.11 Root moment	51
2.2.12 Gimbal equation	53
2.2.13 Teeter equation	53
2.2.14 Modal equations	54
2.2.15 Modal expansion	56
2.2.16 Lag damper	59
2.2.17 Gravitational forces	61
2.2.18 Equations of motion	61
2.2.19 Inertial constants	68
2.2.20 Aerodynamic spring and damping	79
2.3 Blade Bending and Torsion Modes	81
2.3.1 Coupled bending modes of a rotating blade	81
2.3.2 Articulated blade modes	89
2.3.3 Torsion modes of a nonrotating blade	90
2.3.4 Kinematic pitch/bending coupling	93
2.3.5 Blade pitch definition	95
2.4 Aerodynamic Analysis	97
2.4.1 Section aerodynamic forces	97
2.4.2 Blade velocity	103
2.4.3 Induced velocity	106
2.4.4 Section aerodynamic characteristics	111
2.4.5 Tip flow corrections	116

2.4.6	Yawed flow correction	117
2.4.7	Dynamic stall model	118
2.4.8	Unsteady lift and moment	124
2.4.9	Circulation	127
2.5	Environment	127
2.6	Normalization Parameters	129
3.	ROTOR WAKE ANALYSIS	130
3.1	Nonuniform Wake-Induced Velocity	130
3.1.1	Rotor vortex wake	130
3.1.2	Wake model	134
3.1.3	Geometry	142
3.1.4	Induced velocity calculation	152
3.1.5	Ground effect	158
3.1.6	Hover or vertical flight (axisymmetric geometry)	159
3.1.7	Finite length vortex line element	163
3.1.8	Rectangular vortex sheet	173
3.2	Free Wake Geometry	179
4.	AIRCRAFT MODEL	183
4.1	Aircraft Configuration Definition	183
4.1.1	Aircraft orientation: flight path and trim Euler angles	183
4.1.2	Rotor position and orientation	185
4.1.3	Wind tunnel case	188
4.1.4	Gust velocity	188
4.1.5	Aircraft description	189
4.1.6	Pilot's controls	191
4.2	Aircraft Analysis	194
4.2.1	Degrees of freedom	195
4.2.2	Hub motion	196
4.2.3	Pitch/mast-bonding coupling	198
4.2.4	Equations of motion	198
4.2.5	Hub forces	200
4.2.6	Aircraft aerodynamic forces	201
4.2.7	Aircraft aerodynamics -- high frequency	210
4.3	Transmission and Engine Analysis	212
4.3.1	Engine model	212
4.3.2	Equations of motion	214
4.3.3	Rotor speed governor	221
5.	SOLUTION FOR THE ROTORCRAFT MOTION	222
5.1	Rotor Motion and Airframe Vibration	222
5.1.1	Fourier series representation	223
5.1.2	Gimbal and teeter motion	224

5.1.3	Rigid pitch motion	228
5.1.4	Harmonic analysis solution	229
5.1.5	Motion evaluation	233
5.1.6	Rotor equations	239
5.1.7	Hub reactions	244
5.1.8	Aircraft equations	248
5.1.9	Transmission and engine equations	251
5.1.10	Static elastic deflection	254
5.1.11	Two-rotor aircraft	255
5.1.12	Circulation convergence	257
5.1.13	Calculation procedure	258
5.2	Rotor Performance, Loads, and Noise	259
5.2.1	Rotor performance	260
5.2.2	Section force	264
5.2.3	Section bending moment	269
5.2.4	Section torsion moment	273
5.2.5	Control load	277
5.2.6	Root forces and moments	278
5.2.7	Hub reactions	281
5.2.8	Vibration	282
5.2.9	Fatigue damage assessment	283
5.2.10	Rotational noise	286
5.3	Steady State or Slowly Varying Aircraft Motion	292
5.3.1	Trim analysis	294
5.3.2	Transient analysis	300
5.3.3	Flight dynamics analysis	303
5.3.4	Transient gust and control	307
5.3.5	Calculation procedure	310
6.	AEROELASTIC STABILITY	311
6.1	Rotor Model	311
6.1.1	Rotor degrees of freedom	311
6.1.2	Rotor equations and hub reactions	317
6.1.3	Inertial constants	322
6.1.4	Aerodynamic forces	324
6.1.5	Inflow dynamics	336
6.1.6	Rotor equations of motion	342
6.1.7	Constant coefficient approximation	349
6.2	Aircraft Model	353
6.2.1	Aircraft degrees of freedom	353
6.2.2	Aircraft equations of motion	354
6.2.3	Drive train equations of motion	356
6.3	Coupled Rotor and Aircraft	357
6.3.1	Coupled equations of motion	357
6.3.2	Quasistatic approximation	365
6.3.3	Symmetric aircraft	366

6.4	Matrices of Rotor Equations of Motion	368
6.4.1	Inertial matrices for rotor equations	368
6.4.2	Aerodynamic matrices for rotor equations in axial flow	379
6.4.3	Aerodynamic matrices for rotor equations in nonaxial flow	388
6.4.4	Inertial matrices for rotor with four or more blades	399
6.4.5	Aerodynamic matrices for rotor with four or more blades in axial flow	403
6.4.6	Inertial matrices for two-bladed rotor	404
6.4.7	Aerodynamic matrices for two-bladed rotor	414
7.	LINEAR SYSTEM ANALYSIS	425
7.1	State Variable Form	425
7.2	Constant Coefficient System	426
7.2.1	Eigen-analysis	426
7.2.2	Static Response	427
7.2.3	Frequency Response	427
7.2.4	Zeros	427
7.2.5	Transient response	428
7.2.6	Rms gust response	429
7.3	Periodic Coefficient System	431
	REFERENCES	433

A COMPREHENSIVE ANALYTICAL MODEL OF
ROTORCRAFT AERODYNAMICS AND DYNAMICS

Part I: Analysis Development

Wayne Johnson

Ames Research Center
and
Aeromechanics Laboratory
AVRADCOM Research and Technology Laboratories

SUMMARY

The development of a comprehensive analytical model of rotorcraft aerodynamics and dynamics is presented. This analysis is designed to calculate rotor performance, loads, and noise; helicopter vibration and gust response; flight dynamics and handling qualities; and system aeroelastic stability. The analysis is a combination of structural, inertial, and aerodynamic models that is applicable to a wide range of problems and a wide class of vehicles. The analysis is intended for use in the design, testing, and evaluation of rotors and rotorcraft, and to be a basis for further development of rotary wing theories. The analysis is implemented in a digital computer program.

1. INTRODUCTION

For the design, testing, and evaluation of rotors and rotorcraft, a reliable and efficient analysis of the aircraft aerodynamics and dynamics is required. It is necessary to predict and explain the rotor performance, loads, and noise; helicopter vibration and gust response; flight dynamics and handling qualities; and system aeroelastic stability. Such capability is also required as a basis for further development of rotary wing theory. This report presents the development of a comprehensive analytical model of rotorcraft aerodynamics and dynamics.

The analysis developed here is a consistent combination of structural, inertial, and aerodynamic models, applicable to a wide range of problems and a wide class of vehicles. Typically rotary wing analyses have been developed or verified for only a particular type of helicopter or a particular technical problem, that reflects the specific interests of the originating organization. The present model is applicable to articulated, hingeless, gimballed, and teetering rotors with an arbitrary number of blades. The rotor degrees of freedom included are blade flap/lag bending, rigid pitch and elastic torsion, and optionally gimbal or teeter motion. This analysis is applicable to general two-rotor aircraft, including single main-rotor and tandem helicopter configurations and side-by-side or tilting proprotor aircraft configurations (fig. 1). The case of a rotor or helicopter in a wind tunnel is also covered. The aircraft degrees of freedom included are the six rigid body motions, elastic airframe motions, and the rotor/engine speed perturbations. The trim operating conditions considered include level flight, steady climb or descent, and steady turns. The analysis of the rotor includes nonlinear inertial and aerodynamic models, applicable to large blade pitch angles and high inflow ratio. The rotor aerodynamic model is based on two-dimensional steady airfoil characteristics with corrections for three-dimensional and unsteady flow effects, including a dynamic stall model. A detailed wake model for the rotor nonuniform inflow calculation is developed, with a lifting surface theory correction for vortex-induced loads. Available prescribed and free-wake-geometry models are used. The aeroelastic stability analysis derives linearized equations consistent with the nonlinear rotor model.

The solution of the equations of motion is separated into two parts, based on the different time scales involved in rotorcraft dynamics. The first part is the solution for the rotor motion and the airframe vibration. This motion is periodic, with fundamental frequency Ω for the rotor and $N\Omega$ for the airframe (Ω is the rotor rotational speed and N is the number of blades). The periodic motion is calculated by a harmonic analysis method. The second part is the solution for the steady state or slowly varying airframe motion (consisting of the aircraft rigid body and rotor speed perturbations, and the static elastic deflection of the airframe and drive train).

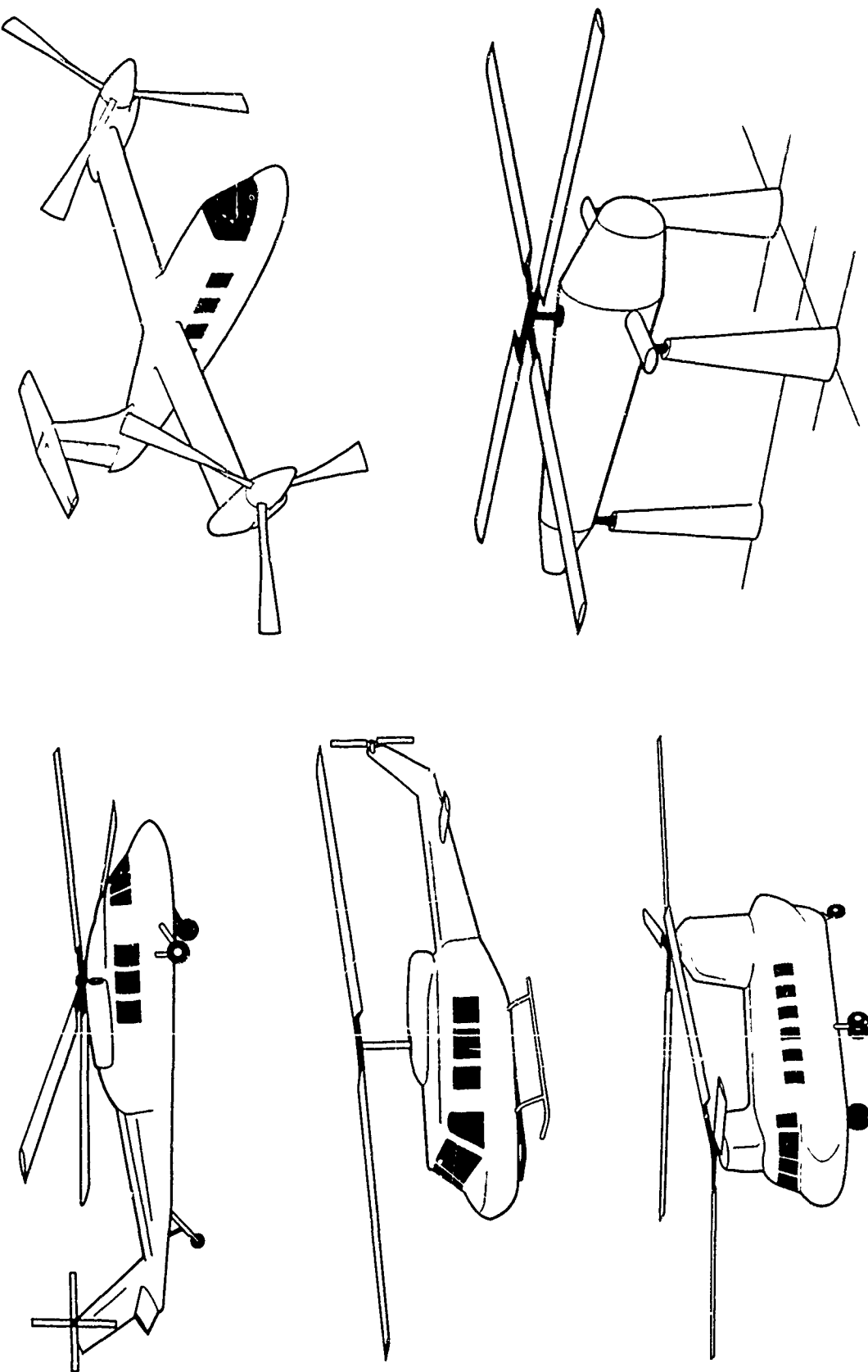


Figure 1. Rotorcraft configurations modelled.

The assumption that the aircraft motion is quasi-static (compared to the rotor speed) allows the periodic rotor solution to be used for transient motions of the helicopter as well as for the trim calculations. Most importantly, by taking advantage of the frequency separation of the rotor and aircraft motions, an economical calculation procedure is realized.

The first computation task is the trim analysis, in which the control position and aircraft orientation are determined for the specified operating condition. The periodic blade motion is calculated, and then the rotor performance, loads, and noise can be evaluated. The rotor model in the trim solution can use uniform inflow, nonuniform inflow with a rigid wake geometry, or nonuniform inflow with a free wake geometry. The aeroelastic stability, flight dynamics, and transient analyses begin from the trim solution. The aeroelastic stability analysis sets up a set of linear differential equations describing the motion of the rotor and aircraft; the eigenvalues of these equations define the system stability. The flight dynamics analysis calculates the rotor and airframe stability derivatives, and sets up linear differential equations for the aircraft rigid body motions; the poles, zeros, and eigenvectors of these equations define the aircraft flying qualities. The transient analysis numerically integrates the rigid body equations of motion for a prescribed control or gust input.

In this analysis all quantities will be dimensionless, based on the air density ρ , the rotor radius R , and the rotor rotational speed Ω .

2. ROTOR MODEL

2.1 Structural Analysis

The rotor structural analysis consists of an engineering beam theory model for the coupled flap/lag bending and torsion of a rotor blade with large pitch and twist. A high aspect ratio (of the structural elements) is assumed, so the beam model is applicable. The objective is to relate the bending moments at the section, and the torsion moment, to the blade deflection and elastic torsion at that section. The analysis follows the work of reference 1.

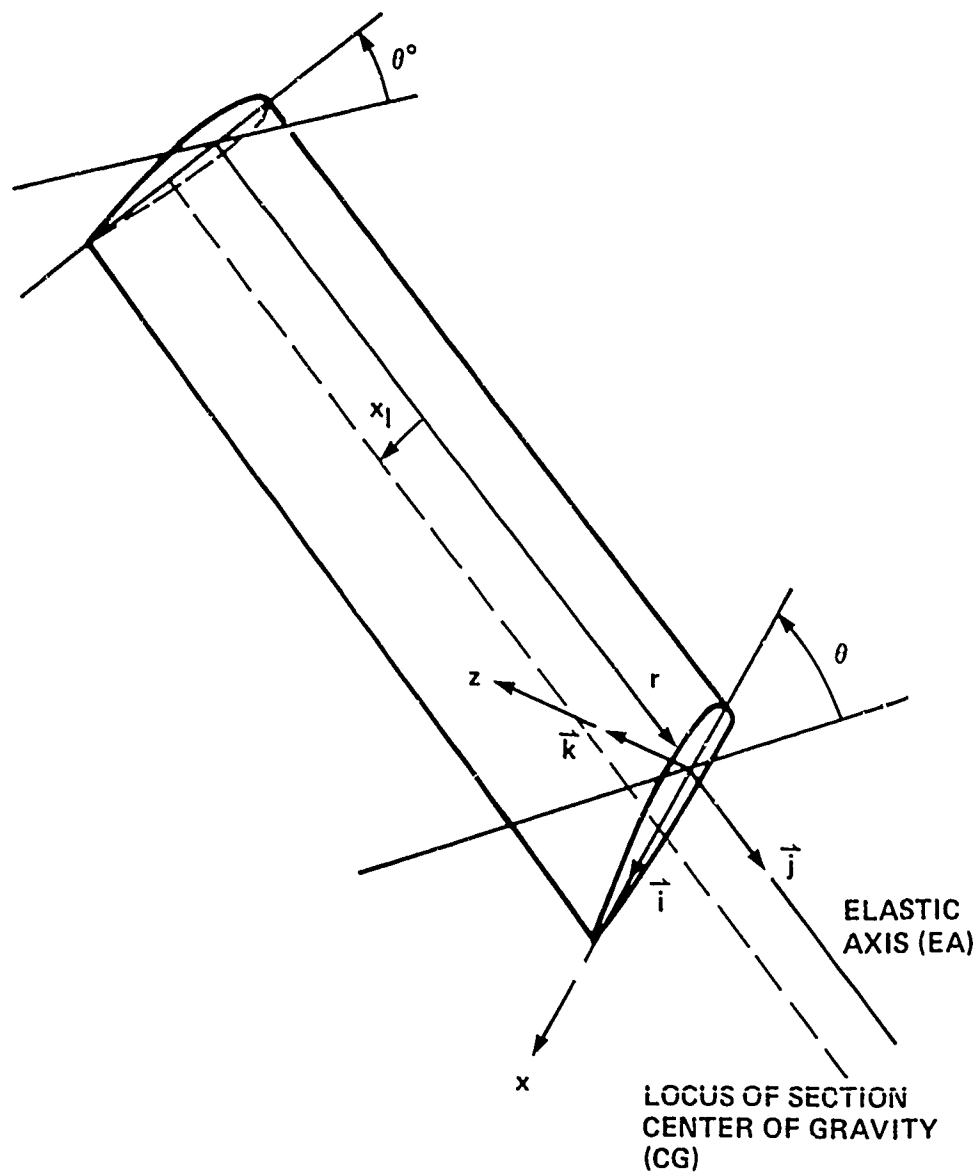


Figure 2. Geometry of the undeformed blade.

2.1.1 *Geometry.*— The basic assumptions are that an elastic axis exists, and the undeformed elastic axis is a straight line; and that the blade has a high aspect ratio (of the structural elements) so engineering beam theory applies. Figure 2 shows the geometry of the undeformed blade. The span variable r is measured from the center of rotation along the straight elastic axis. The section coordinates x and z are the principal axes of the section, with origin at the elastic axis. Then by definition, $\int(z) dA = 0$. Really this integral is over the tension carrying elements, i.e., a modulus weighted integral: $\int x z E dA = 0$. This remark holds for all the section integrals in the structural analysis. The tension center (modulus weighted centroid) is on the x axis, at a distance x_C aft of the elastic axis: $\int x dA = x_C A$ and $\int z dA = 0$. Again, these are modulus weighted integrals. If E is uniform over the section, then x_C is the area centroid; and if the section mass distribution is the same as the E distribution, then the tension center coincides with the section center of gravity.

The angle of the major principal axis (the x axis) with respect to the hub plane is θ . The existence of the elastic axis means that twist about the elastic axis occurs without bending. In general, the elastic torsion deflection will be included in θ . The blade pitch bearing is at the radial station r_{FA} . The blade pitch is described by root pitch θ^0 (rigid pitch about the feathering axis, including that due to the elastic distortion of the control system), built-in twist θ_{tw} , and elastic torsion about the elastic axis θ_e . So $\theta = \theta^0 + \theta_{tw} + \theta_e$, where $\theta^0(\psi)$ is the root pitch, $\theta(r_{FA}) = \theta^0$; $\theta_{tw}(r)$ is the built-in twist, $\theta_{tw}(r_{FA}) = 0$; and $\theta_e(r, \psi)$ is the elastic torsion, $\theta_e(r_{FA}, \psi) = 0$. There is shear stress in the blade due to θ_e only. It is assumed that θ_e is small, but θ^0 and θ_{tw} are allowed to be large angles.

The unit vectors in the rotating hub plane axis system are \hat{i}_B , \hat{j}_B , and \hat{k}_B (fig. 2). The unit vectors for the principal axes of the section (x , r , z) are \hat{i} , \hat{j} , and \hat{k} ; these are for no bending, but include the elastic torsion in the pitch angle θ . So the principal unit vectors are rotated by θ from the hub plane:

$$\begin{aligned}\vec{i} &= \vec{i}_0 \cos \theta - \vec{k}_0 \sin \theta \\ \vec{j} &= \vec{j}_0 \\ \vec{k} &= \vec{i}_0 \sin \theta + \vec{k}_0 \cos \theta\end{aligned}$$

2.1.2 *Description of the bending.*— Now the engineering beam theory assumption is introduced: plane sections perpendicular to the elastic axis remain so after the bending of the blade. Figure 3 shows the geometry of the deformed section. The deformation of the blade is described by (a) deflection of the elastic axis, x_0 , r_0 , and z_0 ; (b) rotation of the section due to bending, by ϕ_x and ϕ_z ; and (c) twist about the elastic axis by θ_e , which is implicit in \vec{i} and \vec{k} . The quantities x_0 , r_0 , z_0 , ψ_x , ϕ_z , and θ_e are assumed to be small.

The unit vectors of the unbent cross section are \vec{i} , \vec{j} , \vec{k} . The unit vectors of the deformed cross section are \vec{i}_{xs} , \vec{j}_{xs} , and \vec{k}_{xs} , where \vec{i}_{xs} and \vec{k}_{xs} are the principal axes of the section, and \vec{j}_{xs} is tangent to the deformed elastic axis. It follows that

$$\begin{aligned}\vec{i}_{xs} &= \vec{i} + \phi_z \vec{j} \\ \vec{j}_{xs} &= \vec{j} - \phi_z \vec{i} + \phi_x \vec{k} \\ \vec{k}_{xs} &= \vec{k} - \phi_x \vec{j}\end{aligned}$$

Now by definition, $\vec{j}_{xs} = d\vec{r}/ds$, where $\vec{r} = x_0 \vec{i} + (r + r_0) \vec{j} + z_0 \vec{k}$ and s is the arc length along the deformed elastic axis. Hence to first order

$$\begin{aligned}\vec{j}_{xs} &= \vec{j} + (x_0 \vec{i} + z_0 \vec{k})' \\ &= \vec{j} + (x_0' + z_0 \theta') \vec{i} + (z_0' - x_0 \theta') \vec{k}\end{aligned}$$

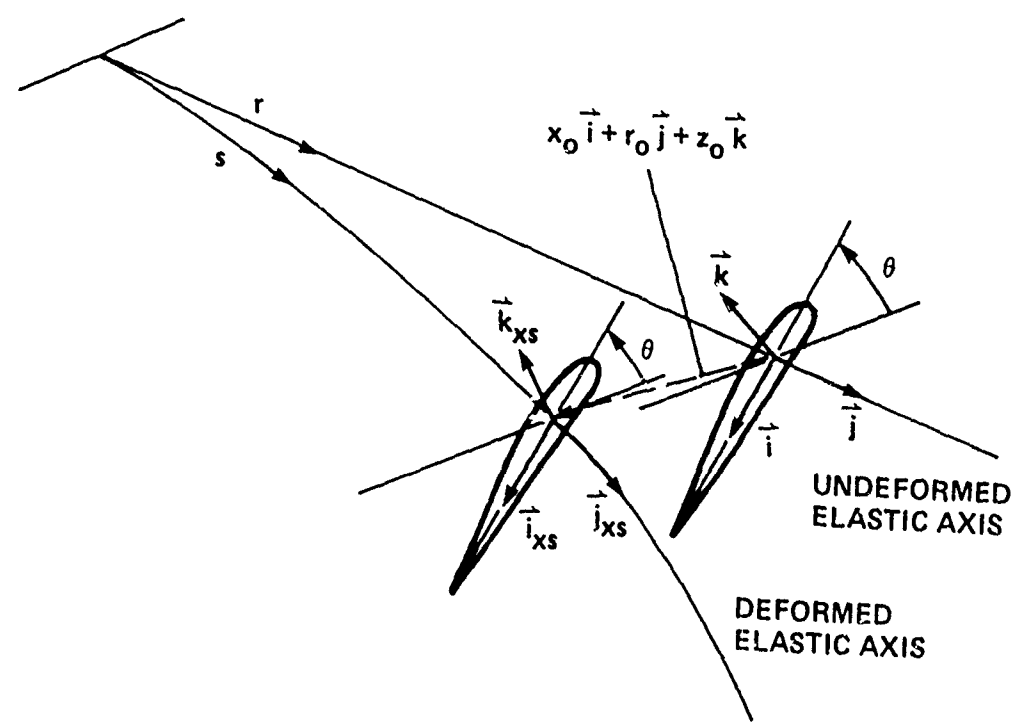


Figure 3. Geometry of the deformed blade.

It follows the rotation of the section is

$$\begin{aligned}-\phi_z &= x'_o + z_o \theta' \\ \phi_x &= z'_o - x_o \theta'\end{aligned}$$

or

$$\phi_x \vec{i} + \phi_z \vec{k} = (z_o \vec{i} - x_o \vec{k})'$$

The undeflected position of the blade element is $\vec{r} = x \vec{i} + r \vec{j} + z \vec{k}$, and the deflected position is

$$\begin{aligned}\vec{r} &= (r + r_o) \vec{j} + x_o \vec{i} + z_o \vec{k} + x \vec{i}_{xs} + z \vec{k}_{xs} \\ &= r \vec{j} + x_o \vec{i} + z_o \vec{k} + (r_o + x \phi_z - z \phi_x) \vec{j} + x \vec{i} + z \vec{k}\end{aligned}$$

The first term in the deflected position is the radial station; the next three terms are the deflection of the elastic axis; the next term is the rotation of the section; and the final two terms are the location of the point on the cross section. For now the elastic extension r_o will be neglected. The strain analysis is simplified since then to first order, $s = r$; r_o gives a uniform strain over the section, which may be reintroduced later.

2.1.3 Analysis of strain.- The fundamental metric tensor g_{mn} of the undistorted blade is defined by:

$$\begin{aligned}(ds)^2 &= d\vec{r} \cdot d\vec{r} \\ &= \left(\frac{\partial \vec{r}}{\partial x_m} dx_m \right) \cdot \left(\frac{\partial \vec{r}}{\partial x_n} dx_n \right) \\ &= g_{mn} dx_m dx_n\end{aligned}$$

Where ds is the differential length in the material, and x_m are general curvilinear coordinates. Similarly, the metric tensor G_{mn} of the deformed blade is

$$\begin{aligned} (ds)^2 &= d\vec{r} \cdot d\vec{r} \\ &= \left(\frac{\partial \vec{r}}{\partial x_m} dx_m \right) \cdot \left(\frac{\partial \vec{r}}{\partial x_n} dx_n \right) \\ &= G_{mn} dx_m dx_n \end{aligned}$$

Then the strain tensor γ_{mn} is defined by the differential length increment

$$2 \gamma_{mn} dx_m dx_n = (ds)^2 - (ds)^2$$

or

$$\gamma_{mn} = \frac{1}{2} (G_{mn} - g_{mn})$$

For engineering beam theory, only the axial components of the strain and stress are required. For a full exposition of the analysis of strain, the reader is directed to reference 2.

The metric of the undeformed blade (no bending, and no torsion so $\theta'_{tw} = \theta'_{tw}$) is obtained from the undistorted position vector $\vec{r} = x\vec{i} + r\vec{j} + z\vec{k}$, giving

$$g_{rr} = \frac{\partial \vec{r}}{\partial r} \cdot \frac{\partial \vec{r}}{\partial r} = 1 + \theta'_{tw}^2 (x^2 + z^2)$$

The metric of the deformed blade, including bending and torsion, is similarly obtained from the position vector $\vec{r} = (x + x_o)\vec{i} + (r + x\phi_z - z\phi_x)\vec{j} + (z + z_o)\vec{k}$:

$$\begin{aligned}
 G_{rr} &= \frac{\partial^2}{\partial r^2} \cdot \frac{\partial^2}{\partial r^2} \\
 &= (1 + x\phi_z' - z\phi_x')^2 \\
 &\quad + (x_0' + \theta'(z + z_0))^2 \\
 &\quad + (z_0' - \theta'(x + x_0))^2
 \end{aligned}$$

Then the axial component of the strain tensor is

$$\begin{aligned}
 \gamma_{rr} &= \frac{1}{2}(G_{rr} - g_{rr}) \\
 &= \frac{1}{2} \left[(1 + x\phi_z' - z\phi_x')^2 - 1 + (x_0' + \theta'(z + z_0))^2 \right. \\
 &\quad \left. - \theta_{tw}'^2 z^2 + (z_0' - \theta'(x + x_0))^2 - \theta_{tw}'^2 x^2 \right]
 \end{aligned}$$

The linear strain (for small x_0 , z_0 , θ_e , ϕ_x , and ϕ_z) is

$$\begin{aligned}
 \gamma_{rr} \cong \epsilon_{rr} &= x\phi_z' - z\phi_x' + \theta_{tw}'^2 (x x_0 + z z_0) \\
 &\quad + \theta_{tw}' (z x_0' - x z_0' + \theta_e' (x^2 + z^2))
 \end{aligned}$$

The strain due to the blade tension, ϵ_T , is a constant such that the tension is given by the integral over the blade section:

$$\tau = \int E \epsilon_{rr} dA = \epsilon_T \int E dA$$

Substituting for ϵ_{rr} and using the results $\int z dA = 0$, $\int x dA = x_C A$, and $\int (x^2 + z^2) dA = I_p = k_p^2 A$ (where k_p is the modulus weighted radius of gyration about the elastic axis), gives

$$\epsilon_r = \frac{T}{EA} = \phi_z' x_c + \theta_{tw}'^z x_0 x_c - \theta_{tw}' z_0 x_c + \theta_{tw}' \theta_e' k_p^2 + r_0'$$

In this expression, the strain due to the blade extension r_0 has been included. It follows that the strain may be written as

$$\epsilon_{rr} = \epsilon_r + (x - x_c) (\phi_z' - \theta_{tw}' \phi_x) - z (\phi_x' + \theta_{tw}' \phi_z) + \theta_{tw}' \theta_e' (x^2 + z^2 - k_p^2)$$

2.1.4 *Section moments.* - To find the moments on the section, the second engineering beam theory assumption is introduced: that all stresses except σ_{rr} are negligible. The axial stress is given by $\sigma_{rr} = E\epsilon_{rr}$. The direction of σ_{rr} is

$$\hat{e} = \frac{\partial \vec{r}}{\partial r} / \left| \frac{\partial \vec{r}}{\partial r} \right|$$

The moment on the deformed cross section (fig. 4) is $M = M_x \vec{I}_{xs} + M_r \vec{J}_{xs} + M_z \vec{k}_{xs}$. The moment about the elastic axis due to the element force $\sigma_{rr} dA$ on the cross section is

$$\begin{aligned} d\vec{M} &= (x \vec{t}_{xs} + z \vec{k}_{xs}) \times (\sigma_{rr} \hat{e}) dA \\ &= [-z \vec{t}_{xs} + x \vec{k}_{xs} + \theta_{tw}' (x^2 + z^2) \vec{J}_{xs}] \sigma_{rr} dA \end{aligned}$$

Integrating over the blade section, there follows the result for the total moments due to bending and elastic torsion:

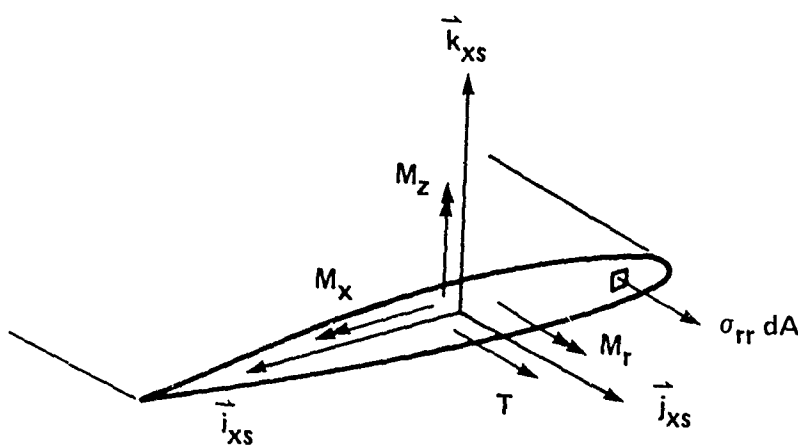


Figure 4. Bending and torsion moments on the blade section.

$$(M_x)_{EA} = - \int z \sigma_{rr} dA$$

$$(M_z)_{EA} = \int x \sigma_{rr} dA$$

$$M_r = GJ \theta'_e + \int (x^2 + z^2) \theta'_{tw} \sigma_{rr} dA$$

To M_r has been added the torsion moment $GJ\theta'_e$, due to shear stresses produced by elastic torsion. These moments are about the elastic axis. For bending it is more convenient to work with moments about the tension center at x_c :

$$M_x = - \int z \sigma_{rr} dA$$

$$M_z = \int (x - x_c) \sigma_{rr} dA$$

Substituting for σ_{rr} and integrating, the moments are

$$M_x = EI_{zz} (\phi'_x + \theta' \phi_z) - \theta'_{tw} \theta'_e EI_{zp}$$

$$M_z = EI_{xx} (\phi'_z - \theta' \phi_x) + \theta'_{tw} \theta'_e EI_{xp}$$

$$\begin{aligned} M_r = & (GJ + k_p^2 T + \theta'_{tw}^2 EI_{pp}) \theta'_e + \theta'_{tw} k_p^2 T \\ & + \theta'_{tw} [EI_{xp} (\phi'_z - \theta' \phi_x) - EI_{zp} (\phi'_x + \theta' \phi_z)] \end{aligned}$$

where

$$\begin{aligned}
 I_{zz} &= \int z^2 dA \\
 I_{xx} &= \int (x-x_c)^2 dA \\
 I_p &= \int (x^2 + z^2) dA = k_p^2 A \\
 I_{xp} &= \int (x-x_c)(x^2 + z^2) dA \\
 I_{zp} &= \int z(x^2 + z^2) dA \\
 I_{pp} &= \int (x^2 + z^2 - k_p^2)^2 dA
 \end{aligned}$$

The integrals are all over the tension carrying elements (i.e., modulus weighted). The tension T acts at the tension center at x_c ; hence the bending moments about the elastic axis may be obtained from those about the tension center by $(M_z)_{EA} = M_z + x_c T$ and $(M_x)_{EA} = M_x$.

2.1.5 *Vector formulation.*— Define the section bending moment vector $\vec{M}_E^{(2)}$, and the flap/lag deflection \vec{w} as follows:

$$\begin{aligned}
 \vec{M}_E^{(2)} &= M_x \vec{i} + M_z \vec{k} \\
 \vec{w} &= z_0 \vec{i} - x_0 \vec{k}
 \end{aligned}$$

$\vec{M}_E^{(2)}$ is not quite the moment on the section, because M_x and M_z are really the i_{xs} and k_{xs} components of the moment). The derivatives of \vec{w} are

$$\begin{aligned}
 (z_0 \vec{i} - x_0 \vec{k})' &= (z'_0 - x_0 \theta') \vec{i} - (x'_0 + z_0 \theta') \vec{k} \\
 &= \phi_x \vec{i} + \phi_z \vec{k} \\
 (z_0 \vec{i} - x_0 \vec{k})'' &= (\phi'_x + \theta' \phi_z) \vec{i} + (\phi'_z - \theta' \phi_x) \vec{k}
 \end{aligned}$$

Then the result for the bending and torsion moments can be written as follows:

$$\vec{M}_E^{(2)} = (EI_{zz}\vec{t}\vec{t} + EI_{xx}\vec{k}\vec{k}) \cdot (\vec{z}_0\vec{t} - \vec{x}_0\vec{k})'' + \theta_{tw}' \theta_e' (EI_{xp}\vec{k} - EI_{zp}\vec{t})$$

$$M_T = (GJ + k_p^z T + \theta_{tw}'^z EI_{pp}) \theta_e' + \theta_{tw}' k_p^z T + \theta_{tw}' (EI_{xp}\vec{k} - EI_{zp}\vec{t}) \cdot (\vec{z}_0\vec{t} - \vec{x}_0\vec{k})''$$

This is the result sought, the relation between the structural moments and deflections of the rotor blade.

Writing the bending stiffness dyadic as $EI = EI_{zz}\vec{t}\vec{t} + EI_{xx}\vec{k}\vec{k}$, and for the purposes of this paragraph neglecting the EI_{xp} and EI_{zp} coupling terms, gives

$$\vec{M}_E^{(2)} = EI \vec{w}''$$

$$M_T = GJ_{eff} \theta_e' + k_p^z T \theta_{tw}'$$

In this form the result appears as a simple extension of the engineering beam theory result for uncoupled bending and torsion (the $\theta_{tw}' = 0$ case). The vector form allows a simultaneous treatment of the coupled inplane and out-of-plane bending of the blade, with considerable simplification of the equations as a consequence.

This relation between the moments and deflections is a linearized result. Thus the vectors \vec{t} and \vec{k} appearing in EI and in \vec{w} are based on the trim pitch angle $\theta = \theta^0 + \theta_{tw}$. The net torsion modulus is

$$GJ_{eff} = GJ + k_p^2 T + \theta_{tw}^2 EI_{pp}$$

where $T = \Omega^2 \int_r^l \rho m dp$ is the centrifugal tension in the blade. For the elastic torsion stiffness characteristic of rotor blades, the GJ term usually dominates. The $k_p^2 T$ term is only important near the root for blades which are very soft torsionally. The $\theta_{tw}^2 EI_{pp}$ term is only important for very soft, highly twisted blades.

2.2 Inertia Analysis

This section derives the inertia forces of a helicopter rotor blade. The blade motion considered includes coupled flap/lag bending (including the rigid modes if the blade is articulated), rigid pitch and elastic torsion, gimbal pitch and roll (which are dropped from the model for articulated and hingeless rotors) or teeter motion (for two-bladed rotors only), and the rotational speed perturbation. The geometric model of the blade and hub includes precone, droop, and sweep; pitch bearing radial offset; feathering axis droop and sweep; and torque offset and gimbal undersling.

2.2.1 Rotor geometry. - Consider an N -bladed rotor, rotating at speed Ω (fig. 5). The m -th blade ($m = 1$ to N) is at the azimuth location $\psi_m = \psi + m\Delta\psi$, where $\Delta\psi = 2\pi/N$ and $\psi = \Omega t$ is the dimensionless time variable. Because for steady flight the blade motion is periodic, it is only necessary to calculate the motion and forces of one of the blades. For this reference blade we choose that identified by $m = N$. The S coordinate system (\vec{i}_S , \vec{j}_S , \vec{k}_S) is a nonrotating, inertial reference frame (fig. 5). The S system coordinates are the rotor shaft axes when there is no hub motion. When the shaft moves however, due to the motion of the helicopter or the wind tunnel support, the S system remains fixed in space. The B system (\vec{i}_B , \vec{j}_B , \vec{k}_B) is a coordinate frame rotating with the m -th blade. The acceleration, angular velocity, and angular acceleration of the hub, and the forces and moments exerted by the rotor on the hub are defined in the nonrotating frame (the S system). Figure 6(a) shows the definition of the linear and angular motion of

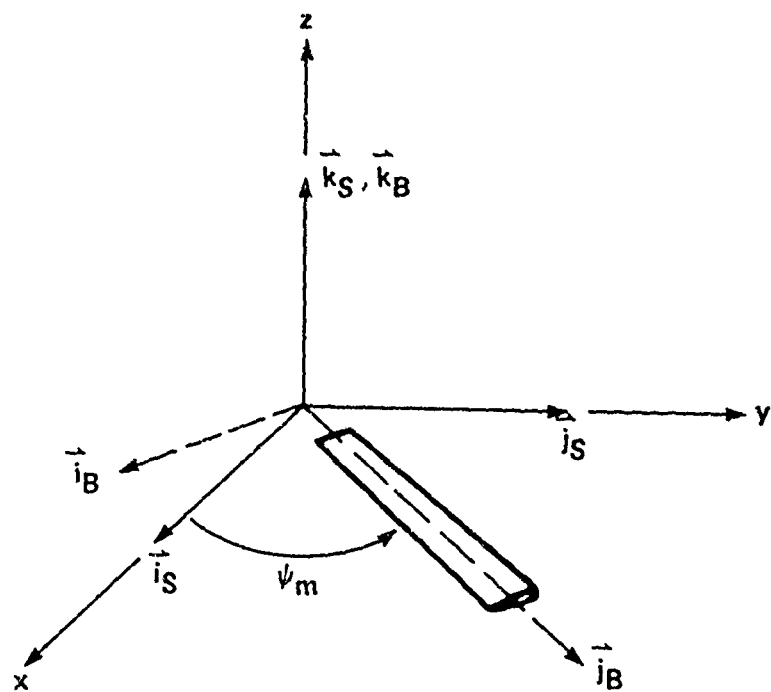
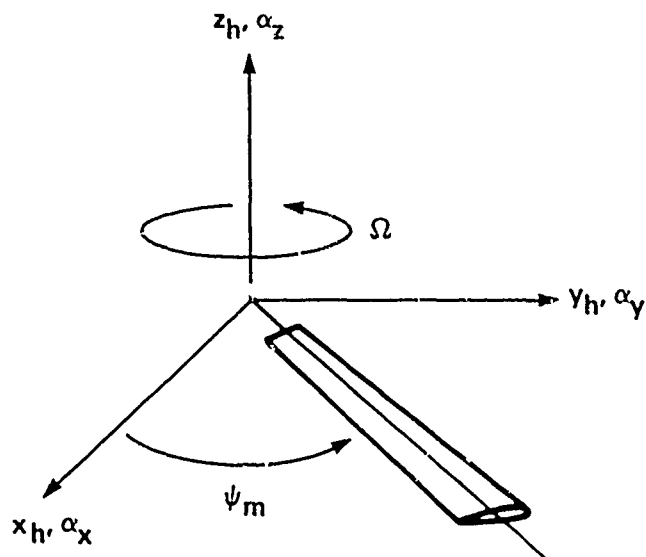
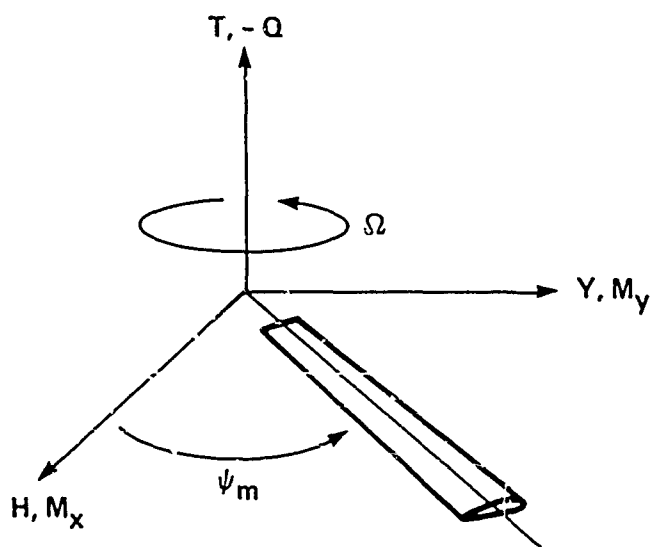


Figure 5. Hub frame coordinate systems: shaft axes and blade axes (nonrotating and rotating frames)



(a) SHAFT MOTION



(b) HUB REACTIONS

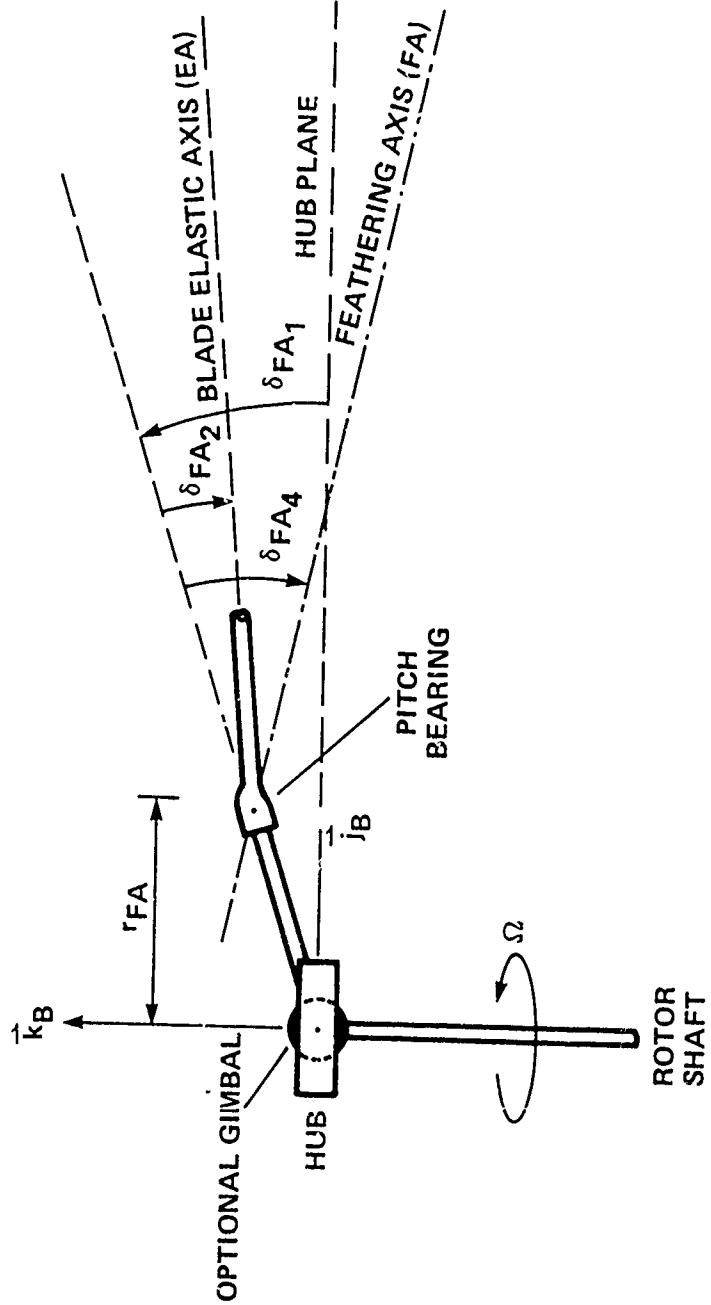
Figure 6. Notation and sign conventions for the linear and angular shaft motion, and the forces and moments acting on the rotor hub.

the rotor hub, and figure 6(b) shows the definition of the rotor forces and moments acting on the hub. The rotor blade equations of motion will be derived in the rotating frame.

Figure 7 shows the blade hub and root geometry considered. The origin of the B and S system is the location of the gimbal (or teeter hinge). For articulated or hingeless rotors, where there is no gimbal, this is simply the point where the shaft motion and hub forces are evaluated. The hub of the rotor is a distance r_{FA} below the gimbal (gimbal undersling, which is not shown in fig. 7). The torque offset x_{FA} is positive in the \hat{r}_B direction. The azimuth ψ_m is measured to the feathering axis line (its projection in the hub plane), so the feathering axis is parallel to the \hat{T}_B axis, and offset x_{FA} from the center of rotation. The precone angle δ_{FA_1} , gives the orientation of the blade elastic axis inboard of the pitch bearing with respect to the hub plane; δ_{FA_1} , is positive upward, and is assumed to be a small angle. The pitch bearing is offset radially from the center of rotation by r_{FA} . The inboard pitch rotation of the blade about the feathering axis occurs at r_{FA} .

The droop angle δ_{FA_2} and sweep angle δ_{FA_3} occur at r_{FA} , just outboard of the pitch bearing; δ_{FA_2} and δ_{FA_3} give the orientation of the elastic axis of the blade outboard of the pitch bearing, with respect to the precone. Both δ_{FA_2} and δ_{FA_3} are assumed to be small angles; δ_{FA_2} is positive downward, and δ_{FA_3} is positive aft. Feathering axis droop δ_{FA_4} and sweep δ_{FA_5} define the orientation of the feathering axis with respect to the precone; δ_{FA_4} is positive downward, δ_{FA_5} is positive aft, and both are small angles. If $\delta_{FA_4} = \delta_{FA_5} = 0$, then the feathering axis orientation is just given by the precone; if $\delta_{FA_4} = \delta_{FA_2}$ and $\delta_{FA_5} = \delta_{FA_3}$ then the orientation is the same as the outboard elastic axis.

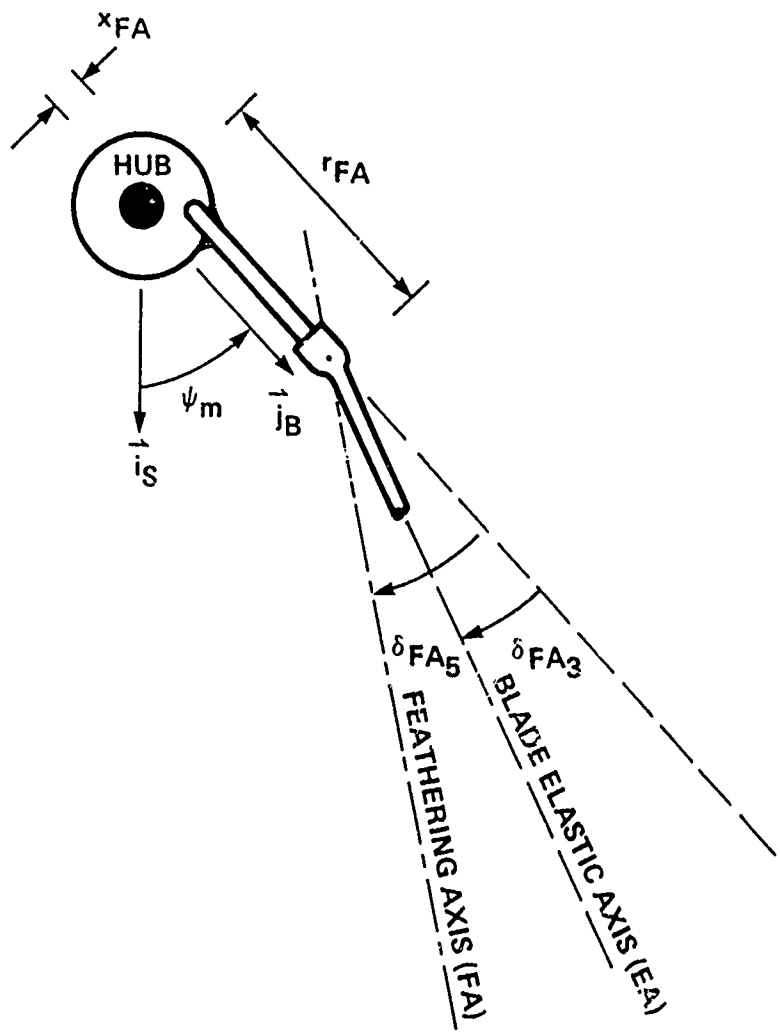
From the root to the pitch bearing (at $r = r_{FA}$), the undistorted elastic axis is a straight line at the precone angle to the hub plane. The blade outboard of the pitch bearing has a straight undistorted elastic axis, with small droop and sweep angles. The feathering axis also has small droop and sweep with respect to the precone. The entire blade is flexible in bending. The portion of the blade outboard of the pitch bearing is flexible in torsion as well. The rotation of the blade about the pitch bearing takes place about the



a) side view

Figure 7. Schematic of the rotor hub and root geometry.

Only a single, undistorted blade is shown, without the gimbal undersling. The gimbal is omitted from the model for articulated and hingeless rotors.



b) top view

Figure 7. Concluded.

local direction of the feathering axis. Incorporation of bending flexibility of the blade inboard of the pitch bearing allows consideration of an articulated rotor with the feathering axis inboard or outboard of the hinges, or a cantilever blade with or without flexibility inboard of the pitch bearing.

Figure 8 shows the undeformed geometry of the blade. The description of the blade for the inertial analysis parallels that for the structural analysis (see fig. 2 and section 2.1.1). It is assumed that an elastic axis exists, and that the undeformed elastic axis is a straight line; and that the blade has a high aspect ratio. Here x_I is the locus of the section center of gravity, x_A is the locus of the section aerodynamic center, and x_C is the locus of the section tension center. The distances x_I , x_A , and x_C are positive aft, measured from the elastic axis; in general they are a function of r . The corresponding z displacements are neglected.

The \vec{i} , \vec{j} , and \vec{k} coordinate system is the elastic axis/principal axis system of the section. The direction of the elastic axis is \vec{j} ; \vec{i} and \vec{k} are the direction of the local principal axes of the section. The spanwise variable is r , measured from the center of rotation. This variable is dimensionless, so $r = 1$ at the blade tip. The section coordinates x and z are mass principal axes, with origin at the elastic axis. It is assumed that the direction of the mass principal axes and the modulus principal axes is the same. The center of gravity is at $z = 0$ and $x = x_I$. The section mass, center of gravity position, and section polar moment of inertia (about the elastic axis) are by definition then as follows:

$$\int dm = m$$

$$\int z dm = 0$$

$$\int xz dm = 0$$

$$\int x dm = x_I m$$

$$\int (x^2 + z^2) dm = I_0$$

where the integrals are over the blade cross section.

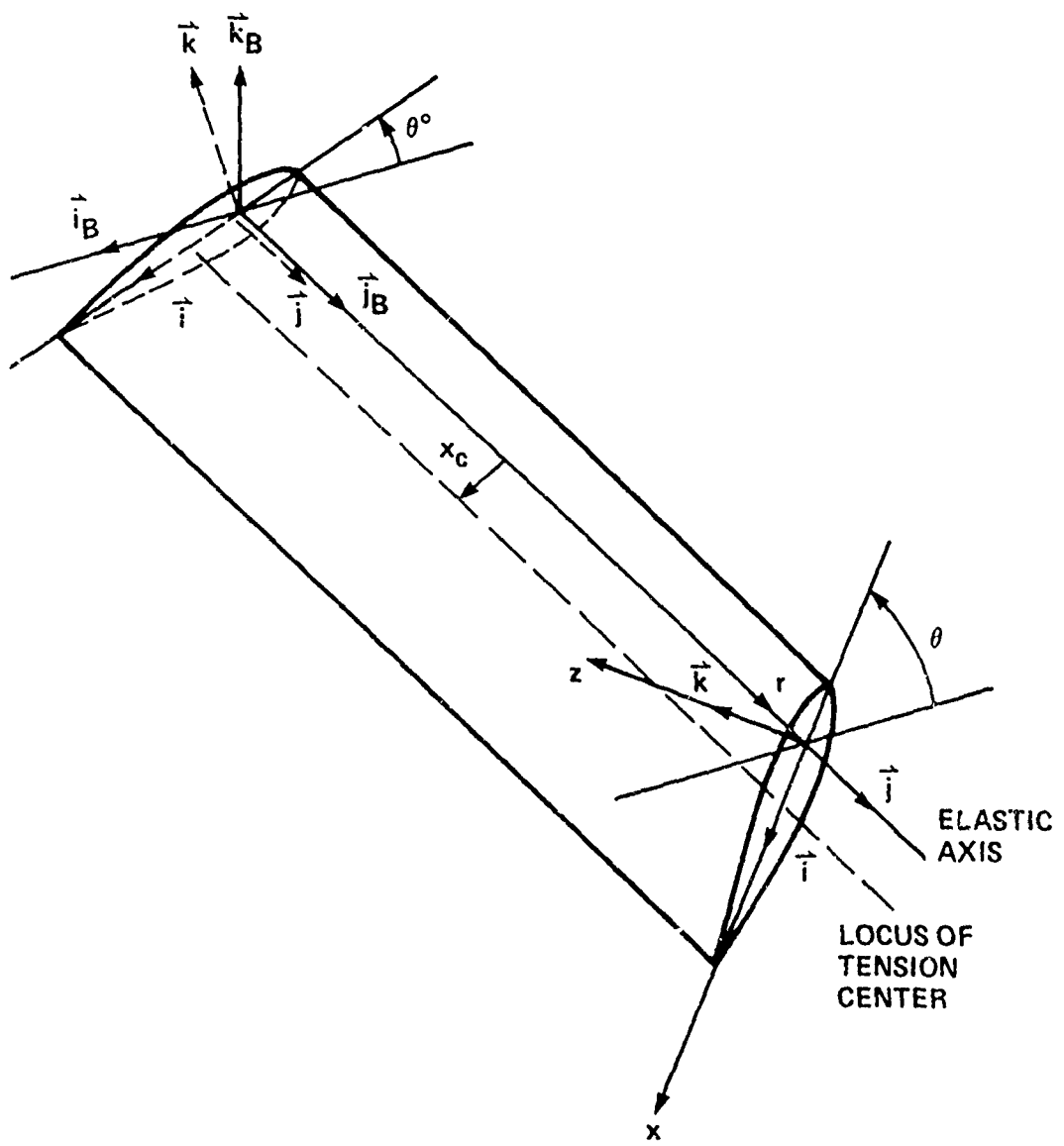


Figure 8. Geometry of the undeformed blade.

The droop and sweep of the blade elastic axis are defined with respect to the hub plane axes, so it follows that unless the feathering axis is parallel to the outboard elastic axis, these angles vary with the pitch of the blade. Let $\delta_{FA_2}^*$ and $\delta_{FA_3}^*$ be the droop and sweep of the blade when the pitch angle at 75% radius is zero. Then the following relation can be obtained from the root geometry:

$$\begin{aligned}\delta_{FA_2} &= \delta_{FA_4} + (\delta_{FA_2}^* - \delta_{FA_4}) \cos \theta_{75} \\ &\quad + (\delta_{FA_3}^* - \delta_{FA_5}) \sin \theta_{75}\end{aligned}$$

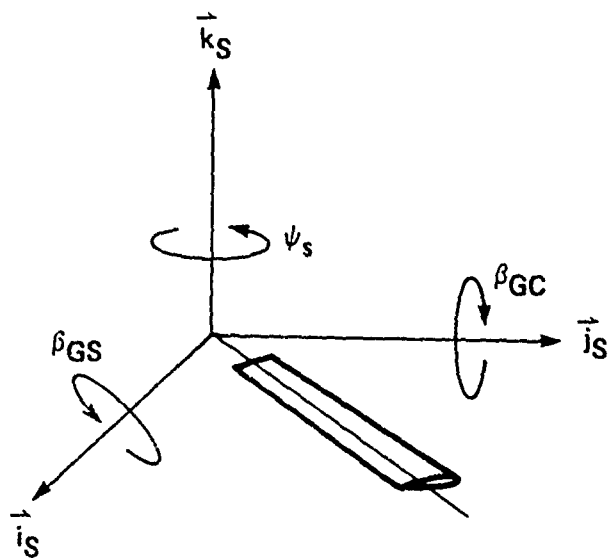
$$\begin{aligned}\delta_{FA_3} &= \delta_{FA_5} - (\delta_{FA_2}^* - \delta_{FA_4}) \sin \theta_{75} \\ &\quad + (\delta_{FA_3}^* - \delta_{FA_5}) \cos \theta_{75}\end{aligned}$$

where θ_{75} is the blade pitch at 75% radius.

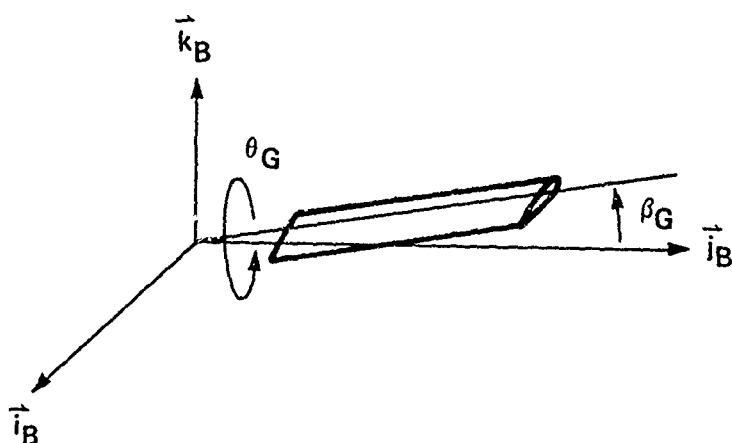
2.2.2 *Rotor motion*.- The rotor blade motion is described by the following degrees of freedom:

- (a) Gimbal pitch and roll motion of the rotor disk (omitted for articulated and hingeless rotors), or teeter motion of the blade (for two-bladed rotors only).
- (b) Rotor speed perturbation.
- (c) Rigid pitch motion about the feathering axis and torsion about the elastic axis.
- (d) Bending deflection of the elastic axis, including rigid flap and lag motion of the blade is articulated.

Figure 9(a) shows the gimbal motion and rotor speed perturbation in the non-rotating frame. The gimbal degrees of freedom are β_{GC} and β_{GS} , respectively



(a) NONROTATING FRAME



(b) ROTATING FRAME

Figure 9. Notation and sign conventions for the gimbal motion and the rotor speed perturbation.

pitch and roll of the rotor disk. The rotor rotational speed perturbation is ψ_s . Figure 9(b) shows the gimbal motion in the rotating frame. The degrees of freedom are β_G and θ_G , given by

$$\begin{aligned}\beta_G &= \beta_{GC} \cos \psi_m + \beta_{GS} \sin \psi_m \\ \theta_G &= -\beta_{GC} \sin \psi_m + \beta_{GS} \cos \psi_m\end{aligned}$$

The blade pitch θ is defined with respect to the hub plane, so only the blade inboard of the pitch bearing sees the pitch rotation due to θ_G . For two-bladed rotors, the teetering degree of freedom β_T may be included. The teetering motion is defined in the rotating frame, hence $\beta_G = \beta_T (-1)^m$ and $\theta_G = 0$ for this case.

Figure 3 showed the geometry of the deformed blade. The blade deformation is described by twist θ about the elastic axis, bending deflection x_0 and z_0 of the elastic axis; and rotations of the section by ϕ_x and ϕ_z due to the bending (see section 2.1.2).

The blade pitch angle θ is measured from the hub plane to the section major principal axis (the x axis). The undeformed pitch angle consists of the collective pitch θ_{coll} plus the built-in twist θ_{tw} . We define θ_{coll} as the pitch at r_{FA} , so $\theta_{tw}(r_{FA}) = 0$. The rotation by θ_{coll} is not present inboard of the pitch bearing, but there can be pitch if the local principal axes with respect to the hub plane, which is included in θ_{tw} for $r < r_{FA}$. The pitch of the deformed blade is composed of the root pitch $\theta^*(\psi)$ (the blade angle at the pitch bearing, $r = r_{FA}$, due to control commands, control system flexibility, and kinematic coupling); the built-in twist $\theta_{tw}(z)$; and torsion about the elastic axis $\theta_e(r, \psi)$ (where $\theta_e(r_{FA}, \psi) = 0$, and only θ_e produces shear stress in the blade). Thus the blade pitch is

$$\theta = \theta^* + \theta_{tw} + \theta_e$$

The commanded root pitch angle is defined as $\theta^c = \theta_{coll} + \theta_{con}$. Here θ_{coll} is the trim value of the collective pitch, which may be large but is steady in time; and θ_{con} is the perturbation control input (including the cyclic control required to trim the rotor), which is time dependent but is assumed to be a small angle. The blade root pitch commanded by the control system is θ^c , while θ^o is the actual root pitch. The difference $(\theta^o - \theta^c)$ is the rigid pitch motion due to control system flexibility or kinematic coupling in the control system. Hence, the blade pitch may be written as

$$\theta = (\theta_{coll} + \theta_{tw}) + (\theta^o - \theta^c) + \theta_{con} + \theta_e$$

The pitch angle may now be separated into trim and perturbation terms, $\theta = \theta_m + \tilde{\theta}$, where the trim term is

$$\theta_m = \theta_{coll} + \theta_{tw}$$

and the perturbation is

$$\tilde{\theta} = (\theta^o - \theta^c) + \theta_{con} + \theta_e$$

The trim pitch θ_m is a large, steady angle; the perturbation pitch $\tilde{\theta}$ is small angle since all the components are small. The pitch at the blade root ($r = r_{FA}$) is then

$$\begin{aligned}\theta(r_{FA}) &= \theta^o = \theta_{coll} + (\theta^o - \theta^c) + \theta_{con} \\ &= \theta_m + \tilde{\theta}^o\end{aligned}$$

For the rigid pitch motion the notation p_o is used:

$$p_o = \tilde{\theta}^\circ = (\theta^\circ - \theta^c) + \theta_{con}$$

(This notation is consistent with that for the modal expansion of the elastic torsion θ_e , as described below.) Note that p_o is the total rigid pitch motion of the blade, including the control angle θ_{con} .

2.2.3 Coordinate frames.- The rotating hub plane coordinate frame is obtained from the nonrotating hub plane frame by rotating about the z - axis:

$$\begin{aligned}\vec{i}_B &= \sin \psi_m \vec{i}_S - \cos \psi_m \vec{j}_S \\ \vec{j}_B &= \cos \psi_m \vec{i}_S + \sin \psi_m \vec{j}_S \\ \vec{k}_B &= \vec{k}_S\end{aligned}$$

The blade coordinate frame is obtained by rotating by the angle $\beta_G + \delta_{FA_1} - \delta_{FA_2}$ about the x-axis, by the angle $\psi_s - \delta_{FA_3}$ about the z-axis, and by the angle θ about the y-axis:

$$\begin{aligned}\vec{i} &= \cos \theta \vec{i}_B - \sin \theta \vec{k}_B \\ &\quad + \vec{j}_B [(\beta_G + \delta_{FA_1} - \delta_{FA_2}) \sin \theta + (\psi_s - \delta_{FA_3}) \cos \theta] \\ \vec{j} &= \vec{j}_B - (\psi_s - \delta_{FA_3}) \vec{i}_B + (\beta_G + \delta_{FA_1} - \delta_{FA_2}) \vec{k}_B \\ \vec{k} &= \sin \theta \vec{i}_B + \cos \theta \vec{k}_B \\ &\quad + \vec{j}_B [-(\beta_G + \delta_{FA_1} - \delta_{FA_2}) \cos \theta + (\psi_s - \delta_{FA_3}) \sin \theta]\end{aligned}$$

The cross section principal axes for the deformed blade are then

$$\vec{t}_{xs} = \vec{\tau} + \psi_z \vec{k}$$

$$\vec{j}_{xs} = \vec{j} - \psi_z \vec{\tau} + \psi_x \vec{k} = \vec{j} + (x_0 \vec{\tau} + z_0 \vec{k})'$$

$$\vec{k}_{xs} = \vec{k} - \psi_x \vec{j}$$

The vector \vec{j}_{xs} is tangent to the deformed elastic axis.

2.2.4 Blade acceleration.- The distance from the rotor hub to the center of gravity of the blade section is:

$$\begin{aligned}\vec{\tau} &= \vec{t}_B [-x_{FA} - (r-r_{FA}) \delta_{FA_3} - r \psi_s - z_{FA} \theta_G] \\ &\quad + \vec{k}_B [-z_{FA} - (r-r_{FA}) \delta_{FA_2} + r (\beta_G + \delta_{FA_1})] \\ &\quad + \vec{j}_B [r + z_{FA} \beta_G - x_{FA} \psi_s] \\ &\quad + (x_0 \vec{\tau} + z_0 \vec{k}) + x_z \vec{\tau} \\ &\quad - \tilde{\theta} x_z \vec{k} + \int_{r_{FA}}^r \partial_e (z_0 \vec{\tau} - x_0 \vec{k})'' (r-g) dg \\ &\quad + \tilde{\theta}^\circ [(z_0 \vec{\tau} - x_0 \vec{k}) - (z_0 \vec{\tau} - x_0 \vec{k})|_{r_{FA}} \\ &\quad \quad - (z_0 \vec{\tau} - x_0 \vec{k})'|_{r_{FA}} (r-r_{FA}) \\ &\quad \quad - ((\delta_{FA_2} - \delta_{FA_4}) \vec{t}_B + (\delta_{FA_3} - \delta_{FA_5}) \vec{k}_B)(r-r_{FA})] \\ &= \vec{t}_B [-x_{FA} - (r-r_{FA}) \delta_{FA_3} - r \psi_s - z_{FA} \theta_G] \\ &\quad + \vec{k}_B [-z_{FA} - (r-r_{FA}) \delta_{FA_2} + r (\beta_G + \delta_{FA_1})] \\ &\quad + \vec{j}_B [r + z_{FA} \beta_G - x_{FA} \psi_s] \\ &\quad + (x_0 \vec{\tau} + z_0 \vec{k}) + x_z \vec{\tau} \\ &\quad - \sum_{k=0}^{\infty} \vec{X}_k P_k\end{aligned}$$

where

$$\vec{X}_k = \vec{\beta}_k \times \vec{k} - \int_{r_{FA}}^r \vec{\beta}_k (z_0 \vec{i} - x_0 \vec{k})'' (r - g) dg$$

for elastic torsion ($k \geq 1$) and

$$\begin{aligned} \vec{X}_0 = & - (z_0 \vec{i} - x_0 \vec{k} - \vec{x}_I \vec{k}) \\ & + (z_0 \vec{i} - x_0 \vec{k})|_{r_{FA}} + (z_0 \vec{i} - x_0 \vec{k})'|_{r_{FA}} (r - r_{FA}) \\ & + ((\delta_{FA2} - \delta_{FA4}) \vec{i}_B + (\delta_{FA3} - \delta_{FA5}) \vec{k}_B) (r - r_{FA}) \end{aligned}$$

for rigid pitch. Then the velocity of the blade section, relative to the rotating frame is

$$\begin{aligned} \vec{v}_r = \left(\frac{d}{dt} \vec{r} \right)_B = & - \vec{i}_B (r \dot{\psi}_s + z_{FA} \dot{\theta}_G) + \vec{k}_B r \dot{\beta}_G \\ & + \vec{j}_B (z_{FA} \dot{\beta}_G - x_{FA} \dot{\psi}_s) \\ & + (x_0 \vec{i} - z_0 \vec{k})' \\ & - \sum_{k=0}^{\infty} \vec{X}_k \dot{p}_k \end{aligned}$$

Neglecting the squares of velocities, the acceleration relative to the rotating frame is

$$\begin{aligned} \vec{a}_r = \left(\frac{d}{dt} \vec{v}_r \right)_B = & - \vec{i}_B (r \ddot{\psi}_s + z_{FA} \ddot{\theta}_G) + \vec{k}_B r \ddot{\beta}_G \\ & + \vec{j}_B (z_{FA} \ddot{\beta}_G - x_{FA} \ddot{\psi}_s) \\ & + (x_0 \vec{i} - z_0 \vec{k})'' \\ & - \sum_{k=0}^{\infty} \vec{X}_k \ddot{p}_k \end{aligned}$$

For the blade Coriolis acceleration the radial velocity component $\vec{J} \cdot \vec{v}_r$ is required, including the effect of the change in the radial position of the section due to bending:

$$\Delta\vec{r} = -\vec{k}_B \frac{1}{2} \int_0^r [(x_0\vec{t} + z_0\vec{k} + x_I\vec{k})' - (\psi_s - \delta_{FA_3})\vec{k}_B \\ + (\beta_G + \delta_{FA_1} - \delta_{FA_2})\vec{k}_B]^2 \, d\vec{r}$$

then

$$\vec{J} \cdot \vec{v}_r = - \int_0^r (z_0\vec{t} - x_0\vec{k})' \cdot (z_0\vec{t} - x_0\vec{k} - x_I\vec{k})' \, d\vec{r} \\ - (z_0\vec{t} - x_0\vec{k})' \cdot ((\delta_{FA_1} - \delta_{FA_2})\vec{k}_B - \delta_{FA_3}\vec{k}_B) \\ - \dot{\beta}_G [-z_{FA} + r\delta_{FA_1} - (r - r_{FA})\delta_{FA_2} \\ + \vec{k}_B \cdot (z_0\vec{t} - x_0\vec{k} - x_I\vec{k})] \\ - \dot{\psi}_s [x_{FA} - (r - r_{FA})\delta_{FA_3} \\ + \vec{k}_B \cdot (z_0\vec{t} - x_0\vec{k} - x_I\vec{k})]$$

The acceleration of the blade is required with respect to an inertial frame, specifically the S system. The B coordinate frame rotates at a constant angular velocity $\vec{\omega} = \Omega \vec{k}_B$ with respect to the S frame. The shaft motion is composed of linear and angular displacement of the origin of the S frame. The acceleration, angular velocity, and angular acceleration of the S system have the following components in the nonrotating, inertial frame:

$$\vec{a}_o = \ddot{x}_s \vec{i}_s + \ddot{y}_s \vec{j}_s + \ddot{z}_s \vec{k}_s$$

$$\vec{\omega}_o = \dot{\alpha}_x \vec{i}_s + \dot{\alpha}_y \vec{j}_s + \dot{\alpha}_z \vec{k}_s$$

$$\ddot{\vec{\omega}}_o = \ddot{\alpha}_x \vec{i}_s + \ddot{\alpha}_y \vec{j}_s + \ddot{\alpha}_z \vec{k}_s$$

It is assumed that \vec{a}_o , $\vec{\omega}_o$, and $\ddot{\vec{\omega}}_o$ are all small quantities.

The acceleration (\vec{a}_r) and velocity (\vec{v}_r) of the blade relative to the B frame have been derived above. Now the acceleration of a blade point in inertial space will be derived, in terms of the motion of the shaft, the rotation of the rotor, and the blade motion in the B frame. From the result for the acceleration in the rotating coordinate frame (the S frame, rotating at rate $\vec{\omega}_o$), there follows:

$$\vec{a} = \vec{a}_o + \vec{a}_{r,s} + 2 \vec{\omega}_o \times \vec{v}_{r,s} + \vec{\omega}_o \times (\vec{\omega}_o \times \vec{r}) + \ddot{\vec{\omega}}_o \times \vec{r}$$

where $\vec{a}_{r,s}$ and $\vec{v}_{r,s}$ are the acceleration and velocity relative to the S frame. The B system rotates at angular velocity $\vec{\Omega} = \Omega \vec{k}_B$ with respect to the S frame. Hence with Ω constant and no angular or linear acceleration of the B frame with respect to the S frame, there follows:

$$\vec{a}_{r,s} = \vec{a}_r + 2 \vec{\omega} \times \vec{r} + \vec{\omega} \times (\vec{\omega} \times \vec{r})$$

$$\vec{v}_{r,s} = \vec{v}_r + \vec{\omega} \times \vec{r}$$

where \vec{a}_r and \vec{v}_r are the acceleration and velocity relative to the B frame.

Thus:

$$\begin{aligned} \vec{a} = & \vec{a}_o + \vec{a}_r + 2 \vec{\omega} \times \vec{v}_r + \vec{\omega} \times (\vec{\omega} \times \vec{r}) \\ & + 2 \vec{\omega}_o \times \vec{r} + 2 \vec{\omega}_o \times (\vec{\omega} \times \vec{r}) + \vec{\omega}_o \times (\vec{\omega}_o \times \vec{r}) + \ddot{\vec{\omega}}_o \times \vec{r} \end{aligned}$$

To first order in the velocity and angular velocity, this becomes finally:

$$\vec{a} \approx \vec{a}_o + 2\vec{\omega}_o \times (\vec{r} \times \vec{v}) + \dot{\vec{\omega}}_o \times \vec{v} \\ + \vec{a}_r + 2\vec{\omega} \times \vec{v}_r + \vec{\omega} \times (\vec{r} \times \vec{v})$$

or in dyadic operator form, with $\vec{\Omega} = \Omega \vec{k}_B$:

$$\vec{a} = \vec{a}_o + 2\vec{\omega} (\vec{k}_B \vec{r} - \vec{r} \vec{k}_B) \vec{\omega}_o - (\vec{r} \times) \dot{\vec{\omega}}_o \\ + \vec{a}_r + 2\vec{\omega} (\vec{j}_B \vec{i}_B - \vec{i}_B \vec{j}_B) \vec{v}_r - 2\vec{\omega}^2 (\vec{i}_B \vec{i}_B + \vec{j}_B \vec{j}_B) \vec{r}$$

The six terms in \vec{a} are respectively the acceleration of the origin, the Coriolis acceleration due to the angular velocity of the origin, the angular acceleration of the origin, the relative acceleration in the rotating frame, the relative Coriolis acceleration, and the centrifugal acceleration.

For the blade bending and torsion equations, the following components of the acceleration will be required:

$$\vec{j} \cdot \vec{a} = -2\vec{\omega}^2 r - 2\vec{\omega} (r \vec{i}_3 + \vec{k}_B \cdot (z_o \vec{i} - x_o \vec{k})) \\ + \ddot{x}_B \cos \psi + \ddot{y}_B \sin \psi - 2\vec{\omega} r \dot{\omega}_2$$

$$\begin{aligned}
\vec{j} \times \vec{\alpha} = & (z_0 \vec{i} - x_0 \vec{k})'' + r \ddot{\psi}_s \vec{k}_B + r \ddot{\beta}_G \vec{i}_B + z_{FA} \ddot{\theta}_G \vec{k}_B \\
& - \sum_{k=0}^{\infty} (\vec{j} \times \vec{x}_k) \ddot{p}_k \\
& + \sum^2 \vec{k}_B [\vec{i}_B \cdot (x_0 \vec{i} + z_0 \vec{k} + x_I \vec{l}) - x_{FA} - r_{FA} \delta_{FA_3}] \\
& + \sum^2 \vec{i}_B r (\beta_G + \delta_{FA_1} - \delta_{FA_2}) \\
& - \sum^2 \vec{k}_B \sum_{k=0}^{\infty} \vec{i}_B \cdot \vec{x}_k p_k \\
& + 2 \sum \vec{k}_B \vec{j} \cdot \vec{v}_r \\
& + 2 \sum [(\delta_{FA_1} - \delta_{FA_2}) \vec{i}_B - \delta_{FA_3} \vec{k}_B] (r \dot{\psi}_s + \vec{k}_B \cdot (z_0 \vec{i} - x_0 \vec{k})) \\
& + \vec{i}_B \ddot{z}_h - \vec{k}_B (\ddot{x}_h \sin \psi - \ddot{y}_h \cos \psi) \\
& + 2 \sum r \vec{i}_B (\ddot{x}_h \cos \psi + \ddot{y}_h \sin \psi) \\
& + r (\vec{k}_B (\ddot{x}_h \sin \psi - \ddot{y}_h \cos \psi) + \vec{k}_B \ddot{x}_2)
\end{aligned}$$

For the hub moment the angular acceleration is required:

$$\begin{aligned}
\vec{r} \times \vec{\alpha} = & r^2 \ddot{\psi}_s \vec{k}_B + r^2 \ddot{\beta}_G \vec{i}_B + r (z_0 \vec{i} - x_0 \vec{k})'' \\
& + r z_{FA} \ddot{\theta}_G \vec{k}_B - \sum_{k=0}^{\infty} (\vec{j} \times \vec{x}_k) r \ddot{p}_k \\
& + \sum^2 r \vec{i}_B [-z_{FA} + r \delta_{FA_1} - (r - r_{FA}) \delta_{FA_2} + r \beta_G \\
& + \vec{k}_B \cdot (x_0 \vec{i} + z_0 \vec{k} + x_I \vec{l}) - \sum_{k=0}^{\infty} \vec{i}_B \cdot \vec{x}_k p_k]
\end{aligned}$$

$$\begin{aligned}
& + 2 \Sigma (r \dot{\psi}_s + \vec{k}_B \cdot (\vec{z}_0 \vec{r} - \vec{x}_0 \vec{r})) [-\vec{k}_B (-x_{FA} + (r - r_{FA}) \delta_{FA_3}) \\
& \quad + \vec{k}_B (-z_{FA} + r \delta_{FA_1}, -(r - r_{FA}) \delta_{FA_2}) \\
& \quad + (\vec{z}_0 \vec{r} - \vec{x}_0 \vec{r}) - \vec{x}_I \vec{r}] \\
& + 2 \Sigma r \vec{k}_B \vec{j} \cdot \vec{v}_r \\
& + \vec{k}_B r \ddot{z}_h - \vec{k}_B r (\ddot{x}_h \sin \psi - \ddot{y}_h \cos \psi) \\
& + 2 \Sigma r^2 \vec{k}_B (\dot{\alpha}_x \cos \psi + \dot{\alpha}_y \sin \psi) \\
& + r^2 (\vec{k}_B (\ddot{\alpha}_x \sin \psi - \ddot{\alpha}_y \cos \psi) + \vec{k}_B \ddot{\alpha}_z)
\end{aligned}$$

and for the hub force we can use

$$\begin{aligned}
\vec{a} = & -r \ddot{\psi}_s \vec{k}_B + r \ddot{\beta}_G \vec{k}_B + (\vec{x}_0 \vec{r} + \vec{z}_0 \vec{r}) \\
& - 2 \Sigma \vec{j}_B (r \dot{\psi}_s + \vec{k}_B \cdot (\vec{z}_0 \vec{r} - \vec{x}_0 \vec{r})) \\
& - \Sigma^2 [\vec{k}_B \vec{k}_B \cdot (\vec{x}_0 \vec{r} + \vec{z}_0 \vec{r} + \vec{x}_I \vec{r}) + \vec{j}_B r \\
& \quad + \vec{k}_B (-x_{FA} + (r - r_{FA}) \delta_{FA_3} - r \dot{\psi}_s)] \\
& + \vec{k}_B (\ddot{x}_h \sin \psi - \ddot{y}_h \cos \psi) + \vec{k}_B \ddot{z}_h \\
& + \vec{j}_B (\ddot{x}_h \cos \psi + \ddot{y}_h \sin \psi) \\
& + 2 \Sigma r (\vec{k}_B (\dot{\alpha}_x \cos \psi + \dot{\alpha}_y \sin \psi) - \vec{j}_B \ddot{\alpha}_z) \\
& + r (\vec{k}_B (\ddot{\alpha}_x \sin \psi - \ddot{\alpha}_y \cos \psi) - \vec{k}_B \ddot{\alpha}_z)
\end{aligned}$$

The approximation $\tilde{r} = r \hat{j}_B^x$ has been used in all cases to evaluate the hub motion terms.

2.2.5 Aerodynamic forces.- The aerodynamic forces acting on the blade section at the elastic axis are F_z , F_x , and F_r (see fig. 11 in section 2.4). These are the components of the aerodynamic lift and drag forces in the hub plane axis system (the B frame). F_x is in the hub plane, positive in the drag direction; F_z is normal to the hub plane, positive upward; and F_r is the radial force, positive outward. There are also radial components of F_x and F_z due to the tilt of the section by blade bending; here F_r is just the radial drag force. Thus the aerodynamic force acting on the section at the deformed elastic axis is:

$$\begin{aligned}\tilde{F}_{\text{aero}} &= F_x \tilde{i}_B + F_z \tilde{k}_B - \tilde{r}_B \tilde{j}_{xs} \cdot (F_x \tilde{i}_B + F_z \tilde{k}_B) + F_r \tilde{j}_{xs} \\ &\cong F_x \tilde{i}_B + F_z \tilde{k}_B + \tilde{F}_r \tilde{j}_B\end{aligned}$$

where

$$\begin{aligned}\tilde{F}_r &= F_r - F_z (\beta_6 + S_{FA_1} - S_{FA_2} + \tilde{k}_B \cdot (x_0 \tilde{i} + z_0 \tilde{k})') \\ &\quad - F_x (-\gamma_5 + S_{FA_3} + \tilde{i}_B \cdot (x_0 \tilde{i} + z_0 \tilde{k})')\end{aligned}$$

The section aerodynamic moment about the elastic axis is M_a , positive nose upward (so $\tilde{M}_{\text{aero}} = M_a \tilde{j}_{xs}$). These section aerodynamic loads are integrated over the blade span to obtain the total forces and moments.

2.2.6 Force and moment equilibrium.- The equations of motion for elastic bending, torsion, and rigid pitch of the blade are obtained from equilibrium of inertial, aerodynamic, and elastic moments on the portion of the blade outboard of r :

$$-\tilde{M}_E + \tilde{M}_A = \tilde{M}_x$$

Where M_E is the structural moment on the inboard face of the defcrmed cross section (so $-M_E$ is the external force on the outboard face); M_A is the total aerodynamic moment on the blade surface outboard of r ; and M_I is the total inertial moment of the blade outboard of r . The structural moment M_E is obtained from the engineering beam theory for bending and torsion (section 2.1.5), from the control system flexibility for rigid pitch, or from the hub spring for gimbal or teeter motion. Alternatively, M_E may be viewed as the force or moment on the hub due to the rotor (so $-M_E$ is the force on the rotor). M_I is the inertial moment of the blade outboard of r , about the point $\vec{r}_o(r)$, obtained by integrating the acceleration times the blade density ($dm/d\phi$) over the volume of the blade:

$$\vec{M}_I = \int_c' \int_{\text{section}} (\vec{r}(\phi) - \vec{r}_o(r)) \times \vec{a} dm d\phi$$

For bending of the blade, engineering beam theory gives

$$\vec{M}_E^{(z)} = M_x \vec{\tau} + M_z \vec{k} = (\vec{\tau} \vec{\tau}_{xs} + \vec{k} \vec{k}_{xs}) \vec{M}_E$$

Therefore the operator $(\vec{\tau}_{xs} + \vec{k}_{xs})$ is applied to \vec{M}_I and \vec{M}_A also. For bending, moments about the tension center ($x = x_C$) are required. Then the desired partial differential equation for bending is obtained from $\partial^2 \vec{M}_E^{(2)} / \partial r^2$. The ordinary differential equation for the k -th bending mode of one blade is obtained by operating with $\int_0^l \vec{\eta}_k \cdot (...) dr$, where $\vec{\eta}_k$ is the flap/lag bending mode shape (see section 2.2.15). For elastic torsion, engineering beam theory gives $M_r = \vec{\tau}_{xs} \cdot \vec{M}_E$. So this same operator is applied to \vec{M}_I and \vec{M}_A . For torsion, moments about the section elastic axis ($x = 0$) at r are required; also, elastic torsion involves only the blade outboard of r_{FA} . The desired partial differential equation for torsion is then obtained from $\partial M_r / \partial r$. The ordinary differential equation for the k -th torsion mode is obtained by operating with $\int_0^l \vec{\xi}_k \cdot (...) dr$, where $\vec{\xi}_k$ is the elastic torsion mode shape (see section 2.2.15). The equation of motion for the rigid pitch degree of freedom p_o is obtained from equilibrium of moments about the feathering axis, $M_{FA} = \hat{e}_{FA} \cdot \vec{M}(r_{FA})$. There \vec{M} is the moment about the feathering axis ($x = 0$)

at $r = r_{FA}$, and \hat{e}_{FA} is the direction of the feathering axis, including perturbations due to blade bending:

$$\hat{e}_{FA} = \vec{\delta}_{FA} + (x_0 \vec{i} + z_0 \vec{k})' \Big|_{r_{FA}} - \delta_{FA4} \vec{T}_B + \delta_{FA5} \vec{U}_B$$

The elastic restraint from the control system flexibility gives the restoring moment about the feathering axis, completing the desired equation of motion.

The total rotor force and moment on the hub (at the gimbal point) are obtained from a sum over the N blades of $\vec{F}^{(m)}$ and $\vec{M}^{(m)}$, the force and moment due to the m -th blade:

$$\vec{F} = \sum_{m=1}^N \vec{F}^{(m)}$$

$$\vec{M} = \sum_{m=1}^N \vec{M}^{(m)}$$

Since $\vec{F}^{(m)}$ and $\vec{M}^{(m)}$ are the forces on the blade, from force and moment equilibrium of the entire blade it follows that

$$\vec{F}^{(m)} = \vec{F}_A - \vec{F}_H$$

$$\vec{M}^{(m)} = \vec{M}_A - \vec{M}_H$$

The hub force and moment are required in the nonrotating hub plane frame (the S system), with components defined as follows:

$$\vec{F} = H \vec{i}_S + V \vec{j}_S + T \vec{k}_S$$

$$\vec{M} = M_x \vec{i}_S + M_y \vec{j}_S - Q \vec{k}_S$$

(see fig. 6).

The equations of motion for the gimbal degrees of freedom β_{GC} and β_{GS} are obtained from equilibrium of moments about the gimbal, $M_x = \vec{i}_S \cdot \vec{M}$ and $M_y = \vec{j}_S \cdot \vec{M}$, where \vec{M} is the total moment (from all N blades) about the gimbal point, in the nonrotating frame. The equation of motion for the teeter degree of freedom β_T is obtained from equilibrium of the moments about the teeter hinge from both blades, in the rotating frame. The equation of motion for the rotor speed perturbation ψ_s is obtained from equilibrium of the shaft torque moments, $Q = -M_z = \vec{k}_S \cdot \vec{M}$. The drive train couples the torque perturbations of both the rotors, hence this degree of freedom is best considered with the other motions of the helicopter body.

2.2.7 *Bending equation.*— The equation of motion for blade bending is obtained from

$$\int_0^1 \vec{\eta}_k \cdot \frac{\partial^2 M^{(2)}}{\partial r^2} dr + \int_0^1 \vec{\eta}_k \cdot \frac{\partial M_E}{\partial r^2} dr = \int_0^1 \vec{\eta}_k \cdot \frac{\partial^2 \vec{M}^{(2)}}{\partial r^2} dr$$

where \vec{M} is the moment about the tension center ($x = x_C$) at r , and

$$\vec{M}^{(2)} = (\vec{i} \vec{i}_{x_S} + \vec{k} \vec{k}_{x_S}) \vec{M} = (\vec{i} \vec{i} + \vec{k} \vec{k} - (x \vec{i} + z \vec{k}) \vec{j}) \vec{M}$$

Considering first the blade outboard of r_{FA} , the inertia moment is

$$\begin{aligned}\vec{M}_I &= \int_r^l \left\{ \text{section } (\vec{r} |_{x_0} - \vec{r} |_{x_c}) \times \vec{a} \ dm \right\} \\ &= \int_r^l \left[\begin{array}{l} (g-r)\vec{j} + (x_0+x_c)\vec{i} + z_0\vec{k} \\ - ((x_0+x_c)\vec{i} + z_0\vec{k}) |_r \end{array} \right] \times \vec{a} \ dm\end{aligned}$$

so

$$\begin{aligned}\frac{\partial \vec{M}}{\partial r} &= - (j + (x_0\vec{i} + z_0\vec{k} + x_c\vec{i})') \times \int_r^l \vec{a} \ dm \\ &\quad - (x_c - x_0)\vec{i} \times \vec{a} \ m\end{aligned}$$

$$\begin{aligned}\frac{\partial^2 \vec{M}}{\partial r^2} &= \vec{j} \times \vec{a} \ m - [(x_0\vec{i} + z_0\vec{k} + x_c\vec{i})' \times \int_r^l \vec{a} \ dm]'' \\ &\quad - [(x_c - x_0)\vec{i} \times \vec{a} \ m]''\end{aligned}$$

$$\vec{j} \cdot \vec{M} = \int_r^l [z_0\vec{i} - (x_0 + x_c)\vec{k} - (z_0\vec{i} - x_0\vec{k} - x_c\vec{k}) |_r] \cdot \vec{a} \ dm$$

Finally:

$$\begin{aligned}\frac{\partial^2 \vec{M}_I}{\partial r^2} &= (\vec{i}\vec{i} + \vec{k}\vec{k}) \frac{\partial \vec{M}_I}{\partial r^2} - [(x_0\vec{i} + z_0\vec{k})' \vec{j} \cdot \vec{M}_I]'' \\ &= \vec{j} \times \vec{a} \ m + [(x_c - x_0)\vec{k} \vec{j} \cdot \vec{a} \ m]'' \\ &\quad + [(z_0\vec{i} - x_0\vec{k} - x_c\vec{k})' \int_r^l \vec{j} \cdot \vec{a} \ dm]'' \\ &\quad - \left\{ (x_0\vec{i} + z_0\vec{k})' \int_r^l [z_0\vec{i} - x_0\vec{k} - x_c\vec{k} \right. \\ &\quad \left. - (z_0\vec{i} - x_0\vec{k} - x_c\vec{k}) |_r] \cdot \vec{a} \ dm \right\}''\end{aligned}$$

The last term in this result will be neglected since it is order $(c/R)^2$ smaller than the first term. Including the case $r < r_{FA}$, which only introduces an effect of the droop and sweep, the result is

$$\begin{aligned} \frac{\partial^2}{\partial r^2} \vec{M}_I^{(2)} &= \vec{j} \times \vec{a}_m + [(x_c - x_I) \vec{k} \vec{j} \cdot \vec{a}_m]^\circ \\ &\quad + [(z_0 \vec{i} - x_0 \vec{k} - x_c \vec{k})^\circ \int_r^1 \vec{j} \cdot \vec{a}_m dr]^\circ \\ &\quad - \delta(r - r_{FA}) (\delta_{FA_2} \vec{i}_B + \delta_{FA_3} \vec{k}_B) \int_{r_{FA}}^1 \vec{j} \cdot \vec{a}_m dr \end{aligned}$$

where $\delta(r)$ is the delta function (an impulse at $r = 0$). Operating with $\int_0^1 \vec{\eta}_k \cdot (\dots) dr$ and integrating the second and third terms by parts gives:

$$\begin{aligned} \int_0^1 \vec{\eta}_k \cdot \frac{\partial^2 \vec{M}_I^{(2)}}{\partial r^2} dr &= \int_0^1 \vec{\eta}_k \cdot (\vec{j} \times \vec{a}_m) m dr \\ &\quad + \int_0^1 \vec{\eta}_k \cdot [(x_c - x_I) \vec{k} \vec{j} \cdot \vec{a}_m]^\circ dr \\ &\quad + \int_0^1 \vec{\eta}_k \cdot [(z_0 \vec{i} - x_0 \vec{k} - x_c \vec{k})^\circ \int_r^1 \vec{j} \cdot \vec{a}_m dr]^\circ dr \\ &\quad - \vec{\eta}_k(r_{FA}) \cdot (\delta_{FA_2} \vec{i}_B + \delta_{FA_3} \vec{k}_B) \int_{r_{FA}}^1 \vec{j} \cdot \vec{a}_m dr \\ &= \int_0^1 \vec{\eta}_k \cdot (\vec{j} \times \vec{a}_m) m dr \\ &\quad + [\vec{\eta}_k \cdot \vec{k} (x_c - x_I) \vec{j} \cdot \vec{a}_m] \Big|_{r=1} \\ &\quad - \int_0^1 \vec{\eta}_k \cdot \vec{k} (x_c - x_I) \vec{j} \cdot \vec{a}_m dr \\ &\quad - \int_0^1 \vec{\eta}_k \cdot (z_0 \vec{i} - x_0 \vec{k} - x_c \vec{k})^\circ \int_r^1 \vec{j} \cdot \vec{a}_m dr dr \\ &\quad - \vec{\eta}_k(r_{FA}) \cdot (\delta_{FA_2} \vec{i}_B + \delta_{FA_3} \vec{k}_B) \int_{r_{FA}}^1 \vec{j} \cdot \vec{a}_m dr \end{aligned}$$

Finally, the torsion terms are introduced; the inertia and centrifugal forces directly due to the blade bending motion are extracted; and the fourth term above is again integrated by parts. Thus the inertia force is:

$$\begin{aligned}
 \int_0^l \vec{\eta}_k \cdot \frac{\partial^2 \vec{M}_x^{(2)}}{\partial r^2} dr = & \\
 & \int_0^l \vec{\eta}_k \cdot (z_0 \vec{r} - x_0 \vec{k})''' m dr - \sum \int_0^l \vec{\eta}_k \cdot \left[\int_r^l g m d\theta (z_0 \vec{r} - x_0 \vec{k})'' \right] dr \\
 & - \int_0^l \vec{\eta}_k \cdot \vec{r} \vec{r} m \vec{r} \cdot (z_0 \vec{r} - x_0 \vec{k})''' m dr \\
 & + \int_0^l \vec{\eta}_k \cdot \left[\vec{r} \times \vec{a} - (z_0 \vec{r} - x_0 \vec{k})''' - \sum E_B \vec{r}_B \cdot (x_0 \vec{r} + z_0 \vec{k}) \right] m dr \\
 & + [\vec{\eta}_k \cdot \vec{k} (x_c - x_I) \vec{r} \cdot \vec{a} m] \Big|_{r=1} \\
 & - \int_0^l \vec{\eta}_k \cdot \vec{k} (x_c - x_I) \vec{r} \cdot \vec{a} m dr - [\vec{\eta}_k \cdot \vec{k} x_c] \Big|_{r=0} \int_0^l \vec{r} \cdot \vec{a} m dr \\
 & - 2 \sum \int_0^l (z_0 \vec{r} - x_0 \vec{k} - x_c \vec{k}) \cdot \left\{ \vec{\eta}_k'' \int_r^l (\dot{\psi}_s \vec{r} + E_B \cdot (z_0 \vec{r} - x_0 \vec{k})) m d\theta \right. \\
 & \quad \left. - \vec{\eta}_k' (\dot{\psi}_s r + E_B (z_0 \vec{r} - x_0 \vec{k})) m \right\} dr \\
 & + \sum \int_0^l x_c \vec{k} \cdot \left\{ \vec{\eta}_k'' \int_r^l g m d\theta - \vec{\eta}_k' r m \right\} dr \\
 & - \vec{\eta}_k (r_{FA}) \cdot (E_{FA_2} \vec{r}_B + E_{FA_3} \vec{k}_B) \int_{r_{FA}}^l \vec{r} \cdot \vec{a} m dr \\
 & - \sum \left[\vec{\eta}_k \cdot \vec{r} \hat{\Theta} (x_c - x_I) m \right] \Big|_{r=1} \\
 & + \sum \int_0^l \vec{\eta}_k \cdot \vec{r} \hat{\Theta} (x_c - x_I) r m dr + \sum \left[\vec{\eta}_k \cdot \vec{r} \hat{\Theta} x_c \right] \Big|_{r=0} \int_0^l r m dr \\
 & + \sum \int_0^l \sum_{k=0}^m \rho_k (\vec{r} \times \vec{X}_k) \cdot \left\{ \vec{\eta}_k'' \int_r^l g m d\theta - \vec{\eta}_k' r m \right\} dr
 \end{aligned}$$

The structural moment (from section 2.1.5) is

$$\begin{aligned}
 \int_0^l \vec{\eta}_k \cdot \frac{\partial^2 \vec{M}_E^{(2)}}{\partial r^2} dr = & \\
 & \int_0^l \vec{\eta}_k \cdot [(EI_{zz} \vec{r}^2 + EI_{xx} \vec{k} \vec{k}) (z_0 \vec{r} - x_0 \vec{k})'''']'' dr \\
 & + \int_0^l \vec{\eta}_k \cdot [(EI_{xp} \vec{k} - EI_{zp} \vec{r}) \theta_m^1 \theta_e^1]'' dr
 \end{aligned}$$

The aerodynamic moment about the tension center ($x = x_C$) at r , due to the blade loading at the elastic axis at station ρ is

$$\begin{aligned}\vec{M}_A &= \int_r^1 (\vec{r} |_{\rho=0} - \vec{r} |_{r=x_C}) \times \vec{F}_{aero} dy \\ &\cong \int_r^1 (y - r) (F_z \vec{i}_B - F_x \vec{k}_B) dy\end{aligned}$$

so

$$\int_0^1 \vec{\eta}_k \cdot \frac{\partial^2 \vec{M}_A}{\partial r^2} dr = \int_0^1 \vec{\eta}_k \cdot (F_z \vec{i}_B - F_x \vec{k}_B) dr$$

2.2.8 Elastic torsion equation.- The equation of motion for elastic torsion is obtained from

$$-\int_0^1 \vec{\eta}_k \frac{\partial M_{r_z}}{\partial r} dr - \int_0^1 \vec{\eta}_k \frac{\partial M_{r_E}}{\partial r} dr = - \int_0^1 \vec{\eta}_k \frac{\partial M_A}{\partial r} dr$$

where \vec{M} is the moment about the elastic axis at r , and

$$\frac{\partial}{\partial r} M_r = \frac{\partial}{\partial r} \vec{\eta}_k \cdot \vec{M} = \vec{\eta} \cdot \frac{\partial \vec{M}}{\partial r} + [(x_0 \vec{i} + z_0 \vec{k})^\circ \cdot \vec{M}]'$$

The inertial moment is

$$\begin{aligned}\vec{M}_I &= \int_r^1 \int_{\text{section}} (\vec{r} |_{\rho=x} - \vec{r} |_{\rho=0}) \times \vec{a} dm dy \\ &= \int_r^1 \int [(y - r) \vec{j} + (x_0 + x) \vec{i} + (z_0 + z) \vec{k}] \times \vec{a} dm dy \\ &\quad - (x_0 \vec{i} + z_0 \vec{k}) |_r\end{aligned}$$

so

$$\frac{\partial \tilde{M}}{\partial r} = -(\vec{j} + (x_0 \vec{i} + z_0 \vec{k})') \times \int_r^1 \vec{a} m dr - \int_r^1 (x_0 \vec{i} + z_0 \vec{k}) \times \vec{a} m dr$$

$$\begin{aligned} \frac{\partial M_{rx}}{\partial r} &= \int_r^1 ((x_0 \vec{i} - z_0 \vec{k}) \cdot \vec{a} m dr - (z_0 \vec{i} - x_0 \vec{k})' \cdot \int_r^1 (r - r) \vec{a} m dr) \\ &\quad - (x_0 \vec{i} + z_0 \vec{k})' \cdot (x_0 \vec{k}) \vec{j} \cdot \vec{a} m \\ &\quad - (x_0 \vec{i} + z_0 \vec{k})'' \cdot \int_r^1 [z_0 \vec{i} - x_0 \vec{k} - x_0 \vec{k} \\ &\quad - (z_0 \vec{i} - x_0 \vec{k})] \vec{j} \cdot \vec{a} m dr \end{aligned}$$

Operating with $\int_{r_{FA}}^1 \xi_k (\dots) dr$ and changing the order of the ρ and r integrations in the second term gives

$$\begin{aligned} \int_{r_{FA}}^1 \int_{\rho} \frac{\partial M_{rx}}{\partial r} dr &= \int_{r_{FA}}^1 \vec{x}_k \cdot \vec{a} m dr \\ &\quad + \int_{r_{FA}}^1 \int_{\rho} \vec{\xi}_k (x_0 \vec{i} - z_0 \vec{k} - x_0 \vec{k}) \cdot \vec{a} m dr dr \\ &\quad - \int_{r_{FA}}^1 \int_{\rho} \vec{\xi}_k (x_0 \vec{i} + z_0 \vec{k})' \cdot (x_0 \vec{k}) \vec{j} \cdot \vec{a} m dr dr \\ &\quad - \int_{r_{FA}}^1 \int_{\rho} \vec{\xi}_k (x_0 \vec{i} + z_0 \vec{k})'' \cdot \int_r^1 [z_0 \vec{i} - x_0 \vec{k} - x_0 \vec{k} \\ &\quad - (z_0 \vec{i} - x_0 \vec{k})] \vec{j} \cdot \vec{a} m dr dr \end{aligned}$$

where

$$\vec{X}_k = \vec{\gamma}_k \times \vec{x}_k - \int_{r_{FA}}^r \vec{\gamma}_k (z_0 \vec{i} - x_0 \vec{k})'' (r - \rho) d\rho$$

Finally, introducing the torsion terms by expanding the unit vectors, the inertia force is:

$$\begin{aligned}
 - \int_{r_{FA}}^r \vec{\gamma}_k \frac{\partial M_{xz}}{\partial r} dr &= \int_{r_{FA}}^r \vec{\gamma}_k \ddot{\theta} I_\theta dr + \sum^2 \int_{r_{FA}}^r \vec{\gamma}_k I_\theta \cos \theta \sin \theta dr \\
 &\quad + \sum^2 \int_{r_{FA}}^r \vec{\gamma}_k I_\theta \tilde{\theta} (\cos^2 \theta - \sin^2 \theta) dr \\
 &\quad - \int_{r_{FA}}^r \vec{X}_k \cdot \vec{a} m dr \\
 &\quad - \sum^2 \int_{r_{FA}}^r \vec{\gamma}_k (x_0 \vec{i} + z_0 \vec{k})' \cdot (x_0 \vec{i}) r m dr \\
 &\quad - \sum^2 \int_{r_{FA}}^r \vec{\gamma}_k (x_0 \vec{i} + z_0 \vec{k})'' \cdot \int_r^1 [z_0 \vec{i} - x_0 \vec{k} - x_0 \vec{i} \\
 &\quad \quad \quad - (z_0 \vec{i} - x_0 \vec{k})] r] g m dr
 \end{aligned}$$

Where $I_\theta = \int (x^2 + z^2) dm$ is the section pitch moment of inertia, about the elastic axis. In the centrifugal acceleration we have neglected a number of terms due to the blade torsion motion which are the same order as the propeller moment, but which are normally much smaller than the structural moment.

With the centrifugal tension $T = \Omega^2 \int_r^1 \rho m dr$, the structural moment (from section 2.1.5) is:

$$\begin{aligned}
 - \int_{r_{FA}}^l \vec{\beta}_x \frac{\partial M_{re}}{\partial r} dr &= - \int_{r_{FA}}^l \vec{\beta}_x (GJ\theta_e')' dr \\
 &\quad + \int_{r_{FA}}^l \vec{\beta}_k' k_p^2 \Omega^2 \int_r^l g m dr (\theta_{rw}' + \theta_e') dr \\
 &\quad - \int_{r_{FA}}^l \vec{\beta}_x [\partial_{rw}^{iz} EI_{pp} \theta_e']' dr \\
 &\quad - \int_{r_{FA}}^l \vec{\beta}_x [\theta_{rw}' (EI_{xp}\vec{k} - EI_{zp}\vec{k}) \\
 &\quad \quad \quad (z_o\vec{r} - x_o\vec{R})"]' dr
 \end{aligned}$$

Finally, the aerodynamic moment about the elastic axis at r is

$$\vec{M}_A = \int_r^l M_a \vec{\beta}_{xs} dg + \int_r^l [(g-r)\vec{f} + (x_o\vec{r} + z_o\vec{R}) \\
 \quad \quad \quad -(x_o\vec{r} + z_o\vec{R})]_r \vec{F}_{aero} dg$$

so

$$\frac{\partial \vec{M}_A}{\partial r} = -M_a \vec{\beta}_{xs} - \vec{\beta}_{xs} \times \int_r^l (F_x \vec{t}_8 + F_z \vec{k}_8) dg$$

$$\begin{aligned}
 \frac{\partial M_{re}}{\partial r} &= \vec{\beta}_{xs} \cdot \frac{\partial \vec{M}_A}{\partial r} + (x_o\vec{r} + z_o\vec{R})'' \cdot \vec{M}_A \\
 &= -M_a - (z_o\vec{r} - x_o\vec{R})'' \cdot \int_r^l (g-r)(F_x \vec{t}_8 + F_z \vec{k}_8) dg
 \end{aligned}$$

Hence

$$-\int_{r_{FA}}^l \vec{\tau}_k \frac{\partial M_{FA}}{\partial r} dr = \int_{r_{FA}}^l \vec{\tau}_k M_a dr - \int_{r_{FA}}^l \vec{X}_{A_k} \cdot (\vec{F}_x \vec{i}_x + \vec{F}_z \vec{i}_z) dr$$

where

$$\vec{X}_{A_k} = - \int_{r_{FA}}^r \vec{\tau}_k (z_0 \vec{i} - x_0 \vec{k})'' (r-g) dg$$

2.2.9 Rigid pitch equation.- The equation of motion for rigid pitch is obtained from $M_{FAI} + M_{FAE} = M_{FAA}$, where

$$M_{FA} = \hat{e}_{FA} \cdot \vec{M} = [\vec{f}_{FA} + (x_0 \vec{i} + z_0 \vec{k})' \Big|_{r_{FA}} - \delta_{FA4} \vec{i}_B + \delta_{FA5} \vec{k}_B] \cdot \vec{M}$$

and \vec{M} is the moment about the feathering axis at $r = r_{FA}$. The inertia moment is

$$\begin{aligned} \vec{M}_I &= \int_{r_{FA}}^l \left\{ \text{Section } (\vec{r})_{r \times z} - \vec{r} \Big|_{r_{FA} \infty} \right\} \times \vec{a} dm dr \\ &= \int_{r_{FA}}^l \left\{ [(r-r_{FA}) \vec{j} + (x_0+x) \vec{i} + (z_0+z) \vec{k}] - (x_0 \vec{i} + z_0 \vec{k}) \Big|_{r_{FA}} \right\} \times \vec{a} dm dr \end{aligned}$$

So

$$\begin{aligned} M_{FAI} &= - \int_{r_{FA}}^l \vec{X}_o \cdot \vec{a} m dr - \int_{r_{FA}}^l \left\{ (x_k^2 - x_z^2 - z_t^2) \cdot \vec{a} \right\} dm dr \\ &\quad + \int_{r_{FA}}^l \left[(- (x_0 \vec{i} + z_0 \vec{k})' \Big|_{r_{FA}} - \delta_{FA5} \vec{i}_B + \delta_{FA4} \vec{k}_B) \cdot \right. \\ &\quad \quad \left. (z_0 \vec{i} - x_0 \vec{k} - x_z \vec{k} - (z_0 \vec{i} - x_0 \vec{k})) \Big|_{r_{FA}} \right] \\ &\quad + (\delta_{FA3} \vec{i}_B - \delta_{FA2} \vec{k}_B) \cdot \\ &\quad \quad (z_0 \vec{i} - x_0 \vec{k} - x_z \vec{k}) \Big] \vec{a} \cdot \vec{a} m dr \end{aligned}$$

where

$$\vec{X}_o = -(z_0 \vec{i} - x_0 \vec{j} - x_I \vec{k}) + ((\delta_{FA_2} - \delta_{FA_4}) \vec{i}_B + (\delta_{FA_3} - \delta_{FA_5}) \vec{k}_B) (r - r_{FA}) \\ + (z_0 \vec{i} - x_0 \vec{k})|_{r_{FA}} + (z_0 \vec{i} - x_I \vec{k})'|_{r_{FA}} (r - r_{FA})$$

Introducing the torsion terms by expanding the unit vectors, the inertia force is

$$M_{FA_I} = \int_{r_{FA}}^r \ddot{\theta} I_{\theta} dr + \Sigma^2 \int_{r_{FA}}^r I_{\theta} \sin \theta \cos \theta dr \\ + \Sigma^2 \int_{r_{FA}}^r I_{\theta} \dot{\theta} (\cos^2 \theta - \sin^2 \theta) dr - \int_{r_{FA}}^r \vec{X}_o \cdot \vec{a}_m dr \\ - \Sigma^2 \int_{r_{FA}}^r [(-(x_0 \vec{i} + z_0 \vec{k})'|_{r_{FA}} - \delta_{FA_5} \vec{i}_B + \delta_{FA_4} \vec{k}_B) \\ (z_0 \vec{i} - x_0 \vec{k} - x_I \vec{k} - (z_0 \vec{i} - x_0 \vec{k})|_{r_{FA}}) \\ + (\delta_{FA_3} \vec{i}_B - \delta_{FA_2} \vec{k}_B) \\ (z_0 \vec{i} - x_0 \vec{k} - x_I \vec{k})] r m dr$$

The aerodynamic moment about the feathering axis at r_{FA} is

$$\vec{M}_A = \int_{r_{FA}}^r M_a \vec{j} \times s dr + \int_{r_{FA}}^r [(r - r_{FA}) \vec{j} + (x_0 \vec{i} + z_0 \vec{k}) \\ - (x_0 \vec{i} + z_0 \vec{k})|_{r_{FA}}] \times \vec{F}_{aero} dr$$

So

$$M_{FAA} = \int_{r_{FA}}^r M_a dr - \int_{r_{FA}}^r (F_x \vec{i}_B + F_z \vec{k}_B) \cdot \vec{X}_{A_0} dr$$

where

$$\vec{X}_{A_0} = \vec{X}_o - x_I \vec{k}$$

The aerodynamic and inertial moments about the feathering axis are reacted by moments due to the deformation of the control system. The restoring moment acting on the blade, about the feathering axis, is $-M_{\text{con}}$. It is given by the product of the elastic deformation in the control system, and the control system stiffness K_θ :

$$M_{\text{con}} = K_\theta (p_o - p_r)$$

where the rigid pitch p_r consists of the kinematic coupling and the blade commanded pitch angle:

$$\begin{aligned} p_r = & \Theta_K \cos \Psi_m + \Theta_{15} \sin \Psi_m + \Delta \Theta_{\text{gov}} + \Delta \Theta_{\text{mast bend}} \\ & - \sum_i K_{p_i} q_i - K_{p_G} \beta_G + (\Theta_{15} \cos \Psi_m - \Theta_{1c} \sin \Psi_m) \psi_s \end{aligned}$$

The first two terms are the lateral and longitudinal cyclic pitch control inputs; the next terms are feedback from the governor, and kinematic coupling due to the rotor mast bending. The term $-K_{p_i} q_i$ is the kinematic pitch/bending coupling due to the control system and blade root geometry, where q_i is the i-th bending degree of freedom (introduced below). Similarly, K_{p_G} is the pitch/flap coupling for the gimbal or teeter motion. For the rigid flap motion of the blade, this coupling is usually expressed in terms of a delta-three (δ_3) angle, such that $K_p = \tan \delta_3$. Finally, the ψ_s term is the pitch change due to the rotor azimuth perturbation with a fixed swashplate. For rigid control system (K_θ very large) the rigid pitch equation of motion reduces to $p_o = p_r$.

Including control system damping in the restoring moment gives

$$M_{\text{con}} = K_\theta (p_o - p_r) + C_\theta (\dot{p}_o - \dot{p}_r)$$

where C_d is the viscous damping coefficient. For consistency with the elastic torsion equations, the control system stiffness can be written in terms of the nonrotating natural frequency of the blade rigid pitch motion, ω_0 :

$$K_d = \omega_0^2 \int_{r_{FA}}^r I_d dr$$

and the damping coefficient in terms of a structural damping coefficient ζ_s :

$$C_d = \zeta_s \omega_0 \int_{r_{FA}}^r I_d dr$$

Then the structural pitch moment is

$$M_{FA_E} = (\int_{r_{FA}}^r I_d dr) (\omega_0^2 (\rho_0 - \rho_r) + g_s \omega_0 (\dot{\rho}_0 - \dot{\rho}_r))$$

2.2.10 Root force.-The net force of the m-th blade acting on the hub is $\vec{F}^{(m)} = \vec{F}_A - \vec{F}_I$. The inertial force is

$$\vec{F}_I = \int_0^r \vec{a}_m dr$$

and the aerodynamic force is

$$\vec{F}_A = \int_0^r (F_x \vec{i}_s + F_z \vec{j}_s + \tilde{F}_r \vec{k}_s) dr$$

The components of the total hub force in the nonrotating frame are

$$\vec{F} = \sum_{m=1}^N \vec{F}^{(m)} = H \vec{i}_s + Y \vec{j}_s + T \vec{k}_s$$

2.2.11 Root moment.- The net moment of the m-th blade acting on the rotor hub is

$$\vec{M}^{(m)} = \vec{M}_A - \vec{M}_I$$

The inertial moment is

$$\vec{M}_I = \int_0^l \vec{r} \times \vec{a} m dr$$

and the aerodynamic moment is

$$\vec{M}_A = \int_0^l (F_z \vec{r}_B - F_x \vec{k}_B) r dr$$

The components of the total hub moment in the nonrotating frame are

$$\vec{M} = \sum_{m=1}^n \vec{M}^{(m)} = M_x \vec{t}_S + M_y \vec{f}_S - Q \vec{k}_S$$

Note that the \vec{t}_B (torsion) component of the root moment in the rotating frame is neglected compared to the \vec{f}_B (fl.) and \vec{k}_B (lag) components.

The flapwise root moment in the rotating frame gives the pitch and roll moments on the gimbal:

$$M_y = \sum_{m=1}^n f_S \cdot \vec{M}^{(m)} = - \sum_{m=1}^n \cos \psi_m \vec{t}_B \cdot \vec{M}^{(m)}$$

$$M_x = \sum_{m=1}^n f_S \cdot \vec{M}^{(m)} = \sum_{m=1}^n \sin \psi_m \vec{t}_B \cdot \vec{M}^{(m)}$$

The inertial moment is

$$\vec{t}_B \cdot \vec{M}_I = \int_0^l \vec{t}_B \cdot (\vec{r} \times \vec{a}) m dr$$

and the aerodynamic moment is

$$\vec{T}_B \cdot \vec{M}_A = \int_0^R F_z r \, dr$$

2.2.12 Gimbal equation.- The equations of motion for the gimbal degrees of freedom are obtained from the pitch and roll components of the total rotor hub force. Allowing for a gimbal spring and damper in the nonrotating frame reacting the rotor moments, the equations of motion are

$$M_y + C_G \dot{\beta}_{GC} + K_G \beta_{GC} = 0$$
$$- M_x + C_G \dot{\beta}_{GS} + K_G \beta_{GS} = 0$$

The gimbal hub spring and damper constants can be written

$$K_G = \frac{\pi}{2} I_0 \Sigma^2 (\nu_G^2 - 1)$$
$$C_G = \frac{\pi}{2} I_b \Sigma C_G^*$$

Where $I_0 = \int_0^R r^2 m \, dr$ and I_b is a characteristic inertia of the blade, and ν_G is the rotating natural frequency of the gimbal flap motion. To allow for different longitudinal and lateral hub spring rates, ν_{GC} and ν_{GS} can be used for the β_{GC} and β_{GS} equations.

2.2.13 Teeter equation.- The equation of motion for the teeter degree of freedom of a two-bladed rotor is obtained from equilibrium of flap moments about the teeter hinge. Allowing for a teeter spring and damper in the rotating frame, the equation of motion is

$$-2M_T + C_T \dot{\beta}_T + K_T \beta_T = 0$$

C_T and K_T are the damper and spring constants about the teeter hinge. In terms of the natural frequency and damping coefficient, we may write

$$\begin{aligned} C_T &= 2 I_b \sum c_T^* \\ K_T &= 2 I_0 \sum^2 (\gamma_T^2 - 1) \end{aligned}$$

where $I_0 = \int_0^R r^2 m dr$.

The teetering moment M_T is the root flapwise moment from the two blades:

$$2M_T = \sum_{m=1}^2 (-1)^m \vec{t}_b \cdot \vec{M}^{(m)}$$

where again

$$\begin{aligned} \vec{t}_b \cdot \vec{M}_I &= \int_0^l \vec{t}_b \cdot (\vec{r} \times \vec{a}) m dr \\ \vec{t}_b \cdot \vec{M}_A &= \int_0^l F_z r dr \end{aligned}$$

2.2.14 *Modal equations.*— Consider the equilibrium of the elastic, inertial, and centrifugal bending moments. From the results of section 2.2.7 these terms give the following homogeneous equation for bending of the blade:

$$\begin{aligned} &[(EI_{zz}\ddot{z} + EI_{xx}\ddot{x}) (z_0\ddot{z} - x_0\ddot{x})'']'' \\ &- \sum^2 \left[\int_0^l g m dr (z_0\ddot{z} - x_0\ddot{x})' \right]' - \sum_m \sum_n (z_0\ddot{z} - x_0\ddot{x}) \\ &+ m (z_0\ddot{z} - x_0\ddot{x})'' = 0 \end{aligned}$$

This equation may be solved by the method of separation of variables. Writing

$$(z_0 \vec{r} - x_0 \vec{k}) = \vec{\eta}(r) e^{i\omega t}$$

it becomes

$$(EI \vec{\eta}'')'' - \omega^2 [\int r^2 m \omega^2 \vec{\eta}']' - \sum_m \vec{\eta} \cdot \vec{\eta} - m^2 \vec{\eta} = 0$$

This is the modal equation for coupled flap/lag bending of the rotating blade. It is an ordinary differential equation for the mode shape $\vec{\eta}(r)$; this mode may be interpreted as the free vibration of the rotating beam at natural frequency ω .

This modal equation, with the appropriate boundary conditions for a cantilever or hinged blade, is a proper Sturm-Liouville eigenvalue problem. It follows that there exists a series of eigensolutions $\vec{\eta}_k(r)$ of this equation, with corresponding eigenvalues ω_k^2 . The eigensolutions or modes are orthogonal with weighting function m ; so if $i \neq k$,

$$\int_0^1 \vec{\eta}_i \cdot \vec{\eta}_k m dr = 0$$

These modes form a complete series, so it is possible to expand the rotor blade bending as a series in the modes:

$$z_0 \vec{r} - x_0 \vec{k} = \sum_{i=1}^{\infty} q_i(t) \vec{\eta}_i(r)$$

The bending modes are normalized to unit amplitude (dimensionless) at the tip: $|\vec{\eta}_i(1)| = 1$.

Consider the homogeneous equation for the elastic torsion motion of the nonrotating blade, i.e., the balance of structural and inertial torsion moments. The results of section 2.2.8 give

$$-(GJ \theta_e')' + I_\theta \ddot{\theta}_e = 0$$

The equation for the torsion motion of a rotating blade, including centrifugal forces and some additional structural torsion moments could be used instead. For the torsional stiffness typical of rotor blades these terms have little effect however, and the nonrotating torsion modes are an accurate representation of the blade motion. Solving this equation by separation of variables, we write $\theta_e = \xi(r)e^{j\omega t}$, so

$$(GJ\ddot{\xi})' + I_0\omega^2\xi = 0$$

This equation is a proper Sturm-Liouville eigenvalue problem, from which it follows that there exists a series of eigensolutions $\xi_k(r)$, and corresponding eigenvalues ω_k^2 ($k = 1 \dots \infty$). The modes are orthogonal with weighting function I_0 , so if $i \neq k$

$$\int_{r_{FA}}^l \xi_i \xi_j I_0 dr = 0$$

The modes form a complete set, so the elastic torsion of the blade may be expanded as a series in the modes:

$$\theta_e = \sum_{i=1}^{\infty} \rho_i(t) \xi_i(r)$$

These modes are the free vibration shape of the nonrotating blade in torsion, at natural frequency ω_k . The torsion modes are normalized to unity at the tip, $\xi_k(1) = 1$.

2.2.15 Modal expansion. - The bending and torsion motion of the blade is expanded as series in the normal modes. By this means the partial differential equations for the motion (in r and t) are converted to ordinary differential equations (in time only) for the degrees of freedom.

For the bending we write:

$$(z_0\ddot{t} - x_0\ddot{k}) = \sum_{i=1}^{\infty} q_i(t) \vec{\eta}_i(r)$$

where $\vec{\eta}_j$ are the rotating, coupled flap/lag bending modes defined above. These modes are orthogonal and satisfy the modal equation given above. The variables q_j are the degrees of freedom for the bending motion of the blade.

For the blade elastic torsion we write

$$\Theta_e = \sum_{i=1}^{\infty} p_i(t) \xi_i(r)$$

where ξ_i are the nonrotating elastic torsion modes. These modes are orthogonal, and satisfy the modal equation given above. The variables p_i ($i \geq 1$) are the degrees of freedom for the elastic torsion motion of the blade. The degree of freedom for rigid pitch motion is $p_0 = \tilde{\theta}^0 = (\theta^0 - \theta^c) + \theta_{\text{con}}$. For rigid rotation about the feathering axis, the mode shape is simply $\xi_0 = 1$. Thus the total blade pitch perturbation is expanded as the series:

$$\tilde{\Theta} = \sum_{i=0}^{\infty} p_i(t) \xi_i(r)$$

The total blade pitch θ (mean and perturbation) is then:

$$\Theta = \Theta_m + \tilde{\Theta} = (\Theta_{m0} + \Theta_{m1}) + \sum_{i=0}^{\infty} p_i(t) \xi_i(r)$$

The partial differential equation for bending of the blade is obtained from $\frac{\partial^2 M}{\partial r^2}$. The ordinary differential equation for the k -th bending mode (the q_k equation) is then obtained by operating with $\int_0^r \vec{\eta}_k \cdot (...) dr$ (which has already been done in section 2.2.7). The modal equation is used to introduce the bending mode natural frequency into the equation, replacing the structural and centrifugal stiffness terms, and the orthogonality of the bending modes decouples the inertial and spring terms as follows:

$$\begin{aligned}
& \int_0^l \vec{\eta}_k \cdot (z_r - x_{0r})'' m dr - \Sigma^2 \int_0^l \vec{\eta}_k \cdot [\int_r^l g_{rr} (z_r - x_{0r})']' dr \\
& - \int_0^l \vec{\eta}_k \cdot \vec{f} - \Sigma^2 \cdot (z_r - x_{0r}) dr \\
& + \int_0^l \vec{\eta}_k \cdot [(EI_{xx} z_r'' + EI_{zz} z_r'^2) (z_r - x_{0r})''] dr \\
= & \sum_{i=1}^{\infty} q_i \int_0^l \vec{\eta}_k \cdot \vec{\eta}_i m dr \\
& + \sum_{i=1}^{\infty} q_i \left[\int_0^l \vec{\eta}_k \cdot [(EI \vec{\eta}_i'')'' - \Sigma^2 (\int_r^l g_{rr} \vec{\eta}_i')' \right. \\
& \quad \left. - \vec{f}] m dr \cdot \vec{\eta}_i \right] dr \\
= & \sum_{i=1}^{\infty} q_i \int_0^l \vec{\eta}_k \cdot \vec{\eta}_i m dr + \sum_{i=1}^{\infty} q_i \nu_i^2 \int_0^l \vec{\eta}_k \cdot \vec{\eta}_i m dr \\
= & I_{q_k} (\ddot{q}_k + \nu_k^2 q_k)
\end{aligned}$$

where

$$I_{q_k} = \int_0^l \eta_k^2 m dr$$

The partial differential equation for torsion of the blade is obtained from $\partial M_r / \partial r$. The ordinary differential equation for the k-th torsion mode (the p_k equation) is then obtained by operating with $\int_{r_{FA}}^l \xi_k(\dots) dr$ (which has already been done in section 2.2.8). The modal equation is used to replace the structural stiffness term with the torsion mode natural frequency, and the orthogonality of the modes decouples the inertial and spring terms as follows:

$$\begin{aligned}
& \int_{C_F A}^t \ddot{\zeta}_k \partial_e I_d dt - \int_{C_F A}^t \dot{\zeta}_k (\zeta J \partial_e')' dt \\
&= \sum_{i=1}^{\infty} \ddot{p}_i \int_{C_F A}^t \ddot{\zeta}_k \ddot{\zeta}_i I_d dt \\
&\quad - \sum_{i=1}^{\infty} p_i \int_{C_F A}^t \dot{\zeta}_k (\zeta J \dot{\zeta}_i')' dt \\
&= \sum_{i=1}^{\infty} \ddot{p}_i \int_{C_F A}^t \ddot{\zeta}_k \ddot{\zeta}_i I_d dt \\
&\quad + \sum_{i=1}^{\infty} p_i \omega_i^2 \int_{C_F A}^t \ddot{\zeta}_k \ddot{\zeta}_i I_d dt \\
&= I_{p_k} (\ddot{p}_k + \omega_k^2 p_k)
\end{aligned}$$

where

$$I_{p_k} = \int_{C_F A}^t \ddot{\zeta}_k^2 I_d dt$$

2.2.16 Lag damper.- Articulated rotors usually have a lag damper, which has an important influence on the blade loads. Therefore a lag damping term is added to the blade bending equation of motion as follows:

$$\begin{aligned}
& I_{q_k} (\ddot{q}_k + g s^2 k \dot{q}_k + \gamma_k^2 q_k) \\
&+ I_b \sum_{i=1}^{\infty} g e n g \tilde{k}_b \cdot \tilde{\eta}_k'(e) \tilde{k}_b \cdot \tilde{\eta}_i'(e) \dot{q}_i + \dots
\end{aligned}$$

where $g_{\text{lag}} = C_\zeta / I_b \Omega$ and C_ζ is the lag damping coefficient (I_b is a characteristic inertia of the blade, used to normalize the inertial constants as described in the next section). The quantity $\vec{k}_B \cdot \vec{\eta}_k'(e)$ is the slope of the k -th bending mode in the lagwise direction, just outboard of the lag hinge. The manner in which the lag damping enters the equation of motion is obtained by a Galerkin or Rayleigh-Ritz analysis. The lag damper results in a bending moment at the lag hinge. Thus it is necessary to evaluate moments at the blade root by integrating along the span, which has in fact been our practice.

Note that structural damping has also been included in the bending equation, modelled as equivalent viscous damping. The structural damping coefficient g_s (equal to twice the equivalent damping ratio) in general is different for each degree of freedom. Structural damping is included in the torsion equations in a similar manner.

Consider also a nonlinear lag damper, for which the lag moment opposing the motion is proportional to $\dot{\xi}^2$ at low lag velocity (hydraulic damping) and constant at M_{LD} for lag velocity above $\dot{\xi}_{LD}$ (friction damping):

$$M_{\text{eng}} = \frac{M_{LD}}{I_b \dot{\xi}^2} (\text{sign } \dot{\xi}) \min(1, (\dot{\xi}/\dot{\xi}_{LD})^2)$$

where

$$\dot{\xi} = \sum_{i=1}^n \vec{k}_B \cdot \vec{\eta}_i(e) \dot{q}_i$$

Hence the term

$$I_b \vec{k}_B \cdot \vec{\eta}_k(e) (g_{\text{eng}} \dot{\xi} - M_{\text{eng}})$$

is added to the right-hand side of the bending equation. Here linear damping is included on the left-hand side still, but only to improve the convergence of the solution; so the $C_\zeta \dot{\xi}$ term must be subtracted from M_{lag} .

2.2.17 *Gravitational forces*. - The acceleration due to gravity is $\vec{g} = g\vec{k}_E = gR_{SF}\vec{k}_E$, where g is the gravitational constant, \vec{k}_E is the vertical vector, and R_{SF} is the coordinate transformation matrix between the rotor shaft axes (S frame) and the aircraft body axes (F frame, see section 4.1.2). In terms of the aircraft trim pitch and roll angles, the vertical vector is

$$\vec{k}_E = -\sin\theta_{FT}\vec{i}_f + \cos\theta_{FT}\sin\phi_{FT}\vec{j}_f + \cos\theta_{FT}\cos\phi_{FT}\vec{k}_f$$

(see section 4.1). The gravitational forces acting on the rotor blades may be accounted for by substituting $\vec{a}_o - \vec{g}$ for \vec{a}_o , the hub linear acceleration. Thus the components of \vec{g} in the S frame are subtracted from the components of the hub acceleration in the nonrotating shaft axes:

$$\vec{a}_o = \ddot{x}_s \vec{i}_s + \ddot{y}_s \vec{j}_s + \ddot{z}_s \vec{k}_s$$

2.2.18 *Equations of motion*. - The rotor blade equations of motion are now obtained by substituting for the expansion of the bending and torsion motion as series in the modes of free vibration. Names are given to all the inertial constants. Also, the equations of motion, hub forces and moments, and inertia constants are normalized at this point in the analysis, using the characteristic blade inertia I_b , and the blade lock number $\gamma = \rho acR^4/I_b$ is introduced. (A good choice for this characteristic inertia is $I_b = \int_0^R r^2 m dr$.) The inertia constants are divided by I_b , with this normalization denoted by a superscript "*". The blade equations of motion are divided by I_b . The hub forces and moments are divided by $N I_b$, so they appear in rotor coefficient form. The equations of motion for blade coupled flap/lag bending and for blade rigid pitch/elastic torsion are thus:

$$\begin{aligned}
& \mathcal{I}_{q_k}^* (\ddot{q}_k + q_s \dot{q}_k \dot{q}_k + \dot{q}_k^2 q_k) \\
& + 2 \sum_i (\mathcal{I}_{q_k \dot{q}_i}^* + \sum_j \mathcal{I}_{q_k \dot{q}_i \dot{q}_j}^* q_j) \dot{q}_i \\
& + \sum_i g_{q_k \dot{q}_i} \vec{k}_k \cdot \vec{\eta}_k^i(\omega) \vec{k}_k \cdot \vec{\eta}_i^i(\omega) \dot{q}_i \\
& - \sum_i (S_{q_k \ddot{q}_i}^* + \sum_j S_{q_k \ddot{q}_i \dot{q}_j}^* q_j) \ddot{q}_i - \sum_i (S_{q_k \dot{q}_i}^* + \sum_j S_{q_k \dot{q}_i \dot{q}_j}^* q_j) \dot{q}_i \\
& + \mathcal{I}_{q_k \alpha}^* \cdot \vec{k}_k (\dot{\psi}_s + \dot{\alpha}_z) + \mathcal{I}_{q_k \alpha}^* \cdot \vec{l}_k (\ddot{\beta}_G + \dot{\beta}_G) \\
& + 2 (\mathcal{I}_{q_k \dot{\psi}}^* + \sum_j \mathcal{I}_{q_k \dot{\psi} \dot{q}_j}^* q_j) (\dot{\psi}_s + \dot{\alpha}_z) \\
& - (\mathcal{I}_{q_k \dot{\beta}}^* + \sum_j \mathcal{I}_{q_k \dot{\beta} \dot{q}_j}^* q_j) (\ddot{\theta}_G - \dot{\theta}_G + 2\dot{\beta}_G) \\
& + S_{q_k \vec{l}_k}^* \ddot{x}_k - S_{q_k \vec{l}_k}^* \vec{l}_k (\ddot{x}_k \sin \psi_m - \ddot{y}_k \cos \psi_m) \\
& + \mathcal{I}_{q_k \alpha}^* \cdot \vec{l}_k ((\ddot{\alpha}_x + 2\dot{\alpha}_y) \sin \psi_m - (\ddot{\alpha}_y - 2\dot{\alpha}_x) \cos \psi_m) \\
& = \mathcal{I}_{q_k \dot{\theta}}^* + \vec{k}_k \cdot \vec{\eta}_k^i(\omega) (g_{q_k \dot{\theta}}^i - M_{q_k \dot{\theta}}) + \partial \frac{M_{q_k \alpha \text{ext}}}{\partial \alpha}
\end{aligned}$$

$$\begin{aligned}
& H_{pk}^* (\ddot{p}_k + g_s \omega_k \dot{p}_k + \omega_k^2 p_k) + \sum_i H_{pkp_i}^* p_i + \sum_i I_{pkp_i}^* \ddot{p}_i \\
& - \sum_i (S_{pkq_i}^* + \sum_j S_{pkq_i q_j}^* q_j) \ddot{q}_i - \sum_i (S_{pkq_i}^* + \sum_j S_{pkq_i q_j}^* q_j) q_i \\
& + (I_{pk\alpha}^* + \sum_j I_{pk\alpha q_j}^* q_j) \cdot [\vec{k}_B (\ddot{\psi}_s + \ddot{\alpha}_z) - \vec{k}_B (\ddot{\beta}_G + \ddot{\gamma}_G) \\
& \quad - \vec{k}_B ((\ddot{\alpha}_x + z \ddot{\alpha}_y) \sin \psi_m - (\ddot{\alpha}_y - z \ddot{\alpha}_x) \cos \psi_m)] \\
& + (S_{pk}^* + \sum_j S_{pkq_j}^* q_j) \cdot [-\vec{k}_B \ddot{z}_B - \vec{k}_B (\ddot{x}_B \sin \psi_m - \ddot{y}_B \cos \psi_m)] \\
& = H_{pk0}^* + I_{po}^* \vec{z}_k(c_R) (\omega_s^2 p_r + \omega_0 g_s \dot{p}_r) + \delta \frac{M_{pk\text{aero}}}{ac}
\end{aligned}$$

The inertia constants are defined in section 2.2.19.

In rotor coefficient form, the rotor hub force and moment are

$$\begin{aligned}
\frac{1}{2} \frac{H}{H_B} &= \gamma \left(\frac{C_f}{\sigma a} \vec{z}_s + \frac{C_f}{\sigma a} \vec{f}_s + \frac{C_f}{\sigma a} \vec{k}_s \right) \\
&= \frac{1}{2} \sum_{m=1}^2 \frac{\vec{F}^{(m)}}{H_B} \\
&= \frac{1}{2} \sum_{m=1}^2 \gamma \left(\frac{C_{fx}}{\sigma a} \vec{z}_s + \frac{C_{fx}}{\sigma a} \vec{f}_s + \frac{C_{fx}}{\sigma a} \vec{k}_s \right)
\end{aligned}$$

$$\begin{aligned}
\frac{1}{2} \frac{M}{H_B} &= \gamma \left(\frac{C_{my}}{\sigma a} \vec{z}_s + \frac{C_{my}}{\sigma a} \vec{f}_s - \frac{C_a}{\sigma a} \vec{k}_s \right) \\
&= \frac{1}{2} \sum_{m=1}^2 \frac{\vec{M}^{(m)}}{H_B} \\
&= \frac{1}{2} \sum_{m=1}^2 \gamma \left(\frac{C_{my}}{\sigma a} \vec{z}_s - \frac{C_{my}}{\sigma a} \vec{k}_s \right)
\end{aligned}$$

or

$$\begin{bmatrix} \delta \frac{C_{fx}}{\sigma a} \\ \delta \frac{C_{fy}}{\sigma a} \\ \delta \frac{C_T}{\sigma a} \\ \delta \frac{C_{Mx}}{\sigma a} \\ \delta \frac{C_{My}}{\sigma a} \\ -\delta \frac{C_Q}{\sigma a} \end{bmatrix} = \frac{1}{N} \sum_{m=1}^N \begin{bmatrix} \sin \psi_m \cdot \delta \frac{C_{fx}}{\sigma a} + \cos \psi_m \cdot \delta \frac{C_{fr}}{\sigma a} \\ -\cos \psi_m \cdot \delta \frac{C_{fx}}{\sigma a} + \sin \psi_m \cdot \delta \frac{C_{fr}}{\sigma a} \\ \delta \frac{C_{fxz}}{\sigma a} \\ \sin \psi_m \cdot \delta \frac{C_{Mx}}{\sigma a} \\ -\cos \psi_m \cdot \delta \frac{C_{Mx}}{\sigma a} \\ -\delta \frac{C_{Mz}}{\sigma a} \end{bmatrix}$$

So the blade root force and moment are resolved in the nonrotating frame, and then filtered by the hub operator $\frac{1}{N} \sum_{m=1}^N$. The harmonics of the forces in the nonrotating frame can be related directly to the harmonics of the rotating forces; the solution of the support equations of motion requires however the hub forces and moment in the time domain.

The components of the blade root force and moment in the rotating frame are as follows:

$$\delta \frac{C_{fx}}{\sigma a} = (\delta \frac{C_{fx}}{\sigma a})_{aero} - M_b^* (\ddot{x}_h \sin \psi_m - \ddot{y}_h \cos \psi_m) + S_b^* (\dot{\alpha}_z + \dot{\psi}_s) - S_b^* \psi_s + \sum_i S_{qi}^* \cdot \vec{k}_b (\ddot{q}_i - q_i) + I_{fx}^*$$

$$\delta \frac{C_{fr}}{\sigma a} = (\delta \frac{C_{fr}}{\sigma a})_{aero} - M_b^* (\ddot{x}_h \cos \psi_m + \ddot{y}_h \sin \psi_m) + 2 S_b^* (\dot{\alpha}_z + \dot{\psi}_s) + \sum_i 2 S_{qi}^* \cdot \vec{k}_b \ddot{q}_i + S_b^*$$

$$\delta \frac{C_{xz}}{\sigma_a} = (\delta \frac{C_{xz}}{\sigma_a})_{aero} - M_b^* \ddot{x}_b - S_b^* ((\ddot{\alpha}_x + 2\dot{\alpha}_y) \sin \psi_m - (\ddot{\alpha}_y - 2\dot{\alpha}_x) \cos \psi_m) - S_b^* \ddot{\beta}_G - \sum_i S_{q_i}^* \cdot \vec{k}_B \ddot{q}_i$$

$$\gamma \frac{C_{mx}}{\sigma_a} = (\gamma \frac{C_{mx}}{\sigma_a})_{aero} - S_b^* \ddot{x}_b - I_0^* ((\ddot{\alpha}_x + 2\dot{\alpha}_y) \sin \psi_m - (\ddot{\alpha}_y - 2\dot{\alpha}_x) \cos \psi_m) - I_0^* (\ddot{\beta}_G + \beta_G) - \sum_i I_{q_i}^* \cdot \vec{k}_B (\ddot{q}_i + q_i) - 2 \sum_i (I_{q_0 \ddot{q}_i}^* + \sum_j I_{q_0 \ddot{q}_i; q_j}^* q_j) \cdot \vec{k}_B \ddot{q}_i - 2 (I_{q_0 \ddot{q}_i}^* + \sum_j I_{q_0 \ddot{q}_i; q_j}^* q_j) (\ddot{q}_i + \dot{\alpha}_z) + \sum_i (S_{q_0 \ddot{p}_i}^* + \sum_j S_{q_0 \ddot{p}_i; q_j}^* q_j) \cdot \vec{k}_B (\ddot{p}_i + p_i) - I_{m_x}^*$$

$$\gamma \frac{C_{mz}}{\sigma_a} = (\gamma \frac{C_{mz}}{\sigma_a})_{aero} - S_b^* (\ddot{x}_b \sin \psi_m - \ddot{y}_b \cos \psi_m) + I_0^* (\ddot{\alpha}_z - \dot{\psi}_s) + \sum_i I_{q_i}^* \cdot \vec{k}_B \ddot{q}_i + 2 \sum_i (I_{q_0 \ddot{q}_i}^* + \sum_j I_{q_0 \ddot{q}_i; q_j}^* q_j) \cdot \vec{k}_B \ddot{q}_i - (I_{q_0 \ddot{p}_i}^* + \sum_j I_{q_0 \ddot{p}_i; q_j}^* q_j) (\ddot{p}_i - p_i + 2\dot{\beta}_G) - \sum_i (S_{q_0 \ddot{p}_i}^* + \sum_j S_{q_0 \ddot{p}_i; q_j}^* q_j) \cdot \vec{k}_B \ddot{p}_i$$

The inertia constants are defined in section 2.2.19.

Note that the total hub forces due to the rotor linear acceleration are simply

$$\Delta \begin{pmatrix} \delta \frac{C_H}{g_a} \\ \delta \frac{C_X}{g_a} \\ \delta \frac{C_T}{g_a} \end{pmatrix} = \frac{1}{2} \sum_{m=1}^n M_b^* \begin{pmatrix} -\ddot{x}_m \\ -\ddot{y}_m \\ -\ddot{z}_m \end{pmatrix}$$

where M_b^* is the normalized mass of a blade. Since the rotor mass is included in the aircraft mass, these hub linear acceleration terms should be omitted when C_{fx} , C_{fr} , and C_{fz} are evaluated for the aircraft equations of motion. These terms should be retained however when evaluating the actual blade root forces.

Similarly, since the rotor weight is included in the aircraft weight, the corresponding gravitational force terms are omitted.

Dividing by $(1/2)NI_b$, the gimbal equations of motion are

$$\gamma \frac{2C_{My}}{\sigma_a} + C_G^* \dot{\beta}_{GC} + I_0^* (\gamma_{GC}^* - 1) \beta_{GC} = 0$$

$$-\gamma \frac{2C_{Mx}}{\sigma_a} + C_G^* \dot{\beta}_{GS} + I_0^* (\gamma_{GS}^* - 1) \beta_{GS} = 0$$

where

$$\gamma \frac{2C_{M\gamma}}{\sigma a} = - \frac{1}{2} \sum_{m=1}^2 2 \cos \psi_m \delta \frac{C_{mx}}{\sigma a}$$

$$\gamma \frac{2C_{Mx}}{\sigma a} = - \frac{1}{2} \sum_{m=1}^2 2 \sin \psi_m \delta \frac{C_{mx}}{\sigma a}$$

Dividing by NI_b , the teetering equation of motion is

$$-\gamma \frac{C_{M\tau}}{\sigma a} + C_\tau^* \dot{\beta}_\tau + H_0^* (\dot{\gamma}_\tau^2 - 1) \beta_\tau = 0$$

where

$$\gamma \frac{C_{M\tau}}{\sigma a} = \frac{1}{2} \sum_{m=1}^2 (-1)^m \delta \frac{C_{mx}}{\sigma a}$$

The equation of motion for the rotor speed perturbation $\dot{\psi}_s$ is obtained from equilibrium of the rotor torque. The speed perturbations of the two rotors are coupled by the helicopter transmission, so the equation of motion for $\dot{\psi}_s$ is best derived with the body equations.

Finally, the aerodynamic forces required for the blade equations of motion and the rotor hub reactions are as follows:

$$\frac{M_{q_k \text{aero}}}{ac} = \int_0^1 \vec{\eta}_k \cdot \left(\frac{F_z}{ac} \vec{t}_B - \frac{F_x}{ac} \vec{k}_B \right) dr$$

$$\frac{M_{p_k \text{aero}}}{ac} = \int_{r_{FA}}^1 \vec{\eta}_k \cdot \frac{M_a}{ac} dr - \int_{r_{FA}}^1 \vec{X}_{A_k} \cdot \left(\frac{F_x}{ac} \vec{t}_B + \frac{F_z}{ac} \vec{k}_B \right) dr$$

$$\left(\frac{C_{mz}}{\sigma a}\right)_{aero} = \int_0^1 \frac{F_z}{ac} r dr$$

$$\left(\frac{C_{mx}}{\sigma a}\right)_{aero} = \int_0^1 \frac{F_x}{ac} r dr$$

$$\left(\frac{C_{fx}}{\sigma a}\right)_{aero} = \int_0^1 \frac{F_x}{ac} dr$$

$$\left(\frac{C_{fr}}{\sigma a}\right)_{aero} = \int_0^1 \frac{F_r}{ac} dr$$

$$\left(\frac{C_{fz}}{ac}\right)_{aero} = \int_0^1 \frac{F_z}{ac} dr$$

2.2.19 *Inertial constants.* - The normalized inertial constants required for the blade equations of motions and the hub reactions given above are defined as follows:

$$M_b^* = \frac{1}{I_b} \int_0^1 m dr$$

$$S_b^* = \frac{1}{I_b} \int_0^1 r m dr$$

$$T_b^* = \frac{1}{I_b} \int_0^1 r^2 m dr$$

$$I_{\eta_k}^* = \frac{1}{I_b} \int_0^1 \eta_k^2 m dr$$

$$S_{\eta_k}^* = \frac{1}{I_b} \int_0^1 \vec{\eta}_k m dr$$

$$I_{\eta_k \alpha}^* = \frac{1}{I_b} \int_0^1 \vec{\eta}_k r m dr$$

$$I_{\eta_k \dot{\eta}_i}^* = \frac{1}{I_b} \left\{ \begin{array}{l} \int_0^1 \vec{\eta}_k \cdot (\vec{\jmath} \times \vec{\eta}_i) (\delta_{FA_1} - \delta_{FA_2}) m dr \\ - \vec{\eta}_k \cdot \vec{k} (x_c - x_i) \vec{k}_B \cdot \vec{\eta}_i m |_{r=1} \\ + \int_0^1 \vec{\eta}_k \cdot \vec{k} (-x_i) \vec{k}_B \cdot \vec{\eta}_i m dr \\ + \vec{\eta}_k \cdot \vec{k} \times |_{r=c} \int_0^1 \vec{k}_B \cdot \vec{\eta}_i m dr \\ + \int_0^1 x_c \vec{k} \cdot (\vec{\eta}_k'' \int_r^1 \vec{k}_B \cdot \vec{\eta}_i m dr) dr \\ + \vec{\eta}_k (r_{FA}) \cdot (\delta_{FA_2} \vec{k}_B + \delta_{FA_3} \vec{k}_B) \int_{r_{FA}}^1 \vec{k}_B \cdot \vec{\eta}_i m dr \\ - \vec{\eta}_i \cdot \vec{k} \times |_{r=c} \int_0^1 \vec{k}_B \cdot \vec{\eta}_k m dr \\ - \int_0^1 x_I \vec{k} \cdot (\vec{\eta}_i'' \int_r^1 \vec{k}_B \cdot \vec{\eta}_k m dr - \vec{\eta}_i' \vec{k}_B \cdot \vec{\eta}_k m) dr \end{array} \right.$$

$$I_{q_k \dot{q}_i \dot{q}_j}^* = \frac{1}{I_b} \left\{ - \int_0^1 \vec{\eta}_k \cdot \vec{k}_B \int_0^r \vec{\eta}'_i \cdot \vec{\eta}'_j \, dr \, m \, dr \right. \\ \left. + \int_0^1 \vec{\eta}'_i \cdot \vec{k}_B \int_0^r \vec{\eta}_k \cdot \vec{\eta}'_j \, dr \, m \, dr \right.$$

$$I_{q_k \dot{q}}^* = \frac{1}{I_b} \left\{ \int_0^1 \vec{\eta}_k \cdot [\vec{t}_B \times (\delta_{FA_1} - \delta_{FA_2}) \right. \\ \left. - \vec{k}_B (x_{FA} + r_{FA} \delta_{FA_3} - x_i \cos \theta)] \, m \, dr \right. \\ \left. - \vec{\eta}_k \cdot \vec{k} \cdot (x_c - x_i) \, m \, |_{r=1} \right. \\ \left. + \int_0^1 \vec{\eta}'_k \cdot \vec{k} \cdot (-x_i) \, r \, m \, dr \right. \\ \left. + \vec{\eta}'_k \cdot \vec{k} \cdot x_c \, |_{r=1} \int_0^1 r \, m \, dr \right. \\ \left. + \int_0^1 x_c \cdot \vec{k} \cdot (\vec{\eta}''_k \int_r^1 g \, m \, dr) \, dr \right. \\ \left. + \vec{\eta}_k \cdot (r_{FA}) \cdot (\delta_{FA_2} \vec{t}_B + \delta_{FA_3} \vec{k}_B) \int_{r_{FA}}^1 r \, m \, dr \right\}$$

$$I_{q_k \dot{q}_i \dot{q}_j}^* = \frac{1}{I_b} \left\{ - \int_0^1 \vec{\eta}_k \cdot \vec{k}_B \vec{\eta}_j \cdot \vec{k}_B \, m \, dr \right. \\ \left. + \int_0^1 r \int_0^r \vec{\eta}'_k \cdot \vec{\eta}'_j \, dr \, m \, dr \right\}$$

$$I_{q_k \dot{q}_i \dot{q}_j}^* = \frac{1}{I_b} \int_0^1 \vec{\eta}_k \cdot \vec{k}_B (-\bar{x}_{FA} + r \delta_{FA_1} - (r - r_{FA}) \delta_{FA_2} - x_i \sin \theta) \, m \, dr$$

$$I_{q_k \dot{q}_i \dot{q}_j}^* = \frac{1}{I_b} \int_0^1 \vec{\eta}_k \cdot \vec{k}_B \vec{\eta}_j \cdot \vec{t}_B \, m \, dr$$

$$S_{q_k p_i}^* = \frac{1}{I_b} \int_{r_{FA}}^l \vec{\eta}_k \cdot [\vec{\beta}_i \times \vec{\tau} + \vec{\beta}_i(r_{FA}) (r - r_{FA}) (\vec{k}_B (\delta_{FA_3} - \delta_{FA_5}) - \vec{k}_B (\delta_{FA_2} - \delta_{FA_4}))] dr$$

$$S_{q_k p_i q_j}^* = \frac{1}{I_b} \int_{r_{FA}}^l \vec{\eta}_k \cdot (\vec{\beta} \times \vec{X}_{ij}) dr$$

$$S_{q_k p_i}^* = \frac{1}{I_b} \left\{ \begin{array}{l} - \int_0^l \vec{\eta}_k \cdot [(EI_{x_F} \vec{k} - EI_{z_F} \vec{l}) \partial_r \vec{\beta}_i] dr \\ + \int_{r_{FA}}^l \vec{\eta}_k \cdot \vec{k}_B [\vec{\beta}_i \times \sin \theta \\ + \vec{\beta}_i(r_{FA}) (r - r_{FA}) (\delta_{FA_2} - \delta_{FA_4})] dr \\ - \int_{r_{FA}}^l \vec{\beta}_i(r_{FA}) (r - r_{FA}) [\vec{k}_B (\delta_{FA_3} - \delta_{FA_5}) \\ - \vec{k}_B (\delta_{FA_2} - \delta_{FA_4})] \cdot \\ [\vec{\eta}_k \cdot \{ \int_r^l g_m dr - \vec{\eta}_k \cdot r_m \}] dr \\ + \vec{\eta}_k \cdot \vec{\tau} \vec{\beta}_i (x_c - x_z) m |_{r=1} \\ - \int_{r_{FA}}^l \vec{\eta}_k \cdot \vec{\tau} \vec{\beta}_i (-x_z) r_m dr \\ - (\vec{\beta}_i \vec{\eta}_k \cdot \vec{\tau} x_c) |_{r=r_{FA}} \int_{r_{FA}}^l r_m dr \\ - \int_{r_{FA}}^l \vec{\beta}_i x_c \vec{\tau} \cdot (\vec{\eta}_k \cdot \{ \int_r^l g_m dr \}) dr \end{array} \right.$$

$$S_{q_k p_i q_j}^* = \frac{1}{I_b} \left\{ \begin{array}{l} \int_{r_{FA}}^l \vec{\eta}_k \cdot \vec{k}_B \vec{\tau}_B \cdot \vec{X}_{ij} dr \\ - \int_{r_{FA}}^l (\vec{\beta} \times \vec{X}_{ij}) \cdot (\vec{\eta}_k \cdot \{ \int_r^l g_m dr - \vec{\eta}_k \cdot r_m \}) dr \end{array} \right.$$

$$I_{q_k^0}^* = \frac{1}{I_b} \left\{ \begin{array}{l} - \int_0^1 \vec{\eta}_k \cdot [\vec{k}_B (-x_{FA} - r_{FA}\delta_{FA_3} + x_I \cos \theta) \\ \quad + \vec{r}_B \cdot (\delta_{FA_1} - \delta_{FA_2})] m dr \\ + \vec{\eta}_k \cdot \vec{k} (x_c - x_I) m \Big|_{r=1} \\ - \int_0^1 \vec{\eta}_k' \cdot \vec{k} (-x_I) r m dr \\ - \vec{\eta}_k' \cdot \vec{k} x_c \Big|_{r=c} \int_c^1 r m dr \\ - \int_0^1 x_c \vec{k} \cdot (\vec{\eta}_k'' \int_r^1 g m dy) dr \\ - \vec{\eta}_k (r_{FA}) \cdot (\delta_{FA_2} \vec{r}_B + \delta_{FA_3} \vec{k}_B) \int_{r_{FA}}^1 r m dr \end{array} \right.$$

$$I_{q_i \dot{q}_i}^* = \frac{1}{I_b} \left\{ \begin{array}{l} \vec{k}_B \int_0^1 \vec{k}_B \cdot \vec{\eta}_i (-z_{FA} + r \delta_{FA_1} - (r - r_{FA}) \delta_{FA_2} - x_I \sin \theta) m dr \\ + \vec{k}_B \int_0^1 \vec{k}_B \cdot \vec{\eta}_i (x_{FA} + r_{FA} \delta_{FA_3} - x_I \cos \theta) m dr \\ - \vec{k}_B \int_0^1 r \vec{\eta}_i \cdot \vec{r}_B (\delta_{FA_1} - \delta_{FA_2}) m dr \\ - \vec{k}_B \vec{\eta}_i' \cdot \vec{k} x_I \Big|_{r=c} \int_c^1 r m dr \\ - \vec{k}_B \int_0^1 x_I \vec{k} \cdot (\vec{\eta}_i'' \int_r^1 g m dy - \vec{\eta}_i' r m) dr \end{array} \right.$$

$$I_{q_i \dot{q}_i q_j}^* = \frac{1}{I_b} \int_0^1 [\vec{k}_B \cdot \vec{\eta}_i \vec{\eta}_j m \\ + \vec{k}_B \vec{\eta}_j \cdot (\vec{\eta}_i'' \int_r^1 g m dy - \vec{\eta}_i' r m)] dr$$

$$I_{q_i \dot{q}_i}^* = \frac{1}{I_b} \int_0^1 r (-z_{FA} + r \delta_{FA_1} - (r - r_{FA}) \delta_{FA_2} - x_I \sin \theta) m dr$$

$$I_{q_i \dot{q}_i q_j}^* = \frac{1}{I_b} \int_0^1 r \vec{k}_B \cdot \vec{\eta}_j m dr$$

$$I_{q_0 \dot{p}}^* = \frac{1}{I_b} \int_0^1 r (-z_{FA} + r \delta_{FA_1} - (r - r_{FA}) \delta_{FA_2} - x_I \sin \theta) m dr$$

$$I_{q_0 \dot{p} q_j}^* = \frac{1}{I_b} \int_0^1 r \vec{t}_B \cdot \vec{\eta}_j m dr$$

$$S_{q_0 \dot{p}_i}^* = \frac{1}{I_b} \int_{r_{FA}}^1 [\ddot{z}_i x_I \vec{t} + \ddot{z}_i (r_{FA}) (r - r_{FA}) [\vec{t}_B (\delta_{FA_3} - \delta_{FA_5}) - \vec{k}_B (\delta_{FA_2} - \delta_{FA_4})]] r m dr$$

$$S_{q_0 \dot{p}_i q_i}^* = \frac{1}{I_b} \int_{r_{FA}}^1 \vec{J} \times \vec{X}_{ij} r m dr$$

$$I_{\dot{x}_0}^* = \frac{1}{I_b} \int_0^1 (-x_{FA} + (r - r_{FA}) \delta_{FA_3} + x_I \cos \theta) m dr$$

$$I_{\dot{m}_0}^* = \frac{1}{I_b} \int_0^1 r (-z_{FA} + r \delta_{FA_1} - (r - r_{FA}) \delta_{FA_2} - x_I \sin \theta) m dr$$

$$I_{p_k}^* = \frac{1}{I_b} \int_{r_{FA}}^1 \ddot{z}_k^2 I_\theta dr$$

$$I_{p_k \alpha}^* = \frac{1}{I_b} \int_{r_{FA}}^1 [\ddot{z}_k x_I \vec{t} + \ddot{z}_k (r_{FA}) (r - r_{FA}) (\vec{t}_B (\delta_{FA_2} - \delta_{FA_4}) + \vec{k}_B (\delta_{FA_3} - \delta_{FA_5}))] r m dr$$

$$I_{p_k \alpha q_j}^* = \frac{1}{I_b} \int_{r_{FA}}^1 \vec{X}_{kj} r m dr$$

$$S_{p_k}^* = \frac{1}{I_b} \int_{r_{FA}}^1 [\ddot{z}_k x_I \vec{t} + \ddot{z}_k (r_{FA}) (r - r_{FA}) (\vec{t}_B (\delta_{FA_2} - \delta_{FA_4}) + \vec{k}_B (\delta_{FA_3} - \delta_{FA_5}))] m dr$$

$$S_{p_k q_j}^* = \frac{1}{I_b} \int_{r_{FA}}^1 \vec{X}_{kj} m dr$$

$$I_{pk\ddot{q}_i}^* = \frac{1}{I_b} \int_{r_{FA}}^l [(\ddot{z}_k - \ddot{z}_k(r_{FA})) \ddot{z}_i(r_{FA}) + (\ddot{z}_i - \ddot{z}_i(r_{FA})) \ddot{z}_k(r_{FA})] I_\theta dr$$

$$I_{pk\ddot{q}_i}^* = \frac{1}{I_b} \left\{ \begin{array}{l} \int_{r_{FA}}^l \ddot{z}_k \ddot{z}_i I_\theta (\cos^2 \theta - \sin^2 \theta) dr \\ + \int_{r_{FA}}^l \ddot{z}_k' k_p^2 \int_r^l gmdy \ddot{z}_i' dr \\ - \int_{r_{FA}}^l (\ddot{z}_k - \ddot{z}_k(r_{FA})) [\Theta_{tw}^{12} E I_{pp} \ddot{z}_i']' dr \end{array} \right.$$

$$S_{pk\ddot{q}_i}^* = \frac{1}{I_b} \int_{r_{FA}}^l \vec{q}_i \cdot [\ddot{z}_k \times \vec{x} + \ddot{z}_k(r_{FA})(l - r_{FA}) (\vec{t}_8 (\delta_{FA_3} - \delta_{FA_5}) - (\delta_{FA_2} - \delta_{FA_4}) \vec{t}_8')] m dr$$

$$S_{pk\ddot{q}_i \ddot{q}_j}^* = \frac{1}{I_b} \int_{r_{FA}}^l \vec{x}_{kj} \cdot (-\vec{j} \times \vec{q}_i) m dr$$

$$I_{pk\ddot{q}_o}^* = \frac{1}{I_b} \left\{ \begin{array}{l} - \int_{r_{FA}}^l \ddot{z}_k I_\theta \cos \theta \sin \theta dr \\ + \int_{r_{FA}}^l \ddot{z}_k \times \vec{x} \cos \theta r (\delta_{FA_1} - \delta_{FA_2}) m dr \\ - \int_{r_{FA}}^l \ddot{z}_k' k_p^2 \int_r^l gmdy \Theta_{tw}' dr \end{array} \right.$$

$$S_{pkq_i}^* = \frac{1}{I_b} \left\{ \begin{aligned} & \int_{r_{FA}}^l \dot{\gamma}_k \left[\theta_{tw}^l (EI_{xp}\vec{k} - EI_{zp}\vec{l}) \cdot \vec{\gamma}_i'' \right] dr \\ & + \int_{r_{FA}}^l \dot{\gamma}_k \vec{\gamma}_i' \cdot \vec{l} x_I r m dr \\ & - \int_{r_{FA}}^l \dot{\gamma}_k \vec{\gamma}_i'' \cdot \int_r^l x_I (\vec{k}_B r \cos \theta - \vec{k}_B r \sin \theta) m dr \\ & + \int_{r_{FA}}^l \dot{\gamma}_k x_I \sin \theta \vec{k}_B \cdot \vec{\gamma}_i m dr \\ & - \int_{r_{FA}}^l \dot{\gamma}_k \vec{\gamma}_i'' \cdot \int_r^l (\vec{k}_B (x_{FA} + r_{FA} \delta_{FA_3}) \\ & + \vec{k}_B g (\delta_{FA_1} - \delta_{FA_2})) (g - r) m dr \end{aligned} \right\}$$

$$S_{pkq_i q_j}^* = \frac{1}{I_b} \left\{ \begin{aligned} & \int_{r_{FA}}^l \dot{\gamma}_k \vec{\gamma}_i'' \cdot \vec{l}_B \int_r^l (r \vec{k}_B \cdot \vec{\gamma}_j \\ & - g \vec{k}_B \cdot \vec{\gamma}_j (r)) m dr \\ & - \int_{r_{FA}}^l \dot{\gamma}_k \vec{\gamma}_i'' \cdot \vec{k}_B \int_r^l (\vec{l}_B \cdot \vec{\gamma}_j \\ & - \vec{l}_B \cdot \vec{\gamma}_j (r)) g m dr \end{aligned} \right\}$$

$$S_{pq_i}^* = \frac{1}{I_b} \left\{ \begin{array}{l} \int_{r_{FA}}^l \vec{r} \cdot \vec{\eta}'_i(r_{FA}) x_I r m dr \\ + \int_{r_{FA}}^l \vec{k}_B \cdot \vec{\eta}_i \times \sin \theta m dr \\ + \int_{r_{FA}}^l \vec{t}_B \cdot \vec{\eta}_i (\delta_{FA3} - \delta_{FA5}) r m dr \\ - \int_{r_{FA}}^l \vec{t}_B \cdot \vec{\eta}_i (\delta_{FA2} - \delta_{FA4}) r_{FA} m dr \\ - \int_{r_{FA}}^l (\delta_{FA4} \vec{k}_B - \delta_{FA5} \vec{t}_B) \cdot \vec{\eta}_i(r_{FA}) r m dr \\ + \int_{r_{FA}}^l [(-\vec{\eta}_i + \vec{\eta}_i(r_{FA}) + \vec{\eta}'_i(r_{FA})(r - r_{FA})) \cdot \\ (\vec{t}_B(x_{FA} + r_{FA} \delta_{FA3} - x_I \cos \theta) \\ + \vec{k}_B (\delta_{FA1} - \delta_{FA2}) r)] m dr \end{array} \right.$$

$$S_{pq_i q_j}^* = \frac{1}{I_b} \left\{ \begin{array}{l} \int_{r_{FA}}^l \vec{t}_B \cdot (-\vec{\eta}_i + \vec{\eta}_i(r_{FA}) - \vec{\eta}'_i(r_{FA}) r_{FA}) \\ \quad \vec{k}_B \cdot \vec{\eta}_j m dr \\ + \int_{r_{FA}}^l \vec{t}_B \cdot \vec{\eta}'_i(r_{FA}) \vec{k}_B \cdot \vec{\eta}_j(r_{FA}) r m dr \\ + \int_{r_{FA}}^l \vec{k}_B \cdot \vec{\eta}'_i(r_{FA}) (\vec{t}_B \cdot \vec{\eta}_j \\ \quad - \vec{t}_B \cdot \vec{\eta}_j(r_{FA})) r m dr \end{array} \right.$$

We have used the relation

$$\begin{aligned}
 \vec{x}_k &= \vec{\beta}_k \vec{x}_{\perp k} - \int_{r_{FA}}^r \vec{\beta}_k (z_0 \vec{r} - x_0 \vec{k})'' (r-g) dg \\
 &= \vec{\beta}_k \vec{x}_{\perp k} - \sum_j q_j \int_{r_{FA}}^r \vec{\beta}_k \vec{\eta}_j'' (r-g) dg \\
 &= \vec{\beta}_k \vec{x}_{\perp k} - \sum_j q_j [\vec{\beta}_k \vec{\eta}_j - \int_{r_{FA}}^r \vec{\beta}_k' (\vec{\eta}_j + \vec{\eta}_j' (r-g)) dg]
 \end{aligned}$$

for elastic torsion ($k \geq 1$), and

$$\begin{aligned}
 \vec{x}_0 &= - (z_0 \vec{r} - x_0 \vec{k} - \vec{x}_{\perp k}) \\
 &\quad + ((\delta_{FA2} - \delta_{FA4}) \vec{l}_B + (\delta_{FA3} - \delta_{FA5}) \vec{k}_B) (r-r_{FA}) \\
 &\quad + (z_0 \vec{r} - x_0 \vec{k})|_{r_{FA}} + (z_0 \vec{r} - x_0 \vec{k})'|_{r_{FA}} (r-r_{FA}) \\
 &= \vec{x}_{\perp k} + ((\delta_{FA2} - \delta_{FA4}) \vec{l}_B + (\delta_{FA3} - \delta_{FA5}) \vec{k}_B) (r-r_{FA}) \\
 &\quad - \sum_j q_j [\vec{\eta}_j - \vec{\eta}_j(r_{FA}) - \vec{\eta}_j'(r_{FA})(r-r_{FA})]
 \end{aligned}$$

for rigid pitch ($k = 0$); or for $k \leq 0$

$$\begin{aligned}
 \vec{x}_k &= \vec{\beta}_k \vec{x}_{\perp k} + \vec{\beta}_k (r_{FA}) ((\delta_{FA2} - \delta_{FA4}) \vec{l}_B + (\delta_{FA3} - \delta_{FA5}) \vec{k}_B) (r-r_{FA}) \\
 &\quad + \sum_j \vec{x}_{kj} q_j
 \end{aligned}$$

where

$$\vec{X}_{kj} = \begin{cases} -\vec{\beta}_k \vec{\gamma}_j + \int_{r_{FA}}^r \vec{\beta}'_k (\vec{\gamma}_j + \vec{\gamma}'_j(r-s)) ds & k \geq 1 \\ -\vec{\gamma}_j + \vec{\gamma}_j(r_{FA}) + \vec{\gamma}'_j(r_{FA})(r-r_{FA}) & k=0 \end{cases}$$

Also then,

$$\vec{X}_{Ak} = \vec{\beta}_k(r_{FA}) ((\delta_{FA2} - \delta_{FA4}) \vec{t}_B + (\delta_{FA3} - \delta_{FA5}) \vec{k}_B) (r - r_{FA}) + \sum_j \vec{X}_{kj} q_j$$

for the aerodynamic coefficients.

The blade inertial and structural properties (m , x_I , x_C , EI , I_θ , GJ , etc.) will be defined at a series of radial stations, r_i , with linear variation between.

The blade bending and torsion mode shapes will be evaluated at $M+1$ equidistant radial stations: $r = 0, \Delta r, \dots M\Delta r$ where $\Delta r = 1/M$. The inertial coefficients are then calculated by numerical integration (using the trapezoidal rule) over these radial stations.

A concentrated mass at the blade tip ($r = 1$) will be allowed, with a corresponding center of gravity offset. This tip mass contributes an equivalent distributed mass, as follows:

$$m_e(1) = m(1) + M_{tip} \frac{2}{\Delta r R}$$

$$x_{Ie}(1) = \frac{1}{m_e(1)} (x_I(1)m(1) + x_{Itip} M_{tip} \frac{2}{\Delta r R})$$

$$I_{\theta e}(1) = I_\theta(1) + x_{Itip}^2 M_{tip} \frac{2R}{\Delta r}$$

where Δr is the segment length for numerical integration. Alternatively, the tip mass can be included in the distributed mass directly (to avoid difficulties with the $(x_C - x_I)m$ terms evaluated at $r = 1$).

The total mass of the blade can be specified, so

$$M_b^* = \frac{R^2}{I_b} M_{bl}$$

Alternatively, a point mass can be added at $r = 0$ to account for the weight of the hub.

2.2.20 Aerodynamic spring and damping.- To improve the convergence of the solution for the blade motion, spring and damping forces should be included on the left-hand-side of the equations of motion. The required perturbation aerodynamic forces are:

$$\Delta \frac{M_{q_k} \text{aero}}{\partial c} = \sum_i M_{q_k q_i} \dot{q}_i + M_{q_k \dot{\beta}} \dot{\beta}_G + \sum_i M_{q_k p_i} \dot{p}_i$$

$$\Delta \frac{M_{p_k} \text{aero}}{\partial c} = \sum_i M_{p_k q_i} \dot{q}_i + M_{p_k \dot{\beta}} \dot{\beta}_G + \sum_i M_{p_k \dot{p}_i} \dot{p}_i + \sum_i M_{p_k p_i} \dot{p}_i$$

$$\Delta \left(\frac{C_m}{\partial \alpha} \right) \text{aero} = \sum_i M_{\dot{q}_i} \dot{q}_i + M_{\dot{\beta}} \dot{\beta}_G + \sum_i M_{\dot{p}_i} \dot{p}_i$$

$$\Delta \left(\frac{C_d}{\partial \alpha} \right) \text{aero} = Q_{\dot{\beta}} \dot{\beta}_S + Q_{\dot{\theta}} \Delta \theta_{gover}$$

These terms will be added to both sides of the equations of motion, so they need not be exact values of the damping and spring forces, but only close enough to achieve good convergence (see section 5.1). The damping terms are needed to avoid unrealistic resonant amplification of the harmonics near the natural frequency, and the spring terms help obtain the correct phase of the

response quickly. Following the aeroelastic analysis (section 6.1.4), the following expressions are used for the aerodynamic coefficients.

$$M_{q_k \dot{q}_i} = \int_0^1 \left\{ \vec{\eta}_k \cdot \vec{k}_B \vec{\eta}_i \cdot \vec{k}_B \left[-\frac{1}{2} \frac{r^2}{U} \right] + \vec{\eta}_k \cdot \vec{k}_B \vec{\eta}_i \cdot \vec{k}_B \left[\frac{r}{U} \left(\frac{\lambda}{2} + r \frac{6C_T}{\sigma^2} \right) \right] \right. \\ \left. + \vec{\eta}_k \cdot \vec{k}_B \vec{\eta}_i \cdot \vec{k}_B \left[\frac{r}{U} \left(\frac{\lambda}{2} - \frac{r}{2} \frac{6C_T}{\sigma^2} \right) \right] \right. \\ \left. - \vec{\eta}_k \cdot \vec{k}_B \vec{\eta}_i \cdot \vec{k}_B \left[\frac{1}{2} \frac{\lambda}{U} (\lambda + r \frac{6C_T}{\sigma^2}) + \frac{C_0}{\alpha} r \right] \right\} \frac{c}{cm} dr$$

$$M_{q_k \dot{B}} = \int_0^1 r \left\{ \vec{\eta}_k \cdot \vec{k}_B \left[-\frac{1}{2} \frac{r^2}{U} \right] \right. \\ \left. + \vec{\eta}_k \cdot \vec{k}_B \left[\frac{r}{U} \left(\frac{\lambda}{2} - \frac{r}{2} \frac{6C_T}{\sigma^2} \right) \right] \right\} \frac{c}{cm} dr$$

$$M_{q_k \ddot{r}} = \int_0^1 \dot{r} \left\{ \vec{\eta}_k \cdot \vec{k}_B \left[\frac{1}{2} Ur \right] - \vec{\eta}_k \cdot \vec{k}_B \left[\frac{1}{2} U\lambda \right] \right\} \frac{c}{cm} dr$$

$$M_{\dot{q}_i} = \int_0^1 r \left\{ \vec{\eta}_i \cdot \vec{k}_B \left[-\frac{1}{2} \frac{r^2}{U} \right] \right. \\ \left. + \vec{\eta}_i \cdot \vec{k}_B \left[\frac{r}{U} \left(\frac{\lambda}{2} + r \frac{6C_T}{\sigma^2} \right) \right] \right\} \frac{c}{cm} dr$$

$$M_{\dot{p}} = \int_0^1 \left[-\frac{1}{2} \frac{r^4}{U} \right] \frac{c}{cm} dr$$

$$M_{p_i} = \int_0^1 \dot{r} \left[\frac{1}{2} Ur \right] \frac{c}{cm} dr$$

$$Q_{\dot{\zeta}} = \int_0^1 \left[\frac{1}{2} \frac{\lambda}{U} (\lambda + r \frac{6C_T}{\sigma^2}) + \frac{C_0}{\alpha} r \right] r^2 \frac{c}{cm} dr$$

$$Q_{\dot{\theta}} = \int_0^1 \frac{1}{2} Ur \lambda r \frac{c}{cm} dr$$

$$M_{PK\dot{q}_i} = \int_{C_{FA}}^l x_A \dot{\xi}_k \left\{ \vec{\eta}_i \cdot \vec{k}_B \left(\frac{1}{2}r \right) - \vec{\eta}_i \cdot \vec{k}_B \left[\frac{\lambda}{2} + r \frac{6C_T}{\alpha} \right] \right\} \frac{c}{cm} dr$$

$$M_{PK\dot{B}} = \int_{C_{FA}}^l x_A \dot{\xi}_k \left\{ \frac{1}{2}r^2 \right\} \frac{c}{cm} dr$$

$$M_{PK\dot{p}_i} = - \int_{C_{FA}}^l \dot{\xi}_k \dot{\xi}_i \frac{c^2}{I_b} r \left[1 + 6 \frac{x_A}{c} + 8 \left(\frac{x_A}{c} \right)^2 \right] \frac{c}{cm} dr$$

$$M_{PKp_i} = - \int_{C_{FA}}^l \dot{\xi}_k \dot{\xi}_i \left[x_A \frac{1}{2} u^2 \right] \frac{c}{cm} dr$$

where

$$u = (r^2 + \lambda^2)^{\frac{1}{2}}$$

$$\lambda = \lambda_i + \mu_z$$

2.3 Blade Bending and Torsion Modes

2.3.1 *Coupled bending modes of a rotating blade.* - Equilibrium of the elastic, inertial, and centrifugal bending moments on the blade gives the differential equation for the coupled flap/lag bending of the rotating blade (see section 2.2.14). For free vibration - the homogeneous equation with harmonic motion at the natural frequency ν - we obtain the modal equation for bending of the blade:

$$(EI\ddot{\gamma}'')' - \Sigma^2 (\int_{C_{FA}}^l \rho g m \omega \dot{\gamma}')' - m \Sigma \Sigma \cdot \dot{\gamma} - m \omega^2 \dot{\gamma} = 0$$

Here $\vec{\eta}(r) = z_0 \vec{i} - x_0 \vec{k}$ is the bending deflection (mode shape),

$$\begin{aligned} EI &= EI_{zz} \vec{i} \vec{i} + EI_{xx} \vec{k} \vec{k} \\ &= (EI_{zz} \cos^2 \theta + EI_{xx} \sin^2 \theta) \vec{i}_B \vec{i}_B \\ &\quad + (EI_{zz} \sin^2 \theta + EI_{xx} \cos^2 \theta) \vec{k}_B \vec{k}_B \\ &\quad + (EI_{xx} - EI_{zz}) \sin \theta \cos \theta (\vec{i}_B \vec{k}_A + \vec{k}_B \vec{i}_B) \end{aligned}$$

is the bending stiffness dyadic $\vec{\Omega} = \Omega \vec{k}_B$ is the rotor rotational speed, and ν is the natural frequency of the mode. The boundary conditions are as follows:

- (a) at the tip ($r = R$): $EI\vec{\eta}'' = (EI\vec{\eta}'')' = 0$
- (b) and at the root ($r = e$): $\vec{\eta} = \vec{\eta}' = 0$ for a cantilever blade;
 $\vec{\eta} = 0$ and $EI\vec{\eta}'' = K_s \vec{\eta}'$ for an articulated blade.

The root boundary condition is applied at the offset $r = e$ to allow for hinge offset of an articulated rotor, or a very stiff hub of a hingeless rotor. Different offsets can be used for the out-of-plane and inplane motion (e_f and e_ℓ). With the hinge springs at an angle θ_s from the hub plane, the hinge spring dyadic is

$$\begin{aligned} K_s &= (K_F \cos^2 \theta_s + K_L \sin^2 \theta_s) \vec{i}_B \vec{i}_B \\ &\quad + (K_F \sin^2 \theta_s + K_L \cos^2 \theta_s) \vec{k}_B \vec{k}_B \\ &\quad + (K_L - K_F) \sin \theta_s \cos \theta_s (\vec{i}_B \vec{k}_B + \vec{k}_B \vec{i}_B) \end{aligned}$$

where K_F is the flap spring and K_L is the lag spring constant.

It is useful to be able to use for the pitch angle of the structural principal axes the effective angle $\theta_e = \theta + \alpha \theta$. The parameter α is zero for no structural coupling of the inplane and out-of-plane blade motion; and

$\mathcal{R} = 1$ for complete coupling. For the hinge spring pitch angle θ_s , an input value can be used; or $\mathcal{R}\theta_{75}$ can be used; or more generally $\theta_s = \mathcal{R}\theta_{75} + \theta_{so}$.

This differential equation is an eigenvalue problem for the mode shapes η and the natural frequencies ν . The equation and boundary conditions constitute a proper Sturm-Liouville problem. It follows that a series of eigensolutions or modes $\vec{\eta}_i(r)$ exists with corresponding natural frequencies ν_i ; and that the modes are orthogonal with weight m . Hence if $i \neq k$,

$$\int_e^R \vec{\eta}_i \cdot \vec{\eta}_k m dr = 0$$

The frequencies satisfy the energy balance relation:

$$\nu^2 = \frac{\vec{\eta}'(e) K_s \vec{\eta}'(e) + \int_e^R [\vec{\eta}'' EI \vec{\eta}'' + S^2 \int_r^R g m dr \vec{\eta}'^2 - m (\vec{\eta} \cdot \vec{\eta}')^2] dr}{\int_e^R \eta^2 m dr}$$

The modal equation will be solved by a modified Galerkin method following reference 3. This approach works better for large radial variations in the bending stiffness than does the Rayleigh-Ritz method in standard form. Write the differential equation as

$$\vec{M}'' - (\int_r^1 g m dr \vec{\eta}')' - m K_s F_s \cdot \vec{\eta} - m \nu^2 \vec{\eta} = 0$$

$$\vec{\eta}'' - \left(\frac{EI}{S^2 R^4} \right)^{-1} \vec{M} = 0$$

with boundary conditions $\vec{M} = \vec{M}' = 0$ at $r = 1$, and $\vec{\eta} = 0$ and $M = K_s \vec{\eta}'$ at $r = e$. The deflection and moment are expanded as finite series in the functions \vec{f}_i and \vec{g}_i

$$\vec{\gamma} = \sum c_i \vec{\xi}_i(r)$$

$$\vec{M} = \sum d_i \vec{\eta}_i(r)$$

It is required that each of the functions \vec{f}_i and \vec{g}_i satisfy the boundary conditions; then the sum automatically does. Since a finite series is required for numerical calculations, this will be an approximate solution. For best numerical accuracy the functions \vec{f}_i and \vec{g}_i must be chosen so that the lower frequency modes can be well represented by the truncated series. Substituting these series into the differential equations and operating with

$$\int_e^l \vec{\xi}_k \cdot (\dots) dr \quad \text{and} \quad \int_e^l \vec{\eta}_k \cdot (\dots) dr$$

gives

$$\begin{aligned} & \sum d_i \int_e^l \vec{\xi}_k \cdot \vec{\eta}_i'' dr \\ & - \sum c_i \int_e^l [(\int_e^l g_m \omega_j \vec{\xi}_i') \cdot \vec{\xi}_k + m k_8 \vec{\xi}_i' \cdot \vec{\xi}_k + m \nu^2 \vec{\xi}_k \cdot \vec{\xi}_i] dr \\ & = 0 \end{aligned}$$

$$\sum c_i \int_e^l \vec{\xi}_k \cdot \vec{\xi}_i'' dr - \sum d_i \int_e^l \vec{\eta}_k \cdot \left(\frac{EI}{\rho I^2 R^4} \right)^{-1} \vec{\eta}_i dr = 0$$

Integrating by parts and applying the boundary conditions gives

$$\begin{aligned} \int_e^l \vec{\xi}_k \cdot \vec{M}'' dr &= \vec{\xi}_k \cdot \vec{M}' \Big|_e^l - \vec{\xi}_k \cdot \vec{M} \Big|_e^l + \int_e^l \vec{\xi}_k'' \cdot \vec{M} dr \\ &= \vec{\xi}_k \cdot \frac{k_s}{\rho I^2 R^3} \vec{\gamma}' \Big|_e^l + \int_e^l \vec{\xi}_k'' \cdot \vec{M} dr \end{aligned}$$

$$\int_e^l (\int_e^l g_m \omega_j \vec{\xi}_i') \cdot \vec{\xi}_k dr = - \int_e^l \int_e^l g_m \omega_j \vec{\xi}_i' \cdot \vec{\xi}_k dr$$

so the first equation becomes

$$\begin{aligned} \sum_{k,i} \int_e \vec{\xi}_k'' \cdot \vec{g}_i dr + \sum_{k,i} \left(\vec{\xi}_k' \frac{k_i}{EI_R^3} \vec{\xi}_i' \right) |_e \\ + \sum_{k,i} \int_e \left[\int_e g_m \vec{\xi}_i' \cdot \vec{\xi}_k' - m k_k \vec{\xi}_k \vec{\xi}_k' - m r^2 \vec{\xi}_k \vec{\xi}_i' \right] dr \\ = 0 \end{aligned}$$

Hence the problem reduces to a set of algebraic equations for $\vec{c} = [c_i]$ and $\vec{d} = [d_j]$

$$\begin{aligned} C \vec{d} + D \vec{c} - r^2 B \vec{c} &= 0 \\ C^T \vec{c} - A \vec{d} &= 0 \end{aligned}$$

or

$$(C A^{-1} C^T + D - r^2 B) \vec{c} = 0$$

For simplicity the functions used for the moment expansion are $\vec{g}_i = \vec{f}_i''$. Then the coefficients of the matrices are

$$A_{ki} = \int_e \vec{\xi}_k'' \left(\frac{EI}{EI_R^4} \right)^{-1} \vec{\xi}_i'' dr$$

$$B_{ki} = \int_e m \vec{\xi}_k \cdot \vec{\xi}_i dr$$

$$C_{ki} = \int_e \vec{\xi}_k'' \cdot \vec{\xi}_i'' dr$$

$$D_{ki} = \vec{\xi}_k'(e) \frac{k_s}{\Sigma^2 R^3} \vec{\xi}_i'(e)$$

$$+ \int_e^R \left[\zeta_r g m d \vec{\xi}_i' \cdot \vec{\xi}_k' - m \vec{k}_s \cdot \vec{\xi}_k \vec{k}_s \cdot \vec{\xi}_i' \right] dr$$

(Note that using $\vec{g}_i = EI \vec{f}_i''$ would give $C = C^T = A$ so $\vec{d} = \vec{c}$, and this solution would reduce to the standard Galerkin form.)

The eigenvalues of the matrix $B^{-1}(CA^{-1}C^T + D)$ are the natural frequencies ν^2 of the coupled bending vibration of the blade; and the corresponding eigenvectors \vec{c} give the mode shape $\vec{\eta}$. As a final step, the modes are normalized to unity at the tip: $|\vec{\eta}(1)| = 1$. This modified Galerkin approach equivalently replaces the Rayleigh energy expression for the natural frequency (given above) by

$$\nu^2 = \frac{\vec{\eta}'(e) k_s \vec{\eta}'(e) + \int_e^R [2 \vec{\eta}'' \cdot \vec{M} - \vec{M} E I^{-1} \vec{M} + \Sigma^2 \int_e^R g m d \eta'^2 - m (\vec{\xi} \cdot \vec{\eta})^2] dr}{\int_e^R \eta'^2 m dr}$$

The blade nonrotating modes and frequencies can be obtained using

$$A_{ki} = \int_e^R \vec{\xi}_k'' \left(\frac{EI}{R^4} \right)^{-1} \vec{\xi}_i'' dr$$

$$D_{ki} = \vec{\xi}_k'(e) \frac{k_s}{R^3} \vec{\xi}_i'(e)$$

A convenient set of functions for \vec{f}_i are the bending mode shapes of a nonrotating, uniform beam. Such functions will satisfy the required boundary conditions, and furthermore are orthogonal (necessary for good numerical conditioning of the Galerkin solution). Let w_n be the series of eigensolutions

of the differential equation $d^4 w/dx^4 = a^4 w$ with appropriate boundary conditions. Using these functions for both out-of-plane and inplane deflections gives

$$\vec{\xi}_1(r) = w_1(x) \vec{e}_B$$

$$\vec{\xi}_2(r) = w_1(x) \vec{k}_B$$

$$\vec{\xi}_3(r) = w_2(x) \vec{e}_B$$

$$\vec{\xi}_4(r) = w_2(x) \vec{k}_B$$

etc.

where $x = (r - e)/(1 - e)$.

For a uniform hinged blade, the nonrotating mode shapes are:

$$w = \frac{\sinh a \sin ax + \sin a \sinh ax}{2 \sin a \sinh a}$$

where a is the solution of

$$\tan a = \tanh a$$

The first mode ($a = 0$) is $w = x$. For a uniform cantilever blade, the nonrotating mode shapes are

$$w = \frac{(\sin a - \sinh a)(\sinh ax - \sin ax)}{2 \sin a \sinh a}$$

$$+ \frac{(\cosh a + \cos a)(\cosh ax - \cos ax)}{2 \sin a \sinh a}$$

where a is the solution of

$$\cos a \cosh a = -1$$

The values of a for the lowest modes are given in the table below.

Mode	Hinged	Cantilever
1	0	1.875104069
2	3.926602313	4.694091134
3	7.068582747	7.854757439
4	10.21017612	10.99554074
5	13.35176878	14.13716839
6	16.49336143	17.27875953
7	19.63495409	20.42035225
8	22.77654674	23.56194490
9	25.91813940	26.70353756
10	29.05973205	29.84513021

The centrifugal force is required for the bending mode calculation.

With the section mass defined at radial stations r_i ($i = 1$ to M) the centrifugal force is

$$\int_{r_{I-1}}^r g_m dr = \int_{r_I}^r g_m dr + \sum_{i=I+1}^M \int_{r_{i-1}}^{r_i} g_m dr$$

where $r_{I-1} \leq r < r_I$. Then for linear variation of the section mass between the stations r_i , the integrals can be evaluated as follows:

$$\begin{aligned}
 S_r^1 g m \delta &= \frac{1}{r_i - r_{i-1}} \left[m_{i-1} \left(\frac{r^3}{3} - \frac{r_i r}{2} + \frac{r_{i-1}^3}{6} \right) \right. \\
 &\quad \left. - m_i \left(\frac{r^3}{3} - \frac{r_{i-1} r^2}{2} + \frac{r_i^3}{6} \right) \right] \\
 &+ \sum_{l=i}^{M-1} m_l [f(r_l, r_{l+1}) - f(r_i, r_{i+1})] + m_M f(r_M, r_{M-1})
 \end{aligned}$$

where

$$f(x, y) = \int_y^x \frac{x-y}{x-y} f dy = \frac{1}{x-y} \left[\frac{x^3}{3} - \frac{x^2 y}{2} + \frac{y^3}{6} \right]$$

2.3.2 Articulated Blade Modes. - For an articulated blade the modal differential equation need not be solved if the higher bending modes are not required. Rigid flap and lag motion about the hinges gives the two lowest frequency modes:

$$\vec{\eta}_1 = \vec{\eta}_{\text{lag}} = - \left(\frac{r - e_f}{1 - e_f} \right) \vec{k}_B$$

$$\vec{\eta}_2 = \vec{\eta}_{\text{flap}} = \left(\frac{r - e_f}{1 - e_f} \right) \vec{l}_B$$

Note that separate hinge offsets may be used for flap and lag motion. The natural frequencies are obtained directly from the energy relation, as follows:

$$\gamma_{\text{eq}}^z = \frac{e_L \int_{r_0}^1 \eta^2 m dr + k_L / 5 z^2 R^3}{(1 - e_L) \int_{r_0}^1 \eta^2 m dr}$$

$$\gamma_{\text{flap}}^z = 1 + \frac{e_F \int_{r_0}^1 \eta^2 m dr + k_F / 5 z^2 R^3}{(1 - e_F) \int_{r_0}^1 \eta^2 m dr}$$

2.3.3 Torsion modes of a nonrotating blade.- Equilibrium of the elastic and inertial torsion moments (see section 2.2.14) gives the model equation

$$(GJ \dot{\psi}')' + I_\theta \omega^2 \psi = 0$$

with the boundary conditions $\dot{\psi}' = 0$ at the tip ($r = R$) and $\psi = 0$ at the root ($r = r_{FA}$). The modes are orthogonal with weight I_θ , so if $i \neq k$

$$\int_{r_{FA}}^R \psi_i \psi_k I_\theta dr = 0$$

The frequencies satisfy the relation

$$\omega^2 = \frac{\int_{r_{FA}}^R GJ \dot{\psi}_i'^2 dr}{\int_{r_{FA}}^R I_\theta \dot{\psi}_i^2 dr}$$

These are the nonrotating torsion modes, so the solution is independent of the rotor speed or collective pitch.

The equation is solved by the modified Galerkin method, as described in detail above for the bending modes. Write the differential equation as

$$-\ddot{\tau} - \frac{I_\theta}{\omega^2 R^2} \dot{\tau} = 0$$

Expand the torsion deflection and torsion moment as series:

$$\ddot{\tau} = \sum c_i f_i(r)$$

$$\tau = \sum d_i g_i(r)$$

where the functions f_i and g_i satisfy the boundary conditions on $\ddot{\tau}$ and τ . Substitute these series in the equations, operate with

$$\int_{r_{FA}}^1 f_k(\dots) dr \quad \text{and} \quad \int_{r_{FA}}^1 g_k(\dots) dr$$

integrate by parts and use the boundary conditions

$$\begin{aligned} \int_{r_{FA}}^1 f_k \ddot{\tau} dr &= f_k \tau \Big|_{r_{FA}}^1 - \int_{r_{FA}}^1 f'_k \tau dr \\ &= - \int_{r_{FA}}^1 f'_k \tau dr \end{aligned}$$

to obtain

$$\sum_{di} \int_{r_{FA}}^l f'_k g_i dr - \omega^2 \sum_{ci} \int_{r_{FA}}^l I_0 f_k f_i dr = 0$$

$$\sum_{ci} \int_{r_{FA}}^l g_k f'_i dr - \sum_{di} \int_{r_{FA}}^l g_k \left(\frac{GJ}{Sc^2 R^2} \right)^{-1} f_i dr = 0$$

Hence the problem reduces to a set of algebraic equations for $\vec{c} = [c_1]$ and $\vec{d} = [d_i]$

$$C \vec{d} - \omega^2 B \vec{c} = 0$$

$$C^T \vec{c} - A \vec{d} = 0$$

or

$$(CA^{-1}C^T - \omega^2 B) \vec{c} = 0$$

For simplicity, the functions used for the torsion moment at $g_i = f'_i$. Then the coefficients of the matrices are

$$A_{ki} = \int_{r_{FA}}^l f'_k \left(\frac{GJ}{Sc^2 R^2} \right)^{-1} f'_i dr$$

$$B_{ki} = \int_{r_{FA}}^l I_0 f_k f_i dr$$

$$C_{ki} = \int_{r_{FA}}^l f'_k f'_i dr$$

(Note using $g_i = GJ f'_i$ would give the standard Galerkin result.)

The eigenvalues of the matrix $B^{-1}(C A^{-1} C^T)$ give the natural frequencies of the torsion vibration, and the corresponding eigenvectors for \vec{c} give the modes. Finally, the torsion modes are normalized to unity at the tip, $\xi(1) = 1$.

A convenient set of functions to use for f_i is the solution for the torsion modes of a uniform beam:

$$w_n = \sin \left[(n - \frac{1}{2}) \pi \frac{r - r_{FA}}{r - r_{HA}} \right]$$

These functions satisfy the boundary conditions, and will often be close to the true mode shapes.

2.3.4 Kinematic pitch/bending coupling. - The kinematic pitch/bending coupling K_{Pi} and the pitch/gimbal coupling K_{PG} have a significant role in the rotor dynamic behavior. The definition of K_{Pi} is the rigid pitch motion due to a unit deflection of the i -th bending mode: $K_{Pi} = -d\theta/dq_i$. For an articulated rotor, the first "bending" modes are rigid lag and flap motion about the hinges. The pitch/flap coupling is often defined in terms of the delta-three angle: $K_p = \tan \delta_3$. It is possible to simply input these kinematic coupling parameters to the dynamics analysis, if values are available from either measurements or some other analysis. It is also desirable to be able to calculate the coupling from a model of the blade root geometry.

Figure 10 is a schematic of the blade root and control system geometry considered, showing the position of the feather bearing, pitch horn, and pitch link for no bending deflection of the blade. The radial locations of the feather bearing and pitch link are r_{PB} and r_{PH} respectively; the length of the pitch horn is x_{PH} . The orientation of the pitch horn and pitch link are given by the angles $\phi_{PH} + \theta_{75}$ and ϕ_{PL} . Control input produces a vertical motion of the bottom of the pitch link, and hence a feathering motion of the blade about the pitch axis. Bending motion of the blade, with either structural flexibility or an actual hinge inboard of the pitch bearing, produces an inplane or out-of-plane deflection of the pitch bearing. With the bottom of the pitch link fixed in space, a pitch change of the blade results.

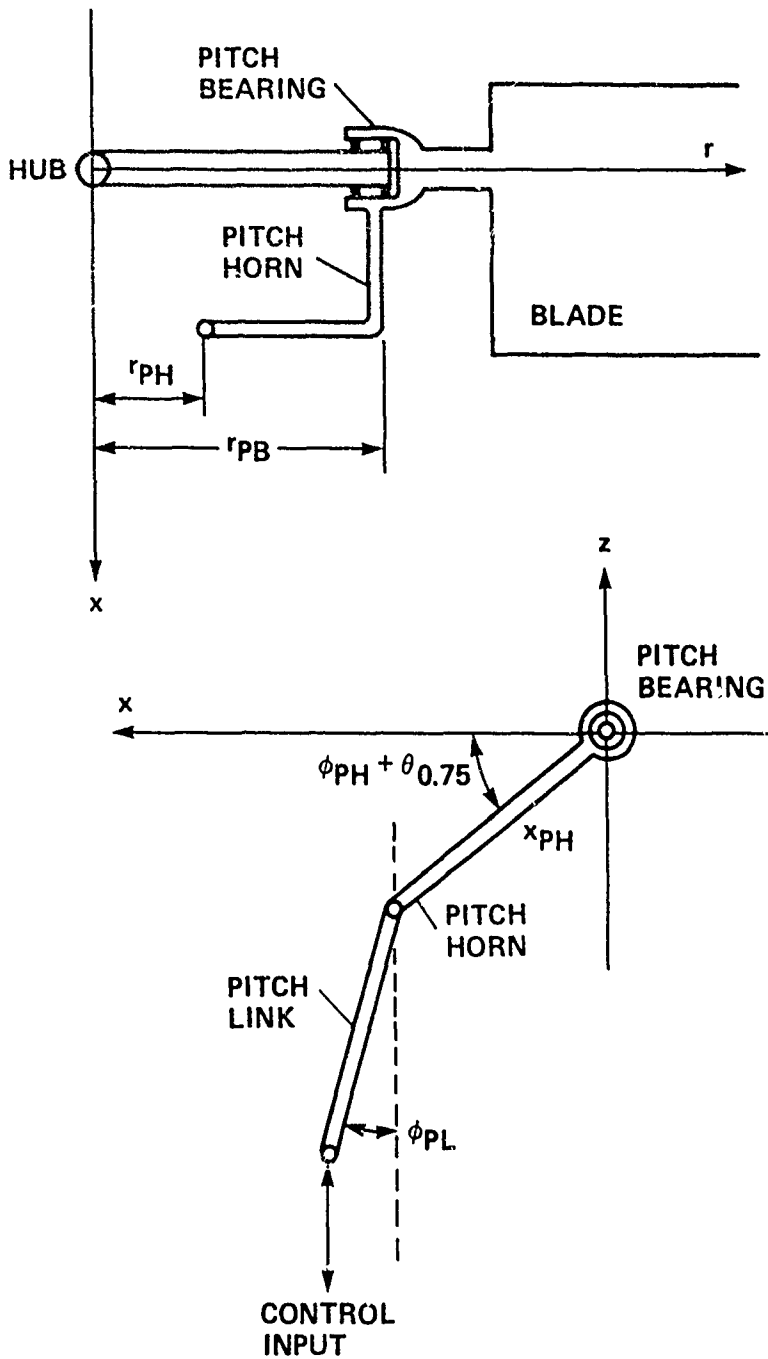


Figure 10. Schematic of blade root and control system geometry for calculating the kinematic pitch/bending coupling.

The vertical and inplane displacements of the pitch horn (the end at r_{PH}) due to bending of the blade in the i -th mode are:

$$\Delta z = q_i \vec{t}_B \cdot (\vec{\eta}_i(r_{PB}) - \vec{\eta}'_i(r_{PB})(r_{PB} - r_{PH}))$$

$$\Delta x = -q_i \vec{k}_B \cdot (\vec{\eta}_i(r_{PB}) - \vec{\eta}'_i(r_{PB})(r_{PB} - r_{PH}))$$

The kinematic pitch/bending coupling is derived from the geometric constraint that the lengths of the pitch horn and pitch link are fixed. The result is:

$$K_{P_i} = \frac{(\cos \phi_{PL} \vec{t}_B + \sin \phi_{PL} \vec{k}_B) \cdot (\vec{\eta}_i(r_{PB}) - \vec{\eta}'_i(r_{PB})(r_{PB} - r_{PH}))}{-x_{PH} \cos(\phi_{PH} + \theta_{75} + \phi_{PL})}$$

Similarly, for a gimballed (or teetering) rotor the pitch/flap coupling is:

$$\begin{aligned} K_{PG} &= \frac{-(r_{PH}/x_{PH}) \cos \phi_{PL}}{\cos(\phi_{PH} + \theta_{75} + \phi_{PL})} \\ &= \frac{(K_{PG})_{\text{pitch horn horizontal}}}{\cos(\phi_{PH} + \theta_{75} + \phi_{PL})} \end{aligned}$$

2.3.5 Blade pitch definition.- Outboard of r_{FA} , the trim pitch angle is given by the collective and twist angles, while inboard of r_{FA} it is given by just the twist angle:

$$\Theta = \begin{cases} \theta_{coll} + \theta_{tw}(r) & r > r_{FA} \\ \theta_{tw}(r) & r < r_{FA} \end{cases}$$

(see section 2.2.2). It is convenient to use the collective pitch value at 75% radius, θ_{75} . Then

$$\Theta = \begin{cases} \theta_{75} + \theta_{tw}(r) & r > r_{FA} \\ \theta_{tw}(r) & r < r_{FA} \end{cases}$$

which requires $\theta_{tw}(r = .75) = 0$ (but no change to θ_{tw} for $r < r_{FA}$). For a rotor without a pitch bearing, it is more appropriate to maintain continuity of θ by adding a linear term inboard of r_{FA} :

$$\Theta = \begin{cases} \theta_{75} + \theta_{tw}(r) & r > r_{FA} \\ \frac{r}{r_{FA}} \theta_{75} + \theta_{tw}(r) & r < r_{FA} \end{cases}$$

For the structural and inertial analysis the pitch angle is multiplied by the structural coupling parameter α .

The twist distribution $\theta_{tw}(r)$ is required at the radial stations for which the inertial and structural properties are defined; and at the radial stations at which the aerodynamic forces are calculated. The aerodynamic twist definition can include the zero lift axis pitch θ_{ZL} (see section 2.4.1). Frequently, a linear twist distribution is used, for which

$$\theta_{tw} = \theta_{tw}^{lin} (r - .75)$$

2.4 Aerodynamic Analysis

In this section the aerodynamic forces and moments on the rotor blade are derived. The general case of a rotor in high or low inflow, axial or nonaxial flight is considered, including the effects of reverse flow and large angles. Lifting line theory (i.e., strip theory or blade element theory) is used to calculate the section loading from the airfoil two-dimensional aerodynamic characteristics, with corrections for yawed and three-dimensional flow effects required. The unsteady aerodynamic lift and moment are obtained from thin airfoil theory, and a dynamic stall model accounts for the unsteady aerodynamic phenomena at large angles of attack.

2.4.1 Section aerodynamic forces.— A hub plane reference frame is used for the aerodynamic forces. All forces and velocities are resolved in the hub plane (i.e., the B coordinate system). The hub plane reference frame is fixed with respect to the shaft, hence it is tilted and displaced by the shaft motion. Figure 11 illustrates the forces and velocities of the blade section aerodynamics. The blade pitch angle is θ , measured from the reference plane. The velocity of the air as seen by the moving blade has components u_T , u_p , and u_R , resolved with respect to the reference frame; $U = (u_T^2 + u_p^2)^{1/2}$ is the resultant air velocity in the plane of the section; and $\phi = \tan^{-1} u_p/u_T$ is the induced angle. The section angle of attack is

$$\alpha = \theta + \theta_{ZL} - \phi$$

where θ_{ZL} is the pitch of the aerodynamic zero-lift axis of the section relative to the structural/inertial principal axis at pitch angle θ (θ_{ZL} may vary along the span, and should not therefore be included in the definition of the section aerodynamic coefficients as a function of α ; θ_{ZL} can however be included in the aerodynamic twist distribution, if θ_{tw} is defined separately for the inertial/structural pitch and for the aerodynamic pitch).

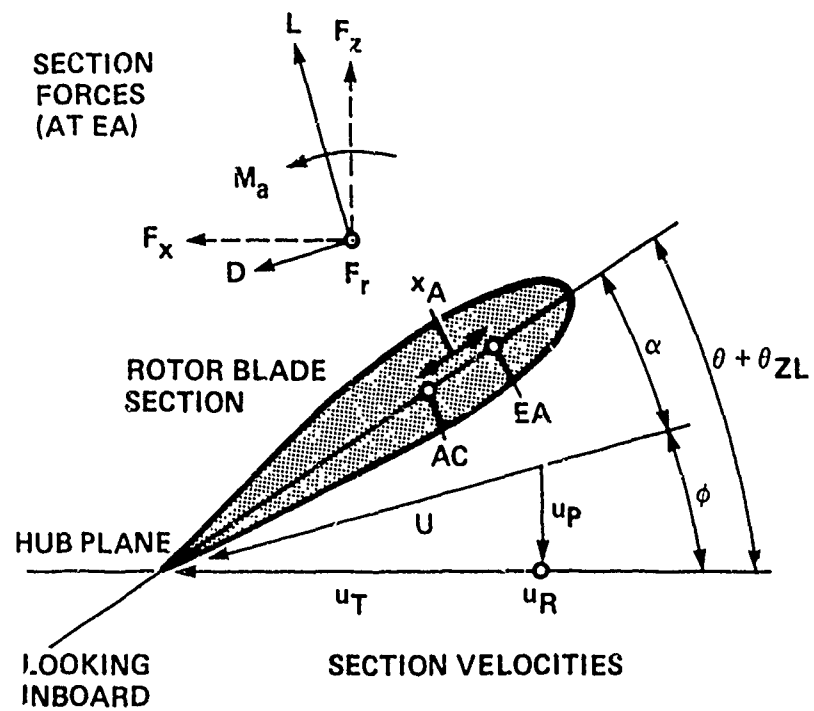


Figure 11. Rotor blade section aerodynamics.

The velocity u_T is in the hub plane, positive in the blade drag direction; u_R is in the hub plane, positive radially outward along the blade; and u_p is normal to the hub plane, positive down through the rotor disk. The aerodynamic forces and moment on the section, at the elastic axis, are defined as follows: L and D are the aerodynamic lift and drag forces on the section, respectively normal and parallel to the resultant velocity U ; F_z and F_x are the components of the total aerodynamic force on the section resolved with respect to the hub plane, normal to and in the plane of the rotor; F_r is the radial drag force on the blade, positive outward (the same direction as positive u_R); and M_a is the section aerodynamic moment about the elastic axis, positive nose up. The radial forces due to the tilt of F_z and F_x are considered separately, hence F_r consists only of the radial drag forces.

The section lift and drag are

$$L = \frac{1}{2} \rho U^2 c c_L + L_{us}$$

$$D = \frac{1}{2} \rho U^2 c c_D$$

where U is the resultant velocity at the section, ρ is the air density, and c is the chord of the blade. (The air density can be dropped since all quantities are actually dimensionless, based on ρ , Ω , and R .) The section lift and drag coefficients, c_L and c_D , are functions of the section angle of attack and Mach number:

$$\alpha = \theta + \Theta_{zL} - \phi = \theta + \Theta_{zL} - \tan^{-1} u_p/u_T$$

$$M = M_{TIP} U$$

where M_{TIP} is the tip Mach number (the motor tip speed ΩR divided by the speed of sound). L_{us} is the unsteady aerodynamic lift force. The radial drag force is

$$F_r = (u_r/u) D = \frac{1}{2} \rho u^2 c_s$$

This radial drag force is based on the assumption that the viscous drag force on the section has the same sweep angle as the local section velocity. The moment about the elastic axis is

$$\begin{aligned} M_a &= -x_A L + M_{AC} + M_{us} \\ &= -x_A \frac{1}{2} \rho u^2 c_m + \frac{1}{2} \rho u^2 c^2 c_m + M_{us} \end{aligned}$$

where x_A is the distance the aerodynamic center is behind the elastic axis, c_m is the section moment about the aerodynamic center (positive nose up), and M_{us} is the unsteady aerodynamic moment.

The components of the section aerodynamic forces relative to the hub plane axes are then

$$F_z = L \cos\phi - D \sin\phi = (L_{u_T} - D_{u_T})/u$$

$$F_x = L \sin\phi + D \cos\phi = (L_{u_T} + D_{u_T})/u$$

Substituting for L and D , and dividing by a , the two-dimensional lift-curve slope, and by c_m , the mean section chord (which enter the Lock number γ also), we obtain:

$$\frac{F_z}{ac} = \left[U(u_r \frac{c_x}{2a} - u_p \frac{c_d}{2a}) + \frac{u_r}{U} \frac{L_{us}}{ac} \right] \frac{c}{cm}$$

$$\frac{F_x}{ac} = \left[U(u_p \frac{c_d}{2a} + u_r \frac{c_x}{2a}) + \frac{u_p}{U} \frac{L_{us}}{ac} \right] \frac{c}{cm}$$

$$\frac{F_r}{ac} = \left[U u_a \frac{c_0}{2a} \right] \frac{c}{cm}$$

$$\frac{M_a}{ac} = \left[-x_A U^2 \frac{c_0}{2a} + U^2 c \frac{cm}{2a} + \frac{M_{us}}{ac} \right] \frac{c}{cm}$$

The net rotor forces required are obtained by integration of these section forces over the span of the blade:

$$\frac{M_{q,aero}}{ac} = \int_0^1 \vec{\eta}_k \cdot \left(\frac{F_z}{ac} \vec{t}_B - \frac{F_x}{ac} \vec{t}_B' \right) dr$$

$$\frac{M_{p_k,aero}}{ac} = \int_{r_{FA}}^1 \vec{\chi}_k \frac{M_a}{ac} dr - \int_{r_{FA}}^1 \vec{\chi}_{A_k} \cdot \left(\frac{F_x}{ac} \vec{t}_B + \frac{F_z}{ac} \vec{t}_B' \right) dr$$

$$\left(\frac{C_{u_x}}{ca} \right)_{aero} = \int_0^1 \frac{F_z}{ac} r dr$$

$$\left(\frac{C_{u_x^2}}{ca} \right)_{aero} = \int_0^1 \frac{F_x}{ac} r dr$$

$$\left(\frac{C_{F_x}}{ca} \right)_{aero} = \int_0^1 \frac{F_x}{ac} dr$$

$$\left(\frac{C_{F_z}}{ca} \right)_{aero} = \int_0^1 \frac{F_z}{ac} dr$$

$$\left(\frac{C_{F_r}}{ca} \right)_{aero} = \int_0^1 \frac{F_r}{ac} dr$$

where

$$\tilde{F}_r = F_r - F_z (\beta_0 + \delta_{FA_1} - \delta_{FA_2}) - F_x (-\gamma_s + \delta_{FA_3}) \\ - \sum_i q_i (F_z \vec{v}_B - F_x \vec{E}_B) \cdot \vec{v}_i'$$

To numerically integrate the aerodynamic loads over the blade span, define K radial segments by the boundaries

$$r_0, r_1, r_2, \dots, r_{k-1}, r_k, \dots, r_K$$

where $r_K = 1$. For the k -th segment, the airloads are calculated at the center:

$$r = \frac{1}{2} (r_k + r_{k-1})$$

Then the spanwise integration is approximated by a summation over all segments:

$$\int_0^1 f(r) dr \cong \sum_{k=1}^K f\left(\frac{r_k + r_{k-1}}{2}\right) \Delta r_k$$

where

$$\Delta r_k = (r_k - r_{k-1})$$

In summary, the rotor blade aerodynamic forces are evaluated as follows. First the section velocity components and pitch angle are evaluated, and then the angle of attack and Mach number. Next the section aerodynamic coefficients

are obtained (see section 2.4.4), and from them the section force components and moment. Finally, the section forces are integrated over the rotor radius to obtain the required generalized forces.

2.4.2 Blade velocity.- The air velocity seen by the blade section is due to the rotor rotation, the helicopter forward speed, the rotor and shaft motion, and the wake induced velocity. The rotor is rotating at speed Ω . The velocity of the air as seen by the rotor disk has the following dimensionless components in the shaft axis system: μ_x , positive aft; μ_y , positive from the right; and μ_z , positive down through the disk:

$$\vec{\mu} = -\frac{v}{SR}\vec{\tau}_w = \mu_x \vec{t}_s - \mu_y \vec{j}_s - \mu_z \vec{k}_s$$

Often the lateral velocity component $\mu_y = -\vec{j}_s \cdot \vec{\mu}$ is assumed to be zero in the rotor aerodynamic analysis, and indeed it is small for most flight conditions. An exception is the case of sideward flight. An alternative to including μ_y is to rotate the shaft axes until $\vec{j}_s \cdot \vec{\mu} = 0$, but that would imply a redefinition of the rotor zero azimuth position for every flight state. Such a redefinition of ψ is not desirable since it changes the values of parameters such as the control system phasing, and even changes the definition of the harmonics of the rotor motion. Hence it is preferable to directly include the effects of the lateral velocity in the analysis.

The rotor wake-induced velocity is $\lambda_i = v_i / \Omega R$, normal to the rotor disk and positive downward. A simple model may be used, such as a uniform or linear variation over the disk, or calculated nonuniform induced velocities may be used. For the latter case, all three components of the wake induced velocity (in shaft axes) will be considered:

$$\vec{\lambda}_i = \lambda_x \vec{t}_s - \lambda_y \vec{j}_s - \lambda_z \vec{k}_s$$

The rotor advance ratio μ and inflow ratio λ as conventionally defined are here

$$\mu = \sqrt{\mu_x^2 + \mu_y^2}$$

$$\lambda = \lambda_i + \mu_z$$

These are the dimensionless inplane and normal components of the total velocity seen by the rotor disk. The hub plane angle of attack and yaw angle are then

$$\alpha_{HP} = \tan^{-1} \frac{\mu_z}{\sqrt{\mu_x^2 + \mu_y^2}}$$

$$\lambda_{HP} = \tan^{-1} \frac{\mu_y}{\mu_x}$$

$$\mu = \frac{V \cos \alpha_{HP}}{\Omega R}$$

$$\lambda = \frac{v_i + V \sin \alpha_{HP}}{\Omega R} = \frac{v_i}{\Omega R} + \mu \tan \alpha_{HP}$$

Here V is the helicopter velocity, with angle of attack α_{HP} relative to the hub plane (α_{HP} is positive for forward tilt of the rotor disk). The advance ratio μ is zero for hover and axial flow, and $\mu > 0$ for helicopter forward flight.

The aerodynamic gust velocity has components u_G , v_G , and w_G in the shaft axis system, normalized by dividing by the tip speed ΩR . The longitudinal gust v_G is positive from the front, the lateral gust v_G is positive from the right, and the vertical gust w_G is positive upward ($\vec{v}_{gust} = u_G \vec{i}_s - v_G \vec{j}_s + w_G \vec{k}_s$ relative to the rotor). This gust velocity is evaluated at azimuth angle ψ and radial station r on the rotor disk

(at $r = r\vec{J}_B = r(\cos \psi \vec{i}_s + \sin \psi \vec{j}_s)$ relative to the hub). The quasisteady shaft motion and the gust velocity at the rotor hub will be included in the advance ratio component μ_x , μ_y , and μ_z (see section 4.1.2).

The blade and shaft motion have been defined in the inertial analysis (section 2.2). The resulting velocity components in the rotor shaft axes are thus:

$$u_T = r + (\mu_x + \lambda_x) \sin \psi + (\mu_y + \lambda_y) \cos \psi - ((\mu_x + \lambda_x) \cos \psi - (\mu_y + \lambda_y) \sin \psi) (\delta_{FA_3} - \vec{k}_B \cdot (\vec{z}_{0T} - \vec{x}_{0T})) + \vec{k}_B \cdot (\vec{z}_{0T} - \vec{x}_{0T}) + (\mu_z \alpha_x + i_{gB} + v_G) \cos \psi + (\mu_z \alpha_y - i_{gB} + u_G) \sin \psi + (\mu_x \cos \psi - \mu_y \sin \psi) (\alpha_z + \psi_s) + r (\dot{\alpha}_z + \dot{\psi}_s)$$

$$u_R = (\mu_x + \lambda_x) \cos \psi - (\mu_y + \lambda_y) \sin \psi + x_{FA} + r_{FA} \delta_{FA_3} + \vec{k}_B \cdot (\vec{z}_{0T} - \vec{x}_{0T}) - r \vec{k}_B \cdot (\vec{z}_{0T} - \vec{x}_{0T}) - (\lambda_z + \mu_z) [\delta_{FA_1} - \delta_{FA_2} + \beta_G + \vec{k}_B \cdot (\vec{z}_{0T} - \vec{x}_{0T})] + ((\mu_x + \lambda_x) \sin \psi + (\mu_y + \lambda_y) \cos \psi) (\delta_{FA_3} - \vec{k}_B \cdot (\vec{z}_{0T} - \vec{x}_{0T})) - (\mu_z \alpha_x + i_{gB} + v_G) \sin \psi + (\mu_z \alpha_y - i_{gB} + u_G) \cos \psi - (\mu_x \sin \psi + \mu_y \cos \psi) (\alpha_z + \psi_s)$$

$$\begin{aligned}
 u_p = & \mu_z + \lambda_z + r\dot{\beta}_G + \vec{t}_B \cdot (\vec{z}_{ol} - \vec{x}_o \vec{r}) \\
 & + ((\mu_x + \lambda_x) \cos \psi - (\mu_y + \lambda_y) \sin \psi) [\delta_{f1}, -\delta_{f1} z + \beta_G \\
 & \quad + \vec{t}_B \cdot (\vec{z}_{ol} - \vec{x}_o \vec{r})'] \\
 & + (\dot{z}_h - w_G - \mu_x \alpha_y - \mu_y \alpha_x) + r(\dot{\alpha}_x \sin \psi - \dot{\alpha}_y \cos \psi)
 \end{aligned}$$

and the pitch angle is

$$\Theta = \Theta_{ee} + \Theta_{tw} + \sum_{i=0}^{\infty} \rho_i \}$$

In body axes, the trim velocity vector is fixed with the reference frame, and would therefore tilt with it. With inertial axes however, a tilt of the rotor by the shaft motion results in a small change in the directions of the components of μ as seen in the reference frame. All the $\mu\alpha$ terms in the expressions above for u_T , u_p , and u_R result from such tilt of the inertial axes relative to the trim velocity vector. The aircraft body yaw, pitch, and roll will be defined as body axis motion however. Hence the body Euler angles are not to be included in the evaluation of α_x , α_y , and α_z for the blade velocities.

2.4.3 *Induced velocity*.- For the case of uniform inflow, the rotor wake-induced velocity is obtained from the momentum theory result

$$\lambda_i = \frac{C_T}{2 \sqrt{\lambda^2 / \kappa_h^4 + \mu^2 / \kappa_f^2}}$$

where $\lambda = \mu_i + \lambda_i$ and $\mu^2 = \mu_x^2 + \mu_y^2$. Empirical correction factors κ_h and κ_f are included for the effects of nonuniform inflow, tip losses, swirl, blockage, etc., in hover and forward flight. An iterative solution of this equation for λ_i is necessary:

$$(\lambda_i)_{n+1} = \left[\frac{\frac{C_T}{2} (\lambda(\lambda + \lambda_i)/k_{\infty}^4 + \mu^2/k_f^2)}{C + \frac{C_T}{2} \lambda/k_{\infty}^4} \right]_n$$

$$C = (\lambda^2/k_{\infty}^4 + \mu^2/k_f^2)^{3/2}$$

with

$$\lambda_i \approx \frac{C_T}{2 \sqrt{C_T/2 k_{\infty}^2 + \mu^2/k_f^2}}$$

to start the solution; 3 or 4 iterations are usually sufficient. For the vortex ring and turbulent wake states this momentum theory result is not applicable. Thus if

$$\mu^2 + (2\mu_z + 3\lambda_{\infty})^2 < \lambda_{\infty}^2$$

the following expression is used instead:

$$\lambda = \mu_z + k_{\infty}/\mu_z \left[\frac{.373 \mu_z^2 + .598 \mu^2}{\lambda_{\infty}^2} - 1.991 \right]$$

where

$$\lambda_{\infty} = \sqrt{C_T/2}$$

The wake-induced velocity is reduced when the rotor disk is in the proximity of the ground plane. The effect of the ground will be accounted for using the following approximate expression from reference 4 for the ratio of the induced velocities in and out of ground effect:

$$\frac{V_w}{V} = \frac{T}{T_\infty} = \frac{1}{1 - (4z/\cos\epsilon)^{-2}}$$

where z is the height of the rotor hub above ground level, normalized by the rotor radius; and ϵ is the angle between the ground and the rotor wake ($\epsilon = 0$ for hover and ϵ approaches 90° in forward flight), which accounts for the effect of forward speed. Note that ground effect is essentially negligible for altitudes greater than the rotor diameter ($z > 2$) or at forward speeds $\mu > 2(C_T/2)^{1/2}$. This expression compares well with test results, down to an altitude of about one-half rotor radius (see reference 4). The rotor wake-induced velocity in ground effect is thus

$$(\lambda_i)_{IGE} = (1 - \frac{\cos^2\epsilon}{16z^2})(\lambda_i)_{OGE}$$

Let h_{AGL} be the height of the helicopter center of gravity above ground level; and (x_R, y_R, z_R) be the components of the rotor hub position relative to the center of gravity, in a body axis system (the F frame, see section 4.1.5). Then the altitude of the rotor hub above ground level is

$$\begin{aligned} z &= h_{AGL} - (x_R \vec{k}_F + y_R \vec{j}_F + z_R \vec{i}_F) \cdot \vec{k}_E \\ &= \frac{1}{R} [h_{AGL} - R_{rotor \#1} (z_R \cos\theta_{FT} \cos\phi_{FT} \\ &\quad + y_R \cos\theta_{FT} \sin\phi_{FT} - x_R \sin\theta_{FT})] \end{aligned}$$

The vertical (\vec{k}_E) is defined relative to the body axes by the trim pitch and roll Euler angles (θ_{FT} and ϕ_{FT} , see section 4.1.1). The angle between the rotor wake and the vertical is

$$\begin{aligned} \cos\epsilon &= (\mu_x \vec{i}_S - \mu_y \vec{j}_S - \lambda \vec{k}_S) \cdot \vec{k}_E / \sqrt{\mu_x^2 + \mu_y^2 + \lambda^2} \\ &= \frac{1}{\sqrt{\mu_x^2 + \mu_y^2 + \lambda^2}} \begin{pmatrix} \mu_x \\ -\mu_y \\ -\lambda \end{pmatrix}^T R_{SF} \begin{pmatrix} -\sin\theta_{FT} \\ \cos\theta_{FT} \sin\phi_{FT} \\ \cos\theta_{FT} \cos\phi_{FT} \end{pmatrix} \end{aligned}$$

where R_{SF} is the transformation matrix between the shaft and body axis coordinate frames.

As a first approximation to the rotor nonuniform induced velocity distribution, a linear variation over the disk is considered:

$$\Delta\lambda = \lambda_i (\kappa_x r \cos \psi + \kappa_y r \sin \psi)$$

where λ_i is the mean value of the induced velocity, calculated as described above. Typically κ_x is positive, roughly 1 at high speed; and κ_y is smaller in magnitude and negative. Both κ_x and κ_y must be zero in hover. Based on references 5 to 7 we will use

$$\kappa_x = \frac{f_x \mu_x}{\sqrt{\mu^2 + \lambda^2} + |\lambda|} - f_y 2 \mu_y$$

$$\kappa_y = -f_y 2 \mu_x - \frac{f_x \mu_x}{\sqrt{\mu^2 + \lambda^2} + |\lambda|}$$

with typically $f_x = 1.5$ and $f_y = 1.0$. There will also be an inflow variation due to any net aerodynamic moment on the rotor disk. The differential form of momentum theory gives

$$\Delta\lambda = \frac{f_m (-2C_{M_y} r \cos \psi + 2C_{M_x} r \sin \psi)}{\sqrt{\mu^2 / x_f^2 + \lambda^2 / k_x^2}}$$

including an empirical factor f_m .

With twin-rotor aircraft it is also necessary to account for the rotor-rotor aerodynamic interference in the wake-induced inflow velocities. The induced velocity at each rotor will be expressed as a linear combination of the isolated rotor induced velocity. Let λ_{i1} and λ_{i2} be the trim induced velocity of the two isolated rotors, calculated as above. Then the trim inflow ratios are

$$\lambda_1 = \mu_{z_1} + \lambda_{i_1} + \kappa_{12} \frac{(S\bar{R})_2}{(S\bar{R})_1} \lambda_{i_2}$$

$$\lambda_2 = \mu_{z_2} + \lambda_{i_2} + \kappa_{21} \frac{(S\bar{R})_1}{(S\bar{R})_2} \lambda_{i_1}$$

Here κ_{12} and κ_{21} are the rotor-rotor aerodynamic interference factors. Separate values are used for the interference factors in hover and forward flight, with a linear variation from $\mu = 0.05$ to 0.10 .

In summary, the isolated rotor mean induced velocity is calculated from the advance ratio and thrust,

$$\lambda_i = f_{GE} \lambda_{i,GE} (\vec{\mu}, c_T)$$

where $f_{GE} = 1$ out of ground effect. Including the rotor-rotor interference and the linearly varying induced velocity components, the inflow ratios are then

$$\begin{aligned} \lambda_i &= \mu_{z_i} + \lambda_{i_1} + \kappa_{12} \frac{(S\bar{R})_2}{(S\bar{R})_1} \lambda_{i_2} \\ &\quad + (\lambda_{i_1} k_x - \cos \psi + \lambda_{i_2} k_y - \sin \psi) \\ &\quad + \frac{c_m (-2Cm_y \cos \psi + 2Cm_x \sin \psi)}{\sqrt{\mu^2/k_x^2 + \lambda^2/k_{2n}^2}} \end{aligned}$$

$$\begin{aligned}
 \lambda_2 = & \lambda_{z_2} + \lambda_{i_2} + k_{z_1} \frac{(S_R)}{(S_R)_2} \lambda_{i_1} \\
 & + (\lambda_{i_2} k_x r \cos \psi + \lambda_{i_2} k_y r \sin \psi) \\
 & + \frac{S_m (-2c_{m_y} r \cos \psi + 2c_{m_x} r \sin \psi)}{\sqrt{\mu^2/k_x^2 + \lambda^2/k_{x_1}^2}}
 \end{aligned}$$

for rotor #1 and rotor #2.

2.4.4 Section aerodynamic characteristics. - The section aerodynamic characteristics required are the static lift, drag, and moment coefficients as a function of angle of attack and Mach number: $c_l(\alpha, M)$, $c_d(\alpha, M)$, and $c_m(\alpha, M)$. Most often rotor loads analyses use two-dimensional airfoil test data in tabular form. The aerodynamic description of the blade also requires θ_{ZL} , the zero lift angle of the section relative to the structural/inertial principal axis at pitch angle θ ; and x_A , the distance the aerodynamic center (in normal flow) is behind the elastic axis. The strict definition of θ_{ZL} is actually the pitch of the axis corresponding to $\alpha = 0$ in the airfoil data used. Similarly the strict definition of x_A is simply the location of the axis about which the moment data c_m are given. It is convenient to use the zero lift axis and the aerodynamic center, but the most important consideration is that the definitions of θ_{ZL} and x_A be consistent with the zero angle of attack and moment axis definitions in the airfoil data used.

The angle of attack α is defined in the range -180 to 180, with the same sense as θ . The lift, drag, and moment as a function of angle of attack are defined as in two-dimensional airfoil tests, where α is varied by pitching the airfoil; and the lift is always positive vertically; the drag is positive in the direction of the free stream; and the moment is positive nose up. For the rotor blade in reverse flow then ($u_T < 0$), a positive pitch θ or

positive (down) normal velocity u_p gives an angle of attack near -180; which gives positive c_ℓ and c_d ; which are down lift L and forward acting drag D . The section moment is given about a fixed axis of the section. In reverse flow the aerodynamic center shifts to near the three-quarter chord (from near the quarter chord in normal flow) so it is expected that the c_m data will show a nose up moment contribution of $\Delta M = \frac{c}{2}L$ or $\Delta c_m = \frac{1}{2}c_\ell$ in reverse flow (see fig. 12).

The steady, two-dimensional airfoil data (c_ℓ , c_d , and c_m as a function of α , M , and r) will be used in tables of the following form. The data will be defined at a finite set of angle of attack points. To facilitate interpolation, these points will consist of several groups, with the same angle of attack increment within each group. Then the set of angle of attack points can be specified by the α at the boundaries between the groups, and the indices of these points: N_a , α_{n1} to α_{nN_a} , and n_1 to n_{N_a} (for N_a-1 groups). The organization will be similar for the variation with Mach number. For the radial variation, the blade will be divided into segments with the same section, defined by the r at the boundaries: N_r , and r_1 to r_{N_r+1} for N_r segments. Hence the data set for the lift coefficient has the form

$$N_a, n_k \text{ (} k = 1 \text{ to } N_a \text{)}, \alpha_k \text{ (} k = 1 \text{ to } N_a \text{)}$$

$$N_m, n_k \text{ (} k = 1 \text{ to } N_m \text{)}, M_k \text{ (} k = 1 \text{ to } N_m \text{)}$$

$$N_r, r_k \text{ (} k = 1 \text{ to } N_r + 1 \text{)}$$

$$c_\ell(i) \text{ for } i = (j_r-1)n_{N_a}n_{N_m} + (j_m-1)n_{N_a} + j_\ell.$$

$$((j_a = 1 \text{ to } n_{N_a}), j_m = 1 \text{ to } n_{N_m}), j_r = 1 \text{ to } N_r)$$

and similarly for the drag and moment coefficient data sets.

The data will be linearly interpolated over angle of attack and Mach number. The boundary point definitions determine the values of α and M for all points in the data set. Consider the angle of attack variation. The boundary point definition of α_{ni} for $i = 1$ to N_a implies that the angles of attack for points between the boundaries α_{ni} and $\alpha_{n,i+1}$ are

$$\alpha_{n,i+j} = \alpha_{ni} + j \frac{\alpha_{n,i+1} - \alpha_{ni}}{n_{i+1} - n_i}$$

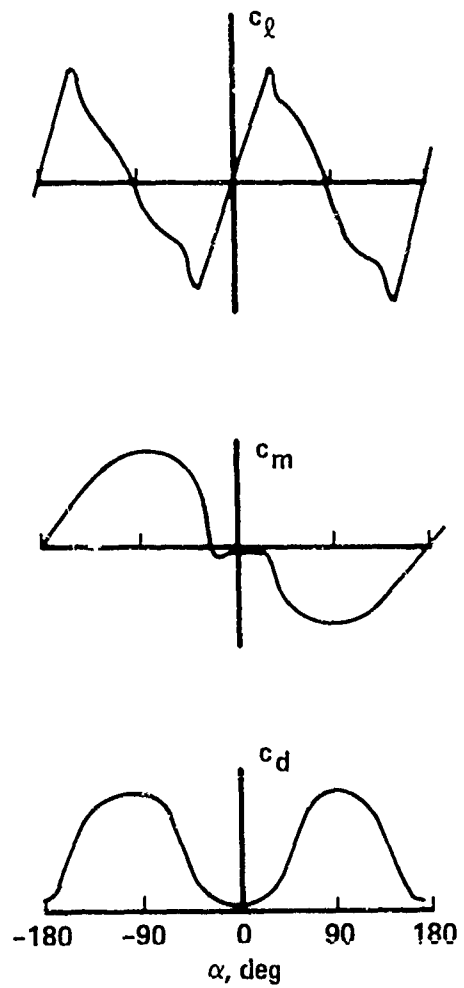


Figure 12. Sketch of section aerodynamic characteristics.

for $j = 0$ to $(n_{i+1} - n_i)$. Hence given α , we search for i such that

$$\alpha_{n_i} \leq \alpha \leq \alpha_{n_{i+1}}$$

It follows immediately that

$$\alpha_j \leq \alpha \leq \alpha_{j+1}$$

where

$$j = n_i + \left[\frac{\alpha - \alpha_{n_i}}{\Delta \alpha} \right]$$

$$\alpha_j = \alpha_{n_i} + (j - n_i) \Delta \alpha$$

$$\Delta \alpha = \frac{\alpha_{n_{i+1}} - \alpha_{n_i}}{n_{i+1} - n_i}$$

([a] means the greatest integer in a ; i.e., integer arithmetic). With a function c defined at α_j and at α_{j+1} , linear interpolation then gives

$$c = \alpha_j c_{j\alpha} + \alpha_{j+1} c_{j+1\alpha}$$

where

$$\begin{aligned} \alpha_{j+1} &= \frac{\alpha - \alpha_j}{\alpha_{j+1} - \alpha_j} = \frac{1}{\Delta \alpha} (\alpha - \alpha_j) = \frac{1}{\Delta \alpha} (\alpha - \alpha_{n_i}) - (j - n_i) \\ &= \frac{\alpha - \alpha_{n_i}}{\Delta \alpha} - \left[\frac{\alpha - \alpha_{n_i}}{\Delta \alpha} \right] \end{aligned}$$

and

$$\alpha_j = \frac{\alpha_{j+1} - \alpha}{\alpha_{j+1} - \alpha_j} = \frac{\alpha_j + \Delta \alpha - \alpha}{\Delta \alpha} = 1 - \alpha_{j+1}$$

If $\alpha < \alpha_1$, set $j_a = 1$ and $a_{j+1} = 0$; if $\alpha > \alpha_{n_{N_a}}$, set $j_a = n_{N_a} - 1$ and $a_{j+1} = 1$. Similarly, for a given Mach number M search for k such that

$$M_{n_k} \leq M \leq M_{n_{k+1}}$$

then calculate

$$j_m = n_k + \left[\frac{M - M_{n_k}}{\Delta M} \right]$$

$$\Delta M = \frac{M_{n_{k+1}} - M_{n_k}}{n_{k+1} - n_k}$$

$$m_{j+1} = \frac{M - M_{n_k}}{\Delta M} - \left[\frac{M - M_{n_k}}{\Delta M} \right]$$

$$m_j = 1 - m_{j+1}$$

If $M < M_1$, set $j_m = 1$ and $m_{j+1} = 0$; if $M > M_{n_{N_m}}$, set $j_m = n_{N_m} - 1$ and $m_{j+1} = 1$. The appropriate radial station is determined by searching for j_r such that

$$r_{j_r} < r \leq r_{j_r+1}$$

The aerodynamic coefficient is evaluated at the four corners, and then the interpolated value is

$$c = \alpha_j m_j c(j_a, j_m, j_r) + \alpha_j m_{j+1} c(j_a, j_m+1, j_r) \\ + \alpha_{j+1} m_j c(j_a+1, j_m, j_r) + \alpha_{j+1} m_{j+1} c(j_a+1, j_m+1, j_r)$$

2.4.5 *Tip flow corrections*.- Three dimensional flow effects at the blade tips significantly alter the wing loading. Principally it is necessary to correct the blade element theory section loading calculation for the lift reduction and compressibility relief near the tip. The standard tip loss correction assumes that the blade has drag but no lift outboard of radial station $r = B$. Hence for a radial segment extending from r_i to r_{i+1} , the lift coefficient is multiplied by the factor

$$\max(0, \min(1, \frac{B - r_i}{r_{i+1} - r_i}))$$

The moment and drag coefficients are not altered. For the tip loss factor $B = .97$ can be used, or

$$B = 1 - \frac{\sqrt{2C_T}}{N}$$

Alternatively, the tip losses can be accounted for by multiplying the blade element theory lift by the Prandtl function:

$$F = \frac{2}{\pi} \cos^{-1} e^{(r-1)N/2\lambda_0}$$

An effective tip loss factor can be evaluated from this function:

$$B = 1 - \frac{\lambda_0}{N} 2 \ln 2$$

hence

$$\begin{aligned} F &= \frac{2}{\pi} \cos^{-1} e^{-(\ln 2)(1-r)/(1-B)} \\ &= \frac{2}{\pi} \cos^{-1} \left(\frac{1}{2}\right)^{(1-r)/(1-B)} \end{aligned}$$

The three dimensional flow at the blade tip increases the critical Mach number of the tip sections, compared to the two dimensional flow characteristics. This compressible tip relief may be accounted for by reducing the effective section Mach number by the factor

$$f_M = \frac{M_{\text{eff}}}{M}$$

The factor f_M must be specified at each blade station, for the lift, drag, and moment.

Swept and tapered tip planforms are defined in the present analysis by the blade chord, aerodynamic center, pitch angle and zero lift angle, and center of gravity distributions (c , x_A , θ and θ_{ZL} , and x_T). Any sweep of the blade elastic axis at the tip is neglected however. The tip planform should also be considered in choosing the tip loss factor and compressible tip relief factors for the rotor blade.

2.4.6 Yawed flow correction.- Yawed flow over the blade section may be accounted for using the equivalence assumption for swept wings: that the yawed section drag coefficient is given by two-dimensional airfoil characteristics, and the normal section lift coefficient is not influenced by yawed flow below stall. Since the wing viewed in a frame moving spanwise at a velocity $V \sin \Lambda$ (where V is the wing velocity, yawed at angle Λ) is equivalent to an unyawed wing with free stream velocity $V \cos \Lambda$, except for changes in the boundary layer, there should then be no effect of spanwise flow on the loading below stall. Accounting for the effective dynamic pressure and angle of attack of the yawed section relative to the normal section leads to

$$c_L(\alpha) = c_{L20} (\alpha \cos^2 \Lambda) / \cos^2 \Lambda$$

$$c_d(\alpha) = c_{d20} (\alpha \cos \Lambda) / \cos \Lambda$$

$$c_m(\alpha) = c_{m20} (\alpha \cos^2 \Lambda)$$

for the section aerodynamic coefficients in terms of two-dimensional airfoil characteristics. These results are largely verified by the experimental data for yawed wings. The section yaw angle is given by

$$\cos \lambda = \sqrt{\frac{u_r^2 + u_p^2}{u_r^2 + u_p^2 + u_R^2}}$$

In reverse flow ($|\alpha| > 90^\circ$) the angle of attack correction is

$$\alpha_y = [(\alpha - 180^\circ) \cos \lambda + 180^\circ] \operatorname{sign} \alpha$$

for the drag, and

$$\alpha_y = [(\alpha - 180^\circ) \cos^2 \lambda + 180^\circ] \operatorname{sign} \alpha$$

for the lift and moment.

2.4.7 Dynamic stall model. - Dynamic stall is characterized by a delay in the occurrence of separated flow due to the blade motion, and high transient loads induced by a vortex shed from the leading edge when stall does occur. These features are modelled by the following procedure adapted from reference 8. McCroskey (reference 9), and Beddoes (reference 10) have found that the dynamic stall delay correlates fairly well in terms of the normalized time constant $\tau = \Delta t V/c$. Their results for lift and moment stall are

	τ_L	τ_M
McCroskey	4.3 ± 0.5	2.8 ± 0.2
Beddoes	5.4 ± 0.6	2.45 ± 0.5

or approximately $\tau_L = 4.8$ and $\tau_M = 2.7$ (a constant τ_D is also required for the drag stall delay). Hence the section lift will be evaluated at the delayed angle of attack

$$\alpha_d = \alpha(\psi - \Delta\psi_L) \approx \alpha - \Delta\psi_L \dot{\alpha}$$

where $\Delta\psi_L = \Omega\Delta t_L = \tau_L c / |\mu_T|$ (radians). A maximum value of the angle increment $(\alpha - \alpha_d)$ should be specified in order to avoid difficulties at small values of u_T . Thus

$$\alpha_d = \alpha - \min(\tau_L |\frac{\dot{\alpha}c}{u_T}|, \Delta\alpha_{\text{max delay}}) \text{ sign } \dot{\alpha}$$

is used. The lift coefficient below stall should not be affected by the dynamic stall model, rather the stall delay should extend the linear range above the static stall angle of attack. Hence the corrected lift coefficient takes the form

$$c_L = \frac{\alpha}{\alpha_d} (c_{L2D}(\alpha_d) - c_{L2D}(0)) + c_{L2D}(0) + \Delta c_L$$

Including the yawed flow correction this becomes

$$c_L = \frac{1}{\cos^2 \Lambda} \left[\frac{\alpha}{\alpha_d} (c_{L2D}(\alpha_d \cos^2 \Lambda) - c_{L2D}(0)) + c_{L2D}(0) \right] + \Delta c_L$$

Here Δc_L is the lift increment due to the loading edge vortex used at dynamic stall, which is discussed below. Similarly a delayed angle of attack is calculated for the drag and moment from appropriate time constants τ_D and τ_M , and the corrected section aerodynamic coefficients are

$$c_d = \frac{1}{\cos \lambda} c_{d20} (\alpha_s \cos \lambda) + \Delta c_d$$

$$c_m = c_{m20} (\alpha_s \cos^2 \lambda) + \Delta c_m$$

including the yawed flow correction. In reverse flow ($90 - |\alpha| < 0$) the lift coefficient correction should be

$$c_d = \frac{1}{\cos^2 \lambda} \left\{ \left(c_{d20} \left[(|\alpha_d| - 180^\circ) \cos^2 \lambda + 180^\circ \right] \operatorname{sign} \alpha_d \right) - c_{d20} (180^\circ) \right\} \frac{(|\alpha| - 180^\circ) \operatorname{sign} \alpha}{(|\alpha_d| - 180^\circ) \operatorname{sign} \alpha_d} + c_{d20} (180^\circ) \} + \Delta c_d$$

and for the drag and moment coefficients

$$c_d = \frac{1}{\cos \lambda} c_{d20} \left[(|\alpha_d| - 180^\circ) \cos \lambda + 180^\circ \right] \operatorname{sign} \alpha_d + \Delta c_d$$

$$c_m = c_{m20} \left[(|\alpha_d| - 180^\circ) \cos^2 \lambda + 180^\circ \right] \operatorname{sign} \alpha_d + \Delta c_m$$

When the blade section angle of attack reaches the dynamic stall angle α_{ds} , a leading edge vortex is shed. As this vortex passes aft over the airfoil upper surface it induces large transient loads. The experimental data

of reference 11 show that the peak incremental aerodynamic coefficients depend on the pitch rate at the instant of stall, $\dot{\alpha} c/V$, approximately as follows:

$$\Delta C_{l_{\max}} = \begin{cases} \Delta c_{l_{ds}} (20 \dot{\alpha} c/V) & \dot{\alpha} c/V < .05 \\ \Delta c_{l_{ds}} & \dot{\alpha} c/V > .05 \end{cases}$$

$$\Delta C_m_{\max} = \begin{cases} 0 & \dot{\alpha} c/V < .02 \\ \Delta c_{m_{ds}} (33.3 \dot{\alpha} c/V - .667) & .02 < \dot{\alpha} c/V < .05 \\ \Delta c_{m_{ds}} & \dot{\alpha} c/V > .05 \end{cases}$$

$$\Delta C_d_{\max} = \begin{cases} \Delta c_{d_{ds}} (20 \dot{\alpha} c/V) & \dot{\alpha} c/V < .05 \\ \Delta c_{d_{ds}} & \dot{\alpha} c/V > .05 \end{cases}$$

with $\Delta c_{l_{ds}} = 2.0$ and $\Delta c_{m_{ds}} = -.65$. In the present model of the dynamic stall loads it is assumed that the incremental coefficients due to the shed vortex (Δc_l , Δc_m , and Δc_d) rise linearly to the above peak values in the small azimuth increment $\Delta\psi_{ds}$ (typically 10° to 15°), and then fall linearly to zero in the time $\Delta\psi_{ds}$ again. Hence the model involves impulsive lift and nose down moment increases when dynamic stall occurs, which produce the blade motion and loads characteristic of rotor stall. After these transient loads decay the blade section is assumed to be in deep stall, and dynamic stall is not allowed to occur again until the flow has reattached. Flow reattachment takes place when the angle of attack drops below the angle α_{re} . Generally a dynamic stall angle about three degrees above the static stall angle gives good results. Different values of α_{ds} , $\Delta\psi_{ds}$, and α_{re} can be used for the lift, drag, and moment characteristic if necessary to adequately model the dynamic stall of an airfoil. The calculation of the vortex induced lift in dynamic stall is outlined in figure 13. The drag and moment are calculated

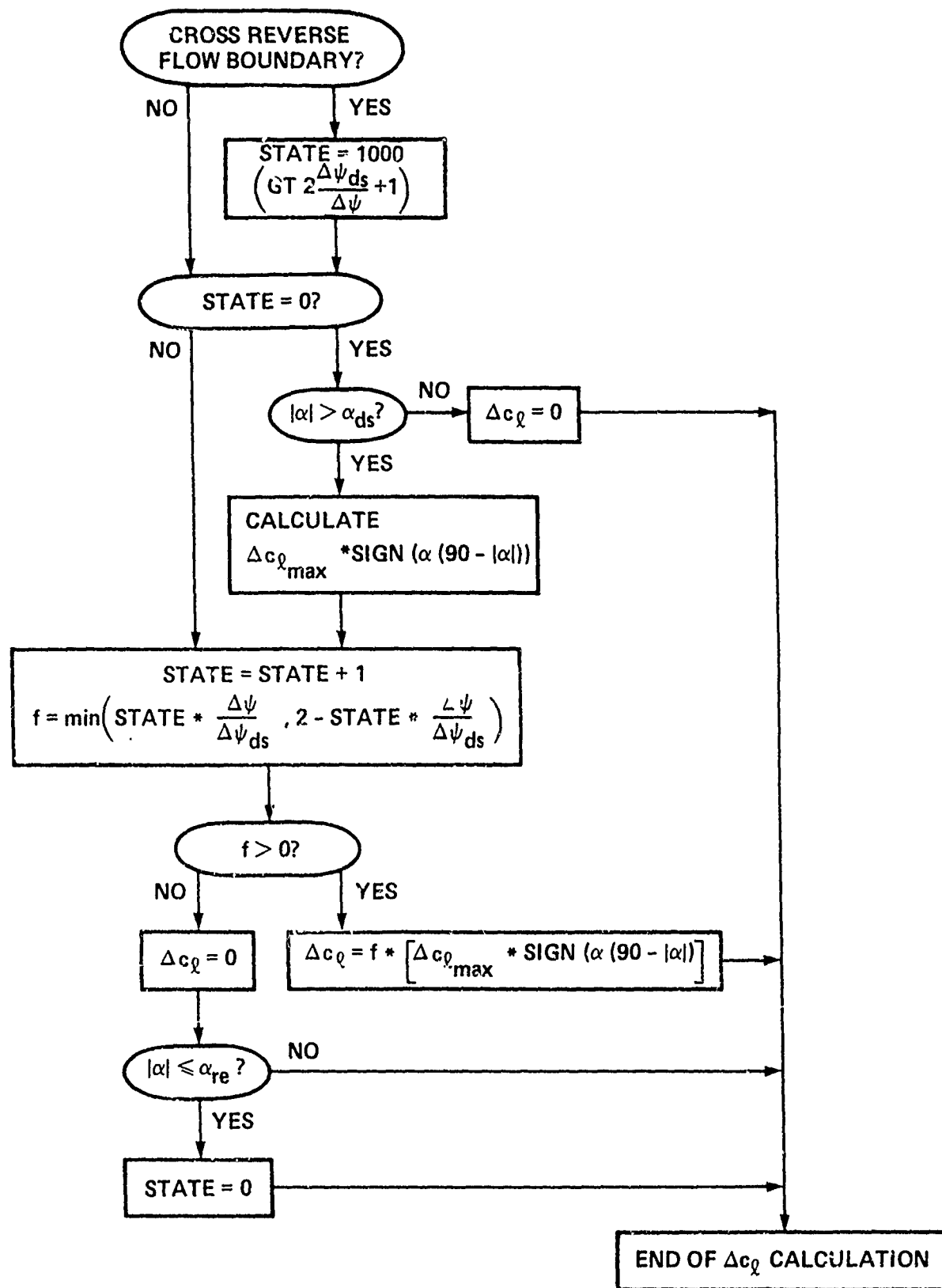


Figure 13. Outline of calculation of dynamic stall vortex-induced lift coefficient.

in a similar fashion, except that the drag is not multiplied by sign of $(\alpha - |\alpha|)$; and $1/2 \Delta c_d$ is added to the moment in reverse flow.

As an alternative dynamic stall model, consider that developed in references 12 to 14. They introduce an effective angle of attack of the form

$$\alpha_{dyn} = \alpha - \min(\tau_L \sqrt{|\frac{\alpha}{c_{L,T}}|}, \Delta \alpha_{max, delay}) \text{sign}\alpha$$

where τ_L is a function of Mach number and the airfoil section obtained from oscillating airfoil tests. This angle α_{dyn} can be used in place of α_d in the expression for c_d given above, with $\Delta c_d = 0$. Similar corrected angles of attack are calculated for the moment and drag coefficients, using appropriate factors τ_M and τ_D . For an NACA 0012 airfoil, reference 14 gives

$$\begin{aligned} \tau_L &= \max(0, \min(1.71, 2.16 - 2.81 M)) \\ \tau_M = \tau_D &= \max(0, \min(1.12, 1.71 - 2.98 M)) \end{aligned}$$

(in radians).

A no-stall model can be implemented by using for α_d the smaller of the actual angle of attack α and a maximum angle of attack α_{max} in the linear range (say 10°):

$$\alpha_d = \begin{cases} \min(|\alpha|, \alpha_{max}) \text{sign}\alpha & |\alpha| < 90^\circ \\ \max(|\alpha|, 180^\circ - \alpha_{max}) \text{sign}\alpha & |\alpha| > 90^\circ \end{cases}$$

The incremental coefficients (Δc_d , Δc_m , and Δc_d) should be set to zero as well.

In summary, the following procedure is used to calculate the section aerodynamic coefficients. First the Mach number correction for tip flow is applied: $M_{eff} = f_M M$. The section coefficients c_d , c_m , and $c_{L,T}$ are calculated from α , $\dot{\alpha}$, Λ , and M_{eff} : first the yawed/delayed effective angle of attack is calculated; then c_{L2D} , c_{d2D} and c_{m2D} for α_{eff} and M_{eff} are obtained from two-dimensional steady airfoil tables; c_{L2D} at $\alpha = 0$ or 180° is also required;

finally the section coefficients are evaluated. Next the dynamic stall vortex loads Δc_l , Δc_d , and Δc_m are evaluated from α and $\dot{\alpha}$. Finally the tip loss correction is applied to the lift coefficient.

The aeroelastic analysis (see section 6.1.4) requires the derivatives of the section coefficients with respect to angle of attack and Mach number. These derivatives are evaluated by applying the above procedure with small increments in α and M (not M_{eff}). For the purpose of evaluating these derivatives, $\dot{\alpha}$, Λ , and the dynamic stall vortex loads are held constant.

2.4.8 Unsteady lift and moment. - The thin airfoil theory result for the unsteady aerodynamic lift and moment about the pitch axis for the rotary wing is

$$\frac{L_{us}}{ac} = \pm \frac{c}{4} VB \left(1 + 2 \frac{x_{Ac}}{c}\right) \pm \frac{c}{8} (\dot{w} + u_R w') \\ \frac{M_{us}}{ac} = \mp \frac{c^2}{32} VB \left(1 + 4 \frac{x_{Ac}}{c}\right)^2 \mp \frac{c^2}{32} (\dot{w} + u_R w')(1 + 4 \frac{x_{Ac}}{c})$$

where x_{Ac} is the distance between the aerodynamic center and the elastic axis:

$$x_{Ac} = \begin{cases} x_{Ac} & \text{normal flow} \\ -(x_{Ac} + \frac{c}{2}) & \text{reverse flow} \end{cases}$$

(here x_{AC} must in fact be the position of the aerodynamic center); and in the double sign the upper one is for normal flow and the lower one for reverse flow, $\pm = \text{sign}(V)$. Here $w = u_T \sin \theta - u_p \cos \theta$ is the upwash velocity normal to the blade surface (with no order c terms); $B = dw/dx$ is the gradient of the upwash along the chord, as due to a pitch rate; and $V = u_T \cos \theta + u_p \sin \theta$.

In this result the order c^2 lift and order c^3 moment terms have been neglected. The virtual mass terms (aerodynamic forces due to the section pitch and heave acceleration) can also be neglected. The sign changes in reverse flow have been accounted for in this result. Radial flow effects are included in the slender body pressure terms (from the radial derivative w') and in the contributions to the upwash w . The time derivative \dot{w} includes terms due to the time varying free stream. Corrections for real flow effects on the lift-curve slope and aerodynamic center have been included (thin airfoil theory gives $a = 2\pi$ and the aerodynamic center at the quarter chord).

For stalled flow, these unsteady aerodynamic forces can be set to zero ($L_{us} = M_{us} = 0$). The unsteady forces at high angle of attack are accounted for in the dynamic stall model for c_l , c_d , and c_m .

Finally, the velocities required for these unsteady aerodynamic forces are as follows:

$$V = u_T \cos \theta + u_p \sin \theta$$

$$\dot{\theta} = \dot{\theta} + \beta_G + \vec{r}_G \cdot (\vec{z}_G - \vec{x}_G)^* + u_R \theta'$$

and from $w = u_T \sin \theta - u_p \cos \theta$, $u_p = \dot{z} + u_R z' + u_{p_0}$, and $u_T = u_{T_0} + \dot{x} + u_R x'$, there follows

$$\begin{aligned} \dot{w} + u_R w' &= V \dot{\theta} + \dot{u}_T \sin \theta - \dot{u}_p \cos \theta \\ &\quad + u_R (V \theta' + u'_T \sin \theta - u'_p \cos \theta) \\ &= V(\dot{\theta} + u_R \theta') + (\dot{u}_T + u_R u'_T) \sin \theta \\ &\quad - (\dot{u}_p + u_R u'_p) \cos \theta \end{aligned}$$

$$\begin{aligned}
&= \nabla(\dot{\theta} + u_R \theta') \\
&\quad + \sin \theta (u_R + u_R \dot{x}' + \dot{u}_R x' + \ddot{x} + u_R + u_R \dot{x}' + u_R^2 x'') \\
&\quad - \cos \theta (u_R \dot{z}' + \dot{u}_R z' + \ddot{z} + u_R \dot{z}' + u_R^2 z'') \\
&= \nabla(\dot{\theta} + u_R \theta') + 2u_R \sin \theta \\
&\quad + (\ddot{x} + 2u_R \dot{x}' + \dot{u}_R x' + u_R^2 x'') \sin \theta \\
&\quad - (\ddot{z} + 2u_R \dot{z}' + \dot{u}_R z' + u_R^2 z'') \cos \theta \\
&= \nabla(\dot{\theta} + u_R \theta') + 2u_R \sin \theta \\
&\quad + 2u_R \sin \theta (\dot{\alpha}_z + \psi_s) + \dot{u}_R \sin \theta (\alpha_z + \psi_s) \\
&\quad - 2u_R \cos \theta \dot{\beta}_G - \dot{u}_R \cos \theta \beta_G \\
&\quad - 2u_R \vec{\tau} \cdot (\vec{z}_0 \vec{\tau} - \vec{x}_0 \vec{\tau})' \\
&\quad - \dot{u}_R \vec{\tau} \cdot (\vec{z}_0 \vec{\tau} - \vec{x}_0 \vec{\tau})' \\
&\quad - u_R^2 \vec{\tau} \cdot (\vec{z} \vec{\tau} - \vec{x} \vec{\tau})'' \\
&\quad + r \sin \theta (\ddot{\alpha}_z + \ddot{\psi}_s) - r \cos \theta \ddot{\beta}_G \\
&\quad - \vec{\tau} \cdot (\vec{z}_0 \vec{\tau} - \vec{x}_0 \vec{\tau})''
\end{aligned}$$

with $u_R = \mu_x \cos \psi - \mu_y \sin \psi$, and using

$$z' = \beta_G + \vec{\tau}_B \cdot (\vec{z}_0 \vec{\tau} - \vec{x}_0 \vec{\tau})'$$

$$x' = \alpha_z + \psi_s + \vec{\tau}_B \cdot (\vec{z}_0 \vec{\tau} - \vec{x}_0 \vec{\tau})'$$

2.4.9 *Circulation*.- The blade bound circulation is required for the wake induced velocity calculation:

$$\Gamma = \frac{1}{2} U_c c_s + \Gamma_{us}$$

Thin airfoil theory gives for the unsteady circulation (below stall)

$$\frac{\Gamma_{us}}{ac} = \frac{c}{4} B \left(1 + 2 \frac{x_{ac}}{c} \right)$$

(see section 2.4.8).

2.5 Environment

The aerodynamic environment of the helicopter is defined by the speed of sound c_s , and the air density ratio to sea level standard ρ/ρ_0 . (The blade Lock number is calculated using ρ_0 .) One approach is to input values of c_s and ρ/ρ_0 . Alternatively these parameters can be calculated from the altitude h for a standard day; or from the pressure altitude and temperature τ .

For a constant temperature lapse rate, the density ratio and speed of sound are obtained from the following expressions.

$$\frac{T_s}{T_0} = 1 - \frac{h}{T_s/3}$$

$$\frac{T}{T_0} = \begin{cases} T_s/T_0 & \text{standard day} \\ (\tau_0 + \tau)/\tau_0 & \text{given temperature} \end{cases}$$

$$\frac{\rho}{\rho_0} = \left(\frac{T_s}{T_0} \right)^{g/3R} \left(\frac{T}{T_0} \right)^{-1}$$

$$c_s = c_{s0} \left(\frac{T}{T_0} \right)^{\frac{1}{2}}$$

For the case of temperature and altitude specified, the density altitude is

$$h_d = \frac{T_0}{g} \left(1 - \left(\frac{g}{g_0} \right)^{\frac{1}{g/\xi R - 1}} \right)$$

Alternatively, the air density and temperature can be specified directly. Then the equivalent altitude can be obtained from

$$h_e = \frac{T_0}{g} \left(1 - \left(\frac{g}{g_0} \frac{T}{T_0} \right)^{\frac{1}{g/\xi R}} \right)$$

The required constants are given in the table below.

<u>Constants</u>	<u>English units</u>	<u>SI units</u>
dimension h	ft	m
dimension τ	$^{\circ}\text{F}$	$^{\circ}\text{C}$
$g/\xi R$	5.256115	
$(g/\xi R - 1)^{-1}$	0.234956	
T_0/ξ	145442 ft	44330.8 m
T_0	518.67 $^{\circ}\text{R}$	288.15 $^{\circ}\text{K}$
T_1	459.67 $^{\circ}\text{R}$	273.15 $^{\circ}\text{K}$
c_s_0	1116.45 ft/sec	340.294 m/sec
g	32.17405 ft/sec 2	9.80665 m/sec 2
ρ_0	.002378 slug/ft 3	1.225 kg/m 3
$(g/\xi R)^{-1}$	0.190255	

2.6 Normalization Parameters

It has been the practice here to deal with dimensionless quantities based on the air density, rotor speed, and rotor radius (ρ , Ω , and R). In addition, the equations of motion, the inertial coefficients, and the aerodynamic forces have been normalized using the following parameters: I_b , a characteristic moment of inertia of the blade; c_m , the blade mean chord; and a , the blade two-dimensional lift-curve slope. The values of these parameters have no influence on the numerical problem and its dimensional solution; they only affect the values of normalized, dimensionless quantities. It is convenient to use the blade Lock number γ and the rotor solidity σ as primary parameters. Then I_b and c_m are obtained from

$$I_b = \frac{g \sigma c_m R^4}{\gamma}$$

$$c_m = \frac{\pi}{N} \sigma R$$

For this purpose, the lift curve slope is set to a value of $a = 5.7$. The Lock number will be defined for standard sea-level conditions (γ_0); then $\gamma = \gamma_0 (\rho/\rho_0)$.

3. ROTOR WAKE ANALYSIS

3.1 Nonuniform Wake-Induced Velocity

3.1.1 *Rotor vortex wake.*— Conservation of vorticity on a three-dimensional wing requires that the bound circulation is trailed into the wake from the blade tip and root. Radial variation of the bound circulation produces trailed vorticity in the wake, parallel to the local free stream direction at the instant it leaves the blade. Azimuthal variation of the bound circulation will produce shed vorticity, oriented radially in the wake. The strength of the trailed and shed vorticity is determined by the radial and azimuthal derivatives of the bound circulation at the time the wake element left the blade. The lift and circulation are concentrated at the tip of the rotating wing, due to the larger dynamic pressure there. Consequently the trailed vorticity strength is high at the outer edge of the rotor wake, and the vortex sheet quickly rolls up into a concentrated tip vortex. The formation of this tip vortex is influenced by the blade tip geometry. With square tips, much of the roll up has occurred by the time the vortex leaves the trailing edge. The rolled up tip vortex quickly attains a strength nearly equal to the maximum bound circulation of the blade. The tip vortex has a small core radius, depending on the blade geometry and loading. The vorticity in the tip vortex is distributed over a small but finite region, called the vortex core, due to the viscosity of the fluid. The vortex core radius is defined at the maximum tangential velocity. The vortex core is an important factor in the wake induced velocity, since it limits the maximum velocity induced near a tip vortex. Only a limited amount of data on the vortex core radius is available, particularly for rotary wings. There is an inboard vortex sheet of trailed vorticity in the wake, with opposite sign as the tip vortex. Since the gradient of the bound circulation is low on the inboard portion of the blade, the root vortex is generally much weaker and more diffuse than the tip vortex.

The trailed and shed vorticity of the rotor wake is created in the flow field as the blades rotate, and then convected with the local velocity of the fluid. This local velocity consists of the free stream velocity, and the wake self-induced velocity. The wake is transported downward, normal to the

disk plane, by a combination of the mean wake induced velocity and the free stream velocity. The wake is transported aft of the rotor disk by the inplane component of the free stream velocity. The self-induced velocity of the wake also produces substantial distortion of the vortex filaments as they are convected with the local flow. Thus the wake geometry basically consists of distorted interlocking helices, one behind each blade, skewed aft in forward flight.

The strong concentrated tip vortices trailed in helices from each blade are the dominant feature of the rotor wake. Due to its rotation, a rotor blade encounters the tip vortex from the preceding blade in both hover and forward flight. These tip vortices produce a highly nonuniform flow field through which the blades must pass. In hover the tip vortex is convected downward only slightly until after it encounters the next blade. The vortex produces a large variation in the tip loading on the following blade therefore, with a substantial influence on the rotor hover performance. In forward flight the rotor wake is convected downstream, so the tip vortices are swept past the entire rotor disk instead of remaining in the tip region. The close vortex/blade encounters occur primarily on the sides of the disk, where the blades sweep over the vortices. The resulting large azimuthal variation in the induced velocity produces a large higher harmonic content of the blade loading. Nonuniform inflow is thus an important factor in the vibration, loads, and noise of the rotor in forward flight. In a tandem helicopter, the rear rotor also encounters the wake of the front rotor.

For close vortex/blade encounters, the induced loading varies rapidly along the blade span. Lifting line theory does not give an accurate prediction of such loading. Thus lifting surface theory is required to accurately estimate the vortex-induced loads on a rotary wing. The most economical approach is to use lifting line theory with a correction factor for close vortex/blade encounters, based on a lifting surface solution for an infinite aspect-ratio, nonrotating wing encountering a straight, infinite, constant-strength free vortex. In the present analysis this correction will be incorporated as a factor reducing the induced velocity as required to obtain the correct loading by lifting line theory. Note however that with this approach the actual blade angle of attack at vortex/blade interactions will

be larger than calculated for the lifting line theory loading solution. Direct application of lifting surface theory to the rotary wing is usually impractical with current computation techniques and machines. An examination of measured rotor airloads indicates that the vortex induced loading is generally high when the blade first encounters a vortex, but decreases as the blade sweeps over the vortex. There is evidently some phenomenon limiting the loads (see reference 15 to 17). Local flow separation due to the high vortex-induced radial pressure gradients on the blade appears at present to be the most likely explanation for the reduction in loading after the initial encounter. Bursting of the vortex core induced by the blade is also a possibility. Another possibility is that the vortex interacts with the trailed wake it induces behind the blade, with the effect of diffusing the circulation in the vortex. Note that the latter two phenomena, involving a change in the vortex itself, will also influence the loading if the vortex encounters yet another blade of the rotor. Following reference 16, the phenomenon limiting vortex induced loads after the initial encounter will be modelled by increasing the core radius of a segment after it encounters the blade, with upstream propagation along the vortex to produce the loads reduction. An increase in core size is a convenient means to reduce the influence of the vortex; the exact physical explanation for this phenomenon is at present speculative.

A possible model for the tip vortex viscous core is solid body rotation, which implies that all the vorticity is concentrated within the core radius r_c (defined at the point of maximum tangential velocity). Measured vortex velocity distributions show that the maximum tangential velocity is much less than $\Gamma/2\pi r_c$, implying that a substantial fraction of the vorticity is outside the core radius. Reference 16 suggests using a circulation distribution

$$\gamma = \Gamma \frac{r^2}{r^2 + r_c^2}$$

based on measured velocity distributions of vortices from nonrotating wings; the corresponding vorticity distribution is

$$\zeta = \frac{\Gamma}{\pi r_c^2} \left(\frac{r_c^2}{r^2 + r_c^2} \right)^2$$

where r is the distance from the vortex line. In this case half the vorticity is outside the core radius. Along a line at right angles to the vortex and a distance h above it (as in a blade/vortex intersection), this vorticity distribution produces a downwash with peak value

$$w_{max} = \frac{\Gamma}{4\pi \sqrt{h^2 + r_c^2}}$$

a distance $\sqrt{h^2 + r_c^2}$ either side of the intersection; compared to $w_{max} = \Gamma/4\pi h$ at a distance h from the intersection for a vortex with no core. (Note that as far as the downwash velocity is concerned, this core effect is equivalent to moving the vortex away from the blade, to an effective distance $h_e = \sqrt{h^2 + r_c^2}$; such a simple interpretation will be useful in the lifting surface correction.) The peak tangential velocity with this vorticity distribution is $\Gamma/4\pi r_c$, half the value obtained with all the vorticity concentrated within the core radius.

The rotor wake induced velocity is calculated by integrating the Biot-Savart law over the vortex elements in the rotor wake. The wake strength is determined by the radial and azimuthal variation of the bound circulation. For the wake geometry a simple assumed model, experimental measurements, or a calculated geometry can be used. With the helical geometry of the rotary wing wake, it is not possible to analytically evaluate the induced velocity, even if the self-induced distortion of the wake is neglected. A direct numerical integration of the Biot-Savart law is not satisfactory either, because the large variations in the induced velocity at close vortex/blade encounters requires a small integration step size for accurate results. It is most accurate and most efficient to calculate the rotor nonuniform inflow with the wake modelled using a set of discrete vortex elements. For each vortex element in the wake the induced velocity at a point in the flow

field is evaluated by an analytical expression, and the total induced velocity is obtained by trimming contributions from all elements. The tip vortex is well represented by a connected series of straight-line vortex segments. The inboard trailed and shed vorticity can be modelled using rectangular vortex sheets, or a lattice of discrete straight-line vortex segments (with a large effective core to limit the induced velocity close to individual line segments). A large core vortex line element might in some cases be a better model than a sheet for the inboard trailing vorticity, if the inboard wake has partially rolled up to form a root vortex. The inboard wake is less important to the nonuniform inflow calculation than the tip vortices, so a more approximate model may be used. The approximations involved in modelling the rotor wake using a set of discrete vortex elements include replacing the curvilinear geometry by a series of straight-line or planar segments; a simplified distribution of vorticity over the individual wake elements (linear variation, or even constant strength); and perhaps physical approximations such as the use of line elements to represent the inboard vortex sheet. The development of a practical model involves a balance between the accuracy and efficiency resulting from such approximations.

3.1.2 *Wake model*. - The blade bound circulation will be calculated at discrete points on the rotor disk radially and azimuthally. Assuming a linear variation of the bound circulation between these known points results in a wake model consisting of vortex sheet panels (see fig. 14). Assume that the blade bound circulation $\Gamma(r, \psi)$ is given at the radial stations r_i ($i = 1$ to M) and at the azimuthal stations $\psi_j = j\Delta\psi$ ($j = 1$ to J , $\Delta\psi = 2\pi/J$). Let ϕ be the age of vortex elements in the wake ($\phi_k = k\Delta\psi$, $k = 0$ to ∞). The strength of the trailed and shed vorticity of a wake element is determined by the bound circulation of the blade at the time the vorticity was created. Consider a wake panel of age $\phi = \phi_k$ to ϕ_{k+1} , arising from the blade between radial stations r_i and r_{i+1} (fig. 15). The strength of the vorticity in this panel is determined by the bound circulation at the time it was created, which is known at the four corners. The bound circulation corresponding to the panel leading edge is that at time $\psi - \phi_k$, where ψ is the current blade position (dimensionless time) and $\phi_k = k\Delta\psi$ is the age of the panel at the leading edge. The bound circulation corresponding to the

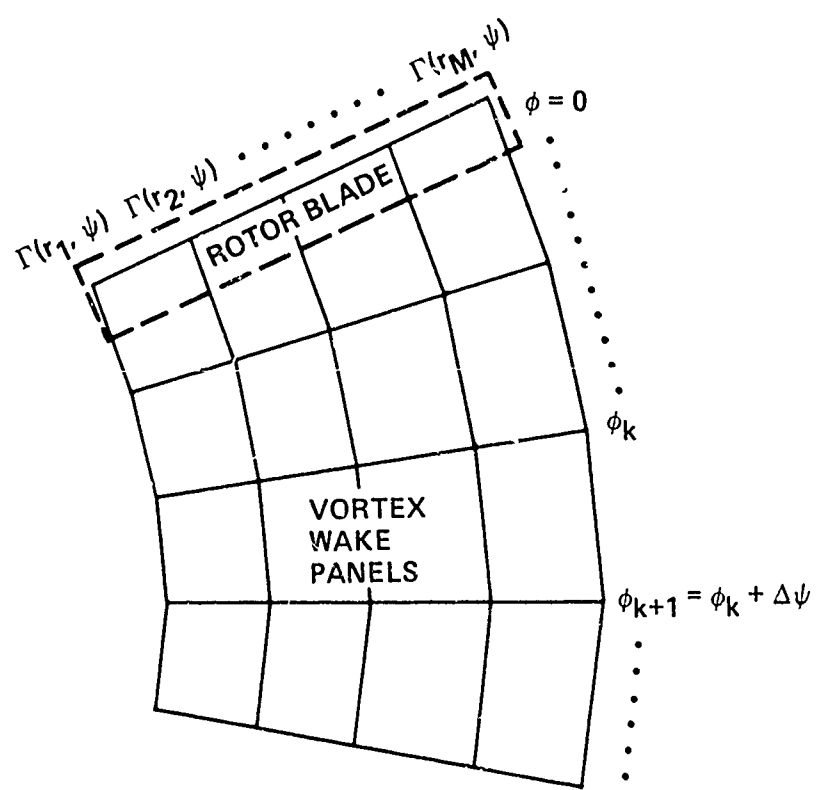


Figure 14. Wake model with bound circulation calculated at discrete points on rotor disk.

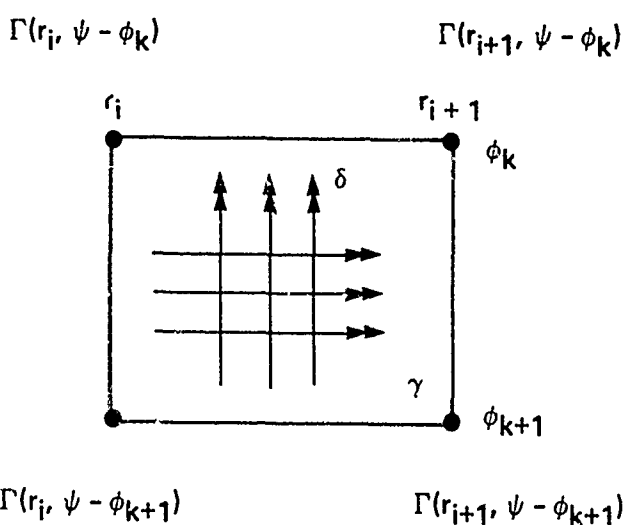


Figure 15. Vortex wake panel.

panel trailing edge is that at $\psi - \phi_{k+1}$, $\Delta\psi$ earlier than the leading edge. The difference between the bound circulation at r_i and r_{i+1} defines the trailed vorticity strength δ , which is constant radially along the panel assuming a linear variation of the bound circulation from r_i to r_{i+1} . When the bound circulation varies azimuthally however the trailed vorticity strength δ is different at the panel leading and trailing edges; a linear variation of δ in the direction of the trailed vorticity will be used. Similarly, the difference between the bound circulation at $\psi - \phi_k$ and $\psi - \phi_{k+1}$ defines the shed vorticity strength γ , which is constant azimuthally along the panel (for a linear azimuthal variation of the bound circulation) but varies linearly from the left to the right panel edges.

A vortex sheet panel in the wake may be economically approximated by shed and trailed line vortices located in the middle of the panel, with a large core to avoid the induced velocity singularity near a vortex line. A vortex lattice model of the rotor wake is produced by collapsing all the wake panels to such finite strength line segments. Since the line segments are in the center of the sheets, the points at which the induced velocity and bound circulation are evaluated lie at the midpoints of the vortex lattice grid, both radially and azimuthally. Positioning the collocation points midway between the trailed vortex elements (radially) is a standard practice of wing theory utilizing the vortex lattice wake model, in order to avoid the singularities at the lines; positioning the collocation points midway azimuthally is required to correctly obtain the unsteady aerodynamic effects of the shed wake (see ref. 18). Simply collapsing the shed and trailed vorticity in the wake panels to lines, the strength of the line segments will vary along their length as described above. The shed and trailed line segments will cross in the middle of the panel. As a further approximation, a stepped (piecewise constant) variation of strength can be used instead of the linear variation, with the jump in strength occurring at the center of the segment where it crosses the other vortex line. Such a vortex lattice wake model with constant strength line segments corresponds to a stepped distribution of the blade bound circulation, azimuthally and radially (with the jumps occurring midway between the points where the circulation is evaluated.)

The rotor vortex wake quickly rolls up at the outer edge to form a concentrated tip vortex. Because of the dominant role of the tip vortex in the wake flow field, it is important to model these rolled up tip vortices in the induced velocity calculation. The lesser role of the inboard wake vorticity also allows a more approximate model to be used for it. Let $\Gamma_{\max}(\psi)$ be the radial maximum of the blade bound circulation. It is assumed that in the far wake, where the rollup process is complete, that all of the bound circulation Γ_{\max} is concentrated in the tip vortex. The tip vortex will be modelled by a vortex line segment with a small but finite core radius. When Γ_{\max} varies azimuthally, the tip vortex strength varies along its length. Furthermore, the inboard portion of the wake will be modelled by a single sheet panel, with trailed and shed vorticity as described above. This far wake model may be viewed as corresponding to the circulation distribution sketched in figure 16. The linear variation from $\Gamma = 0$ at the root to $\Gamma = \Gamma_{\max}$ at the tip defines the single inboard sheet, and the sharp drop from Γ_{\max} to zero at the tip defines the tip vortex line. (This circulation distribution should not be associated with the actual bound circulation at the rotor blade. Rather it is an approximation for the vorticity distribution in the far wake, which is determined by the rollup process. Since an analysis of the rollup is not attempted here, the actual vorticity distribution over the inboard sheet is not known. An approximation involving constant strength determined by the known maximum bound circulation is appropriate therefore.) This far wake model is computationally efficient, since it depends only on the maximum bound circulation Γ_{\max} .

The rollup process may not be complete by the time the tip vortex encounters the following blade. The induced loads will be significantly lower if the tip vortex has strength less than the maximum bound circulation. Therefore the tip vortex rollup must be included in the wake model. Figure 16 sketches the radial circulation distribution assumed, which produces the model for the rolling up wake. The circulation goes from zero at the root to Γ_{\max} at radial station r_{RU} ; to $f_{RU}\Gamma_{\max}$ at the tip. Thus there is a line tip vortex of strength $f_{RU}\Gamma_{\max}$, and two inboard wake panels. The rollup process will take place over the wake from $\phi = 0$ to $\phi = \phi_{RU}$. The position of the maximum circulation and the rollup fraction will vary linearly

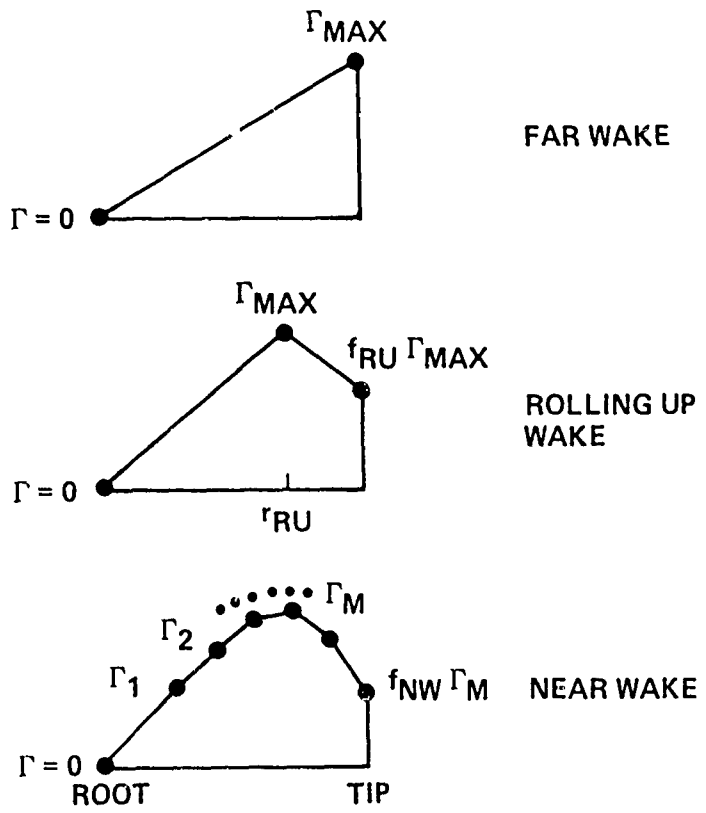


Figure 16. Equivalent circulation distribution for models of far wake, rolling up wake, and near wake.

from r_{RU} and f_{RU} at $\phi = 0$ to $r = 1$ and $f = 1$ at $\phi = \phi_{RU}$. An analysis of the rollup process is not part of the present work, so the parameters ϕ_{RU} , r_{RU} , and f_{RU} will be prescribed inputs to the calculation procedure. Note that the velocity induced by the rolling up wake will also depend only on the single bound circulation value Γ_{max} .

Just behind the reference blade, where the induced velocity is being calculated, it is the detailed radial and azimuthal variation of the wake vorticity which is important, not the rollup process (except for the influence of the rollup on the tip loads). Hence for the near wake of the reference blade the full vortex panel representation is retained. The corresponding radial distribution of the circulation is also sketched in figure 16 for the near wake; in this case it is the actual blade bound circulation distribution. The tip vortex rollup is often partially complete at the blade trailing edge, so a line vortex at the tip is included, with strength equal to a fraction f_{NW} of the calculated bound circulation at the most outboard radial station. The complete model of the rotor wake is shown in figure 17.

The very first panels of the near wake require special consideration. In order to correctly calculate the unsteady aerodynamic effects, the shed wake is stopped a quarter chord behind the bound vortex (ref. 19). The singularity near the side edges of the trailed vortex sheets presents a difficulty in calculating the induced velocity at a point due to the immediately adjacent panels. Thus if the induced velocity is to be calculated near a junction between two panels, they should be replaced by one panel with the collocation point well away from the edges of the single panel. This difficulty can be also avoided by using line vortex elements for the trailed vorticity in the near wake, or by moving the panel side edge away from the collocation point. Finally, the front edges of the individual panels should all be aligned with the bound vortex.

When calculating the induced velocity at points off the rotor blade, as at another rotor or for the airframe aerodynamics, the near wake model need not be used. Often calculating the induced velocity away from the rotor will require a consideration of more wake spirals than are needed for points on the rotor disk.

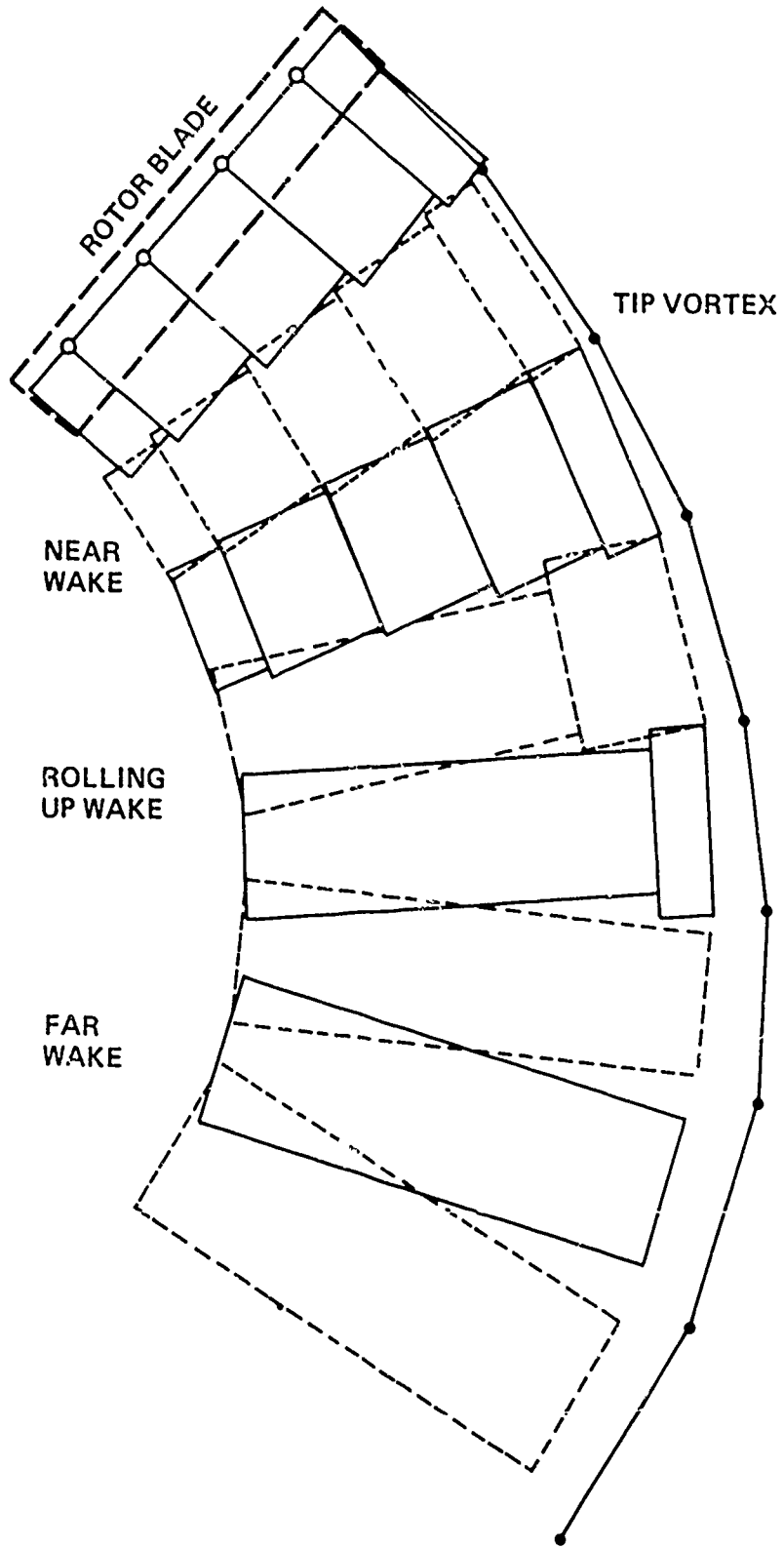


Figure 17. Sketch of wake model for nonuniform induced velocity calculation.

For computing the induced velocity, the tip vortices will be represented by a connected series of straight vortex line segments, with a small viscous core radius. Normally a linear variation of the strength along each segment will be used; a piecewise constant variation corresponding to a stepped bound circulation distribution is also possible. The inboard wake panels will be represented by planar, rectangular vortex sheets, with shed and trailed vorticity varying linearly along its length. For computational economy, the vortex sheets can be replaced by line segments in the middle of the sheets, with a large core radius (which in this case does not have physical significance, rather a viscous core is a convenient means for eliminating the singularity near a line used to represent a sheet element; unless the inboard trailed vorticity does rollup to form a diffuse root vortex). If the induced velocity is to be calculated near the side edge of a vortex sheet element, it can be replaced by a line element in order to avoid the edge velocity singularity.

3.1.3 *Geometry.* - A nonrotating tip path plane coordinate frame with origin at the rotor hub will be used for the induced velocity calculation. The solution process will iterate between the induced velocity calculation, and the harmonic blade motion and helicopter trim solution (using uniform inflow to start the cycle). Thus the hub plane orientation (S system) will be updated based on a new induced velocity estimate. In contrast, the tip path plane orientation is well defined by the helicopter or rotor trim, hence is less sensitive to changes in the induced velocity estimate. Also, the rotor wake geometry is simplest when defined relative to the tip path plane. The tip path plane tilt relative to the hub plane is given by the first harmonics of the tip deflection $z_{TIP} = \beta_G + \sum_i \vec{\tau}_B \cdot \vec{\eta}_i(1)$:

$$\beta_c = (\beta_G)_{lc} + \sum_i \beta_{lc}^{(i)} \vec{\tau}_B \cdot \vec{\eta}_i(1)$$

$$\beta_s = (\beta_G)_{ls} + \sum_i \beta_{ls}^{(i)} \vec{\tau}_B \cdot \vec{\eta}_i(1)$$

The rotation matrix

$$R_{TS} = \begin{bmatrix} 1 & 0 & \beta_c \\ 0 & 1 & \beta_s \\ -\beta_c & -\beta_s & 1 \end{bmatrix}$$

will transform position and velocity vectors from the shaft axes (S system) to the tip path plane axes (T system).

The induced velocity is required at the radial stations r_n along the rotor blade. The radial stations at which the induced velocity and bound circulation are evaluated will each be a subset of the blade loading radial stations, but the two sets need not be identical. From section 2.2.4, the position vector of the rotor blade is

$$\begin{aligned} \vec{r}_b &= \vec{t}_B [-x_{FA} + (r - r_{FA}) \delta_{FA_3} - r \psi_s - \vec{t}_B \cdot (\vec{z}_0 \vec{r} - \vec{x}_0 \vec{k})] \\ &\quad + \vec{j}_B r \\ &\quad + \vec{k}_B [-z_{FA} - (r - r_{FA}) \delta_{FA_2} + r (\beta_c + \delta_{FA_1}) + \vec{t}_B \cdot (\vec{z}_0 \vec{r} - \vec{x}_0 \vec{k})] \\ &= (\sin \psi \vec{t}_s - \cos \psi \vec{j}_s) [-x_{FA} + (r - r_{FA}) \delta_{FA_3} - r \psi_s \\ &\quad - \vec{t}_B \cdot (\vec{z}_0 \vec{r} - \vec{x}_0 \vec{k})] \\ &\quad + (\cos \psi \vec{t}_s + \sin \psi \vec{j}_s) r \\ &\quad + \vec{k}_B [-z_{FA} - (r - r_{FA}) \delta_{FA_2} + r (\beta_c + \delta_{FA_1}) + \vec{t}_B \cdot (\vec{z}_0 \vec{r} - \vec{x}_0 \vec{k})] \end{aligned}$$

Transforming to the tip path plane (neglecting second order terms) gives then

$$\begin{aligned}\vec{r}_b = & \vec{\tau}_T \left\{ \sin \psi [-x_{FA} + (r - r_{FA}) \delta_{FA_3} - r \psi_s - \vec{t}_B \cdot (\vec{z}_0 \vec{r} - \vec{x}_0 \vec{r})] + r \cos \psi \right\} \\ & + \vec{\gamma}_T \left\{ -\cos \psi [-x_{FA} + (r - r_{FA}) \delta_{FA_3} - r \psi_s - \vec{t}_B \cdot (\vec{z}_0 \vec{r} - \vec{x}_0 \vec{r})] + r \sin \psi \right\} \\ & + \vec{\tau}_T \left\{ -z_{FA} - (r - r_{FA}) \delta_{FA_2} + r (\beta_c + \delta_{FA_1}) + \vec{t}_B \cdot (\vec{z}_0 \vec{r} - \vec{x}_0 \vec{r}) \right. \\ & \quad \left. - r (\beta_c \cos \psi + \beta_s \sin \psi) \right\}\end{aligned}$$

The induced velocity is to be evaluated at the points $\vec{r}_b(r_n)$ along the rotor blade. It is useful in the computation of \vec{r}_b to have the option to suppress the inplane deflection, to suppress all harmonics except the mean, or to linearly interpolate the geometry between the root and the tip.

The wake induced velocity is also required at points in the flow field off the rotor disk:

- a. at the wing/body, horizontal tail, and vertical tail for the rotor/airframe aerodynamic interference;
- b. at the other rotor hub for rotor/rotor aerodynamic interference;
- c. at an arbitrary point in the flow field;
- d. and at the reference blade of the other rotor, for detailed rotor/rotor aerodynamic interference.

For the first two, only the mean value of the induced velocity will be used in the present analysis. The induced velocity distribution over the disk of the other rotor can be used in the present analysis only if the two rotors have the same rotational speed (see section 5.1.11); so for the single main rotor and tail rotor configuration the rotor/rotor interference can be accounted for only in terms of the induced velocity at the rotor hub. The position vector of the wing/body is

$$R_{TS} R_{SF} (-\vec{r}_k + \vec{r}_{we})$$

where \vec{r}_R and \vec{r}_{WB} are the position of the rotor hub and the wing/body center of action, in the body axes (F system). The vectors for the horizontal tail, vertical tail, and other rotor hub are similar. For the induced velocity of rotor #2, these vectors must be multiplied by R_1/R_2 . For the induced velocity at the disk of rotor #2 due to the wake of rotor #1, the position vector is

$$\begin{aligned}\vec{r}_{2/1} &= (R_{TS} R_{SF})_{\text{rotor } \#1} [-\vec{r}_{R1} + \vec{r}_{R2} \\ &\quad + \frac{R_2}{R_1} (R_{TS} R_{SF})_{\text{rotor } \#2}^T \vec{r}_{b2}(r_{n2}, \psi + \Delta\psi_{21})] \\ &= \vec{r}_{\text{other}} + R_{21} \vec{r}_{b2}(r_{n2}, \psi + \Delta\psi_{21})\end{aligned}$$

where $\Delta\psi_{21}$ is the azimuth angle of the reference blade of rotor #2 when $\psi = 0$ for rotor #1 (see section 5.1.5) and

$$R_{21} = (R_{TS} R_{SF})_{\text{rotor } \#1} (R_{TS} R_{SF})_{\text{other rotor}}^T \frac{\text{Rotator rotor.}}{R_{\text{two rotors}}}$$

The position vector for the induced velocity at the disk of rotor #1 due to the wake of rotor #2 is

$$\begin{aligned}\vec{r}_{1/2} &= \frac{R_1}{R_2} (R_{TS} R_{SF})_{\text{rotor } \#2} [-\vec{r}_{R2} + \vec{r}_{R1} \\ &\quad + (R_{TS} R_{SF})_{\text{rotor } \#1}^T \vec{r}_{b1}(r_{n1}, \psi - \Delta\psi_{21})] \\ &= \vec{r}_{\text{other}} + R_{21} \vec{r}_{b1}(r_{n1}, \psi - \Delta\psi_{21})\end{aligned}$$

If the rotor rotates clockwise it is necessary to change the sign of the \vec{r} 's component of \vec{r} (between the R_{TS} and R_{SF} rotation matrices).

The geometry of the tip vortex behind the reference blade will be defined by the vector $\vec{r}_w(\psi, \phi)$, where ψ is the present azimuth angle of the blade and ϕ is the age of the vortex element. The wake geometry is required at

the discrete azimuth positions $\psi_\lambda = \lambda \Delta\psi$ and wake ages $\phi_k = k \Delta\psi$, where λ ranges from 1 to J (one revolution of the blade, with $\Delta\psi = 2\pi/J$) and k ranges from zero to the specified number of wake spirals for the induced velocity calculation. The tip vortex geometry behind the other blades of the rotor can be obtained for \vec{r}_w at the appropriate azimuth angle. The tip vortex elements are created at the blade tip (\vec{r}_b at radial station $r = 1$), convected with the free stream velocity $\vec{\mu}$, and distorted by the self-induced velocity in the wake. The rotation of the wing together with convection by the free stream velocity produces the basic helical geometry of the rotor wake. As at the rotor disk, the induced velocity throughout the wake is highly nonuniform. The actual position of the wake elements, determined by the integral of the local convection velocity, is thus highly distorted from the basic helical form. The resulting wake geometry is

$$\vec{r}_w(\psi, \phi) = \vec{r}_b(\psi - \phi) + \phi \vec{\mu} + \vec{D}(\psi, \phi)$$

where $\vec{D}(\psi, \phi)$ is the distortion due to the wake self-induced velocity (note $\vec{D}(\psi, 0) = 0$) and the free stream convection velocity is

$$\vec{\mu} = R_{TS} \begin{pmatrix} \mu_x \\ -\mu_y \\ -\mu_z \end{pmatrix} = \begin{pmatrix} \mu_x - \beta_c \mu_z \\ -\mu_y - \beta_s \mu_z \\ -\mu_z - \beta_c \mu_x + \beta_s \mu_y \end{pmatrix}$$

relative to the tip path plane.

Similarly the geometry of the inboard wake sheet will be defined at the root and tip edges, trailing from the blade position \vec{r}_b at radial stations $r = r_{ROOT}$ and $r = 1$ respectively. The distortion \vec{D} will be different for the tip vortex and the inboard sheet. Because of the dominant role of the tip vortices, the most important information in the wake geometry is the tip

vortex position, and a less accurate definition of the inboard sheet geometry is often acceptable.

The induced velocity calculation may require the wake geometry beyond the point where the stored distortion ends. For this portion of the wake rigid geometry will be used. Consider the distortion $\vec{D}(\psi, \phi)$ when the age ϕ is greater than the age of the last element in the known distortion, ϕ_{last} = $K_{WG} \Delta\psi$. The wake geometry will be extrapolated from ϕ_{last} to ϕ , using only vertical convection due to the mean induced velocity:

$$\vec{D}(\psi, \phi) = \vec{D}(\psi - (\phi - \phi_{last}), \phi_{last}) - (\phi - \phi_{last}) k_z \vec{k}$$

Note that the azimuth angle of the blade at the time the wake element was created, $\psi - \phi$, has been held constant.

For the self-induced distortion of the rotor wake geometry, the following models are considered:

- a. rigid or prescribed wake, with contraction and two-stage convection;
- b. and a calculated free wake geometry (section 3.2).

In the rigid wake geometry it is assumed that all elements in the wake are convected downward by the mean induced velocity at the rotor disk, giving

$$\vec{D} = \begin{pmatrix} 0 \\ 0 \\ D_z \end{pmatrix}$$

relative to the tip path plane, where

$$D_z = -\phi \lambda_i$$

Note that this distortion is independent of the azimuth angle ψ . The convection velocity λ_i is the mean induced velocity at the rotor disk, including ground effect and rotor/rotor interference in general. This model can be generalized to a two-stage convection:

$$D_z = \begin{cases} -K_1 \phi & \phi < \frac{\pi}{N} \\ -K_1 \frac{\pi}{N} - K_2 (\phi - \frac{\pi}{N}) & \phi > \frac{\pi}{N} \end{cases}$$

with

$$K_1 = f_1 \lambda_i$$

$$K_2 = f_2 \lambda_i$$

determined by the constants f_1 and f_2 . To improve convergence, $\bar{\lambda} = 1/2 (\lambda_i + \bar{\lambda}_{\text{old}})$ should be used in place of λ_i . Including contraction of the wake gives for the distortion

$$\vec{D} = \begin{pmatrix} D_r \cos(\psi - \phi) \\ D_r \sin(\psi - \phi) \\ D_z \end{pmatrix}$$

where the radial displacement (also independent of ψ) is

$$D_r = - (1 - e^{-K_3 \phi}) (1 - K_4) r_i$$

($r_i = 1$ for the tip vortex and the outside edge of the inboard sheet, and $r_i = r_{\text{ROOT}}$ for the inside edge.) Hence the rigid wake geometry is determined by the parameters f_1 , f_2 , K_3 , and K_4 , which may be different for the tip vortex and inboard sheet. Alternatively, the constants K_1 and K_2 can be specified, instead of f_1 and f_2 .

Landgrebe (ref. 20) developed a prescribed wake geometry model for a hovering rotor from experimental model rotor flow visualization data. The model consists of contraction and two-stage convection as defined above, with the constants as follows:

a. tip vortex

$$K_1 = .25 (C_r/\sigma + .001 \theta_{tw})$$

$$K_2 = (1 + .01 \theta_{tw}) \sqrt{C_r}$$

b. sheet tip edge

$$K_1 = 1.55 \sqrt{C_r}$$

$$K_2 = 1.9 \sqrt{C_r}$$

c. sheet root edge

$$K_1 = 0$$

$$K_2 = -(0.0025 \theta_{tw}^2 + 0.099 \theta_{tw}) \sqrt{C_r}$$

d. radial contraction

$$K_3 = .145 + 27 C_r$$

$$K_4 = -78$$

where θ_{tw} is here the blade linear twist rate in degrees. Kocurek and Tangler (ref. 21) revised the tip vortex geometry based on experimental data for low aspect-ratio two-bladed rotors, obtaining

$$K_1 = B + C (C_r/N^n)^m$$

$$K_2 = [C_r - N^n (-B/C)^{Vm}]^{\frac{1}{2}}$$

$$K_3 = 4.0 \sqrt{C_r}$$

with

$$B = .000729 \theta_{tw}$$

$$C = 2.3 - .206 \theta_{tw}$$

$$m = 1.0 - .25 e^{.04 \theta_{tw}}$$

$$n = 0.5 - .0172 \theta_{tw}$$

In reference 22 it was found that the prediction of measured rotor hover performance was improved when the wake geometry was prescribed based on the blade maximum bound circulation rather than C_T as above. Hence

$$C_T = \frac{N\bar{\Gamma}_{max}}{2\pi}$$

can be used in place of C_T ; in general $\bar{\Gamma}_{max}$ must be averaged over ψ as well. These prescribed wake models were developed for a hovering rotor. To apply them in more general flight conditions we can use

$$C_T = \left(\lambda_i \frac{\sqrt{2}}{K_2} \right)^2$$

with λ_i the mean induced velocity including ground effect and rotor/rotor interference (the blade loading C_T/σ is retained.)

The wake geometry arrays will be organized as follows. The rigid or prescribed wake geometry is defined by D_z and D_r at $\phi = k\Delta\psi$, $k = 1$ to K_{RWG} (independent of ψ). So the structure of the array is

$$D(k), \text{ for } k = 1 \text{ to } K_{RWG}$$

for D_z and D_r , for the tip vortex and the two inboard sheet edges. The convection rate K_2 is also required, for extrapolation of the geometry beyond $\phi = K_{RWG}\Delta\psi$. The free wake geometry is defined by $\overrightarrow{D}(\psi, \phi)$. The first

subscript in the array will be the age $\phi = k\Delta\psi$ for $k = 1$ to K_{FWG} ; the second subscript will be the blade azimuth angle $\psi = \ell\Delta\psi$, $\ell = 1$ to J . So the structure of the array is

$$\vec{D}(n), \quad n = (\ell - 1)K_{FWG} + k \quad \text{for } ((k = 1 \text{ to } K_{FWG}), \quad \ell = 1 \text{ to } J)$$

The free wake geometry will be used for the tip vortex only (see section 3.2).

In the near wake and the rolling up wake, the position of a panel corner at an arbitrary radial station ρ is required ($r_{Root} \leq \rho \leq 1$). Linear interpolation between the root and tip edges of the inboard sheet gives

$$\vec{r}_w = \frac{\vec{r}_{w_{root}}(1-\gamma) + \vec{r}_{w_{tip}}(\gamma - r_{Root})}{1 - r_{Root}}$$

The geometry of the near wake panels should include the increment

$$\Delta \vec{r} = \vec{r}_b(\gamma, \psi) - \frac{\vec{r}_b(r_{Root}, \psi)(1-\gamma) + \vec{r}_b(1, \psi)(\gamma - r_{Root})}{1 - r_{Root}}$$

to account for the blade bending (the variation with wake age is neglected).

The first panels of the near wake are aligned with the bound vortex. Let \vec{r}_1 and \vec{r}_3 be the position vectors of the right and left front corners of a near wake panel, obtained from the wake geometry at $\phi = 0$. Let \vec{r}_2 and \vec{r}_4 be the position vectors of the right and left rear corners, obtained from the wake geometry at $\phi = \Delta\psi$. Then a rectangular panel aligned with the bound vortex is obtained if \vec{r}_2 and \vec{r}_4 are replaced by $\vec{r}_1 + \Delta \vec{r}$ and $\vec{r}_3 + \Delta \vec{r}$ respectively where

$$\Delta \vec{r} = \left[1 - \frac{(\vec{r}_1 - \vec{r}_3)(\vec{r}_1 - \vec{r}_3)}{|\vec{r}_1 - \vec{r}_3|^2} \right] \cdot \left(\frac{\vec{r}_2 + \vec{r}_4 - \vec{r}_1 - \vec{r}_3}{2} \right)$$

For the shed vorticity in these first panels, the front corners are also moved aft by a quarter chord, which is accomplished by adding

$$\Delta \vec{r}_s = \frac{c}{4} \frac{\Delta \vec{r}}{|\Delta \vec{r}|}$$

to \vec{r}_1 and \vec{r}_3 , with $\Delta \vec{r}$ given above. The blade chord at the induced velocity radial station will be used; and the shed wake panel will be omitted entirely if $c/4 > |\Delta \vec{r}|$.

That portion of the first tip vortex segment extending from the bound vortex to the trailing edge (a length $3c/4$) should be perpendicular to the bound vortex. Let \vec{r}_1 and \vec{r}_2 be the position vectors of the vortex segment end points, at the blade tip and at the first downstream point respectively. Let \vec{r}_3 be the position vector of the first blade point inboard of the tip. Then this line vortex segment will be replaced by two segments extending from \vec{r}_1 to

$$\vec{r}_1 + \frac{3c}{4} \frac{\Delta \vec{r}}{|\Delta \vec{r}|}$$

and from there to \vec{r}_2 , where

$$\begin{aligned}\Delta \vec{r} &= ((\vec{r}_3 - \vec{r}_1) \times (\vec{r}_2 - \vec{r}_1)) \times (\vec{r}_3 - \vec{r}_1) \\ &= (\vec{r}_3 - \vec{r}_1) (\vec{r}_3 - \vec{r}_1) \cdot (\vec{r}_3 - \vec{r}_1) \\ &\quad - (\vec{r}_3 - \vec{r}_1) (\vec{r}_3 - \vec{r}_1) \cdot (\vec{r}_2 - \vec{r}_1)\end{aligned}$$

and c is the tip chord. Constant strength will be assumed for the portion from the bound vortex to the trailing edge.

3.1.4 Induced velocity calculation.— The blade bound circulation is calculated at discrete points on the rotor disk: $\Gamma_{ij} = \Gamma(r_i, \psi_j)$. The solution is periodic, so the azimuthal points cover one revolution of the blade: $\psi_j = j\Delta\psi$ for $j = 1$ to J ($\Delta\psi = 2\pi/J$). The radial stations r_i ($i = 1$ to M) will be a subset of the aerodynamic loading radial stations. Except for the

near wake, the vorticity strength in the present wake model actually depends only on the maximum circulation Γ_j , defined as the value of Γ_{ij} with maximum magnitude over all radial stations r_i at a given azimuth ψ_j (the computation will allow the use of the maximum over the radial stations outboard of station r_{Gmax}).

Summing the contributions from all vortex elements in the wake gives the induced velocity as the product of the blade bound circulation and influence coefficients:

$$\vec{v} = \sum_{j=1}^J \Gamma_j \vec{C}_j + \sum_{j=2-K_{NW}}^{\lambda} \sum_{i=1}^M \Gamma_{ij} \vec{C}_{ij}$$

The second term is due to the near wake (extending from $\phi = 0$ to $\phi = K_{NW} \Delta\psi$ behind the reference blade at azimuth angle $\psi = \lambda \Delta\psi$). A set of influence coefficients is obtained for each point in the flow field at which the induced velocity is calculated: at points distributed radially and azimuthally over the rotor disk, and at points off the rotor disk (see section 3.1.3). The influence coefficient arrays will be organized as follows. Consider $\vec{C}_j(\vec{r})$; the first subscript is the index due the azimuth angle of the bound circulation ($j = 1$ to J). The second subscript is the index over all the field points \vec{r} at a given azimuth angle ($k = 1$ to MR). The third subscript is the index over the azimuth angle of the field points ($\lambda = 1$ to J). So the structure of the array is

$$\vec{C}(n), \quad n = (\lambda - 1) * MR * J + (k - 1) * J + j \\ \text{for } (((j = 1 \text{ to } J), k = 1 \text{ to } MR), \lambda = 1 \text{ to } J)$$

The field points at a given azimuth angle ψ_λ consist of the induced velocity points along the rotor blade span; perhaps the induced velocity points along the blade of the other rotor, or at the hub of the other rotor; and perhaps the points at the wing/body, horizontal tail, vertical tail, or an arbitrary field point. The organization of the array for the near wake influence coefficients $\vec{C}_{ij}(\vec{r})$ is similar, except there is an additional subscript which

is the index over the circulation radial stations ($i = 1$ to M), and the index over the azimuth angle of the bound circulation covers only the near wake ($j = \lambda - K_{NW}$ to λ):

$$\vec{C}_{NW}(n), \quad n = (\lambda - 1) * MR * (K_{NW} + 1) * M + (k - 1) * (K_{NW} + 1) * M + (j - \lambda + K_{NW}) * M + i$$

for ((($i = 1$ to M), $j = \lambda - K_{NW}$ to λ), $k = 1$ to MR),
 $\lambda = 1$ to J)

Also, for the near wake the field points at a given azimuth station consist of only the induced velocity points along the rotor blade span (no points off the rotor disk).

The calculation of the influence coefficients proceeds as follows. The outermost loop involves the dimensionless time ψ , which is also the azimuth angle of the reference blade. The solution is periodic so the induced velocity is evaluated for $\psi = 0$ to 2π (at the discrete points $\psi = \lambda\Delta\psi$, $\lambda = 1$ to J , $\Delta\psi = 2\pi/J$). For a given ψ , the position vectors at which the induced velocity is required can be evaluated: at the radial stations along the reference blade; at the wing/body, horizontal tail, vertical tail, other rotor hub, or an arbitrary point; and at the radial stations along the reference blade of the other rotor.

Next there is a loop over all the blades of the rotor ($m = 0$ to $N-1$; $m = 0$ is the reference blade). The azimuth angle of the m -th blade is $\psi_m = \psi + m 2\pi/N = (\lambda + mJ/N)\Delta\psi$. Finally there is a loop over the wake age $\phi = k\Delta\psi$ ($k = 0$ to the maximum extent of the far wake, which may be different when calculating the velocity at points on or off the rotor disk).

The blade specification plus the wake age determines the vortex panel being considered, extending from ϕ to $\phi + \Delta\psi$ behind the m -th blade. Given ψ_m and ϕ , the position vectors of this wake panel can be evaluated: the end points of the tip vortex line segment, and the four corners of the inboard sheet (at the side edges, as described in section 3.1.3). The wake strength at the panel leading edge is determined by the bound circulation at $\psi_m - \phi$, and the strength at the trailing edge by the bound circulation

at $\psi_m - \phi - \Delta\psi$. These azimuth angles define to which influence coefficients the induced velocity of this panel contributes.

The wake age determines whether the panel considered is part of the near wake, the rolling up wake, or the far wake models (as described in section 3.1.2). The near wake model is only used behind the reference blade ($m = 0$). The near way is not used in calculating the velocity at points off the rotor disk.

The far wake model consists of a tip vortex line segment and a single inboard wake panel. The line segment has strength Γ_{max} . The sheet is due to a circulation distribution linear from zero at the inside edge to Γ_{max} at the outside edge. The induced velocity expressions for a line segment and a rectangular vortex sheet then give the contributions to the influence coefficients.

The rolling up wake model consists of a tip vortex line segment of strength $f\Gamma_{max}$, where

$$\delta = \delta_{R_u} - (1 - \delta_{R_u}) (\phi / \phi_{R_u})$$

and an inboard wake sheet divided into two panels at radial station

$$\gamma = \gamma_{R_u} - (1 - \gamma_{R_u}) (\phi / \phi_{R_u})$$

Linear interpolation between the side edges gives the wake geometry at ρ . The circulation corresponding to these panels goes from zero at the inside edge, to Γ_{max} at ρ , to $f\Gamma_{max}$ at the outside edge. The induced velocity expressions for these vortex elements then give the contributions to the influence coefficients.

The near wake model consists of a tip vortex line segment of strength $f_{NW} \Gamma_{Mj}$ (where Γ_{Mj} is the bound circulation at the most outboard radial station); and separate inboard wake panels between the bound circulation radial stations. Linear interpolation between the side edges gives the wake geometry at r_i ($i = 1$ to M). An increment accounting for the blade bending must also be added to the position vectors in the near wake. The circulation

corresponding to these panels goes from zero at the inside edge, to Γ_{ij} at r_i , to $f_{NW} \Gamma_{Mj}$ at the outside edge. The induced velocity expressions for these vortex elements then give the contributions to the influence coefficients.

The inboard wake panels in the near wake directly behind the blade ($\phi = 0$ to $\Delta\psi$) require special consideration (see section 3.1.2). First, the position vectors at the rear corners of each element are adjusted so the front edge of the rectangular vortex sheet is exactly aligned with the bound vortex. When evaluating the induced velocity near the junction of two trailing vorticity sheets, they can be replaced by a single sheet. The leading edges of the shed vorticity sheets must be moved a quarter chord behind the bound vortex. However, if line segments rather than rectangular vortex sheets are used for the trailing or shed wake, the above modifications are not required.

Finally, the contribution of the bound vortex of each blade is calculated. The bound vortex is a straight line segment extending from the root to the tip of the blade at azimuth angle ψ_m , with strength varying from zero at the root to Γ_{max} at the tip. The contribution of the bound vortex of the reference blade to the induced velocity at the reference blade is not included.

By this procedure the influence coefficients are calculated for a given wake geometry. Then from a circulation estimate at some stage in the blade motion and helicopter trim solution, the induced velocity \vec{v} can be evaluated. The vector \vec{v} is at the induced velocity radial station, in the tip path plane coordinate frame. The aerodynamic analysis requires the induced velocity at the loads radial stations, in the hub plane coordinate frame ($\lambda = \lambda_x \vec{i}_s - \lambda_y \vec{j}_s - \lambda_z \vec{k}_s$). Transforming to the S system gives

$$\begin{pmatrix} \lambda_x \\ -\lambda_y \\ -\lambda_z \end{pmatrix} = R_{TS}^T \vec{v}$$

using the current values of the tip path plane tilt angles (β_c and β_s). The induced velocity is then calculated at the loads radial stations by linear interpolation.

The induced velocity for the rotor/airframe aerodynamic interference (at the wing/body, horizontal tail, vertical tail, or an arbitrary point) is required in the body axis system (the F frame):

$$\begin{pmatrix} \lambda_x \\ \lambda_y \\ \lambda_z \end{pmatrix} = (R_{TS} R_{SF})^T \vec{v}$$

For the induced velocity from rotor #2, a factor $\Omega R_2 / \Omega R_1$ is required as well. The induced velocity for the rotor/rotor interference (at the hub or over the disk) is required in the shaft axis system of the other rotor. The interference velocity at rotor #2 due to the loading of rotor #1 is then

$$\begin{pmatrix} \lambda_x \\ -\lambda_y \\ -\lambda_z \end{pmatrix}_{2/1} = \frac{\Omega R_1}{\Omega R_2} (R_{SF})_{\text{rotor } \#2} (R_{TS} R_{SF})_{\text{rotor } \#1}^T \vec{v}_{2/1}$$

and at rotor #1 due to rotor #2

$$\begin{pmatrix} \lambda_x \\ -\lambda_y \\ -\lambda_z \end{pmatrix}_{1/2} = \frac{\Omega R_2}{\Omega R_1} (R_{SF})_{\text{rotor } \#1} (R_{TS} R_{SF})_{\text{rotor } \#2}^T \vec{v}_{1/2}$$

These coordinate rotations normally should not be included in the influence coefficients because the updated values of the tip path plane tilt angles are to be used in the matrix R_{TS} (although the rotation of the induced velocity by the small angles β_c and β_s should not be important). The factor $\Omega R_1 / \Omega R_2$ can be incorporated in the influence coefficients however. For a clockwise

rotating rotor, the sign of the \vec{j}_s component of the induced velocity must be changed (between the R_{TS} and R_{SF} rotation matrices).

The interference induced velocity due to rotor #1 is calculated at rotor #2 for the azimuth angles $\psi = l\Delta\psi + \Delta\psi_{21}$ ($l = 1$ to J). When $\Delta\psi_{21} \neq 0$ it will be necessary to linearly interpolate the velocity to the azimuth angles $\psi = k\Delta\psi$ ($k = 1$ to J). Similarly, the induced velocity due to rotor #2 at rotor #1 must be interpolated from $\psi = l\Delta\psi - \Delta\psi_{21}$ to $\psi = k\Delta\psi$. The velocity moved off the rotor disk by rotor #2 is also calculated for $\psi = l\Delta\psi - \Delta\psi_{21}$, and must be interpolated to $\psi = k\Delta\psi$.

3.1.5 *Ground effect.*— Ground effect can be included in the nonuniform induced velocity calculation by introducing an image element for every vortex element in the rotor wake. The image element position is obtained by reflecting the actual wake element position about the ground plane, and changing the sign of the vorticity. Let z_{AGL} be the distance the rotor hub is above the ground (see section 2.4.3). The position of the image element is required in the tip path plane axes relative to the hub. First the position vector of the actual element is rotated to earth axes; then the origin is shifted to the ground, the sign of the \vec{k}_E component is changed, and the origin is shifted back to the hub; finally the vector is rotated back to the tip path plane axes:

$$\begin{aligned}\vec{r}_{\text{image}} &= R_{TE} [z_{AGL} \vec{k}_E + (\vec{\tau}_E \vec{\tau}_E + \vec{j}_E \vec{j}_E - \vec{k}_E \vec{k}_E) (-z_{AGL} \vec{k}_E + R_{TE}^T \vec{r})] \\ &= R_{TE} [2z_{AGL} \vec{k}_E + (\vec{\tau}_E \vec{\tau}_E + \vec{j}_E \vec{j}_E - \vec{k}_E \vec{k}_E) R_{TE}^T \vec{r}]\end{aligned}$$

where

$$R_{TE} = R_{TS} R_{SF} R_{FE}$$

The induced velocity of the vortex element is calculated, and subtracted from the induced velocity contribution of the actual element. The actual element is below the ground plane if

$$\vec{k}_E \cdot (R_{TE}^T \vec{r}) > z_{AGL}$$

(This can occur if the wake geometry does not allow for ground effect.) In this case the induced velocity contributions of both the actual element and its image are set to zero.

3.1.6 Hover or vertical flight (axisymmetric geometry). - The nonuniform inflow calculation can be simplified in hover due to the axisymmetry of the wake geometry. For the hover case the influence coefficients will be the same for the induced velocity at all azimuth angles, except for an azimuth shift and axis rotation:

$$\vec{C}_j (\psi = \lambda \Delta\psi) = \begin{bmatrix} \cos(\psi - \Delta\psi) & -\sin(\psi - \Delta\psi) & 0 \\ \sin(\psi - \Delta\psi) & \cos(\psi - \Delta\psi) & 0 \\ 0 & 0 & 1 \end{bmatrix} \vec{C}_{j-\lambda+1} (\psi = \Delta\psi)$$

Even in hover the rotor may have a net pitch or roll moment if the center of gravity is offset from the shaft (with offset hinges or a hingeless rotor). Hence in general the hover case will not involve induced velocity and bound circulation independent of azimuth angle. These considerations apply to the general vertical flight case as well.

An accurate calculation of the induced velocity of a rotor in axial flight usually requires consideration of the wake very far from the rotor disk. The detailed wake model described above is required only close to the disk however. Very far from the disk a more approximate and more efficient model will be used, obtained by spreading the vorticity vertically over the distance h between successive sheets, as sketched in figure 18. The axial convection velocity in the far wake is taken from the prescribed wake model:

$$v = -\vec{k} \cdot \vec{\mu}_{tip} + (k_z)_{tip \text{ vortex}}$$

giving for the spiral axial spacing

$$s_r = 2\pi v$$

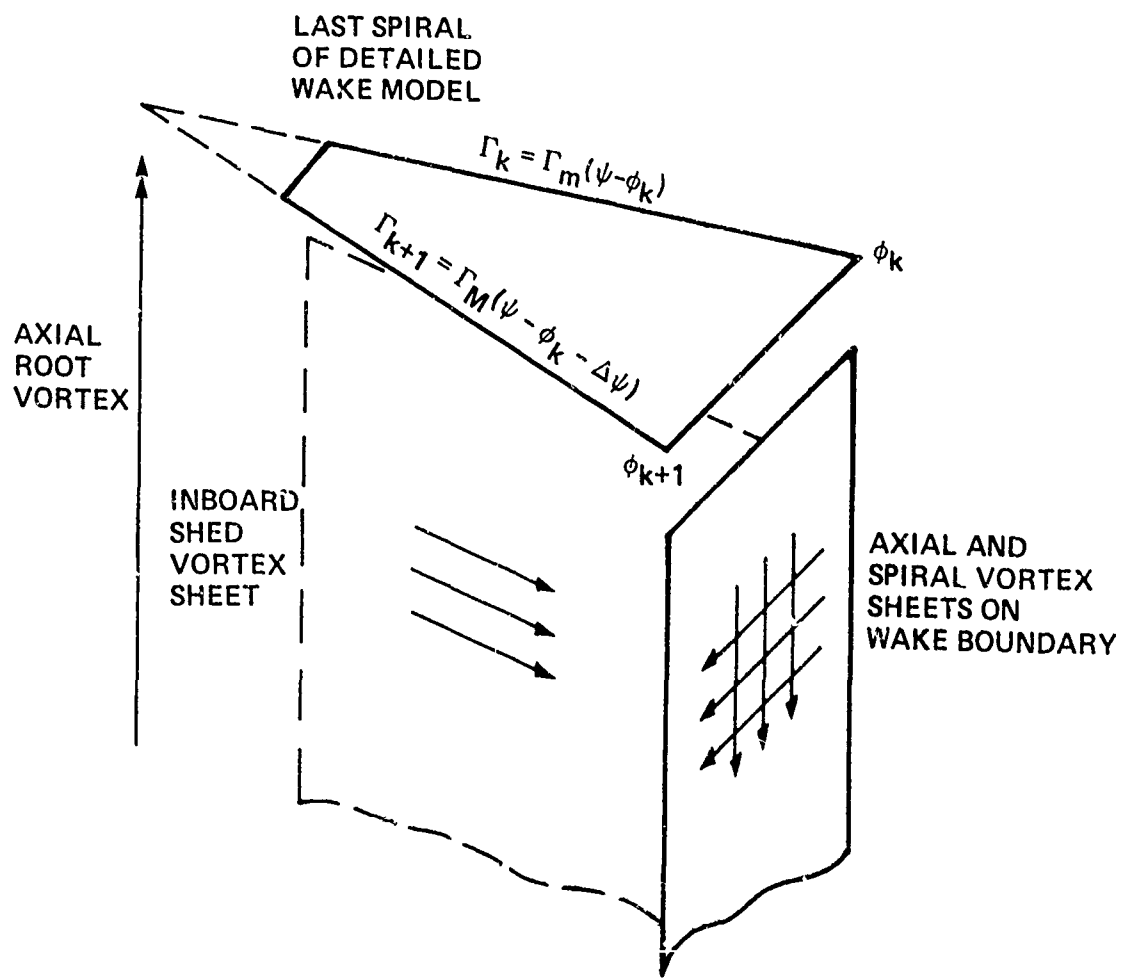


Figure 18. Far wake model for hover or vertical flight.

The tip vortex elements are spread vertically to form a vortex sheet with axial and spiral components. There is a corresponding axial root vortex from the inboard trailing vorticity. The shed vorticity is spread vertically to form a vortex sheet. This wake model extends L turns (an axial distance Lh) beyond the last spiral of the detailed wake model from each blade.

The influence coefficients of this very far wake model are calculated as follows. For a panel in the last spiral in the wake, the geometry is specified by the location of the ends of the tip vortex line segment, and the corners of the inboard panel. The wake strength is determined by the bound circulation corresponding to the panel leading and trailing edges:

$$\Gamma_k = \Gamma_{\max} (\psi_m - \phi_k)$$

$$\Gamma_{k+1} = \Gamma_{\max} (\psi_m - \phi_k - \Delta\psi)$$

The geometry of the sheet vorticity on the wake boundary is obtained from the position of the tip vortex segment, \vec{r}_k and \vec{r}_{k+1} (vectors to the segment ends). The vectors to the sheet vector are then

$$\vec{\tau}_1 = \vec{r}_k - \frac{1}{2} L \vec{k}$$

$$\vec{\tau}_2 = \vec{\tau}_1 - L \vec{k}$$

$$\vec{\tau}_3 = \vec{r}_{k+1} - \vec{\tau}_{k+1} \cdot \vec{k} \vec{k} + \vec{\tau}_1 \cdot \vec{k} \vec{k}$$

$$\vec{\tau}_4 = \vec{\tau}_3 - L \vec{k}$$

The induced velocity of the tip axial vorticity is given by the trailed sheet vorticity solution with

$$\Gamma_1 = \Gamma_2 = -\Gamma_k$$

$$\Gamma_3 = \Gamma_4 = -\Gamma_{k+1}$$

(see section 3.1.8). The induced velocity of the tip spiral vorticity is given by the shed sheet vorticity solution with

$$\Gamma_1 = L\Gamma_k$$

$$\Gamma_2 = 0$$

$$\Gamma_3 = L\Gamma_{k+1}$$

$$\Gamma_4 = 0$$

Let \vec{r}_i and \vec{r}_o be the position vectors of the inboard wake panel (the inside and outside edges respectively, at $\phi_k + \Delta\psi/2$). Then the vectors to the inboard shed vortex sheet are:

$$\vec{\gamma}_1 = \vec{r}_o - \frac{1}{2}L\vec{k}$$

$$\vec{\gamma}_2 = \vec{r}_o - L\vec{k}$$

$$\vec{\gamma}_3 = \vec{r}_i - \vec{v} \cdot \vec{k} \vec{k} + \vec{v} \cdot \vec{T} \vec{T}$$

$$\vec{\gamma}_4 = \vec{r}_3 - L\vec{k}$$

and the induced velocity is given by the shed sheet vorticity with

$$\Gamma_1 = L\Gamma_k$$

$$\Gamma_2 = L\Gamma_{k+1}$$

$$\Gamma_3 = L\Gamma_k$$

$$\Gamma_4 = L\Gamma_{k+1}$$

(see section 3.1.8). Finally, the vectors to the ends of the root axial vortex are

$$\vec{r}_2 = \vec{r}_i \cdot \hat{k} \hat{k} - \frac{1}{2} L \hat{k}$$

$$\vec{r}_i = \vec{r}_2 - L \hat{k}$$

and the induced velocity is given by the line vortex solution with

$$\Gamma_1 = \Gamma_2 = \Gamma_k - \Gamma_{k+1}$$

(see section 3.1.7).

3.1.7 Finite length vortex line element.- Consider a straight vortex line segment of length s , as shown in figure 19. The vortex segment has linearly varying circulation, between Γ_1 and Γ_2 at the end points (Γ_1 is the circulation at ϕ and Γ_2 is the circulation at $\phi + \Delta\psi$). The induced velocity is required at the point P , defined by the position vectors \vec{r}_1 and \vec{r}_2 from the ends of the segment. The vectors \vec{r}_1 and \vec{r}_2 can be in any convenient coordinate frame; the components of the induced velocity will be obtained in the same coordinate frame. The Biot-Savart law gives the induced velocity due to this line segment:

$$\Delta \vec{v} = - \frac{1}{4\pi} \oint \frac{\Gamma \vec{r} \times d\vec{\sigma}}{r^3}$$

where \vec{r} is the vector from the element $d\vec{\sigma}$ on the segment, to the point P ; and $r = |\vec{r}|$. The coordinate σ is measured along the vortex segment, from s_1 to s_2 :

$$s_1 = \frac{\vec{r}_1 \cdot \vec{r}_2 - r_1^2}{s}$$

$$s_2 = \frac{r_2^2 - \vec{r}_1 \cdot \vec{r}_2}{s} = s_1 + s$$

where s is the length of the segment:

$$s^2 = |\vec{r}_1 - \vec{r}_2|^2 = r_1^2 + r_2^2 - 2 \vec{r}_1 \cdot \vec{r}_2$$

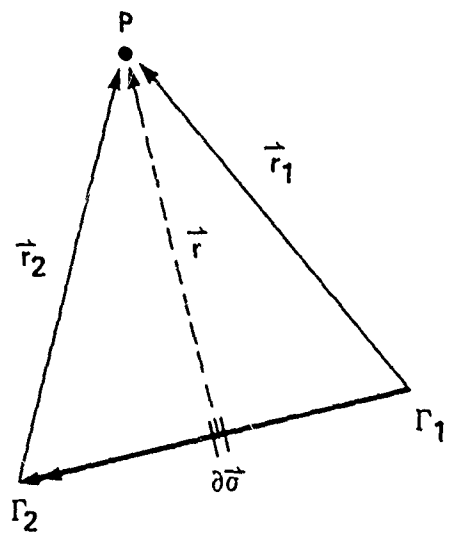


Figure 19. Finite length vortex line element.

Write $\vec{r} = \vec{r}_m - \sigma \hat{e}$, where \vec{r}_m is the minimum distance from the vortex line (including its extension beyond the end points of the segment) to the point P, and \hat{e} is the unit vector in the direction of the vortex:

$$\begin{aligned}\vec{r}_m &= \frac{\vec{r}_1 (r_2^2 - \vec{r}_1 \cdot \vec{r}_2) + \vec{r}_2 (r_1^2 - \vec{r}_1 \cdot \vec{r}_2)}{s^2} = \frac{\vec{r}_1 s_2 - \vec{r}_2 s_1}{s} \\ \hat{e} &= \frac{\vec{r}_1 - \vec{r}_2}{s}\end{aligned}$$

The vectors \vec{r}_m and \hat{e} are perpendicular, and

$$r_m^2 s^2 = r_1^2 r_2^2 - (\vec{r}_1 \cdot \vec{r}_2)^2$$

The vortex strength varies linearly along the segment:

$$\begin{aligned}\Gamma &= \frac{\Gamma_1 (s_2 - \sigma) + \Gamma_2 (\sigma - s_1)}{s} = \frac{\Gamma_1 s_2 - \Gamma_2 s_1}{s} + \sigma \frac{\Gamma_2 - \Gamma_1}{s} \\ &= \Gamma_m + \sigma \Gamma_s\end{aligned}$$

It follows that

$$\begin{aligned}\Delta \vec{v} &= \frac{\vec{r}_1 \times \vec{r}_2}{4\pi s} \left\{ \begin{array}{l} s_2 \\ s_1 \end{array} \right. \frac{\Gamma_m + \sigma \Gamma_s}{(r_m^2 + \sigma^2)^{3/2}} \downarrow \sigma \\ &= \frac{\vec{r}_1 \times \vec{r}_2}{4\pi s} \left[\frac{\Gamma_m \sigma / r_m^2 - \Gamma_s}{(r_m^2 + \sigma^2)^{3/2}} \right] \left| \begin{array}{l} \sigma = s_2 \\ \sigma = s_1 \end{array} \right. \\ &= \frac{\vec{r}_1 \times \vec{r}_2}{4\pi s r_m^2} \left[\Gamma_m \left(\frac{s_2}{r_2} - \frac{s_1}{r_1} \right) - \Gamma_s r_m^2 \left(\frac{1}{r_2} - \frac{1}{r_1} \right) \right] \\ &= \frac{\vec{r}_1 \times \vec{r}_2}{4\pi s r_m^2} \left[\Gamma_1 \left\{ \frac{s_2}{s} \left(\frac{s_2}{r_2} - \frac{s_1}{r_1} \right) + \frac{r_m^2}{s} \left(\frac{1}{r_2} - \frac{1}{r_1} \right) \right\} \right. \\ &\quad \left. + \Gamma_2 \left\{ \frac{s_1}{s} \left(\frac{s_1}{r_1} - \frac{s_2}{r_2} \right) + \frac{r_m^2}{s} \left(\frac{1}{r_1} - \frac{1}{r_2} \right) \right\} \right]\end{aligned}$$

for the induced velocity of the vortex line segment with linearly varying circulation.

Consider also the induced velocity of a line vortex segment with a stepped circulation distribution. The distance from the midpoint of the segment to the point P is

$$\vec{r}_3 = \frac{1}{2} (\vec{r}_1 + \vec{r}_2)$$

and the midpoint is located at

$$s_3 = \frac{1}{2} (s_1 + s_2) = \frac{1}{2s} (r_2^2 - r_1^2)$$

The line segment has constant strength Γ_1 from s_1 to s_3 , and constant strength Γ_2 from s_3 to s_2 . Applying the above result (with $\Gamma_s = 0$) to both values of the line segment gives

$$\begin{aligned} \Delta \vec{v} &= \frac{\vec{r}_1 \times \vec{r}_3}{4\pi(s/2)r_m^2} \Gamma_1 \left(\frac{s_3}{r_3} - \frac{s_1}{r_1} \right) + \frac{\vec{r}_3 \times \vec{r}_2}{4\pi(s/2)r_m^2} \Gamma_2 \left(\frac{s_2}{r_2} - \frac{s_3}{r_3} \right) \\ &= \frac{\vec{r}_1 \times \vec{r}_2}{4\pi s r_m^2} \left[\Gamma_1 \left\{ \frac{s_3}{r_3} - \frac{s_1}{r_1} \right\} + \Gamma_2 \left\{ \frac{s_2}{r_2} - \frac{s_3}{r_3} \right\} \right] \end{aligned}$$

The influence of the vortex core is accounted for by multiplying the induced velocity of the line segment by the factor

$$\min \left(\frac{r_m^2}{r_c^2}, 1 \right)$$

for concentrated vorticity (solid body rotation) or by

$$\frac{r_m^2}{r_m^2 + r_c^2}$$

for distributed vorticity (from ref. 16). The core radius r_c is the location of the maximum tangential velocity.

In references 23 and 24 a lifting surface theory solution was developed for the vortex induced loads on an infinite aspect-ratio, nonrotating wing encountering a straight, infinite vortex at an angle Λ with the wing (fig. 20). The vortex lies in a plane parallel to the wing, a distance h below it, and is convected past the wing by the free stream. The distortion of the vortex line by interaction with the wing is not considered. In linear lifting surface theory, the blade and wake are represented by a planar distribution of vorticity. This model problem was solved for the case of a sinusoidal induced velocity distribution, with wave fronts parallel to the vortex line. An approximate solution was obtained by fitting analytical expressions to the numerical solution for sinusoidal loading. The vortex induced velocity distribution can be obtained by a suitable combination of sinusoidal waves of various wavelengths, and the same super-position gives the vortex induced loading from the sinusoidal loading solution. The approximate solution is not valid for extremely small wavelengths, but the range of validity is sufficient to handle the cases arising in rotary wing applications. For the velocity induced along the wing span by a vortex of strength Γ :

$$w = \frac{\Gamma}{2\pi(c/2)} \frac{-r \sin \Lambda}{(r \sin \Lambda)^2 + h^2}$$

(where r and h are here divided by the wing semichord) the approximate lifting surface solution (from ref. 23) for the section lift is:

$$\begin{aligned} L_{es} = & \rho V \Gamma \left\{ \frac{r \sin \Lambda}{(r \sin \Lambda)^2 + (h + c_0)^2} \right. \\ & - a'_0 \frac{2_0 (- (r \sin \Lambda)^2 + (h + c'_0)^2 + b_0^2)}{(- (r \sin \Lambda)^2 + (h + c'_0)^2 + b_0^2)^2 + 4(r \sin \Lambda)^2(h + c'_0)^2} \\ & \left. - \sum_{n=1}^{\infty} a_n \left(\frac{d}{r \sin \Lambda} \right)^{2n} \left[\frac{-(r \sin \Lambda + b_0) \cos b_0 z + (h + c_n) \sin b_0 z}{(r \sin \Lambda + b_0)^2 + (h + c_n)^2} \right] \right\} \end{aligned}$$

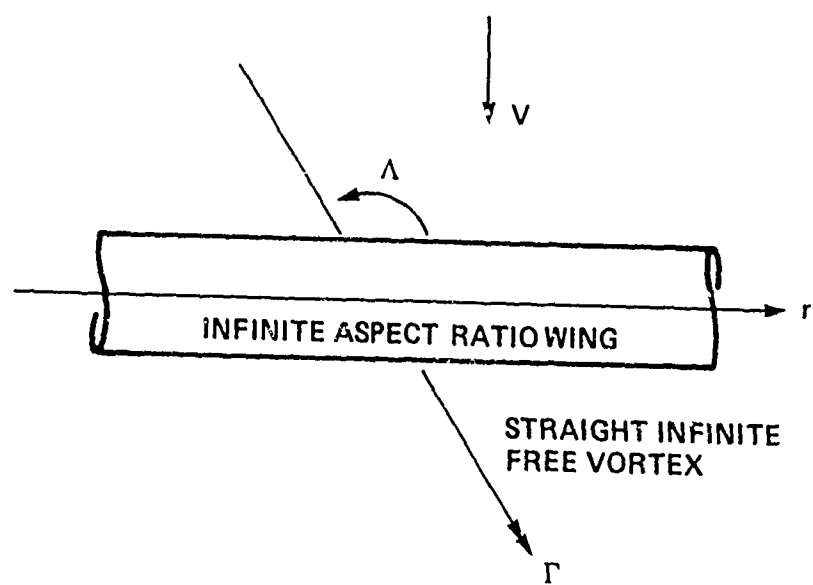


Figure 20. Lifting surface theory solution for vortex-induced loads.

For the incompressible case, the coefficients in this expression are functions of the vortex angle Λ :

$$b_0 = 5.12 + 1.88 (\Lambda/90^\circ)$$

$$b_1 = -\cos\Lambda$$

$$b_2 = \frac{\pi}{4} (\Lambda/90^\circ - 1)$$

$$a'_0 = .544 (-\cos\Lambda) + .07 \sin 2\Lambda$$

$$a'_1 = -.434 - 1.09 (1-\sin\Lambda)^{.94} + .607 (1-\sin\Lambda)^{2.46}$$

$$a'_2 = .0084 + .0069 (-\cos\Lambda)^{1.8}$$

$$c'_0 = 5.9$$

$$c'_0 = 1.683 + .27 (1-\sin\Lambda)^{.90} - .154 (1-\sin\Lambda)^{2.9}$$

$$c'_1 = 1.417 + .366 (1-\sin\Lambda)^{.84} - .392 (1-\sin\Lambda)^{2.0}$$

$$c'_2 = .91 + .93 (1-\sin\Lambda)^{1.0} - 1.025 (1-\sin\Lambda)^{1.45}$$

(Λ is in the range 90° to 180° ; the solution for Λ from 0 to 90° is obtained by symmetry considerations). The corresponding lifting line theory solution for the vortex induced loading is

$$L_{xx} = \rho V \Gamma \left\{ \frac{c \sin \Lambda}{(c \sin \Lambda)^2 + (b_0 + c_0)^2} - a_1 \left(\frac{d}{c \sin \Lambda} \right)^2 \left[\frac{-c \sin \Lambda}{(c \sin \Lambda)^2 + (b_0 + c_1)^2} \right] \right\}$$

where $a_1 = -0.662$, $c_1 = 1.296$, and $c_0 = \pi/2$. This lifting surface solution will be used in the present analysis in the following manner. For each line segment it will be determined whether it is close enough to the blade for lifting surface effects to be important (it is more economical to apply such a test than to always use the correction). If so, the induced velocity contribution of the line segment as calculated above, will be multiplied by the ratio L_{ls}/L_{ll} .

The parameters required to apply this lifting surface correction for vortex induced loads are h , $r \sin \Lambda$, and Λ . From the minimum distance \overrightarrow{r}_m between the point P and the vortex segment (in the tip path plane coordinate frame), and including the influence of the viscous core on the induced velocity, the vortex/blade separation is

$$\lambda = \frac{2}{c} \sqrt{(\vec{r}_T \cdot \vec{r}_m)^2 + c_c^2}$$

Let $\vec{i}^* = (\vec{r}_1 - \vec{r}_2)/s$ be the unit vector along the vortex segment; and $\vec{j}^* = \vec{i}_T \cos \psi + \vec{j}_T \sin \psi$ the unit vector along the blade. Then the intersection angle is

$$\Lambda = 180^\circ - \sin^{-1} \sqrt{1 - (\vec{j}^* \cdot \vec{r}^*)^2}$$

$$\sin \Lambda = \sqrt{1 - (\vec{j}^* \cdot \vec{r}^*)^2}$$

$$\cos \Lambda = -|\vec{j}^* \cdot \vec{r}^*|$$

Finally, the distance from the vortex line is

$$r \sin \Lambda = \frac{2}{c} \sqrt{(\vec{r}_T \cdot \vec{r}_m)^2 + (\vec{j}_T \cdot \vec{r}_m)^2} \operatorname{sign}(\vec{j}^* \cdot \vec{r}_m) \operatorname{sign}(\vec{j}^* \cdot \vec{r}^*) \\ + \frac{1}{2} \cos \Lambda$$

The lifting surface correction will be used if the distance from the segment midpoint is less than a specified distance d_{ls} :

$$r_3 = \frac{1}{2} |\vec{r}_1 + \vec{r}_2| < d_{ls}$$

Typically d_{ls} should be around $10c$ (see ref. 24).

The use of a larger viscous core radius after a blade/vortex interaction will be allowed, to model such affects as vortex induced stall or core bursting, which limit the induced loads (see section 3.1.1). Let $\phi_{inter}(\psi)$ be the age of the tip vortex segment which first intersects the following blade, with the generating blade at azimuth angle ψ . Then a larger core radius r_b will be used if the line segment age is greater than $\phi_b(\psi)$. The transition at ϕ_b occurs initially a fixed increment $\Delta\phi_b$ after the intersection at ϕ_{inter} , and then propagates up the tip vortex at a rate $v_b = \partial\phi/\partial\psi$:

$$\begin{aligned}\phi_b(\psi) &= \min \left\{ \begin{array}{l} \phi_{inter}(\psi) + \Delta\phi_b \\ \phi_b(\psi - \Delta\psi) + \Delta\psi - v_b \Delta\psi \end{array} \right. \\ &= \min_{j=0 \rightarrow \infty} (\phi_{inter}(\psi - j\Delta\psi) + \Delta\phi_b + j(1-v_b)\Delta\psi)\end{aligned}$$

(only $j = 1$ to J need be tested if $v_b < 1$, and $\phi_b = 0$ for all ψ if $v_b > 1$). The initial, small tip vortex core radius r_c is used if $\phi_{k+1} < \phi_b$; the large core radius r_b is used if $\phi_k > \phi_b$; and if $\phi_k < \phi_b < \phi_{k+1}$ the core radius is obtained by linear interpolation between r_c and r_b . The initial, small core radius r_c is always used for the near wake.

The wake age ϕ_{inter} at the first blade/vortex intersection can be determined by examining the projection of the tip vortex wake geometry $\vec{r}_w(\psi, \phi)$ on the disk plane. Consider a line segment extending from \vec{r}_1 at ϕ_k to \vec{r}_2 at ϕ_{k+1} , and the m -th blade at azimuth angle $\psi_m = \psi + m2\pi/N$. The vortex segment line is defined by

$$\vec{r}_{vortex} = \vec{r}_1 + \sigma (\vec{r}_2 - \vec{r}_1)$$

with $c = 0$ at \vec{r}_1 and $c = 1$ at \vec{r}_2 ; while the blade line is defined by

$$\vec{r}_{\text{blade}} = g (\vec{\tau}_T \cos \psi_m + \vec{\gamma}_T \sin \psi_m)$$

with $\rho = 0$ at the hub and $\rho = 1$ at the tip. The intersection of these two lines is obtained by equating the $\vec{\tau}_T$ and $\vec{\gamma}_T$ components of \vec{r}_{vortex} and \vec{r}_{blade} :

$$\vec{r}_1 \cdot \vec{\tau}_T + r (\vec{r}_2 \cdot \vec{\tau}_T - \vec{r}_1 \cdot \vec{\tau}_T) = g \cos \psi_m$$

$$\vec{r}_1 \cdot \vec{\gamma}_T + \sigma (\vec{r}_2 \cdot \vec{\gamma}_T - \vec{r}_1 \cdot \vec{\gamma}_T) = g \sin \psi_m$$

which gives

$$\tau_{\text{inter}} = \frac{\vec{r}_1 \cdot \vec{\tau}_T \sin \psi_m - \vec{r}_1 \cdot \vec{\gamma}_T \cos \psi_m}{(\vec{r}_1 - \vec{r}_2) \cdot \vec{\tau}_T \sin \psi_m - (\vec{r}_1 - \vec{r}_2) \cdot \vec{\gamma}_T \cos \psi_m}$$

$$\gamma_{\text{inter}} = \frac{\vec{r}_1 \cdot \vec{\tau}_T \vec{r}_2 \cdot \vec{\gamma}_T - \vec{r}_1 \cdot \vec{\gamma}_T \vec{r}_2 \cdot \vec{\tau}_T}{(\vec{r}_1 - \vec{r}_2) \cdot \vec{\tau}_T \sin \psi_m - (\vec{r}_1 - \vec{r}_2) \cdot \vec{\gamma}_T \cos \psi_m}$$

(There is no intersection if the denominator is zero). The vertical separation of the vortex and rotor blade is

$$h = \frac{1}{2} (\vec{r}_1 + \vec{r}_2) \cdot \vec{k}_T$$

A blade/vortex intersection is defined to occur if $0 < \sigma_{\text{inter}} < 1$ and $0.2 < \rho_{\text{inter}} < 1.0$; and if $|h| < d_{bv}$ as well. The intersections will be identified by examining each line segment in the tip vortex behind the blade at ψ , beginning with the wake age $\phi_k = \Delta\psi$. The segment will be tested against the blade index m such that the magnitude of

$$\min \left\{ \left| \psi_m - \tan^{-1} \frac{\vec{\gamma}_T \cdot \vec{r}}{\vec{\tau}_T \cdot \vec{r}} \right|, 2\pi - \left| \psi_m - \tan^{-1} \frac{\vec{\gamma}_T \cdot \vec{r}}{\vec{\tau}_T \cdot \vec{r}} \right| \right\}$$

is minimized. If an intersection occurs, then

$$\Psi_{\text{inter}} = \phi_k + \tau_{\text{inter}} \Delta \Psi$$

If an intersection does not occur, the next line segment is tested.

3.1.8 *Rectangular vortex sheet*. - Consider a planar rectangular vortex sheet element, as shown in figure 21. The induced velocity is required at an arbitrary point P in the flow field, defined by vectors from the four corners. The strength of the sheet is defined by the circulation values at the four corners (Γ_1 and Γ_3 at ϕ_k , Γ_2 and Γ_4 at ϕ_{k+1} ; Γ_1 and Γ_2 at the outside edge, Γ_3 and Γ_4 at the inside edge). This vortex element is approximated by a planar, rectangular sheet with sides s and t (fig. 21). The point P is defined by a vector \vec{r}_o from the center of the sheet. The orientation of the sheet is defined by orthogonal unit vectors \hat{e}_s and \hat{e}_t parallel to the sides of the sheet, and the normal unit vector $\hat{e}_n = \hat{e}_s \times \hat{e}_t$:

$$\hat{e}_t \cdot t = \frac{1}{2} (\vec{r}_2 + \vec{r}_4 - \vec{r}_1 - \vec{r}_3)$$

$$\hat{e}_s \cdot s = \frac{1}{2} (\vec{r}_3 + \vec{r}_4 - \vec{r}_1 - \vec{r}_2)$$

$$\vec{r}_o = \frac{1}{4} (\vec{r}_1 + \vec{r}_2 + \vec{r}_3 + \vec{r}_4)$$

The vorticity strength is δ in the \hat{e}_t direction and γ in the \hat{e}_s direction, varying linearly along the length of the vortex filaments. The minimum distance from P to the sheet or its extension is \vec{r}_m :

$$\vec{r}_m = \vec{r}_o \cdot \hat{e}_n \hat{e}_n = r_m \hat{e}_n$$

The vector \vec{r}_m is perpendicular to the plane of the sheet and intersects it at a point M . A coordinate system (c, τ) will be used on the sheet plane, with origin at M so the center of the sheet is at

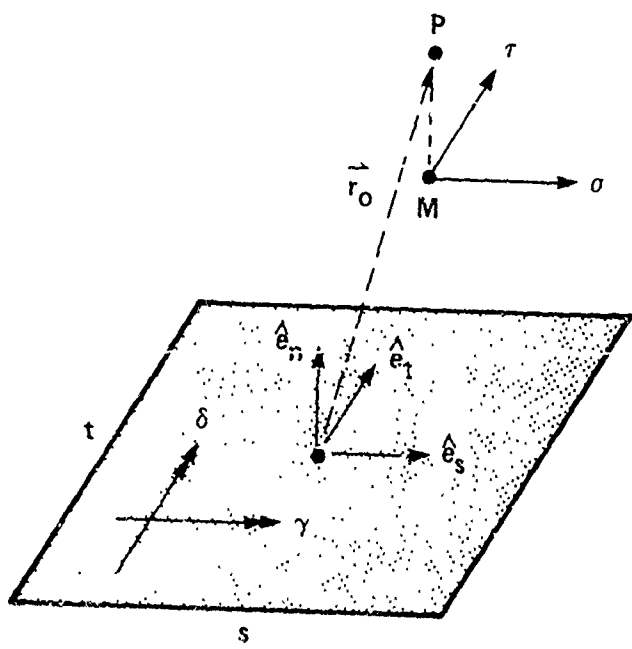
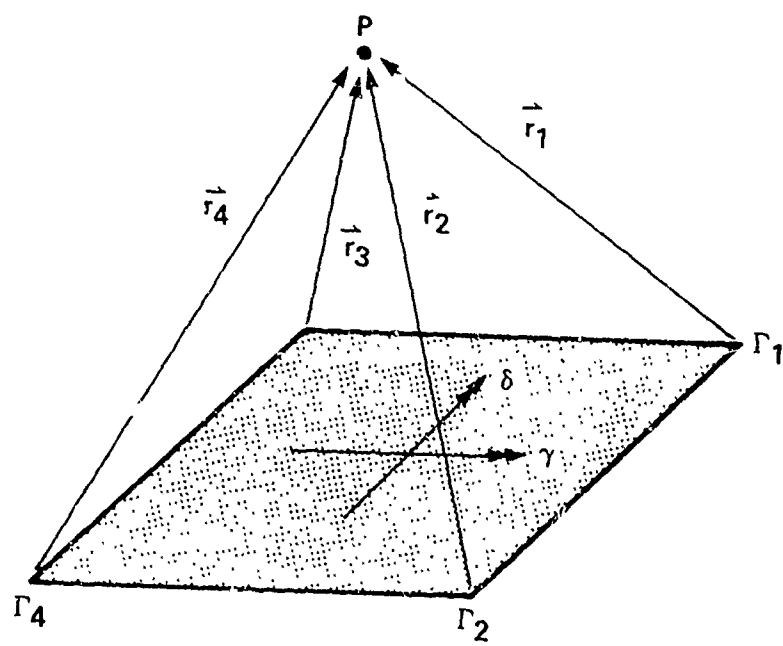


Figure 21. Rectangular vortex sheet.

$$\sigma = s_0 = -\vec{r}_0 \cdot \hat{\mathbf{e}}_s$$

$$\tau = t_0 = -\vec{r}_0 \cdot \hat{\mathbf{e}}_t$$

The edges of the rectangle are then given by $\sigma = s_0 \pm s/2$ and $\tau = t_0 \pm t/2$.
The distance from a point on the sheet to P is

$$\vec{r} = \vec{r}_m - \sigma \hat{\mathbf{e}}_s - \tau \hat{\mathbf{e}}_t$$

The linearly varying vorticity of the sheet is

$$\vec{\omega} = \sigma \hat{\mathbf{e}}_s + \delta \hat{\mathbf{e}}_t = (\kappa_m + \sigma \gamma_s) \hat{\mathbf{e}}_s + (\delta_m + \tau \delta_t) \hat{\mathbf{e}}_t$$

or in terms of the circulation at the corners:

$$\begin{aligned} \delta &= \frac{r_1 - r_3}{s} \frac{\tau - (t_0 - \frac{t}{2})}{t} + \frac{r_2 - r_4}{s} \frac{(t_0 + \frac{t}{2}) - \tau}{t} \\ &= \frac{1}{st} [(r_3 - r_1)(t_0 - \frac{t}{2}) + (r_2 - r_4)(t_0 + \frac{t}{2})] + \frac{1}{st} [r_1 - r_3 - r_2 - r_4] \tau \\ \gamma &= \frac{r_2 - r_1}{t} \frac{\sigma - (s_0 - \frac{s}{2})}{s} + \frac{r_4 - r_2}{t} \frac{(s_0 + \frac{s}{2}) - \sigma}{s} \\ &= \frac{1}{st} [(r_1 - r_2)(s_0 - \frac{s}{2}) + (r_4 - r_3)(s_0 + \frac{s}{2})] + \frac{1}{st} [r_2 - r_1 - r_4 + r_3] \sigma \end{aligned}$$

Note that conservation of vorticity gives $\partial \gamma / \partial \sigma = -\partial \delta / \partial \tau$ or $\gamma_s = -\delta_t$.

The Biot-Savart law gives the induced velocity of this vortex sheet:

$$\begin{aligned} \Delta \vec{v} &= -\frac{1}{4\pi} \oint \frac{\vec{r} \times \vec{\omega}}{r^3} dA \\ &= -\frac{1}{4\pi} \iint_{t_0 - \frac{t}{2}}^{t_0 + \frac{t}{2}} \iint_{s_0 - \frac{s}{2}}^{s_0 + \frac{s}{2}} \frac{r_m \delta \hat{\mathbf{e}}_t - r_m \delta \hat{\mathbf{e}}_s + (\tau \delta - \sigma \delta) \hat{\mathbf{e}}_n}{(r_m^2 + \sigma^2 + \tau^2)^{3/2}} d\sigma d\tau \end{aligned}$$

$$= -\frac{1}{4\pi} \left[(\delta_m \hat{e}_t - \delta_m \hat{e}_s) I_1 + (-\epsilon_m \delta_t \hat{e}_s + \epsilon_m \hat{e}_n) I_2 \right. \\ \left. + (\epsilon_m \delta_s \hat{e}_t - \delta_m \hat{e}_n) I_3 + \hat{e}_n (\delta_s - \delta_t) I_4 \right]$$

where

$$I_1 = \iint \frac{\sigma}{r^3} d\sigma d\tau = \tan^{-1} \frac{\sigma \tau}{\epsilon_m r} \Big|_{t_0 - \frac{t}{2}}^{t_0 + \frac{t}{2}} \Big|_{s_0 - \frac{s}{2}}^{s_0 + \frac{s}{2}} \\ = \tan^{-1} \frac{(s_0 + \frac{s}{2})(t_0 + \frac{t}{2})}{\epsilon_m r_1} + \tan^{-1} \frac{(s_0 - \frac{s}{2})(t_0 - \frac{t}{2})}{\epsilon_m r_4} \\ - \tan^{-1} \frac{(s_0 + \frac{s}{2})(t_0 - \frac{t}{2})}{\epsilon_m r_2} - \tan^{-1} \frac{(s_0 - \frac{s}{2})(t_0 + \frac{t}{2})}{\epsilon_m r_3}$$

$$I_2 = \iint \frac{\tau}{r^3} d\sigma d\tau = \ln(r - \sigma) \Big|_{t_0 - \frac{t}{2}}^{t_0 + \frac{t}{2}} \Big|_{s_0 - \frac{s}{2}}^{s_0 + \frac{s}{2}} \\ = \ln \frac{(r_1 - (s_0 + \frac{s}{2})) (r_4 - (s_0 - \frac{s}{2}))}{(r_2 - (s_0 + \frac{s}{2})) (r_3 - (s_0 - \frac{s}{2}))}$$

$$I_3 = \iint \frac{\sigma}{r^3} d\sigma d\tau = \ln(r - \tau) \Big|_{t_0 - \frac{t}{2}}^{t_0 + \frac{t}{2}} \Big|_{s_0 - \frac{s}{2}}^{s_0 + \frac{s}{2}} \\ = \ln \frac{(r_1 - (t_0 + \frac{t}{2})) (r_4 - (t_0 - \frac{t}{2}))}{(r_2 - (t_0 - \frac{t}{2})) (r_3 - (t_0 + \frac{t}{2}))}$$

$$\begin{aligned} I_4 &= \iint \frac{\tau z}{r^3} dr d\tau = -r \left[\begin{array}{l} t_0 + \frac{\tau}{2} \\ t_0 - \frac{\tau}{2} \end{array} \right] \left[\begin{array}{l} s_0 + \frac{z}{2} \\ s_0 - \frac{z}{2} \end{array} \right] \\ &= -(\tau_1 + \tau_4 - \tau_2 - \tau_3) \end{aligned}$$

Finally, the induced velocity in terms of the circulation at the four corners is:

$$\begin{aligned} \Delta \vec{v} &= -\frac{(\Gamma_1 - \Gamma_3)}{4\pi st} \left[(t_0 - \frac{\tau}{2}) \hat{e}_s I_1 - c_m \hat{e}_s I_2 + (t_0 + \frac{\tau}{2}) \hat{e}_n I_3 - \hat{e}_n I_4 \right] \\ &\quad - \frac{(\Gamma_2 - \Gamma_4)}{4\pi st} \left[-(t_0 + \frac{\tau}{2}) \hat{e}_s I_1 + c_m \hat{e}_s I_2 - (t_0 + \frac{\tau}{2}) \hat{e}_n I_3 + \hat{e}_n I_4 \right] \\ &\quad - \frac{(\Gamma_1 - \Gamma_2)}{4\pi st} \left[(s_0 - \frac{z}{2}) \hat{e}_t I_1 + (s_0 - \frac{z}{2}) \hat{e}_n I_2 - c_m \hat{e}_t I_3 - \hat{e}_n I_4 \right] \\ &\quad - \frac{(\Gamma_3 - \Gamma_4)}{4\pi st} \left[-(s_0 + \frac{z}{2}) \hat{e}_t I_1 - (s_0 + \frac{z}{2}) \hat{e}_n I_2 + c_m \hat{e}_t I_3 + \hat{e}_n I_4 \right] \end{aligned}$$

where the first two terms are due to the trailed vorticity, and the last two terms are due to the shed vorticity. This may be written as

$$\begin{aligned} \Delta \vec{v} &= (\Gamma_1 - \Gamma_3) [-\vec{v}_{t_1} + \vec{v}_{t_2}] + (\Gamma_2 - \Gamma_4) [\vec{v}_{t_1} + \vec{v}_{t_2}] \\ &\quad + (\Gamma_1 - \Gamma_2) [-\vec{v}_{s_1} + \vec{v}_{s_2}] + (\Gamma_3 - \Gamma_4) [\vec{v}_{s_1} + \vec{v}_{s_2}] \end{aligned}$$

where

$$\vec{v}_{t_1} = \frac{1}{4\pi s t} [t_0 \hat{e}_s I_1 - r_m \hat{e}_s I_2 + t_0 \hat{e}_n I_3 - \hat{e}_n I_4]$$

$$\vec{v}_{t_2} = \frac{1}{4\pi s t} \left[\frac{t}{2} \hat{e}_s I_1 + \frac{t}{2} \hat{e}_n I_3 \right]$$

$$\vec{v}_{s_1} = \frac{1}{4\pi s t} [s_0 \hat{e}_c I_1 + s_0 \hat{e}_n I_2 - r_m \hat{e}_c I_3 - \hat{e}_n I_4]$$

$$\vec{v}_{s_2} = \frac{1}{4\pi s t} \left[\frac{s}{2} \hat{e}_c I_1 + \frac{s}{2} \hat{e}_n I_2 \right]$$

There is a logarithmic singularity in the velocity induced at the vortex sheet side edges (the $\gamma_m \hat{e}_n I_2$ and $\delta_m \hat{e}_n I_3$ terms in $\Delta \vec{v}$). This singularity will be avoided by replacing the trailed or shed sheet vorticity by a line segment with a large core radius. Hence if

$$r_m^2 + (s_0 \pm \frac{s}{2})^2 < d_{vs}^2 \quad \text{and} \quad |t_0| < \frac{t}{2} + d_{vs}$$

then the point P is near a side edge of the trailed vorticity; if

$$r_m^2 + (t_0 \pm \frac{t}{2})^2 < d_{vs}^2 \quad \text{and} \quad |s_0| < \frac{s}{2} + d_{vs}$$

then it is near a side edge of the shed vorticity; and if

$$|r| < d_{vs}$$

for any corner, the point P is near the side edges of both the shed and trailed vorticity.

An economical approximation is to replace the vortex sheet by a line segment, with either a linear or a stepped circulation distribution, and a large core size to eliminate the large induced velocity near the line. The

strength and position of the line segments are determined from the circulation and position of the four corners of the sheet: for the trailed vorticity

$$\Gamma_{2\text{line}} = \Gamma_1 - \Gamma_3$$

$$\Gamma_{1\text{line}} = \Gamma_2 - \Gamma_4$$

$$\vec{\Gamma}_{2\text{line}} = \frac{1}{2} (\vec{\Gamma}_1 + \vec{\Gamma}_3)$$

$$\vec{\Gamma}_{1\text{line}} = \frac{1}{2} (\vec{\Gamma}_2 + \vec{\Gamma}_4)$$

and for the shed vorticity

$$\Gamma_{2\text{line}} = \Gamma_2 - \Gamma_1$$

$$\Gamma_{1\text{line}} = \Gamma_4 - \Gamma_3$$

$$\vec{\Gamma}_{2\text{line}} = \frac{1}{2} (\vec{\Gamma}_1 + \vec{\Gamma}_2)$$

$$\vec{\Gamma}_{1\text{line}} = \frac{1}{2} (\vec{\Gamma}_3 + \vec{\Gamma}_4)$$

Note that with line segments it is not necessary to approximate the sheet geometry by a planar rectangle. The core radius can be specified arbitrarily; or $r_c = s/2$ can be used for the trailed vorticity and $r_c = t/2$ for the shed vorticity.

3.2 Free Wake Geometry

A method was developed in reference 16 for calculating the free wake geometry of a single rotor in steady state flight out of ground effect, which will be adapted for use in the present analysis. The wake model for the free wake calculation consists of line segments for the tip vortices; and

rectangular sheets or line segments for the inboard shed and trailede wake (similar to the far wake model used here for the induced velocity calculation; see section 3.1.2). The near wake or rolling up wake as described above are not considered.

Only the distorted geometry of the tip vertices is calculated in the analysis of reference 16. The rigid or prescribed wake geometry is thus still used for the inboard vorticity. The distortion of the tip vortex geometry from the basic helix is defined in reference 16 as a vector $\vec{D}_s(\psi, \delta)$, giving the displacement of the wake element with current age δ which was created when the blade was at azimuth angle ψ . A tip path plane coordinate frame is used, with the x axis to the right (the advancing side), the y axis aft, and the z axis down. The procedure for calculating the wake geometry consists basically of integrating the induced velocity at each wake element. The outer loop in the calculation is an iteration on the wake age δ . The induced velocity $\vec{q}(\psi)$ are calculated at all wake elements for a given age δ , and all azimuth angles ψ . Then the increment in the distortion as the wake age increases by $\Delta\psi$ is:

$$\vec{D}_s(\psi, \delta) = \vec{D}_s(\psi, \delta - \Delta\psi) + \Delta\psi \vec{q}(\psi)$$

An efficient calculation of the wake geometry requires many variations in this basic procedure. Reference 16 adapted the near-wake and far-wake scheme for reducing the computation. The first time the induced velocity is evaluated at a point in the wake, the contributions from all wake elements must be found. For subsequent evaluations of the induced velocity at that point, only the induced velocity, due to the nearby wake elements are recalculated. The other major consideration for minimizing the computation is the matter of updating the induced velocity calculation. At a given point in the wake geometry calculation, there is a boundary in the wake between the distorted geometry and the initial, rigid geometry. The distortion has been calculated

between the rotor disk and the boundary; downstream of the boundary the wake is undistorted. As time increases by $\Delta\psi$, the entire wake is convected downstream, and the rotor blades move forward by $\Delta\psi$, adding new trailed and shed vorticity at the beginning of the wake. If there were no distortion of the wake during the time $\Delta\psi$, then the induced velocity at a given wake element would not change except for the contributions from the newly created wake vorticity just behind the blade. Thus the normal calculation procedure consists of calculating the induced velocity at the boundary, by just adding at each step the contribution from the new wake directly behind the blade. Of course, the wake does distort as it is convected and as the estimate of the distortion improves, thus it is necessary to update the calculation of the induced velocity in the wake. In boundary updating, the induced velocity is calculated at the boundary still, by summing the contributions from all elements in the wake. In general updating, the induced velocity is recalculated at all points in the wake upstream of the boundary. Boundary updating is typically done every 90° on the front and rear portions of the helices, and every 45° along the sides where the distortion is greater. General updating is typically done every 180° . General updating can not be done often if the amount of computation is to be kept low, but it does improve the accuracy and convergence. Numerous techniques for secondary improvements in the efficiency and accuracy were also included. The distorted wake geometry is required for m revolutions, where m decreases with forward speed. A single iteration of the free wake analysis consists of calculating the distortion $D_s(\psi, \delta)$ for $\psi = 0$ to 2π and $\delta = 0$ to $2\pi m$. Usually two iterations are sufficient to obtain the converged solution for the wake geometry.

The present analysis requires the wake geometry in the form of $D(\psi, \phi)$ where ψ is the current azimuth angle of the blade and ϕ is the wake age ($\psi + \delta$ and δ respectively in the notation of ref. 16). The present analysis uses a tip path plane coordinate system with x aft, y to the right, and z upward. Hence

$$\vec{D}(\psi, \phi) = [\vec{\tau}_\tau \vec{\gamma}_\tau + \vec{\delta}_\tau \vec{\zeta}_\tau - \vec{k}_\tau \vec{k}_\tau] \vec{D}_s(\psi - \phi, \phi)$$

is the distortion as used in section 3.1.3. The rotor velocity components μ_x and μ_z are required relative to the tip path plane. The hub motion and gust velocity at the hub can be included in these velocity components. Ground effect and rotor/rotor interference can be accounted for by using an effective normal velocity:

$$\mu_{z_{eff}} = \mu_{z_{TPI}} + (1 - f_{GE}^{-1}) \lambda_i + \lambda_{int}$$

where f_{GE} is the ground effect factor defined in section 2.4.3, and λ_{int} is the interference induced velocity. The total uniform induced velocity

$$\lambda = \mu_{z_{TPI}} + \lambda_i + \lambda_{int}$$

is required to define the wake geometry at the start of the calculation.

4. AIRCRAFT MODEL

4.1 Aircraft Configuration Definition

A general two rotor aircraft is considered, with rigid body and elastic motion of the airframe. Aerodynamic forces on the wing/body, horizontal tail, and vertical tail are modelled, including aerodynamic control surfaces. The drive train connecting the rotors is modelled, with engine dynamics and a rotor speed governor. The case of a rotor or helicopter on a flexible support in a wind tunnel is included in the model.

4.1.1 *Aircraft orientation: flight path and trim Euler angles.* - The aircraft flight path is specified by the velocity magnitude V , and the orientation of the velocity vector with respect to earth axes (fig. 22). The velocity vector has a yaw angle ψ_{FP} (positive to the right), and a pitch angle θ_{FP} (positive upward). Thus the climb and side velocities of the aircraft are $v_{climb} = V \sin \theta_{FP}$ and $v_{side} = V \sin \psi_{FP} \cos \theta_{FP}$. The aircraft attitude with respect to earth axes is specified by the trim Euler angles, first pitch θ_{FT} (positive nose up), then roll ϕ_{FT} (positive to the right). Airplane convention is followed here for the coordinate systems -- x positive forward, y positive to the right, and z positive downward (see reference 25). Between the earth axes (E system) and the velocity axes (V system) there are the rotations ψ_{FP} and θ_{FP} . Between the earth axes and the body axes (F system) there are the rotations θ_{FT} and ϕ_{FT} . Thus the rotation matrix between the V system and the F system is:

$$R_{FV} = \begin{bmatrix} C_{\theta_{FT}} C_{\theta_{FP}} C_{\psi_{FP}} & -C_{\theta_{FT}} S_{\psi_{FP}} & C_{\theta_{FT}} S_{\theta_{FP}} C_{\psi_{FP}} \\ + S_{\theta_{FT}} S_{\psi_{FP}} & & -S_{\theta_{FT}} C_{\psi_{FP}} \\ S_{\theta_{FT}} S_{\phi_{FT}} C_{\theta_{FP}} C_{\psi_{FP}} & -S_{\theta_{FT}} S_{\phi_{FT}} S_{\psi_{FP}} & S_{\theta_{FT}} S_{\phi_{FT}} S_{\theta_{FP}} C_{\psi_{FP}} \\ + C_{\phi_{FT}} C_{\theta_{FP}} S_{\psi_{FP}} & + C_{\phi_{FT}} C_{\psi_{FP}} & + C_{\phi_{FT}} S_{\theta_{FP}} S_{\psi_{FP}} \\ - C_{\theta_{FT}} S_{\phi_{FT}} S_{\theta_{FP}} & + C_{\phi_{FT}} S_{\psi_{FP}} & + C_{\theta_{FT}} S_{\phi_{FT}} C_{\theta_{FP}} \\ S_{\theta_{FT}} C_{\phi_{FT}} C_{\theta_{FP}} C_{\psi_{FP}} & -S_{\theta_{FT}} C_{\phi_{FT}} S_{\psi_{FP}} & S_{\theta_{FT}} C_{\phi_{FT}} S_{\theta_{FP}} C_{\psi_{FP}} \\ - S_{\phi_{FT}} C_{\theta_{FP}} S_{\psi_{FP}} & -S_{\phi_{FT}} C_{\psi_{FP}} & - S_{\phi_{FT}} S_{\theta_{FP}} S_{\psi_{FP}} \\ - C_{\theta_{FT}} C_{\phi_{FT}} S_{\theta_{FP}} & & + C_{\theta_{FT}} C_{\phi_{FT}} C_{\theta_{FP}} \end{bmatrix}$$

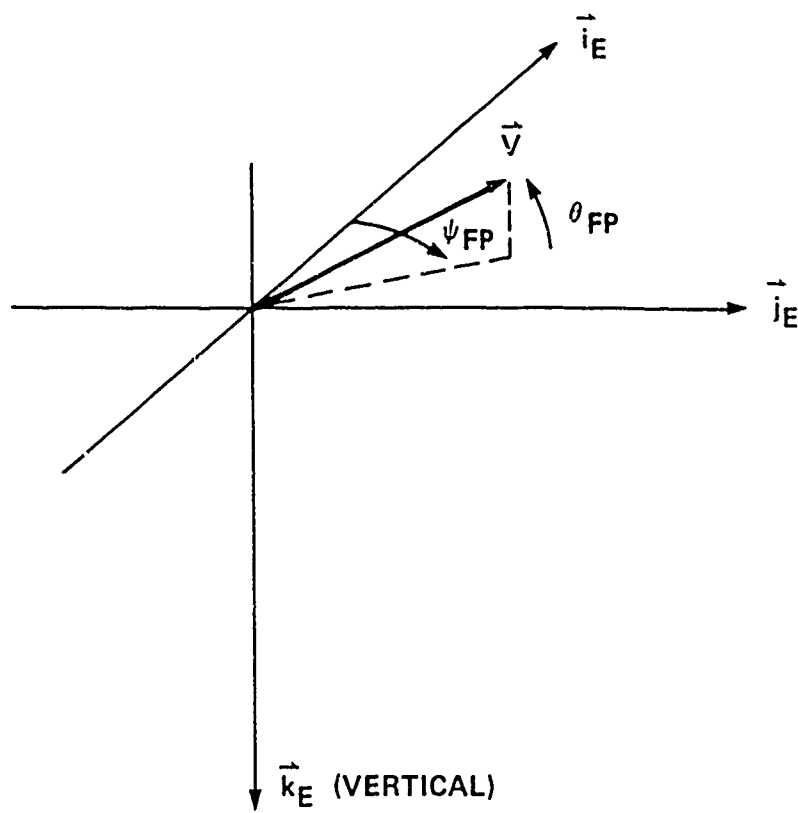


Figure 22. Earth axes and aircraft flight path definition.

The trim calculation determines the Euler angles θ_{FT} and ϕ_{FT} (and perhaps the flight path climb angle θ_{FP} also).

The velocity of the aircraft is $\vec{V} = V \vec{i}_V$, so the components in the body axes are:

$$\begin{pmatrix} v_x \\ v_y \\ v_z \end{pmatrix} = V R_{FV} \vec{i}_V$$

The acceleration due to gravity is $\vec{g} = g \vec{k}_E$ or in body axes

$$\vec{g} = g \vec{k}_E = g \begin{pmatrix} -\sin\theta_{FT} \\ \cos\theta_{FT} \sin\phi_{FT} \\ \cos\theta_{FT} \cos\phi_{FT} \end{pmatrix}$$

4.1.2 Rotor position and orientation. - The rotor hub position is specified in the body axes relative to the aircraft center of gravity position, $\vec{r}_{hub} = (x_F \vec{i}_F + y \vec{j}_F + z \vec{k}_F)_{hub}$. The rotor orientation is defined by the rotation matrix between the shaft axes (S system) and the aircraft body axes (F system).

$$\begin{pmatrix} \vec{i}_S \\ \vec{j}_S \\ \vec{k}_S \end{pmatrix} = R_{SF} \begin{pmatrix} \vec{i}_F \\ \vec{j}_F \\ \vec{k}_F \end{pmatrix}$$

The position and orientation of the rotors relative to the body axes are fixed geometric parameters. The aircraft velocity is $\vec{V} = -\mu_x \vec{i}_S + \mu_y \vec{j}_S + \mu_z \vec{k}_S = V \vec{i}_V$, so the shaft axes components of the velocity seen by the rotor are

$$\begin{pmatrix} -\mu_x \\ \mu_y \\ \mu_z \end{pmatrix} = R_{SF} R_{FV} \begin{pmatrix} V \\ 0 \\ 0 \end{pmatrix}$$

The hub plane angle of attack and yaw angle may then be obtained from

$$\alpha_{HP} = \tan^{-1} \mu_z / \sqrt{\mu_x^2 + \mu_y^2}$$

$$\mu_{HP} = \tan^{-1} \mu_y / \mu_x$$

and the advancing tip Mach number from

$$M_{AT} = M_{Tip} \sqrt{(1 + \sqrt{\mu_x^2 + \mu_y^2})^2 + \mu_z^2}$$

The sign of the lateral velocity μ_y must be changed for a clockwise rotating rotor; and for rotor #2 the velocity components must be multiplied by $\Omega R_1 / \Omega R_2$. The quasistatic hub motion and the gust velocity at the rotor hub will be included in the advance ratio components:

$$\begin{pmatrix} -\mu_x \\ \mu_y \\ \mu_z \end{pmatrix} = R_{SF} R_{FV} \begin{pmatrix} V + u_e \\ v_g \\ w_g \end{pmatrix} + \begin{pmatrix} x_e \\ y_e \\ z_e \end{pmatrix}_{\text{Static}}$$

For a helicopter main rotor, the orientation with respect to the body axes will be specified by a shaft angle of attack θ_R (positive for rearward tilt), and a roll angle ϕ_R (positive to the right). Thus:

$$R_{SF} = \begin{bmatrix} -c_\theta & 0 & s_\theta \\ s_\phi c_\theta & c_\phi & s_\phi s_\theta \\ -c_\phi s_\theta & s_\phi & -c_\phi c_\theta \end{bmatrix}$$

The orientation of a tail rotor will be specified by a cant angle ϕ_R (positive upward), and a shaft angle of attack θ_R (positive rearward). The tail rotor thrust is to the right for a counterclockwise rotating main rotor, and to the left for clockwise rotation. Thus the definition of the tail rotor shaft axes depends on the main rotor rotation direction. Let Ω_{mr} have the value +1 for a counterclockwise rotating main rotor, and $\Omega_{mr} = -1$ for a clockwise rotation. Then the rotation matrix for the tail rotor is:

$$R_{SF} = \begin{bmatrix} -c_\theta & -\Omega_{mr} c_\phi s_\theta & s_\phi s_\theta \\ 0 & s_\phi & \Omega_{mr} c_\phi \\ -s_\theta & \Omega_{mr} c_\phi c_\theta & -s_\phi c_\theta \end{bmatrix}$$

The nacelle and rotor of a tilting proprotor aircraft can be tilted by an angle α_p , where $\alpha_p = 0$ for axial flow (airplane configuration), and $\alpha_p = 90^\circ$ for edgewise flow (helicopter configuration). The rotor orientation is also described by a cant angle ϕ_R (positive inward in helicopter mode, zero in airplane mode), and a pitch angle θ_R (positive nose upward) which is the angle of attack of the shaft with respect to the body axes when $\alpha_p = 0$. Thus the rotation matrix is:

$$R_{SF} = \begin{bmatrix} -c_\phi s_\alpha c_\theta - c_\alpha s_\theta & -s_\phi s_\alpha & c_\phi s_\alpha s_\theta - c_\alpha c_\theta \\ -c_\phi s_\phi (1 - c_\alpha) c_\theta - s_\phi s_\alpha s_\theta & c_\phi^2 + s_\phi^2 c_\alpha & c_\phi s_\phi (1 - c_\alpha) s_\theta - s_\phi s_\alpha c_\theta \\ (c_\phi^2 c_\alpha + s_\phi^2) c_\theta - c_\phi s_\alpha s_\theta & -c_\phi s_\phi (1 - c_\alpha) & -(c_\phi^2 c_\alpha + s_\phi^2) s_\theta - c_\phi s_\alpha c_\theta \end{bmatrix}$$

The rotor hub location \vec{r}_{hub} for the tilting proprotor aircraft is defined by the pivot location \vec{r}_{pivot} and the mast height h , so

$$\vec{r}_{\text{hub}} = \vec{r}_{\text{pivot}} + h \begin{pmatrix} (c_{\phi}^2 c_{\alpha} + s_{\phi}^2) c_{\theta} - c_{\phi} s_{\alpha} s_{\theta} \\ -c_{\phi} s_{\phi} (1 - c_{\alpha}) \\ -(c_{\phi}^2 c_{\alpha} + s_{\phi}^2) s_{\theta} - c_{\phi} s_{\alpha} c_{\theta} \end{pmatrix}$$

4.1.3 Wind tunnel case. - For the case of a rotor or rotorcraft in a wind tunnel, the forces and moments on the body are reacted by the model support system, so trim of the body forces is no longer a concern. The flight path and trim Euler angles can be set to zero ($\theta_{FT} = \phi_{FT} = \theta_{FP} = \psi_{FP} = 0$), so the wind, earth, and body axes coincide ($R_{FV} = I$). The wind axes and body axes are therefore the tunnel axes system, with the x-axis directed upstream, the y-axis to the right, and the z-axis vertically downward. The rotor orientation is specified by the matrix R_{SF} as above. To accommodate the case of a wind tunnel with a turntable, the R_{SF} matrices can be post-multiplied by the matrix

$$R_{FT} = \begin{bmatrix} c_{\alpha} c_{\psi} & c_{\alpha} s_{\psi} & -s_{\alpha} \\ -s_{\psi} & c_{\psi} & 0 \\ s_{\alpha} c_{\psi} & s_{\alpha} s_{\psi} & c_{\alpha} \end{bmatrix}$$

where ψ_T is the turntable yaw angle, positive to the right, and θ_T is the test module pitch angle, positive rearward.

4.1.4 Gust velocity. - The aerodynamic gust velocity will be defined relative to the velocity axes, with longitudinal component u_G positive rearward, lateral component v_G positive from the right, and vertical component w_G positive upward ($\vec{v}_{\text{gust}} = -u_G \vec{i}_V - v_G \vec{j}_V - w_G \vec{k}_V$). The components in the body axes are then

$$\begin{pmatrix} u_G \\ v_G \\ w_G \end{pmatrix}_F = R_{FV} \begin{pmatrix} u_G \\ v_G \\ w_G \end{pmatrix}_V$$

The components in the rotor shaft axes are

$$\begin{pmatrix} u_G \\ -v_G \\ w_G \end{pmatrix}_S = R_{SF} R_{FV} \begin{pmatrix} -u_G \\ -v_G \\ -w_G \end{pmatrix}_V$$

For a clockwise rotating rotor, the sign of v_G is changed; for rotor #2 the gust velocities must be multiplied by $\Omega R_1 / \Omega R_2$. Hence define

$$R_G = \begin{bmatrix} -1 & 0 & 0 \\ 0 & 1 & 0 \\ 0 & 0 & -1 \end{bmatrix} R_{SF} R_{FV}$$

including also the factor $\Omega R_1 / \Omega R_2$ and the sign change for a clockwise rotating rotor as appropriate.

4.1.5 Aircraft description.— The aircraft geometrical description consists of the location of rotor #1, rotor #2, and wing/body, the horizontal tail, and the vertical tail relative to the center of gravity. The orientation and position of the aircraft components will be defined in a body axis system (the F frame) with origin at an arbitrary reference point, as in figure 23. Given the dimensional positions relative to the reference point, for example

center of gravity:	FSCG, WLCG, BLCG
rotor #1:	FSRL, WLRL, BLRL

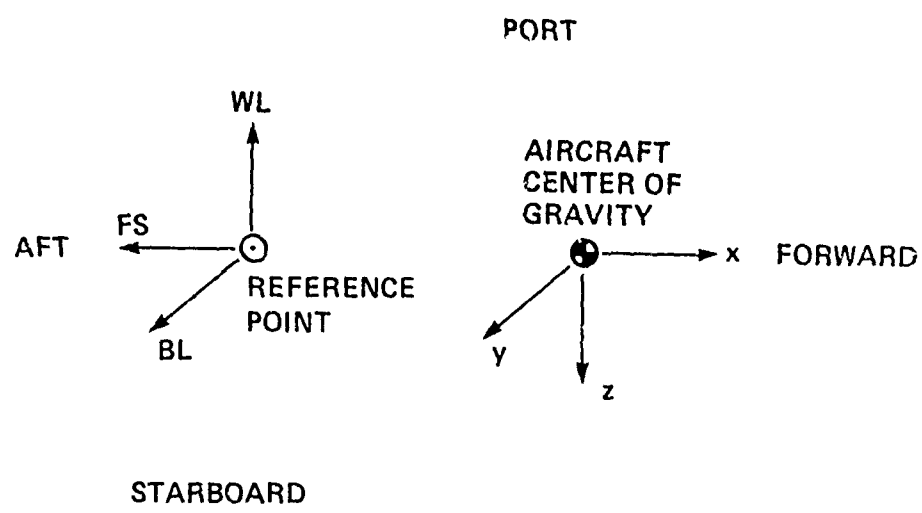


Figure 23. Definition of aircraft geometry.

Then the coordinates of the location of rotor #1 relative to the center of gravity (in the F frame) are

$$\begin{aligned}x &= (\text{FSCG} - \text{FSR1})/R \\y &= (\text{BLR1} - \text{BLCG})/R \\z &= (\text{WLCG} - \text{WLR1})/R\end{aligned}$$

and similarly for the rotor #2, wing/body, horizontal tail, and vertical tail.

The mode shapes of the airframe elastic motion are described by the six components of linear and angular hub motion, in the F frame: ξ_k and γ_k at \vec{r}_{hub} (for each rotor). Assuming that the generalized coordinate q_k has dimensions of m or ft, it follows that the generalized mass M_k has dimensions of kg or slug; that the hub linear motion ξ_k is dimensionless; and that the hub angular motion γ_k has dimensions rad/m or rad/ft. These elastic vibration modes can be arbitrarily scaled; if ξ_k and γ_k are multiplied by a factor S , then M_k should be multiplied by S^2 and the solution for q_k will be divided by S .

For the case of a wind tunnel with a turntable, the geometry will be defined for zero yaw angle, relative to a reference point at the center of the rotation. Then

$$\begin{pmatrix} x \\ y \\ z \end{pmatrix} = R_{TF} \begin{pmatrix} x \\ y \\ z \end{pmatrix}_{\psi=\theta=0}$$

where R_{TF} is defined in section 4.1.3.

4.1.6 Pilot's controls. - The control variables included in the rotorcraft model are collective and cyclic pitch of the two rotors, and the aircraft controls, which consist of engine throttle θ_t , wing flaperon angle δ_f , wing aileron angle δ_a , elevator angle δ_e , and rudder angle δ_r . The control vector is thus

$$\vec{\nabla}^T = [(\theta_0 \ \theta_{1c} \ \theta_{1s})_1 \ (\theta_0 \ \theta_{1c} \ \theta_{1s})_2 \ \delta_f \ \delta_e \ \delta_a \ \delta_r \ \theta_t]$$

The pilot's controls consist of collective stick δ_o (positive upward), lateral cyclic stick δ_c (positive to the right), longitudinal cyclic stick δ_s (positive forward), pedal δ_p (positive yaw right), and the throttle δ_t :

$$\vec{v}_p^T = [\delta_o \ \delta_c \ \delta_s \ \delta_p \ \delta_t]$$

For the purpose of trimming the helicopter, a linear relation between the pilot's control inputs and the rotor and aircraft control variables is assumed:

$$\vec{v} = T_{CFE} \vec{v}_p + \vec{v}_o$$

where \vec{v}_o is the control input with all sticks centered ($\vec{v}_p = 0$), and T_{CFE} is a transformation matrix defined by the control system geometry.

The control transformation matrices for the single main-rotor and tail-rotor, the tandem main rotor, and the side-by-side main-rotor configurations are given below. The K's are gain factors in the control system, and the $\Delta\psi$'s are swashplate azimuth lead angles. The main rotor, front rotor, or right rotor is assumed to be rotor #1; and the tail rotor, rear rotor, or left rotor is rotor #2. The parameter Ω here takes the value +1 for counter-clockwise rotation of the rotor, and $\Omega = -1$ for clockwise rotation.

$$(T_{CFE})_{\text{single main rotor}} = \begin{bmatrix} K_0 & 0 & 0 & 0 & 0 & 0 \\ 0 & -S_{mr} K_c \cos \Delta \Psi_c & -K_s \sin \Delta \Psi_s & 0 & 0 & 0 \\ 0 & -S_{mr} K_c \sin \Delta \Psi_c & -K_s \cos \Delta \Psi_s & 0 & 0 & 0 \\ 0 & 0 & 0 & -J_{mr} K_p & 0 & 0 \\ 0 & 0 & 0 & 0 & 0 & 0 \\ 0 & 0 & 0 & 0 & 0 & 0 \\ K_f & 0 & 0 & 0 & 0 & 0 \\ 0 & 0 & K_e & 0 & 0 & 0 \\ 0 & -K_a & 0 & 0 & 0 & 0 \\ 0 & 0 & 0 & K_r & 0 & 0 \\ K_t & 0 & 0 & 0 & 0 & 1 \end{bmatrix}$$

$$(T_{CFE})_{\text{tandem main rotors}} = \begin{bmatrix} K_{f0} & 0 & -K_{fs} & 0 & 0 & 0 \\ 0 & -S_1 K_{fc} \cos \Delta \Psi_{fc} & 0 & -S_1 K_{fp} \cos \Delta \Psi_{fp} & 0 & 0 \\ 0 & S_1 K_{fc} \sin \Delta \Psi_{fc} & 0 & S_1 K_{fp} \sin \Delta \Psi_{fp} & 0 & 0 \\ K_{r0} & 0 & K_{rs} & 0 & 0 & 0 \\ 0 & -S_2 K_{rc} \cos \Delta \Psi_{rc} & 0 & S_2 K_{rp} \cos \Delta \Psi_{rp} & 0 & 0 \\ 0 & S_2 K_{rc} \sin \Delta \Psi_{rc} & 0 & -S_2 K_{rp} \sin \Delta \Psi_{rp} & 0 & 0 \\ K_f & 0 & 0 & 0 & 0 & 0 \\ 0 & 0 & K_e & 0 & 0 & 0 \\ 0 & -K_a & 0 & 0 & 0 & 0 \\ 0 & 0 & 0 & K_r & 0 & 0 \\ K_t & 0 & 0 & 0 & 0 & 1 \end{bmatrix}$$

$$(T_{CFE})_{\text{side-by-side main rotors}} = \begin{bmatrix} k_o & -k_c & 0 & 0 & 0 \\ 0 & 0 & -k_s \sin \Delta \psi_s & k_p \sin \Delta \psi_p & 0 \\ 0 & 0 & -k_s \cos \Delta \psi_s & k_p \cos \Delta \psi_p & 0 \\ k_o & k_c & 0 & 0 & 0 \\ 0 & 0 & -k_s \sin \Delta \psi_s & -k_p \sin \Delta \psi_p & 0 \\ 0 & 0 & -k_s \cos \Delta \psi_s & -k_p \cos \Delta \psi_p & 0 \\ k_f & 0 & 0 & 0 & 0 \\ 0 & 0 & k_c & 0 & 0 \\ 0 & -k_a & 0 & 0 & 0 \\ 0 & 0 & 0 & k_r & 0 \\ k_t & 0 & 0 & 0 & 1 \end{bmatrix}$$

4.2 Aircraft Analysis

The aircraft motion consists of the six rigid body degrees of freedom and the elastic free vibration modes. A body axis coordinate frame with origin at the aircraft center of gravity (the F system) is used for the description of the motion. Airplane practice is followed for these axes -- x is forward, y is to the right, and z is downward (ref. 25). The coordinate frame used is not a principal axis system however; moreover, the airplane practice of aligning the x-axis with the trim velocity is not followed, since for rotorcraft it is necessary to consider the hovering case ($V = 0$).

The parameters of rotor #1 are used in making quantities dimensionless and in normalizing the aircraft equations of motion. It is assumed that

rotor #1 is the main-rotor of a single main rotor and tail rotor helicopter; the front rotor of a tandem rotor helicopter; or the right rotor of a side-by-side rotor helicopter. With the hub forces in rotor coefficient form it is convenient to normalize the equations by dividing by the characteristic inertia ($\frac{1}{2}NI_b$)₁.

4.2.1 *Degrees of freedom.* - The linear and angular rigid body motion of the aircraft is defined in the body axes (F system). The linear degrees of freedom are x_F (positive forward), y_F (positive to the right), and z_F (positive downward). These variables are dimensionless based on the rotor radius R; thus the velocity perturbations are normalized using the rotor tip speed ΩR rather than the forward speed V as is airplane practice. The angular degrees of freedom are the Euler angles ψ_F (yaw to the right), θ_F (pitch nose up), and ϕ_F (roll right). Then the linear and angular velocity perturbations are

$$\begin{aligned}\vec{u}_F &= \dot{x}_F \vec{i}_F + \dot{y}_F \vec{j}_F + \dot{z}_F \vec{k}_F \\ \vec{\omega}_F &= R_e (\dot{\phi}_F \vec{i}_F + \dot{\theta}_F \vec{j}_F + \dot{\psi}_F \vec{k}_F)\end{aligned}$$

where

$$R_e = \begin{bmatrix} 1 & 0 & -\sin\theta_{FT} \\ 0 & \cos\phi_{FT} & \sin\phi_{FT} \cos\theta_{FT} \\ 0 & -\sin\phi_{FT} & \cos\phi_{FT} \cos\theta_{FT} \end{bmatrix}$$

For the elastic motion of the aircraft in flight, the displacement \vec{u} and rotation $\vec{\theta}$ at an arbitrary point \vec{r} are expanded in a series of the orthogonal free vibration modes:

$$\vec{u}(\vec{r}, t) = \sum_{k=1}^{\infty} q_{sk}(t) \vec{\xi}_k(\vec{r})$$

$$\vec{\theta}(\vec{r}, t) = \sum_{k=1}^{\infty} q_{Sk}(t) \vec{\delta}_k(\vec{r})$$

The first six degrees of freedom are the rigid body motions: $q_{S1} \dots q_{S6}$ are respectively $\phi_F, \theta_F, \psi_F, x_F, y_F$, and z_F . The generalized coordinates q_{Sk} for $K \geq 7$ are the elastic modes of the aircraft. Orthogonality implies that the elastic vibration modes produce no net displacement of the aircraft center of gravity, or rotation of the principal axes.

For the rigid body motions the mode shapes are simply

$$\begin{bmatrix} \vec{z}_1 & \dots & \vec{z}_6 \end{bmatrix} = \begin{bmatrix} (-\vec{r}_x) R_e & I \end{bmatrix}$$

$$\begin{bmatrix} \vec{\delta}_1 & \dots & \vec{\delta}_6 \end{bmatrix} = \begin{bmatrix} R_e & 0 \end{bmatrix}$$

since

$$\vec{u} = \vec{x}_F + \vec{\alpha}_F \times \vec{r} = \vec{x}_F - (\vec{r}_x) R_e \vec{\alpha}_e$$

$$\vec{\theta} = \vec{\alpha}_F = R_e \vec{\alpha}_e$$

4.2.2 Hub motion.- The rotor equations of motion require the six components of the hub linear and angular motion in the shaft axis system:

$$\begin{pmatrix} x_h \\ y_h \\ z_h \\ \alpha_x \\ \alpha_y \\ \alpha_z \end{pmatrix} = \begin{bmatrix} R_{SF} \vec{z}_k(\vec{r}_{hub}) \\ \dots \\ R_{SF} \vec{\delta}_k(\vec{r}_{hub}) \end{bmatrix} \quad \{ q_{Sk} \}$$

or

$$\alpha = \begin{bmatrix} R_{SF} (-\vec{r}_{hub} \times) R_e & R_{SF} & \dots R_{SF} \vec{z}_k \dots \\ R_{SF} R_e & 0 & \dots R_{SF} \vec{\delta}_k \dots \end{bmatrix} x_s = c x_s$$

The matrix R_{SF} transforms the motion from body to shaft axes. The moment arm of the rotor hub about the aircraft center of gravity is in body axes, $\vec{r}_{hub} = x\vec{i}_F + y\vec{j}_F + z\vec{k}_F$.

The total velocity of a point is the sum of the trim and perturbation velocities, $\vec{u} = \vec{V} + \sum q_{sk} \vec{\xi}_k$, in body axes. The rotor equations require the velocity components at the hub in an inertial frame however (the S system), and the Euler angle rotations between the body and inertial axes introduce perturbations of the trim velocity \vec{V} . So the perturbation velocity becomes $\vec{u} = \vec{\alpha}_F \times \vec{V} + \sum q_{sk} \vec{\xi}_k$, where in the S system

$$\vec{\alpha}_F \times \vec{V} = \begin{pmatrix} \mu_z \alpha_y - \mu_y \alpha_z \\ -\mu_z \alpha_x - \mu_x \alpha_z \\ \mu_x \alpha_y + \mu_y \alpha_x \end{pmatrix}$$

These contributions to the hub velocities ($\dot{x}_h, \dot{y}_h, \dot{z}_h$) cancel the terms in the blade velocity due to the Euler angle rotation of the inertial axes relative to the trim velocity (the $\mu \alpha$ terms in u_T, u_p , and u_R). Thus the evaluation of the hub rotation ($\alpha_x, \alpha_y, \alpha_z$) for the aerodynamic analysis should not include the body Euler angle contributions, as discussed in section 2.4.2.

Finally, the rotor hub acceleration is $\ddot{\vec{u}} = \vec{\omega}_F \times \vec{V} + \sum \ddot{q}_{sk} \vec{\xi}_k$, where the first term is the inertial acceleration due to the rotation of the trim velocity vector by the body axes angular velocity. This additional contribution of the Euler angle velocity to the hub linear acceleration, in the shaft axes system, is

$$\Delta \begin{pmatrix} \dot{x}_h \\ \dot{y}_h \\ \dot{z}_h \end{pmatrix} = \vec{\omega}_F \times \vec{V} = R_{SF} (-\vec{V} \times) R_e \begin{pmatrix} \dot{\phi}_F \\ \dot{\theta}_F \\ \dot{\psi}_F \end{pmatrix}$$

which can be written $\Delta \ddot{\vec{u}} = \bar{c} \vec{x}_S$ with

$$\bar{c} = \begin{bmatrix} R_{SF} (-\vec{V} \times) R_e & 0 \\ 0 & 0 \end{bmatrix}$$

For rotor #2 the linear hub displacement (x_h , y_h , z_h) must be multiplied by R_1/R_2 to account for the differences in normalization, c being based on rotor #1 parameters while α is based on rotor #2 parameters in this case. For a clockwise rotating rotor it is necessary to change the signs of y_h , α_x , and α_z . These conversions will be included in the definition of c and \bar{c} , by

- multiplying rows 1, 2, and 3 by R_1/R_2
- changing the signs of rows 2, 4, and 6

as appropriate. In addition, the derivatives of the hub motion of rotor #2 must be corrected for the different time base, by multiplying the velocities by Ω_1/Ω_2 and the acceleration by Ω_1^2/Ω_2^2 :

$$\dot{\alpha} = \frac{\dot{z}_1}{\dot{z}_2} c \dot{x}_s$$

$$\ddot{\alpha} = \left(\frac{\dot{z}_1}{\dot{z}_2} \right)^2 (c \ddot{x}_s + \bar{c} \dot{x}_s)$$

(See section 5.1.5 for the time scale correction in the case of harmonic body motion.)

4.2.3 *Pitch/mast-bending coupling.* - Flexibility between the rotor swash-plate and hub will produce a blade pitch change due to elastic motion of the airframe. This coupling between the rotor pitch and mast bending is accounted for by introducing kinematic feedback of the following form:

$$\Delta\theta_{\text{mast bend}} = - \sum_{i=1}^{\infty} q_s; (k_{mc}; \cos\psi_m + k_{ms}; \sin\psi_m)$$

4.2.4 *Equations of motion.* - Following the usual steps of airplane flight dynamics analysis (see ref. 25), the linearized rigid body equations of motion are obtained by equating the angular and linear acceleration to the net moments and forces on the aircraft: $I\dot{\omega}_F = \Sigma M$ and $M(\dot{u}_F + \dot{\omega}_F \times \dot{v}) = \Sigma F$. In terms of the body axis degrees of freedom, including the gravitational forces, the equations are:

$$R_e^T I^* R_e \begin{pmatrix} \dot{\phi}_F \\ \dot{\theta}_F \\ \dot{\psi}_F \end{pmatrix} = \begin{pmatrix} Q_1^* \\ Q_2^* \\ Q_3^* \end{pmatrix}$$

$$M^* \begin{pmatrix} \dot{x}_F \\ \dot{y}_F \\ \dot{z}_F \end{pmatrix} - M^* (\vec{v} \times) \vec{k}_E \begin{pmatrix} \dot{\phi}_F \\ \dot{\theta}_F \\ \dot{\psi}_F \end{pmatrix} =$$

$$\begin{pmatrix} Q_4^* \\ Q_5^* \\ Q_6^* \end{pmatrix} + M^* g \vec{k}_E - G \begin{pmatrix} \dot{\phi}_F \\ \dot{\theta}_F \\ \dot{\psi}_F \end{pmatrix}$$

where

$$G = -M^* g \begin{bmatrix} \frac{\partial \vec{k}_E}{\partial \phi_F} & \frac{\partial \vec{k}_E}{\partial \theta_F} & \frac{\partial \vec{k}_E}{\partial \psi_F} \end{bmatrix} = M^* g \begin{bmatrix} 0 & C_{\phi F T} & 0 \\ -C_{\theta F T} C_{\phi F T} & S_{\theta F T} S_{\phi F T} & 0 \\ C_{\theta F T} S_{\phi F T} & -S_{\theta F T} C_{\phi F T} & 0 \end{bmatrix}$$

Here M is the aircraft mass, including the rotors, and I is the moment of inertia matrix:

$$I = \begin{bmatrix} I_x & -I_{xy} & -I_{xz} \\ -I_{xy} & I_y & -I_{yz} \\ -I_{xz} & -I_{yz} & I_z \end{bmatrix}$$

($I_{xy} = I_{yz} = 0$ if lateral symmetry is assumed). These equations are dimensionless, and have been normalized by dividing by the characteristic inertia $(\frac{1}{2} N I_b)$. Thus $M^* = M / (\frac{1}{2} N I_b / R^2)$ and $I^* = I / (\frac{1}{2} N I_b)$. Note that the gravitational constant g is also dimensionless, based on the acceleration $\Omega^2 R$; and $M^* g = \gamma 2 C_W / c_a$, where $W = Mg$ is the gross weight.

For the elastic degrees of freedom, since orthogonal free vibration modes are used the equations of motion are simply

$$M_k^* (\ddot{q}_{sk} + g_s \omega_k \dot{q}_{sk} + \omega_k^2 q_{sk}) = Q_k^* \quad (k \geq 7)$$

where M_k^* is the generalized mass including the rotors (in normalized form $M_k^* = M_k / (1/2 N I_b / R^2)$), ω_k is the natural frequency of the mode, and g_s is the structural damping coefficient.

The generalized forces Q_k^* are due to the hub reactions of the two rotors, and the aerodynamic forces on the aircraft. Since the rotor mass is included in the aircraft inertia, the hub linear acceleration terms should not be included in the evaluation of the hub forces for these equations of motion. The aircraft aerodynamic forces are considered in section 4.2.6.

Similarly, the rotor gravitational forces are not included in the rotor hub forces, since the rotor weight is included in the aircraft gross weight.

4.2.5 Hub forces.- The aircraft generalized force due to the rotor hub reactions is

$$Q_k = \vec{\beta}_k(\vec{r}_{hub}) \cdot \vec{F}_{hub} + \vec{\delta}_k(\vec{r}_{hub}) \cdot \vec{M}_{hub}$$

Normalizing Q_k by dividing by $1/2 N I_b$ gives then

$$\{Q_k^*\} = \begin{bmatrix} & & & \vdots & \\ \vec{\beta}_k \cdot \vec{\beta}_k & \vec{\beta}_k \cdot \vec{\beta}_k & \vec{\beta}_k \cdot \vec{\beta}_k & \vec{\beta}_k \cdot \vec{\beta}_k & \vec{\beta}_k \cdot \vec{\beta}_k \\ \vdots & & & & \end{bmatrix} \left| \begin{array}{c} \gamma \frac{2C_H}{\sigma a} \\ \gamma \frac{2C_Y}{\sigma a} \\ \gamma \frac{2C_R}{\sigma a} \\ \gamma \frac{2C_M}{\sigma a} \\ \gamma \frac{2C_{My}}{\sigma a} \\ -\gamma \frac{2C_Q}{\sigma a} \end{array} \right.$$

or $Q = c^T F$, with c defined above for the hub motion.

For rotor #2 it is also necessary to account for the differences in normalization, Q and c being based on rotor #1 parameters while F is based on rotor #2 parameters. Thus the force coefficients of rotor #2 must be multiplied by

$$\frac{(N I_b \Omega^2 / R)_2}{(N I_b \Omega^2 / R)_1}$$

and the moment coefficients by

$$\frac{(N I_b \Omega^2)_2}{(N I_b \Omega^2)_1}$$

For a clockwise rotating rotor it is also necessary to change the signs of C_Y , C_Q , and C_{Mx} . Using c corrected for rotor #2 normalization and the rotor rotation direction as required for the hub motion, it is then only necessary to multiply the matrix by

$$\frac{(N I_b \Omega^2)_2}{(N I_b \Omega^2)_1}$$

to obtain c^T for rotor #2.

4.2.6 *Aircraft aerodynamic forces.* - The aircraft aerodynamic forces considered are those acting on the wing/body (WB), horizontal tail (HT), and vertical tail (VT). The generalized forces for the aircraft rigid body degrees of freedom, due to the aerodynamic forces and moments, are as follows.

$$\begin{aligned}
 \begin{pmatrix} Q_1^* \\ Q_2^* \\ Q_3^* \\ Q_4^* \\ Q_5^* \\ Q_6^* \end{pmatrix} &= \frac{2\gamma}{\alpha} \frac{q}{\sigma A R} \begin{bmatrix} R_e^T \\ 0 \end{bmatrix} \begin{pmatrix} M_x/q \\ M_y/q \\ M_z/q \end{pmatrix}_{WB} \\
 &+ \frac{2\gamma}{\alpha} \frac{q}{\sigma A} \begin{bmatrix} R_e^T (\vec{r}_{WB} \cdot \vec{x}) \\ 1 \end{bmatrix} \begin{pmatrix} -(\cos \alpha D/q - \sin \alpha L/q) \\ Y/q \\ -(\cos \alpha L/q + \sin \alpha D/q) \end{pmatrix}_{WB} \\
 &+ \frac{2\gamma}{\alpha} \frac{q}{\sigma A} \begin{bmatrix} R_e^T (\vec{r}_{HT} \cdot \vec{x}) \\ 1 \end{bmatrix} \begin{pmatrix} -(\cos \alpha D/q - \sin \alpha L/q) \\ -\sin \phi (\cos \alpha L/q + \sin \alpha D/q) \\ -\cos \phi (\cos \alpha L/q + \sin \alpha D/q) \end{pmatrix}_{HT} \\
 &+ \frac{2\gamma}{\alpha} \frac{q}{\sigma a} \begin{bmatrix} R_e^T (\vec{r}_{VT} \cdot \vec{x}) \\ 1 \end{bmatrix} \begin{pmatrix} -(\cos \alpha D/q - \sin \alpha L/q) \\ -\cos \phi (\cos \alpha L/q + \sin \alpha D/q) \\ -\sin \phi (\cos \alpha L/q + \sin \alpha D/q) \end{pmatrix}_{VT}
 \end{aligned}$$

Here L , D , and Y are respectively the aerodynamic lift, drag, and side forces; M_x , M_y , and M_z are the roll, pitch, and yaw moments on the wing/body; and q is the dynamic pressure. The horizontal tail cant angle is ϕ_{HT} (positive to left), and the vertical tail cant angle is ϕ_{VT} (positive to right). The moment arms of the aerodynamic centers of action about the aircraft center of gravity are in the body axes, $\vec{r} = x\vec{i}_F + y\vec{j}_F + z\vec{k}_F$. The factor $2\gamma/\alpha a$ results from normalizing the equations by dividing by $\frac{1}{2}NI_b$. The parameter A is the rotor disk area.

The aircraft aerodynamic analysis thus requires the wing/body lift, drag, and pitch moment (L/q , D/q , and M_y/q) as a function of angle of attack α and of the flaperon deflection δ_f ; and wing/body side force, roll moment, and yaw moment (Y/q , M_x/q , M_z/q) as a function of sideslip angle β and aileron deflection δ_a ; the horizontal tail lift and drag (L_{HT}/q , D_{HT}/q) as a function of angle of attack α_{HT} and elevator deflection δ_e ; and the vertical tail lift and drag (L_{VT}/q , D_{VT}/q) as a function of angle of attack α_{VT} .

and rudder deflection δ_r . These force and moment characteristics have dimensions of length-squared and length-cubed respectively.

The aircraft aerodynamic forces depend on the air velocity seen by the components and on the aircraft control positions. The air velocity consists of the trim aircraft velocity, the perturbation linear and angular rigid body contributions, the gust velocity and the rotor-induced aerodynamic interference velocity. In body axes (the F system) the total velocity is thus

$$\begin{pmatrix} u \\ v \\ w \end{pmatrix} = \begin{pmatrix} V_x \\ V_y \\ V_z \end{pmatrix} + \begin{pmatrix} \dot{x}_F \\ \dot{y}_F \\ \dot{z}_F \end{pmatrix} - (\vec{r}_x) R_e \begin{pmatrix} \dot{\phi}_F \\ \dot{\theta}_F \\ \dot{\psi}_F \end{pmatrix} + R_{FV} \begin{pmatrix} u_G \\ v_G \\ w_G \end{pmatrix} - \vec{\lambda}$$

which must be evaluated at the wing/body, at the horizontal tail, and at the vertical tail. The angular velocity of the aircraft is

$$\begin{pmatrix} p \\ q \\ r \end{pmatrix} = R_e \begin{pmatrix} \dot{\phi}_F \\ \dot{\theta}_F \\ \dot{\psi}_F \end{pmatrix}$$

The rate of change of angle of attack is also required ($\dot{\alpha} = \ddot{z}_F/V_x$). The aircraft controls consist of flaperon, elevator, aileron, and rudder (δ_f , δ_e , δ_a , δ_r).

The aerodynamic interference velocity due to each rotor is required. With a nonuniform induced velocity calculation, $\vec{\lambda}$ is the mean value of the wake velocity calculated at the position of the fixed aerodynamic surface (see section 3.1). The complete time history of the velocity, required to evaluate the mean, can be useful information itself.

As a simple model for the aerodynamic interference, the rotor-induced velocities at the wing/body, horizontal tail, and vertical tail can be obtained as a linear combination of the mean induced velocity at the two rotors:

$$\vec{\lambda} = k_1 c_1 \lambda_{i_1} R_{SF}^T (-\vec{k}_1) + k_2 c_2 \lambda_{i_2} R_{SF}^T (-\vec{k}_2)$$

assuming that the induced velocity is normal to the disk plane (\vec{k}_s direction). The K factors account for the maximum fraction of the aerodynamic surface which is affected by the wake, and the fraction of the fully developed wake velocity which is achieved. Typical values would be $K = 1.5$ to 1.8 (or zero for no interference). The C multiplicative factors account for the decrease in the wake induced velocity away from the wake surface, using the following expression:

$$C = \frac{1}{\max(1, 1+\lambda)}$$

where λ is the perpendicular distance from the aerodynamic surface to the nearest wake boundary ($\lambda < 0$ if the surface is inside the rotor wake cylinder). Consider the geometry sketched in figure 24. The aerodynamic surface is located at $(\vec{r} - \vec{r}_R)$ relative to the rotor hub. The unit vector along the wake center-line is

$$\vec{e} = \frac{\mu_x \vec{i}_s - \mu_y \vec{j}_s - \lambda \vec{k}_s}{\sqrt{\mu_x^2 + \mu_y^2 + \lambda^2}}$$

and we write

$$\vec{e} \times (\vec{r} - \vec{r}_R) = (\vec{e} \times) R_{SF} (\vec{r} - \vec{r}_R) = x \vec{i}_s + y \vec{j}_s + z \vec{k}_s$$

(times R_1/R_2 for rotor #2). Now the unit vector in the $\vec{e}/\vec{r} - \vec{r}_R$ plane, perpendicular to \vec{e} is

$$\vec{j} = \frac{(\vec{e} \times (\vec{r} - \vec{r}_R)) \times \vec{e}}{|\vec{e} \times (\vec{r} - \vec{r}_R)|}$$

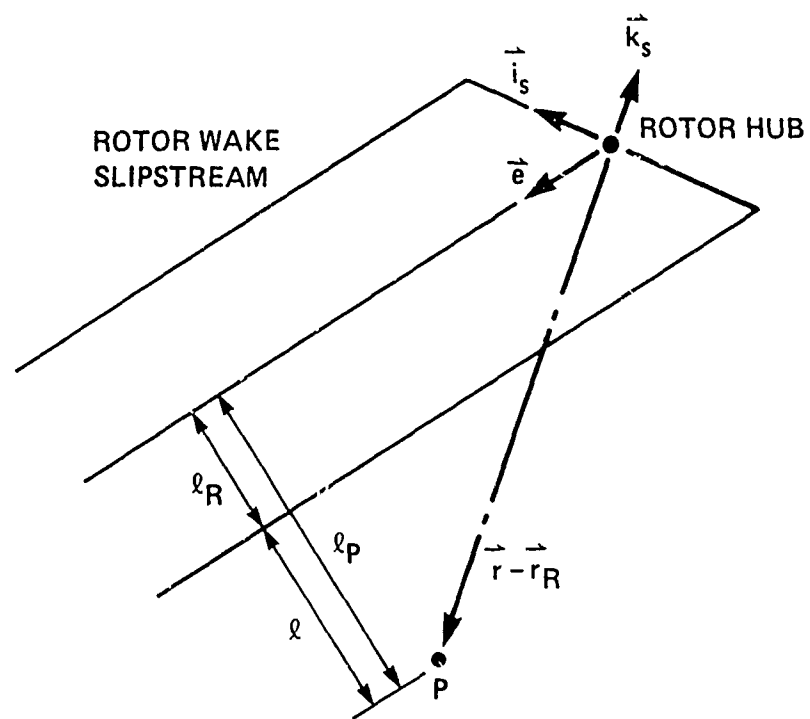


Figure 24. Model for rotor/airframe aerodynamic interference.

So the distance from P to the wake center-line is

$$\lambda_P = (\vec{r} - \vec{r}_R) \cdot \vec{j} = |\vec{e} \times (\vec{r} - \vec{r}_R)|$$

A point on the edge of the rotor disk is a unit vector perpendicular to \vec{k}_s ; the point also in the $\vec{e}/\vec{r} - \vec{r}_R$ plane (perpendicular to $\vec{e} \times (\vec{r} - \vec{r}_R)$) is then

$$\vec{\xi} = \frac{\vec{k}_s \times (\vec{e} \times (\vec{r} - \vec{r}_R))}{|\vec{k}_s \times (\vec{e} \times (\vec{r} - \vec{r}_R))|}$$

The distance of the wake edge to the wake center-line is thus

$$\lambda_R = \vec{\xi} \cdot \vec{j} = -\vec{e} \cdot \vec{k}_s \frac{|\vec{e} \times (\vec{r} - \vec{r}_R)|}{|\vec{k}_s \times (\vec{e} \times (\vec{r} - \vec{r}_R))|}$$

So the distance from P to the wake boundary is

$$\begin{aligned} \lambda &= \lambda_P - \lambda_R = |\vec{e} \times (\vec{r} - \vec{r}_R)| \left(1 - \frac{|\vec{e} \cdot \vec{k}_s|}{|\vec{k}_s \times (\vec{e} \times (\vec{r} - \vec{r}_R))|} \right) \\ &= \sqrt{x^2 + y^2 + z^2} \left(1 - \frac{|\vec{e} \cdot \vec{k}_s|}{\sqrt{x^2 + y^2}} \right) \end{aligned}$$

and

$$C = \frac{1}{\max(1, 1 - \lambda)}$$

From the velocity components at the wing/body, the angle of attack and sideslip angle are:

$$\alpha_{WB} = \tan^{-1} \frac{w}{u}$$

$$\beta_{WB} = \tan^{-1} \frac{v}{u}$$

and the dynamic pressure is

$$q_{WB} = \frac{1}{2} (u^2 + v^2 + w^2)$$

The aircraft aerodynamic interference at the tail will be accounted for by an angle of attack change ϵ and a sideslip angle σ (positive when decreasing α and β at the tail) so the net velocity components are

$$\begin{pmatrix} u + \epsilon w + \sigma v \\ v - \sigma u \\ w - \epsilon u \end{pmatrix}$$

Then the horizontal tail angle of attack and dynamic pressure are

$$\alpha_{HT} = \tan^{-1} \frac{(w - \epsilon u) \cos \phi_{HT} + (v - \sigma u) \sin \phi_{HT}}{u + \epsilon w + \sigma v}$$

$$\begin{aligned} q_{HT} &= \frac{1}{2} ((u + \epsilon w + \sigma v)^2 + (v - \sigma u)^2 + (w - \epsilon u)^2) \\ &\approx \frac{1}{2} (u^2 + v^2 + w^2) \end{aligned}$$

and similarly for the vertical tail

$$\alpha_{VT} = \tan^{-1} \frac{(v - \sigma u) \cos \phi_{VT} + (w - \epsilon u) \sin \phi_{VT}}{u + \epsilon w + r v}$$

$$q_{VT} \approx \frac{1}{2} (u^2 + v^2 + w^2)$$

where ϕ_{HT} and ϕ_{VT} are the tail surface cant angles. The time-varying non-uniform inflow will increase the mean dynamic pressure in the wake:

$$q = \frac{1}{2} (u^2 + v^2 + w^2) + \frac{1}{2} \sigma^2$$

where σ^2 is the mean-square wake velocity perturbation, at the wing/body or tail as appropriate:

$$\sigma^2 = \bar{x}^2 - \bar{x}^2$$

For best results, experimental data should be used for the aircraft aerodynamic characteristics, including the airframe interference effects. As a simple model, the following expressions can be used for the wing/body:

$$\frac{L}{q} = \frac{L\alpha}{q} (\alpha_{ws} + i_{ws}) + \frac{L\delta_F}{q} \delta_F + \frac{L\delta_S}{q} \delta_S$$

$$\begin{aligned} \frac{D}{q} = & f_{ws} + f_{vent} \sin^2(\alpha_{ws} + i_{ws}) + \frac{(1/q)^2}{\pi e \rho w^2} \\ & + \frac{D_0 \delta_F}{q} \delta_F + \frac{D_0 \delta_S}{q} \delta_S \end{aligned}$$

$$\frac{M_y}{q} = \frac{M_0}{q} + \frac{M\alpha}{q} (\alpha_{ws} + i_{ws}) + \frac{M\delta_F}{q} \delta_F + \frac{M\delta_S}{q} \delta_S$$

$$\frac{Y}{q} = \frac{Y_0}{q} \beta + \frac{V Y_p}{q} \frac{p}{V} + \frac{V Y_r}{q} \frac{r}{V}$$

$$\frac{M_x}{q} = \frac{N_{xp}}{q} \beta + \frac{V N_{xp}}{q} \frac{p}{V} + \frac{V N_{xr}}{q} \frac{r}{V} + \frac{N_x \epsilon}{q} \delta_a$$

$$\frac{M_z}{q} = \frac{N_{zp}}{q} \beta + \frac{VN_{zp}}{q} \frac{\ell}{V} + \frac{VN_{zr}}{q} \frac{c}{V} + \frac{N_{zs}}{q} \delta_a$$

(y_p , y_r , and N_{zr} are often negligible); and for the horizontal and vertical tails

$$\begin{aligned}\frac{L_{HT}}{q} &= \frac{L\alpha}{q} (\alpha_{HT} + i_{HT}) + \frac{L\delta_e}{q} \delta_e \\ \frac{L_{VT}}{q} &= \frac{L\alpha}{q} (\alpha_{VT} + i_{VT}) + \frac{L\delta_r}{q} \delta_r\end{aligned}$$

To account for stall, $\alpha = \text{sign } \alpha * \min(|\alpha|, \alpha_{\max})$ is used in the wing/body lift and pitch moment, and in the tail forces. Here i_{WB} , i_{HT} , and i_{VT} are the zero lift angles relative to the reference body axis system; and δ_F is a wing flap angle.

The wing/tail interference is evaluated from

$$c = \frac{(L/q)_{WB}}{f_e}$$

The area f_e can be estimated from the wing area, span, and chord (S_w , λ_w , c_w) and the horizontal tail length (ℓ_{HT}) by

$$f_e = 2.2 S_w (\lambda_w^2 / S_w)^{.725} (\lambda_{HT} / c_w)^{.25}$$

(from ref. 26). A lag in the wake velocity at the tail is also included:

$$\Delta c = - \frac{\partial c}{\partial \alpha} \frac{\ell_{HT}}{V} \dot{\alpha}_{WB} = - \frac{(L\alpha/q)_{WB}}{f_e} \frac{\ell_{HT}}{V} \dot{\alpha}_{WB}$$

(ref. 25). The wing-induced velocity could be obtained from the first order differential equation

$$\tau \dot{\epsilon} + \epsilon = \frac{\partial \epsilon}{\partial \alpha} \alpha_{WB}$$

The usual approach for airplane flight dynamics analysis is to write this equation as

$$\epsilon = \frac{\frac{\partial \epsilon}{\partial \alpha} \alpha_{WB}}{1 + \tau s} \approx (1 - \tau s) \frac{\partial \epsilon}{\partial \alpha} \alpha_{WB} = \frac{\partial \epsilon}{\partial \alpha} \alpha_{WB} - \tau \frac{\partial \epsilon}{\partial \alpha} \dot{\alpha}_{WB}$$

Using $\tau = l_{HT}/V$ for the time lag gives the above result. From reference 25, the sideslip interference angle is approximately

$$\sigma = \frac{\partial \sigma}{\partial \beta} \beta + \left(\frac{V}{x_{VT}} \frac{\partial \sigma}{\partial r} \right) \frac{x_{VT} \dot{r}}{V} + \left(\frac{V}{z_{VT}} \frac{\partial \sigma}{\partial p} \right) \frac{z_{VT} \dot{p}}{V}$$

$$\approx \frac{z_{VT}}{V} \dot{p}$$

where z_{VT} is the vertical tail position (positive upward).

In summary, the aircraft aerodynamic forces are calculated as follows. The aerodynamic environment is defined by the helicopter trim velocity, perturbation linear and angular velocity, gust velocity, rotor-induced interference velocity, and the aircraft controls. The total velocity components are calculated at the wing/body, horizontal tail, and vertical tail; from these the angle of attack and dynamic pressure are calculated. Then the aerodynamic forces and moments on the aircraft are calculated. Finally, the generalized aerodynamic forces are evaluated.

4.2.7 Aircraft aerodynamics - high frequency. - The aerodynamic model described in the preceding sections deals with the steady forces on the aircraft, and the stability derivatives for the rigid body motions involved in flight dynamics. Such a model would not be appropriate however for the high frequencies of rotor-induced vibration, for either rigid body or elastic

motions of the airframe. An accurate analytical evaluation of the generalized forces at high frequencies would require a sophisticated model of the wing/body and tail aerodynamics, including the effects of the rotor wake-induced flow field, for the normal modes of elastic vibration of the airframe. Such an analysis is not attempted in the present investigation.

The only generalized aerodynamic forces considered for the airframe elastic modes are the direct damping and control forces. In dimensional form, the equations of motion are then

$$M_k (\ddot{\tilde{q}}_{sk} + g_s \omega_k \dot{\tilde{q}}_{sk} + \omega_k^2 q_{sk}) = (Q_k)_{\text{rotors}} \\ + \frac{1}{2} \rho V^2 \left[- F_{q_k \dot{q}_k} \frac{\dot{\tilde{q}}_{sk}}{V} + F_{q_k \delta} \begin{pmatrix} \delta_e \\ \delta_a \\ \delta_r \end{pmatrix} \right]$$

where $F_{q_k \dot{q}_k}$ and $F_{q_k \delta}$ are constants (with dimensions of length-squared and length-squared per radian respectively) that depend only on the airframe characteristics; $F_{q_k \dot{q}_k}$ is the damping force divided by $\frac{1}{2} \rho V$:

$$F_{q_k \dot{q}_k} = \frac{\partial Q_k / \frac{1}{2} \rho V^2}{\partial \dot{\tilde{q}}_{sk} / V}$$

and $F_{q_k \delta}$ is the control force derivative divided by $\frac{1}{2} \rho V^2$:

$$F_{q_k \delta} = \frac{\partial Q_k / \frac{1}{2} \rho V^2}{\partial \delta}$$

The dimensionless form, normalized by dividing by $\frac{1}{2} N I_b$, is then

$$M_k^* \ddot{\tilde{q}}_{sk} + (M_k^* g_s \omega_k + \frac{2\delta}{\sigma \alpha A} \frac{g}{V} F_{q_k \dot{q}_k}) \dot{\tilde{q}}_{sk} + M_k^* \omega_k^2 q_{sk} \\ = (Q_k^*)_{\text{rotors}} + \frac{2\delta}{\sigma \alpha A} g \left[F_{q_k \delta} \begin{pmatrix} \delta_e \\ \delta_a \\ \delta_r \end{pmatrix} \right]$$

4.3 Transmission and Engine Analysis

The rotor rotational speed degree of freedom can be an important factor in the helicopter dynamics, and the rotor torque perturbations can produce significant drive train loads. A model is required which accounts for the coupling of the two rotors through the flexible drive-train, and for the engine damping and inertia. The drive train dynamics will be described by the rotor speed, the interconnect shaft torsion, and the engine shaft torsion degrees of freedom. The equations of motion are derived from the balance of rotor and engine torques (in the nonrotating frame). A model for a governor with throttle or collective feedback of the rotor speed error is also considered.

4.3.1 *Engine model.* -The engine model includes the inertia, damping, and control torques:

$$I_E \dot{\Omega}_E = Q_E - Q_{\Omega} \Omega_E + Q_t \theta_t$$

The engine speed is Ω_E , and Q_E is the torque on the engine. The engine rotary inertia is I_E . Q_{Ω} is the engine speed damping coefficient, i.e., the torque per unit speed change at constant throttle setting:

$$Q_{\Omega} = \left. \frac{\partial Q_E}{\partial \Omega_E} \right|_{\theta_t = \text{constant}}$$

The variable θ_t is the engine throttle control position. Q_t is the torque applied due to a throttle change at constant speed:

$$Q_t = \left. \frac{\partial Q_E}{\partial \theta_t} \right|_{\Omega_E = \text{constant}} = \frac{1}{\Omega_E} \left. \frac{\partial P_E}{\partial \theta_t} \right|_{\Omega_E = \text{constant}}$$

Thus Q_t and Q_{Ω} can be obtained from data on the engine power as a function of throttle position and engine speed.

The engine damping may be related to the engine trim operating condition by

$$\omega_{sr} = \frac{\partial Q_E}{\partial \Sigma_E} \approx k \frac{Q_{E\text{trim}}}{\Sigma_{E\text{trim}}} = k \frac{P_{\text{trim}}}{\Sigma_{E\text{trim}}^2}$$

where k is a constant depending on the engine type. This approximation is applicable to a wide variety of engines. The constant takes the value $k = 1$ for a turboshaft engine (ref. 27) or for a series DC electric motor (ref. 28). It takes a value $k = 1/(1 - \eta)$ for an induction electric motor or an armature controlled shunt DC electric motor (ref. 28; η is the motor efficiency). For a field controlled shunt DC motor, the only damping is mechanical and the damping of the load, so $k = 0$ (ref. 28). For a synchronous electric motor there is a spring on the rotational speed due to the motor, so the above model is not applicable (ref. 28). Generally, the inertia of the engine or motor is more of a factor in the dynamics than the damping.

The normalized engine damping and throttle coefficients are:

$$r_E^2 Q_{sr}^* = \frac{r_E^2 Q_{sr}}{(NI_b \Sigma^2)} \approx \frac{r_E^2 k Q_E / \Sigma_E}{(NI_b \Sigma^2)} = \frac{r_E^2 k P_E}{(NI_b \Sigma^2) \Sigma_E^2} = \frac{k P_E}{(NI_b \Sigma^3)},$$

$$r_E Q_t^* = \frac{r_E Q_t}{(NI_b \Sigma^2)} = \frac{r_E \partial P_E / \partial \theta_t}{(NI_b \Sigma^2) \Sigma_E} = \frac{\partial P_E / \partial \theta_t}{(NI_b \Sigma^3)},$$

where r_E is the ratio of the engine speed to the rotor speed. When the throttle control is only involved in the governor, the parameters required for Q_t^* is not really $\partial P_E / \partial \theta_t$, but rather just over all loop gain of the governor -- the torque perturbation due to a rotor speed error.

The transmission losses may be viewed as a viscous damping source, with a coefficient equal to

$$\frac{\partial Q}{\partial \Sigma} = \frac{(1-\gamma) P_t}{\Sigma^2}$$

where η is the transmission efficiency. This loss can be included in the engine damping coefficient $r_E^2 Q_\Omega^*$, by increasing the factor κ by $\Delta\kappa = 1 - \eta$. In the equations for interconnect shaft torsion and engine shaft torsion, structural damping can be included as well.

4.3.2 *Equations of motion.*— Figure 25 is a schematic of the transmission/engine model considered for asymmetric drive train configurations, such as for a single main and tail rotor helicopter. The two rotors are connected by a shaft, and the engine is geared to one rotor (rotor #1 in fig. 25). The torsional flexibility of the drive train is represented by the rotor shaft springs K_{M1} and K_{M2} , the interconnect shaft spring K_I , and the engine shaft spring K_E . The transmission gear ratios are r_E (the ratio of the engine speed to rotor #1 speed), and r_{I1} and r_{I2} (the ratio of the interconnect shaft speed to the rotor speeds). Thus $r_{I1}/r_{I2} = \Omega_2/\Omega_1$ is the ratio of the trim rotational speeds of rotor #2 and rotor #1.

The degrees of freedom are the rotational speed perturbations of the two rotors ($\dot{\psi}_{s1}$ and $\dot{\psi}_{s2}$), and the engine speed perturbation $\dot{\psi}_e$. The engine shaft azimuth perturbation ψ_e is defined relative to rotor #1 rotation, so the total engine speed perturbation with respect to space is $r_E(\dot{\psi}_{s1} + \dot{\psi}_e)$. With the rotation of the two rotors coupled by the drive system, it is more appropriate to use the following degrees of freedom:

$$\begin{aligned}\Psi_s &= \dot{\psi}_{s1} \\ \Psi_I &= \dot{\psi}_{s2} - (c_{x1}/c_{x2}) \Psi_{s1}\end{aligned}$$

Here Ψ_I is the differential azimuth perturbation between the two rotors. The degrees of freedom Ψ_I and ψ_e therefore involve elastic torsion in the drive train. The degrees of freedom $\dot{\psi}_s$ is the rotational speed perturbation of the drive system as a whole: both rotors, the engine, and the transmission.

The differential equation of motion for the rotor speed dynamics are obtained from equilibrium of the torques on the two rotors and the engine. The resulting equations for $\dot{\psi}_s$, $\dot{\Psi}_I$, and $\dot{\psi}_e$ are as follows:

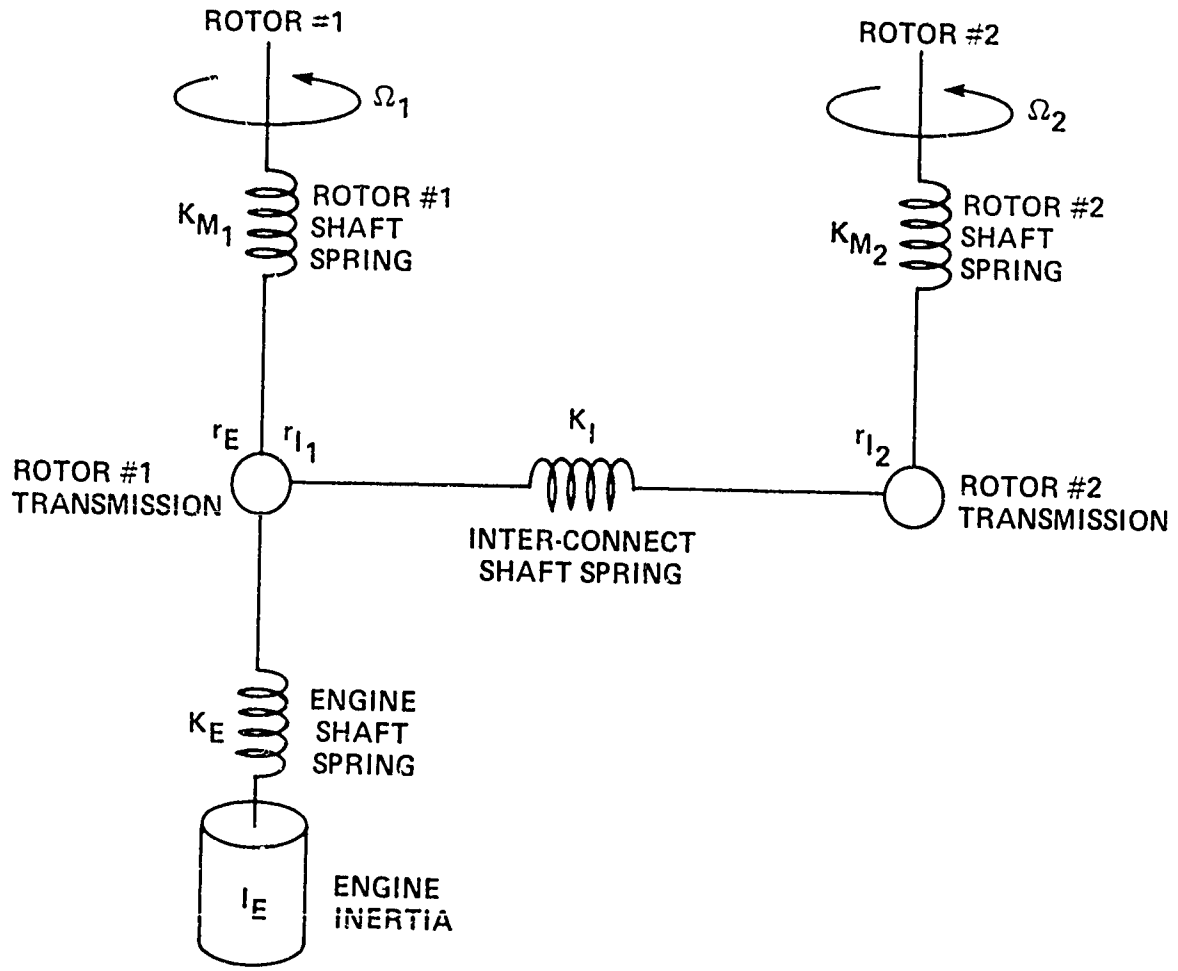


Figure 25. Schematic of rotorcraft transmission and engine dynamics model (asymmetric configuration)

$$\left(\frac{\partial \frac{C_E}{\sigma_a}}{\partial \alpha}\right)_1 + \frac{r_{I_1}}{r_{I_2}} \frac{(N I_b \dot{\sigma}^2)_2}{(N I_b \dot{\sigma}^2)_1} \left(\frac{\partial \frac{C_E}{\sigma_a}}{\partial \alpha}\right)_2 \\ + r_E^2 I_E^* (\ddot{\psi}_s + \ddot{\psi}_e) + r_E^2 Q_{S2}^* (\dot{\psi}_s + \dot{\psi}_e) = r_E \dot{\theta}_t^* \dot{\theta}_t + \left(\frac{\partial C_E}{\partial \alpha}\right)_{\text{trim}}$$

$$-k_{M_{I_1}} \left(\frac{\partial \frac{C_E}{\sigma_a}}{\partial \alpha}\right)_1 + \frac{(N I_b \dot{\sigma}^2)_2}{(N I_b \dot{\sigma}^2)_1} \left(\frac{\partial \frac{C_E}{\sigma_a}}{\partial \alpha}\right)_1 \\ + k_{MR} r_E^2 I_E^* \ddot{\psi}_I + k_{MR} r_E^2 Q_{S2}^* \dot{\psi}_I + k_{M_{I_2}}^* \psi_I = 0$$

$$r_E^2 I_E^* (\ddot{\psi}_s + \ddot{\psi}_e) + r_E^2 Q_{S2}^* (\dot{\psi}_s + \dot{\psi}_e) \\ + k_{ME_1}^* \psi_e - k_{ME_2}^* \psi_I = r_E \dot{\theta}_t^* \dot{\theta}_t + \left(\frac{\partial C_E}{\partial \alpha}\right)_{\text{trim}}$$

where $\psi_{s1} = \psi_s$ and $\psi_{s2} = (r_{I1}/r_{I2}) \psi_s + \psi_I$; and with the engine by rotor #1 as in figure 25, the constants are:

$$K_{M_{I_1}} = \frac{(r_{I_1}/r_{I_2}) K_{M_2} r_{I_2}^2 K_I}{K_{M_1} (K_{M_2} + r_{I_2}^2 K_I)}$$

$$K_{M_{I_2}} = \frac{K_{M_2} r_{I_2}^2 K_I}{K_{M_2} + r_{I_2}^2 K_I}$$

$$K_{ME_1} = \frac{r_E^2 K_E K_{MM}}{r_E^2 K_E (K_{M_2} + r_{I_2}^2 K_I) + K_{MM}}$$

$$K_{ME_2} = \frac{r_E^2 K_E r_{I_1} K_{M_2} r_{I_2} K_I}{r_E^2 K_E (K_{M_2} + r_{I_2}^2 K_I) + K_{MM}}$$

$$K_{MM} = K_{M_1} K_{M_2} + K_I (r_{I_2}^2 K_{M_1} + r_{I_1}^2 K_{M_2})$$

$$K_{MR} = 0$$

The spring constants are normalized by dividing by $(NI_b \Omega^2)_1$; and $I_E^* = I_E / (NI_b)_1$. When evaluating the derivatives of $\dot{\psi}_{s2}$ for use in the analysis of rotor #2, it is necessary to account for the difference in time scales:

$$\ddot{\psi}_{s2} = \frac{5\zeta_1}{5\zeta_2} \left(\frac{r_{I_1}}{r_{I_2}} \dot{\psi}_s + \dot{\psi}_I \right)$$

In these equations the gear ratio r_{I_1}/r_{I_2} between the two rotors is a positive number, regardless of the rotor direction of rotation. Therefore here the sign of C_Q is not changed for a clockwise rotating rotor.

With the engine by rotor #2, the constants in the equations of motion are:

$$K_{MI_1} = \frac{(r_{I_1}/r_{I_2}) K_{M2} (K_M + r_{I_1}^2 K_I)}{K_M, r_{I_1}^2 K_I}$$

$$K_{MI_2} = K_{M2}$$

$$K_{ME_1} = \frac{(r_{I_1}/r_{I_2})^2 r_E^2 K_E K_{MM}}{r_E^2 K_E (K_M + r_{I_1}^2 K_I) + (r_{I_1}/r_{I_2})^2 K_{MM}}$$

$$K_{ME_2} = \frac{(r_{I_1}/r_{I_2}) r_E^2 K_E K_{M2} (K_M + r_{I_1}^2 K_I)}{r_E^2 K_E (K_M + r_{I_1}^2 K_I) + (r_{I_1}/r_{I_2})^2 K_{MM}}$$

Figure 26 sketches a symmetric drive train configuration, as might be used for a side-by-side main rotor helicopter. The two rotors are connected by a cross-shaft, and there are two engines, one geared to each rotor. The degrees of freedom of this system are symmetric and antisymmetric rotor speed perturbations, and symmetric and antisymmetric engine speed perturbations. Dropping the antisymmetric engine speed perturbation and antisymmetric throttle input, the system has three degrees of freedom as for the asymmetric configurations above. Let

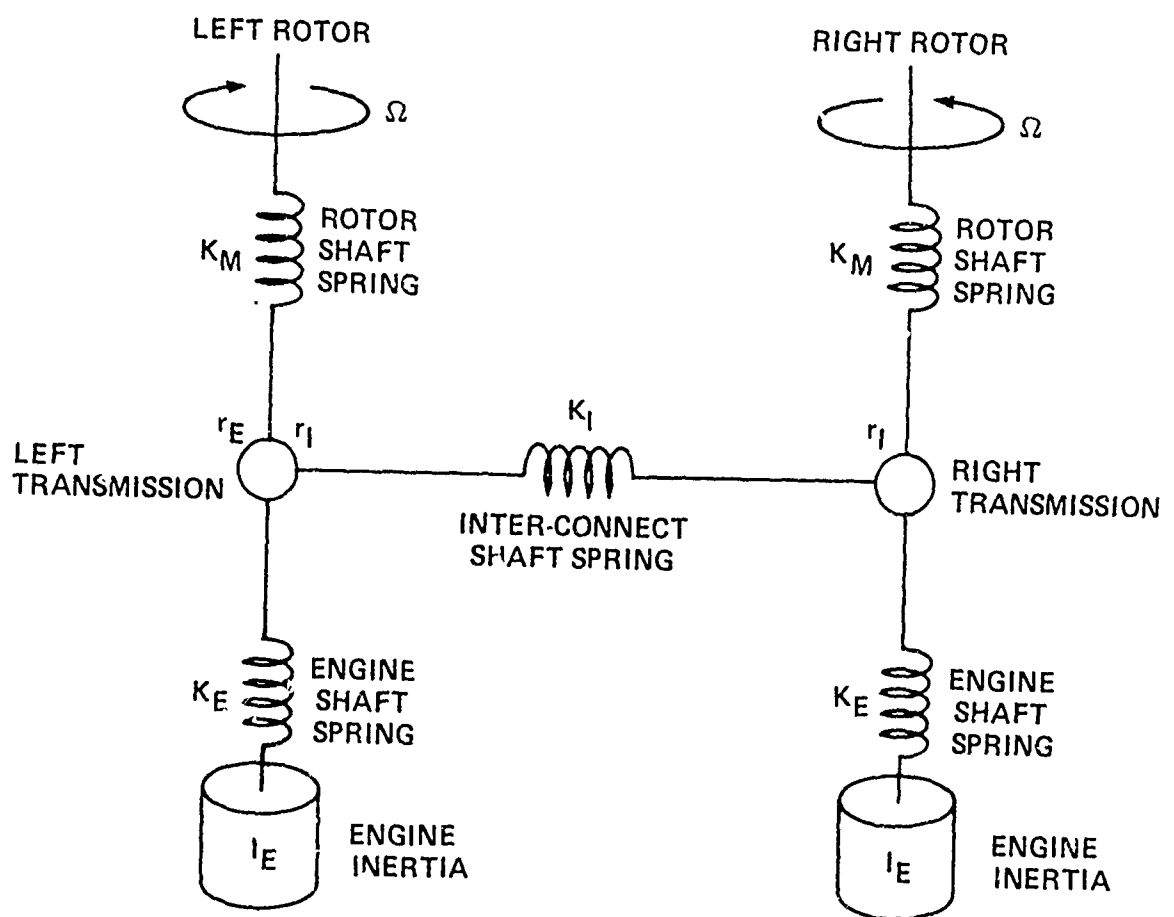


Figure 26. Schematic of rotorcraft transmission and engine dynamics model (symmetric configuration).

$$\Psi_{S_1} = \Psi_S$$

$$\Psi_{S_2} = (r_I, / r_{I2}) \Psi_S + \Psi_I$$

again, where here $r_{I1}/r_{I2} = 1$. The constants in the equations of motion are:

$$K_{MI_1} = 1$$

$$K_{ME} = \frac{1}{2} \frac{K_M}{K_M + 2r_E^2 K_I}$$

$$K_{MI_2} = \frac{K_M 2r_E^2 K_I}{K_M + 2r_E^2 K_I}$$

$$K_{ME_1} = 2 \frac{r_E^2 K_E K_M}{K_M + r_E^2 K_E}$$

$$K_{ME_2} = \frac{r_E^2 K_E K_M}{K_M + r_E^2 K_E}$$

Here the engine inertia I_E is for both engines, as are the damping and throttle coefficients (Q_Ω and Q_t). The resulting symmetric and antisymmetric drive train motions can then be obtained from

$$\Psi_{\text{sym}} = \Psi_S + \frac{1}{2} \Psi_I$$

$$\Psi_{\text{anti}} = -\frac{1}{2} \Psi_I$$

$$\Psi_{\text{eng}} = \Psi_E - \frac{1}{2} \Psi_I$$

as required.

With just one rotor (as in a wind tunnel), the equations of motion for the rotor and engine speed perturbations reduce to:

$$\begin{aligned} \delta \frac{CQ}{\sigma a} + r_E^2 I_E^* (\ddot{\psi}_s + \ddot{\psi}_e) + r_E^2 Q_{s2}^* (\dot{\psi}_s + \dot{\psi}_e) \\ = r_E Q_t^* \theta_t + (\delta \frac{Cp_E}{\sigma a}) \end{aligned}$$

$$\begin{aligned} r_E^2 I_E^* (\ddot{\psi}_s + \ddot{\psi}_e) + r_E^2 Q_{s2}^* (\dot{\psi}_s + \dot{\psi}_e) + K_{ME_1}^* N_e \\ = r_E Q_t^* \theta_t + (\delta \frac{Cp_E}{\sigma a}) \end{aligned}$$

where here

$$K_{ME_1} = \frac{r_E^2 K_E K_M}{K_M + r_E^2 K_E}$$

Hence the equations for the asymmetric drive train configuration can be used, dropping the ψ_I degree of freedom and the rotor #2 torque.

The case of a rotorcraft in autorotation can be treated with this model by dropping the engine speed degree of freedom ($\dot{\psi}_e$), dropping the engine terms from the ψ_s and ψ_I equations (helicopters usually have an over-running clutch to disconnect the rotors from the engine at zero torque), and dropping the throttle governor control input (θ_t). The engine out case (engine and rotors still connected) requires dropping the engine damping term (or reducing it to just the transmission losses contribution) and dropping the throttle governor control input. The case of constant rotor speed is modelled by dropping the rotor and engine speed degrees of freedom and equations from the system.

4.3.3 Rotor speed governor.- When the rotor rotational speed perturbation is included in the dynamics analysis, it is usually necessary to also include the rotor speed governor for a consistent calculation of the rotor and aircraft behavior. The governor model considered is integral and proportional feedback of the rotor speed to the throttle, and to the collective pitch of rotors #1 and #2. The governor dynamics are represented by a second order lag. The control equations are thus:

$$\tau_{z_e} \ddot{\Delta\theta_t} + \tau_{I_e} \dot{\Delta\theta_t} + \Delta\theta_t = -k_{P_e} \dot{\psi}_s - k_{I_e} \psi_s$$

$$\tau_{z_1} \ddot{\Delta\theta_{gov_1}} + \tau_{I_1} \dot{\Delta\theta_{gov_1}} + \Delta\theta_{gov_1} = k_{P_1} \dot{\psi}_s + k_{I_1} \psi_s$$

$$\tau_{z_2} \ddot{\Delta\theta_{gov_2}} + \tau_{I_2} \dot{\Delta\theta_{gov_2}} + \Delta\theta_{gov_2} = k_{P_2} \dot{\psi}_s + k_{I_2} \psi_s$$

Note that $\epsilon = \dot{\psi}_s$ is the rotor speed error, and ψ_s is the integral of the error. The integral gains are dimensionless (with θ and ψ_s both in radians or both in degrees), and the proportional gains have units of seconds (k_p/k_I is the lead in the integral control). When the throttle control is only used for this governor model, it is only necessary that the product of $\partial P_E / \partial \theta_t$ and the governor gains be correct:

$$k_{P_e} \frac{\partial P_E}{\partial \theta_t} = - \frac{\partial P}{\partial \dot{\psi}_s}$$

$$k_{I_e} \frac{\partial P_E}{\partial \theta_t} = - \frac{\partial P}{\partial \psi_s}$$

($P = \Omega_R Q_R = \Omega_E Q_E$), or in terms of the dimensionless parameters

$$k_{P_e} (r_e Q_t^*) = - \frac{\partial C_a / r_a}{\partial \dot{\psi}_s / S_2}$$

$$k_{I_e} (r_e Q_t^*) = - \frac{\partial C_a / r_a}{\partial \psi_s}$$

The time constants in the governor equations can be alternatively described in terms of frequency and damping ratio:

$$\tau_z = \frac{1}{\omega_n^2}$$

$$\zeta_c = \frac{25}{\omega_n}$$

5. SOLUTION FOR THE ROTORCRAFT MOTION

The solution of the equations of motion will be divided into two parts, based on the frequency content of the motion. The first part is the solution for the rotor motion and the airframe vibration. This motion is periodic with fundamental frequency Ω for the rotor, and $N\Omega$ for the airframe, hence it is high frequency motion. The second part is the solution for the steady state or slowly varying airframe motion, consisting of the aircraft rigid body and rotor speed perturbations. The assumption that this airframe motion occurs slowly relative to the rotor speed allows the solution of the equations of motion to be separated into these two parts.

5.1 Rotor Motion and Airframe Vibration

The equations of motion for the rotor and aircraft will be solved for the periodic motion by a harmonic analysis method, which obtains directly the harmonics of a Fourier series representation of the motion. After a converged solution for the blade motion and airframe vibration is obtained, the rotor performance is evaluated, including the mean aerodynamic hub reactions (in particular the rotor thrust and power). The hub motion includes the static or quasistatic contributions from the aircraft rigid body motion.

The helicopter state is determined by the control positions; the flight path angles and trim Euler angles (or test module pitch and yaw for the wind tunnel case); the quasisteady linear and angular velocity perturbations of the airframe; the quasisteady rotor speed perturbation; and the aerodynamic

gust velocities. The rotor motion and airframe vibration are calculated for this state. Then the generalized forces acting on the rotor and airframe can be evaluated, as well as the various performance parameters of the aircraft.

5.1.1 Fourier series representation.- For the case of steady state flight, all the rotor blades execute the same periodic motion. It follows that the blade motion in the rotating frame can be written as a Fourier series:

$$\begin{aligned} q_k &= \sum_{n=-\infty}^{\infty} \beta_n^{(k)} e^{in\psi_m} \\ &= \beta_0^{(k)} + \sum_{n=1}^{\infty} (\beta_{nc}^{(k)} \cos n\psi_m + \beta_{ns}^{(k)} \sin n\psi_m) \\ p_k &= \sum_{n=-\infty}^{\infty} \theta_n^{(k)} e^{in\psi_m} \\ &= \theta_0^{(k)} + \sum_{n=1}^{\infty} (\theta_{nc}^{(k)} \cos n\psi_m + \theta_{ns}^{(k)} \sin n\psi_m) \end{aligned}$$

where $\psi_m = \psi + m\Delta\psi$ is the azimuth angle of the m-th blade ($\Delta\psi = 2\pi/N$, $m = 1$ to N), and $\psi = \Omega t$ is the dimensionless time variable. The complex and real Fourier coefficients are related by $\beta_n = (\beta_{nc} - i\beta_{ns})/2$ and $\theta_n = (\theta_{nc} - i\theta_{ns})/2$ for $n \geq 1$. The complex representation is most convenient for solving the equations of motion, while the real representation is best for interpreting the motion. The notation $\beta_n^{(k)}$ is used for the harmonics of the k-th bending mode. With the modes ordered according to natural frequency, $\beta_n^{(1)}$ is usually the fundamental lag mode and $\beta_n^{(2)}$ the fundamental flap mode. Similarly $\theta_n^{(k)}$ are the harmonics of the k-th torsion mode, with $\theta_n^{(0)}$ rigid pitch and the remaining modes elastic motion of the blade. The Fourier representation of the gimbal or teeter motion is discussed in the next section.

The degrees of freedom in the nonrotating frame are the aircraft rigid body and elastic motion, and the rotor speed perturbations. These degrees

of freedom are excited by the net rotor hub reactions, obtained by summing the root forces and moments from all N blades. Ideally, the rotor hub acts as a filter, transmitting to the nonrotating frame only those harmonics at multiples of N/rev . The vibratory motion in the nonrotating frame is then also periodic, with fundamental frequency $N\Omega$, and can be written as a Fourier series:

$$q_{Sk} = \sum_{p=-\infty}^{\infty} \psi_{pN}^{(k)} e^{ipN\psi}$$

for the body motion, and

$$\psi_s = \sum_{p=-\infty}^{\infty} \psi_{pN}^{(s)} e^{ipN\psi}$$

for the rotor azimuth perturbation (similarly for ψ_I and ψ_e). The static or mean terms are obtained from the low frequency solution of the airframe equation.

5.1.2 Gimbal and veeter motion. - The rotor gimbal motion (if present) is in the nonrotating frame, but it is most convenient to solve an equation in the rotating frame for the gimbal motion, along with the other rotor blade equations. From section 2.2.18, the gimbal equations of motion are given by equilibrium of the net longitudinal and lateral moments on the rotor hub:

$$-\frac{1}{N} \sum_{m=1}^N 2 \cos \psi_m \delta \frac{C_{mx}}{\sigma_a} + C_{Gc}^* \dot{\beta}_{Gc} + I_0^* (\dot{\beta}_{Gc}^2 - 1) \beta_{Gc} = 0$$

$$-\frac{1}{N} \sum_{m=1}^N 2 \sin \psi_m \delta \frac{C_{mx}}{\sigma_a} + C_{Gs}^* \dot{\beta}_{Gs} + I_0^* (\dot{\beta}_{Gs}^2 - 1) \beta_{Gs} = 0$$

where C_{mx} is the flap moment at the blade root. All harmonics of the longitudinal and lateral hub moments cancel within the hub, except those at multiples of N/rev . The pN harmonics of the gimbal equations of motion are:

$$-\left[\left(\delta \frac{C_{mx}}{\sigma a} \right)_{pN-1} + \left(\delta \frac{C_{mx}}{\sigma a} \right)_{pN+1} \right] \\ + C_{GC}^* i p N (\beta_{GC})_{pN} + I_0^* (J_{GS}^2 - 1) (\beta_{GS})_{pN} = 0$$

$$i \left[\left(\delta \frac{C_{mx}}{\sigma a} \right)_{pN-1} + \left(\delta \frac{C_{mx}}{\sigma a} \right)_{pN+1} \right] \\ + C_{GS}^* i p N (\beta_{GS})_{pN} + I_0^* (J_{GS}^2 - 1) (\beta_{GS})_{pN} = 0$$

where $(C_{mx})_n$ is the n-th complex harmonic of C_{mx} .

The flap motion in the rotating frame due to the gimbal tilt is $\beta_G = \beta_{GC} \cos \psi + \beta_{GS} \sin \psi$. Only the pN harmonics of β_{GC} and β_{GS} are excited, hence only the $pN \pm 1$ harmonics of β_G :

$$(\beta_G)_{pN+1} = \frac{1}{2} [(\beta_{GC})_{pN} - i(\beta_{GS})_{pN}]$$

$$(\beta_G)_{pN-1} = \frac{1}{2} [(\beta_{GC})_{pN} + i(\beta_{GS})_{pN}]$$

so

$$(\beta_{GC})_{pN} = (\beta_G)_{pN-1} + (\beta_G)_{pN+1}$$

$$(\beta_{GS})_{pN} = -i [(\beta_G)_{pN-1} - (\beta_G)_{pN+1}]$$

for $p \neq 0$, and

$$(\beta_{GC})_0 = 2 \operatorname{Re} (\beta_G)_1$$

$$(\beta_{GS})_0 = -2 \operatorname{Im} (\beta_G)_1$$

Note that with the restriction that only the $pN = 1$ harmonics of β_G exist, this is equivalent to the relation

$$\beta_{GC} = \frac{N}{2} \sum_{m=1}^N \cos \gamma_m \beta_G^{(m)}$$

$$\beta_{GS} = \frac{N}{2} \sum_{m=1}^N \sin \gamma_m \beta_G^{(m)}$$

Substituting for the harmonics of β_{GC} and β_{GS} in terms of the harmonics of β_G , the gimbal equations of motion give:

$$-\left[(\delta \frac{C_{mx}}{\sigma \alpha})_{pN-1} + (\delta \frac{C_{mx}}{\sigma \alpha})_{pN+1} \right] + C_{GC}^* i p N [(\beta_G)_{pN-1} + (\beta_G)_{pN+1}] + I_0^* (J_{GC}^2 - 1) [(\beta_G)_{pN-1} + (\beta_G)_{pN+1}] = 0$$

$$-\left[(\delta \frac{C_{mx}}{\sigma \alpha})_{pN-1} - (\delta \frac{C_{mx}}{\sigma \alpha})_{pN+1} \right] + C_{GS}^* i p N [(\beta_G)_{pN-1} - (\beta_G)_{pN+1}] + I_0^* (J_{GS}^2 - 1) [(\beta_G)_{pN-1} - (\beta_G)_{pN+1}] = 0$$

or

$$-\left(\delta \frac{C_{mx}}{\sigma \alpha} \right)_{pN-1} + \frac{1}{2}(C_{GC}^* + C_{GS}^*) i p N (\beta_G)_{pN-1} + I_0^* \left(\frac{1}{2}(J_{GC}^2 + J_{GS}^2) - 1 \right) (\beta_G)_{pN-1} + \frac{1}{2}(C_{GC}^* - C_{GS}^*) i p N (\beta_G)_{pN+1} + I_0^* \frac{1}{2}(J_{GC}^2 - J_{GS}^2) (\beta_G)_{pN+1} = 0$$

$$-\left(\delta \frac{C_{mx}}{\sigma \alpha} \right)_{pN+1} + \frac{1}{2}(C_{GC}^* + C_{GS}^*) i p N (\beta_G)_{pN+1} + I_0^* \left(\frac{1}{2}(J_{GC}^2 + J_{GS}^2) - 1 \right) (\beta_G)_{pN+1} + \frac{1}{2}(C_{GC}^* - C_{GS}^*) i p N (\beta_G)_{pN-1} + I_0^* \frac{1}{2}(J_{GC}^2 - J_{GS}^2) (\beta_G)_{pN-1} = 0$$

which we note are just the $pN \pm 1$ harmonics of the equation

$$-\gamma \frac{C_{m\alpha}}{\sigma_\alpha} + C_G^* \dot{\beta}_G + \Xi_0^* (\vartheta_G^2 - 1) \beta_G = 0$$

(except for the effects of unsymmetric gimbal springs or dampers, and the fact that the damping is in the nonrotating frame).

The equation for the teeter motion of a two-bladed rotor is

$$-\frac{1}{2} \sum_{m=1}^2 (-1)^m \gamma \frac{C_{m\alpha}}{\sigma_\alpha} + C_T^* \dot{\beta}_T + \Xi_0^* (\vartheta_T^2 - 1) \beta_T = 0$$

All the even harmonics of the root flap moments cancel within the rotor hub. The summation operator only transmits the odd harmonics to produce teeter motion. Hence the solution for the teeter motion can be obtained by solving the equation

$$-\gamma \frac{C_{m\alpha}}{\sigma_\alpha} + C_T^* \dot{\beta}_T + \Xi_0^* (\vartheta_T^2 - 1) \beta_T = 0$$

for the odd harmonics (i.e., for the $pN \pm 1$ harmonics, just as for the gimbal motion).

Thus the gimbal or teeter motion can be obtained by solving the rigid flapping equation in the rotating frame:

$$-\gamma \frac{C_{m\alpha}}{\sigma_\alpha} + C_G^* \dot{\beta}_G + \Xi_0^* (\vartheta_G^2 - 1) \beta_G = 0$$

for just the $pN \pm 1$ harmonics of β_G . Then the harmonics of the gimbal motion are

$$(\beta_{GC})_{PN} = (\beta_G)_{PN-1} + (\beta_G)_{PN+1}$$

$$(\beta_{GS})_{PN} = -i [(\beta_G)_{PN-1} - (\beta_G)_{PN+1}]$$

from which the gimbal motion can be evaluated

$$\beta_{GC} = \sum_{p=-\infty}^{\infty} (\beta_{GC})_{pn} e^{ipn\psi}$$

$$\beta_{GS} = \sum_{p=-\infty}^{\infty} (\beta_{GS})_{pn} e^{ipn\psi}$$

and so

$$\beta_G = \beta_{GC} \cos \psi + \beta_{GS} \sin \psi = \sum_{n=PN \pm 1} (\beta_G)_n e^{in\psi}$$

The harmonics of the teetering motion are

$$(\beta_T)_n = (\beta_G)_n$$

for the odd harmonics, from which

$$\beta_G = \beta_T = \sum_{n \text{ odd}} (\beta_G)_n e^{in\psi}$$

5.1.3 Rigid pitch motion.- In the limit of infinite control stiffness, the equation of motion for the blade rigid pitch degree of freedom reduces to $M_{TAE} = 0$ (see section 2.2.9), with the solution

$$\begin{aligned} p_0 = p_r &= \theta_{1c} \cos(\psi + \psi_s) + \theta_{1s} \sin(\psi + \psi_s) \\ &- \sum K_F q_i - K_{PG} \beta_G \\ &+ \Delta \theta_{govr} + \Delta \theta_{west bend} \end{aligned}$$

Write the total root pitch motion p_0 as the sum of p_r and the motion due to elastic distortion of the control system: $p_0 = p_r + p_d$. Substituting for p_0 , the rotor equations of motion will be solved for the harmonics of p_d . The case of infinite control system stiffness then requires only that the equations for p_d be dropped from the solution procedure. Writing $p_0 = p_r + p_d$ introduces terms due to p_r , \dot{p}_r , and \ddot{p}_r in the equations of motion.

Allowance will be made for different stiffnesses in the collective and cyclic control systems by using different natural frequencies for the collective motion ($\omega_0^{(d)}$), cyclic motion ($\omega_1^{(d)}$), and the reactionless motion ($\omega_n^{(d)}$, $n \geq 2$). Given the collective, cyclic, and reactionless control stiffnesses, the dimensionless natural frequencies are obtained from

$$\omega_0^2 = \frac{k_0}{\rho^2 \int_0^R I_\theta dr / r_{FA}}$$

or the natural frequencies can be specified directly.

The control system damping will be specified for the collective motion, the cyclic motion, and for the rotating frame motion. The total damping is then $C_{\theta_{coll}} + C_{\theta_{rot}}$ for the collective mode, $C_{\theta_{cyc}} + C_{\theta_{rot}}$ for the cyclic modes, and $C_{\theta_{rot}}$ for the reactionless modes ($n \geq 2$).

5.1.4 Harmonic analysis solution.-- A harmonic analysis method will be used to integrate the differential equations of motion, solving directly for the harmonics of the motion. Consider equations of the form

$$M \ddot{\beta} + K \beta = g(\beta, \dot{\beta}, \psi)$$

where β is the degree of freedom, K and M are the appropriate stiffness and mass, and g is the forcing function (usually nonlinear). To avoid the singularity of the resonant response at harmonics near the natural frequency, it is necessary to include the damping terms on the left-hand-side of this equation. Thus the term $C\dot{\beta}$ is added to both sides, giving

$$M\ddot{\beta} + C\dot{\beta} + K\beta = g + C\dot{\beta} = F$$

where C is the damping coefficient. For good convergence the damping coefficient used should be close to the actual damping of the particular degree of freedom, including structural, mechanical, and aerodynamic damping sources. The damping estimate does not have to be exact however, since it is added to both sides of the equation. In fact the actual damping in the forcing function g will often be time varying and even nonlinear, so the viscous damping coefficient has to be an approximation. The sole function of this damping term is to avoid divergence of the solution near resonance, and the value of C has no influence on the final converged solution.

Now the function F is evaluated at J points around the rotor azimuth:

$$F_j = F(\psi_j) = g(\psi_j) + C\dot{\beta}(\psi_j)$$

where $\psi_j = j\Delta\psi$ ($j = 1$ to J and $\Delta\psi = 2\pi/J$). Then the harmonics of a complex Fourier series representation of F are

$$F_n = \frac{1}{J} \sum_{j=1}^J F_j e^{-in\psi_j} K_n$$

where

$$K_n = \left(\frac{J}{\pi n} \sin \frac{\pi n}{J} \right)^2$$

With $K_n = 1$ these harmonics would give a Fourier interpolation representation of $F(\psi)$. While it matches the function exactly at the known points $F(\psi_j)$ (or with least squared-error if the number of harmonics used is less than $(J-1)/2$), the Fourier interpolation gives a poor representation elsewhere, with large excursions due to the higher harmonics. In particular, poor estimates of the derivatives of the function F are obtained. With the above values for K_n (which reduce the magnitude of the higher harmonics), and an infinite number of harmonics ($n = -\infty$ to ∞), a linear interpolation between the known points $F(\psi_j)$ is obtained. By truncating the Fourier series ($n = -L$ to L) the representation of F is smoothed, the corners of the linear interpolation being rounded off. Usually $L = J/3$ is satisfactory, that is the number of azimuth stations should be about 3 times the maximum harmonic of interest. The azimuth step thus should be $\Delta\psi = 2\pi/J \approx 120/n_{\max}$ degrees. Then the solution of the equation of motion for the harmonics of β is obtained from the harmonics of F by

$$\beta_n = \frac{f_n}{H_n}$$

$$\text{where } H_n = K - Mn^2 + C \sin.$$

The iterative solution, required because the nonlinear forcing function F depends on β and $\dot{\beta}$, proceeds as follows. At a given azimuth ψ_j , the blade motion is calculated using the current estimates of the harmonics:

$$\begin{aligned}\beta &= \sum_{n=-L}^L \beta_n e^{in\psi_j} \\ \dot{\beta} &= \sum_{n=-L}^L \beta_n i n e^{in\psi_j}\end{aligned}$$

The forcing function F_j is evaluated next. The estimates of the flapping harmonics are then updated to account for the difference between the current value of F_j and that found in the last revolution:

$$\Delta\beta_n = [f_j - (f_j)_{\text{start}}] \frac{k_n}{J} \frac{e^{-in\psi_j}}{H_n}$$

After adding $\Delta\beta_n$ to the flap harmonics β_n , the azimuth angle is incremented to $\psi_j + 1$. The calculation proceeds around the azimuth in this fashion until the solution converges. The test for convergence is performed once each revolution. Requiring that the root-mean-squared change in the blade motion from one revolution to the next be below a specified tolerance, the criterion is $(\Delta\beta)_{\text{rms}} < \epsilon$ for all degrees of freedom, where

$$\begin{aligned}\Delta\beta_{\text{rms}}^2 &= \frac{1}{2\pi} \int_0^{2\pi} (\Delta\beta)^2 d\psi \\ &= (\Delta\beta_s)^2 + \frac{1}{2} \sum_n ((\Delta\beta_{nc})^2 + (\Delta\beta_{ns})^2)\end{aligned}$$

and

$$\Delta\beta = \beta - \beta_{\text{start}}$$

This test is applied to all degrees of freedom, for both the rotor and the airframe.

In the present problem, the system of equations and degrees of freedom can be separated into two sets: the rotor motion, consisting of flap/lag bending, rigid pitch/elastic torsion, and gimbal or teeter flapping; and the aircraft rigid body and elastic motion, with the engine/transmission as an independent subset. The coupling between these sets is accounted for in the nonlinear forcing functions. As long as the coupling is weak, it is possible to solve the two sets of equations separately, in parallel. Within each of these subsystems, it is necessary to solve all the equations simultaneously, including in particular the inertial coupling on the left-hand side. Thus a vector equation must be solved for each harmonic of the motion. The solution proceeds as follows. At a given azimuth station, the blade motion and hub motion are evaluated using the current estimates of the harmonics. Then the generalized forces are evaluated, and the rotor equations are solved to update the harmonics of the blade motion. Next the rotor hub reactions are evaluated (for which the updated blade motion harmonics can be used), and the aircraft

equations solved to update the harmonics of the body motion. The azimuth angle is then incremented, and the calculation repeated until a converged solution is obtained.

5.1.5 Motion evaluation.- To begin the solution at a new azimuth station, the deflection, velocity, and acceleration of each degree of freedom must be evaluated from the harmonics. For the rotor blade bending:

$$\dot{\theta}_k = \sum_{n=-\infty}^{\infty} \beta_n^{(k)} e^{in\psi} = \beta_0^{(k)} + \sum_{n=1}^{\infty} (\beta_{nc}^{(k)} \cos n\psi + \beta_{ns}^{(k)} \sin n\psi)$$

$$\ddot{\theta}_k = \sum_{n=-\infty}^{\infty} in \beta_n^{(k)} e^{in\psi} = \sum_{n=1}^{\infty} n (-\beta_{nc}^{(k)} \sin n\psi + \beta_{ns}^{(k)} \cos n\psi)$$

$$\dddot{\theta}_k = \sum_{n=-\infty}^{\infty} (-n^2) \beta_n^{(k)} e^{in\psi} = \sum_{n=1}^{\infty} n^2 (-\beta_{nc}^{(k)} \cos n\psi - \beta_{ns}^{(k)} \sin n\psi)$$

Similarly for the blade pitch/torsion, p_k , \dot{p}_k , and \ddot{p}_k are obtained from the harmonics $\phi_n^{(k)}$. Note that for rotor #2 these time derivatives are based on Ω_2 . For the gimbal/teeter motion, recall from section above

$$\beta_G = \sum_{n=pN \pm 1} (\beta_G)_n e^{in\psi}$$

and similarly for $\dot{\beta}_G$ and $\ddot{\beta}_G$.

Recalling that only the pN harmonics are excited in the nonrotating frame, the rigid body and elastic airframe motion of the aircraft is

$$\dot{\theta}_{sk} = \sum_{n=pN} \phi_n^{(k)} e^{in\psi} + (\dot{\theta}_{sk})_{static}$$

$$\ddot{\theta}_{sk} = \sum_{n=pN} in \phi_n^{(k)} e^{in\psi} + (\ddot{\theta}_{sk})_{static}$$

$$\dddot{\theta}_{sk} = \sum_{n=pN} (-n^2) \phi_n^{(k)} e^{in\psi}$$

where $q_{s1} \dots q_{s6}$ are the six rigid body degrees of freedom, and q_{sk} for $k \geq 7$ are the airframe elastic modes. The steady state or slowly varying rigid body motion contributes the static velocity terms $(\dot{q}_{sk})_{\text{static}}$ ($k \leq 6$; this motion is static compared to the high frequency rotor motion and airframe vibration). The static elastic airframe deflection gives $(q_{sk})_{\text{static}}$ ($k \geq 7$). The rotor hub motion is then

$$\alpha = \begin{pmatrix} x_h \\ y_h \\ z_h \\ \alpha_x \\ \alpha_y \\ \alpha_z \end{pmatrix} = c \{ \dot{q}_{sk} \}$$

where c is given in section 4.2.2. Recall that in the evaluation of α_x , α_y , and α_z (for the aerodynamic analysis) the contributions of the rigid body Euler angles ϕ_F , θ_F and ψ_F (q_{s1} to q_{s3}) are not included; also the linear hub displacements (x_h , y_h , and z_h) are not used in the rotor analysis. Hence α is evaluated due to the elastic airframe modes only (q_{sk} , $k \geq 7$). The velocity and acceleration of the hub are

$$\dot{\alpha} = c \{ \dot{q}_{sk} \}$$

$$\ddot{\alpha} = c \{ \ddot{q}_{sk} \} + \bar{c} \{ \dot{q}_{sk} \}$$

For rotor #2, $\dot{\alpha}$ and $\ddot{\alpha}$ are multiplied by Ω_1/Ω_2 and $(\Omega_1/\Omega_2)^2$ respectively. Also for rotor #2, the aircraft motion harmonics are at $n = pN \Omega_2/\Omega_1$ (relative to the time scale of the nonrotating frame, Ω_1). We can write the hub velocity as follows therefore:

$$\begin{aligned}
 (\ddot{\alpha})_{\text{rotor } \#2} &= \frac{\Sigma_1}{\Sigma_2} c \left\{ \sum \sin \phi_n^{(k)} e^{in\psi} \right\} \\
 &= \frac{\Sigma_1}{\Sigma_2} c \left\{ \sum i p N \frac{\Sigma_2}{\Sigma_1} \phi_n^{(k)} e^{ipN(R_2/R_1)\psi} \right\} \\
 &= c \left\{ \sum i p N \phi_n^{(k)} e^{ipN\psi_2} \right\}
 \end{aligned}$$

Hence by evaluating the hub motion as a sum of harmonics at $n = pN$, with the azimuth angle of rotor #2, the time scale will be automatically accounted for. Similarly for the acceleration

$$\begin{aligned}
 (\ddot{\alpha})_{\text{rotor } \#2} &= c \left\{ - \sum (pN)^2 \phi_n^{(k)} e^{ipN\psi_2} \right\} \\
 &\quad + \frac{\Sigma_1}{\Sigma_2} \bar{c} \left\{ \sum i p N \phi_n^{(k)} e^{ipN\psi_2} \right\}
 \end{aligned}$$

A factor of Ω_1/Ω_2 is still required in the second term of $\ddot{\alpha}$, to account for the scaling of the aircraft velocity in \bar{c} .

The acceleration due to gravity, considered as an equivalent linear acceleration, is

$$\Delta \begin{pmatrix} x_m \\ y_m \\ z_m \end{pmatrix} = -g R_{SF} \vec{k}_e$$

For rotor #2, the factor $(\Omega^2 R)_1 / (\Omega^2 R)_2$ is also required.

The rotor shaft angular motion perturbation is evaluated from

$$\begin{aligned}
 \psi_s &= \sum_{n=pN} \psi_{sn} e^{in\psi} \\
 \dot{\psi}_s &= \sum_{n=pN} in \psi_{sn} e^{in\psi} + (\dot{\psi}_s)_{\text{static}} \\
 \ddot{\psi}_s &= \sum_{n=pN} (-n)^2 \psi_{sn} e^{in\psi}
 \end{aligned}$$

$$\begin{aligned}\psi_I &= \sum_{n=pN} \psi_{In} e^{in\psi} + (\psi_I)_{\text{static}} \\ \dot{\psi}_I &= \sum_{n=pN} in \psi_{In} e^{in\psi} \\ \ddot{\psi}_I &= \sum_{n=pN} (-n^2) \psi_{In} e^{in\psi}\end{aligned}$$

From section 4.3.2, the angular motion perturbations of the two rotors are then obtained from

$$\begin{aligned}\psi_{S1} &= \psi_S \\ \psi_{S2} &= \frac{c_{z1}}{r_{z2}} \psi_S + \psi_I\end{aligned}$$

As for the airframe motion, the time scales of the velocity and acceleration perturbations for rotor #2 are accounted for without additional factors of Ω_1/Ω_2 .

The solution for the helicopter trim or transient motion (section 5.3) supplies the static motion of the airframe rigid body degrees of freedom (\dot{q}_{sk} for $k = 1$ to 6) and of the rotational speed degree of freedom ($\dot{\psi}_S$). The solution for the static elastic deflection of the airframe and drive train (q_{sk} for $k \geq 7$, ψ_I , and ψ_e) is given in section 5.1.10.

The dimensionless time variable is ψ , the azimuth angle of rotor #1. The azimuth angle of rotor #2 is

$$\psi_2 = \frac{S_{z2}}{S_{z1}} \psi + \Delta\psi_{21}$$

where $\Delta\psi_{21}$ is the angle when $\psi = 0$ at rotor #1. Hence the analysis of rotor #2 must account for this phase difference of the two rotors, by evaluating the blade motion, the airloads, and the hub reactions of rotor #2 at $\psi + \Delta\psi_{21}$. The phase of the time variable for the airframe motion is the same as that for rotor #1. Note that if $\Omega_2/\Omega_1 \neq 1$ the rotors do not maintain a fixed azimuthal phase difference. For that case the rotors will effectively be analyzed separately however, so $\Delta\psi_{21} = 0$ can be used.

Hence the harmonics of the rotor hub motion are obtained from the harmonics of the aircraft degrees of freedom by the following expressions:

$$\alpha_n = c \{ \phi_n^{(k)} \}$$

$$\dot{\alpha}_n = i n c \{ \phi_n^{(k)} \}$$

$$\ddot{\alpha}_n = -n^2 c \{ \phi_n^{(k)} \} + i n \bar{c} \{ \phi_n^{(k)} \}$$

for n a nonzero multiple of N ; and the "static" components are

$$\alpha_{\text{static}} = c \{ \dot{q}_{sk} \}_{\text{static}}$$

$$\dot{\alpha}_{\text{static}} = c \{ \ddot{q}_{sk} \}_{\text{static}}$$

$$\ddot{\alpha}_{\text{static}} = \bar{c} \{ \dot{q}_{sk} \}_{\text{static}} + \begin{bmatrix} -g \rho_F k_E \\ 0 \end{bmatrix}$$

for the displacement (α_n and α_{static}) the summation is over the elastic air-frame modes only; also, only the angular displacement components are required ($\alpha_x, \alpha_y, \alpha_z$). For rotor #2, a factor of $(\Omega^2 R)_1 / (\Omega^2 R)_2$ is required in the gravity term, $(\dot{q}_{sk})_{\text{static}}$ is multiplied by Ω_1 / Ω_2 , and the matrix c is multiplied by Ω_1 / Ω_2 . Also, for rotor #2 the harmonics are multiplied by

$$e^{-in\Delta\psi_{21}}$$

since for the azimuth angle of rotor #2 equal to ψ , the hub motion at $\psi - \Delta\psi_{21}$ is required (only if $\Omega_1 = \Omega_2$). The harmonics of the rotor azimuth perturbation are obtained from the harmonics of the drive train degrees of freedom by the following expressions:

$$(\psi_{s1})_n = (\psi_s)_n$$

$$(\psi_{s2})_n = \frac{\omega_2}{\omega_1} (\psi_s)_n + (\psi_i)_n$$

or

$$\begin{pmatrix} \psi_{s1} \\ \psi_{s2} \end{pmatrix} = \begin{bmatrix} 1 & 0 \\ \frac{\omega_2}{\omega_1} & 1 \end{bmatrix} \begin{pmatrix} \psi_s \\ \psi_i \end{pmatrix}_n = \begin{bmatrix} c_{\psi_s} \\ c_{\psi_i} \end{bmatrix} \begin{pmatrix} \psi_s \\ \psi_i \end{pmatrix}_n$$

for n a nonzero multiple of N ; and the "static" components are

$$(\psi_{s1})_{\text{static}} = 0$$

$$(\psi_{s2})_{\text{static}} = (\psi_i)_{\text{static}}$$

$$(\dot{\psi}_{s1})_{\text{static}} = (\dot{\psi}_s)_{\text{static}}$$

$$(\dot{\psi}_{s2})_{\text{static}} = \underline{(\dot{\psi}_s)_{\text{static}}}$$

For rotor #2, $(\dot{\psi}_s)_{\text{static}}$ has been multiplied by ω_1/ω_2 ; also for rotor #2 the harmonics are multiplied by

$$e^{-in\Delta\psi_{21}}$$

The blade rigid pitch motion p_r requires the pitch increment due to the governor and due to the rotor mast bending. The harmonics of the governor pitch increment are obtained by summing the contributions from the two rotors; and for rotor #2 multiplying by

$$e^{-in\Delta\psi_{21}}$$

The pitch increment due to mast bending is

$$\begin{aligned}
 \Delta\theta_{\text{mast}}^{\text{bend}} &= - \sum_{k=1}^{\infty} q_{sk} (K_{Mck} \cos \psi + K_{MSk} \sin \psi) \\
 &= - \sum_{k=1}^{\infty} ((q_{sk})_{\text{static}} + \sum_n \phi_n^{(k)} e^{in\psi}) (K_{Mck} \cos \psi \\
 &\quad + K_{MSk} \sin \psi) \\
 &= \sum_n \left[- \sum_{k=1}^{\infty} \phi_n^{(k)} \frac{K_{Mck} - iK_{MSk}}{2} e^{i(n+1)\psi} \right. \\
 &\quad \left. - \sum_{k=1}^{\infty} \phi_n^{(k)} \frac{K_{Mck} + iK_{MSk}}{2} e^{i(n-1)\psi} \right]
 \end{aligned}$$

So the harmonics are obtained from the harmonics of the airframe elastic motion by the following expression:

$$\begin{aligned}
 (\Delta\theta_{\text{mast}}^{\text{bend}})_n &= - \sum_{k=1}^{\infty} \phi_{n-1}^{(k)} \frac{K_{Mck} - iK_{MSk}}{2} \\
 &\quad - \sum_{k=1}^{\infty} \phi_{n+1}^{(k)} \frac{K_{Mck} + iK_{MSk}}{2}
 \end{aligned}$$

where $\phi_n^{(k)}$ is zero except when n is a nonzero multiple of N , and the convention $\phi_0^{(k)} = (q_{sk})_{\text{static}}$ is used here. For rotor #2, the harmonics $\phi_n^{(k)}$ are multiplied by

$$e^{-in\Delta\psi_{21}}$$

in this calculation.

5.1.6 Rotor equations. - The differential equations of motion for the rotor degrees of freedom are given in section 2.2.18. For the n -th harmonic, these equations take the form

$$H_n \begin{pmatrix} \beta_n^{(1)} \\ \vdots \\ \beta_n^{(i)} \\ \theta_n^{(d)} \\ \theta_n^{(1)} \\ \vdots \\ \theta_n^{(i)} \\ \beta_{G,n} \end{pmatrix} = F_n$$

where $\theta_n^{(d)}$ is the n-th harmonic of p_d , and $\beta_{G,1}$ is only present for the $n = pN \pm 1$ harmonics for gimballed or teetering rotors. From the equations of section 2.2.18, the transfer functions matrix H_n and the forcing function F are as follows.

$H_n =$

$\mathcal{I}_{\vec{k}}^* (-n^2 + g_s \nu_k i n + \nu_k^2)$ $+ 2(\mathcal{I}_{\vec{k}q_i}^* + \sum_j \mathcal{I}_{\vec{k}q_j}^* q_j q_i) i n$ $+ g_{sq} \vec{k}_s \cdot \vec{\eta}_k'(e) \vec{k}_s \cdot \vec{\eta}'(e) i n$ $- \delta M_{q_k q_i} i n + \delta M_{q_k p_i} k_{p_i}$	$(S_{i \vec{k} \vec{p} i}^* + \sum_j S_{i \vec{k} \vec{p} j}^* q_j q_i) n^2$ $- (S_{q_k \vec{p} i}^*$ $+ \sum_j S_{q_k \vec{p} j}^* q_j q_i)$	$\mathcal{I}_{\vec{q}_k \alpha}^* \cdot \vec{k}_s (-n^2 + 1)$ $- (\mathcal{I}_{\vec{q}_k \vec{p} i}^*$ $+ \sum_j \mathcal{I}_{\vec{q}_k \vec{p} j}^* q_j q_i) i L_{G1}$ $- \delta M_{q_k \vec{p} i} i n + \delta M_{q_k p_i} k_{p_i}$
$(S_{A \vec{q} i}^* + \sum_j S_{A \vec{q} j}^* q_i q_j) n^2$ $- (S_{P \vec{q} i}^* + \sum_j S_{P \vec{q} j}^* q_i q_j)$ $- \delta M_{P \vec{q} i} i n$	$\mathcal{I}_{P \vec{k}}^* (-n^2 + g_s \nu_k i n + \nu_k^2)$ $- \mathcal{I}_{P \vec{p} i}^* n^2 + \mathcal{I}_{P \vec{p} i}^*$ $- \delta M_{P \vec{p} i} i n - \delta M_{P \vec{p} i}$	$-(\mathcal{I}_{P \vec{q} \alpha}^*$ $+ \sum_j \mathcal{I}_{P \vec{q} j}^* q_j q_i) \cdot \vec{k}_s (-n^2 + 1)$
$\mathcal{I}_{\vec{q}_\beta \alpha}^* \cdot \vec{k}_s (-n^2 + 1)$ $+ 2(\mathcal{I}_{\vec{q}_\beta q_i}^*$ $+ \sum_j \mathcal{I}_{\vec{q}_\beta q_j}^* q_i q_j) \cdot \vec{k}_s i n$ $- \delta M_{q_\beta i} i n + \delta M_{q_\beta p_i} k_{p_i}$	$-(S_{\vec{q}_\beta \vec{p} i}^*$ $+ \sum_j S_{\vec{q}_\beta \vec{p} j}^* q_i q_j) \cdot \vec{k}_s (-n^2 + 1)$	$\mathcal{I}_\alpha^* (-n^2 + \frac{1}{2}(\nu_{\alpha C}^2 + \nu_{\alpha S}^2))$ $+ \frac{1}{2}(C_{\alpha C}^2 + C_{\alpha S}^2) i D_{G2}$ $- \delta M_\beta i n + \delta M_{q_\beta p_i} k_{p_i}$

$F =$

$$\begin{aligned}
 & I_{q_0}^* - I_{q_k \alpha}^* \cdot \vec{k}_B (\ddot{\psi}_S + \ddot{\alpha}_Z) - 2(I_{q_k \dot{\alpha}}^* + \sum_j I_{q_k \dot{\alpha} q_j}^* \dot{q}_j)(\dot{\psi}_S + \dot{\alpha}_Z) \\
 & - S_{q_k}^* \cdot \vec{l}_B \ddot{z}_B + S_{q_k}^* \cdot \vec{l}_B (\ddot{x}_B \sin \psi - \ddot{y}_B \cos \psi) \\
 & - I_{q_k \alpha}^* \cdot \vec{l}_B ((\ddot{\alpha}_X + 2\ddot{\alpha}_Y) \sin \psi - (\ddot{\alpha}_Y - 2\ddot{\alpha}_X) \cos \psi) \\
 & + (S_{q_k \dot{\beta}}^* + \sum_j S_{q_k \dot{\beta} q_j}^* \dot{q}_j) \ddot{p}_r + (S_{q_k \dot{\beta}}^* + \sum_j S_{q_k \dot{\beta} q_j}^* \dot{q}_j) \ddot{p}_r \\
 & + \delta \frac{M_{q_k \text{geo}}}{\omega} + \vec{k}_B \cdot \vec{l}_k(r) (g \sin \dot{\psi} - M_{q_k}) \\
 & - \delta \left[\sum_i M_{q_k \dot{q}_i} \dot{q}_i + M_{q_k \dot{\beta}} \dot{\beta}_G - M_{q_k \dot{\beta} \dot{\beta}} (\sum_i k_{\dot{\beta} i} \dot{q}_i + k_{\dot{\beta} G} \dot{\beta}_G) \right]
 \end{aligned}$$

$$\begin{aligned}
 & I_{p_k 0}^* - (I_{p_k \alpha}^* + \sum_j I_{p_k \alpha q_j}^* \dot{q}_j) \cdot \vec{l}_B (\ddot{\psi}_S + \ddot{\alpha}_Z) \\
 & + (S_{p_k}^* + \sum_j S_{p_k q_j}^* \dot{q}_j) \cdot (\vec{k}_B \ddot{z}_B + \vec{l}_B (\ddot{x}_B \sin \psi - \ddot{y}_B \cos \psi)) \\
 & + (I_{p_k \alpha}^* + \sum_j I_{p_k \alpha q_j}^* \dot{q}_j) \cdot \vec{k}_B ((\ddot{\alpha}_X + 2\ddot{\alpha}_Y) \sin \psi - (\ddot{\alpha}_Y - 2\ddot{\alpha}_X) \cos \psi) \\
 & + \delta \frac{M_{p_k \text{geo}}}{\omega} - I_{p_0}^* \dot{\beta}_k(r_F) \ddot{p}_r - I_{p_k 0}^* \ddot{p}_r - I_{p_k 0}^* p_r \\
 & - \delta \left[\sum_i M_{p_k \dot{q}_i} \dot{q}_i + M_{p_k \dot{\beta}} \dot{\beta}_G + \sum_i M_{p_k \dot{\beta} i} (\dot{p}_i - \dot{\beta}_i(r_F) \ddot{p}_r) \right. \\
 & \quad \left. + \sum_i M_{p_k \dot{\beta} i} (\dot{p}_i - \dot{\beta}_i(r_F) p_r) \right]
 \end{aligned}$$

$$\begin{aligned}
 & - I_0^* ((\ddot{\alpha}_X + 2\ddot{\alpha}_Y) \sin \psi - (\ddot{\alpha}_Y - 2\ddot{\alpha}_X) \cos \psi) \\
 & + (\delta \frac{C_{\text{geo}}}{\omega})_{\text{geo}} + (S_{q_k \dot{\beta} 0}^* + \sum_j S_{q_k \dot{\beta} q_j}^* \dot{q}_j) \cdot \vec{l}_B (\ddot{p}_r + p_r) \\
 & - \delta \left[\sum_i M_{q_k \dot{q}_i} \dot{q}_i + M_{\dot{\beta}} \dot{\beta}_G - M_{\dot{\beta} 0} (\sum_i k_{\dot{\beta} i} \dot{q}_i + k_{\dot{\beta} G} \dot{\beta}_G) \right] \\
 & - \sum_{n=pN} \left[\frac{1}{2} (\zeta_{G\dot{\beta}}^* - C_{G\dot{\beta}}^*) i n + \frac{1}{2} I_0^* (p_{G\dot{\beta}}^2 - q_{G\dot{\beta}}^2) \right] \left[\beta_{G_{n+1}} e^{i(n+1)\psi} \right. \\
 & \quad \left. + \beta_{G_{n+1}} e^{i(n-1)\psi} \right]
 \end{aligned}$$

where

$$\Delta_{G1} = \begin{cases} -(n-1)^2 & \text{gimbal, } n = pN+1 \\ (n+1)^2 & \text{gimbal, } n = pN-1 \\ 2n & \text{teeter} \end{cases}$$

$$\Delta_{G2} = \begin{cases} (n-1) & \text{gimbal, } n = pN+1 \\ (n+1) & \text{gimbal, } n = pN-1 \\ n & \text{teeter} \end{cases}$$

Note that estimates of the aerodynamic spring and damping forces have been added to both sides of the equations. In the matrix H_n these terms must be multiplied by $((J/n\pi)\sin(n\pi/J))^2$, to be consistent with the Fourier analysis of the forcing function F (see section 5.1.4).

The solution for the blade motion requires the inverse of H_n for each harmonic. One approach is to invert H_n every azimuth step. A more efficient approach is to invert H_n^{-1} once and store the result. It will still be necessary to update H_n^{-1} occasionally however, because it depends on the bending solution (q_j terms). The blade motion harmonics should be completely recalculated whenever H_n^{-1} is updated.

Hence at each azimuth step ψ_j the forcing function F_j is evaluated. Then the blade motion harmonics are updated by adding the following increment:

$$\Delta \begin{pmatrix} \beta_n^{(1)} \\ \vdots \\ \beta_n^{(1)} \\ \theta_n^{(d)} \\ \theta_n^{(1)} \\ \vdots \\ \theta_n^{(1)} \\ \beta_n \end{pmatrix} = H_n^{-1} (F_j - (F_j)_{\text{east rev}}) \frac{k_n e^{-in\psi_j}}{J}$$

5.1.7 Hub reactions.- The generalized aircraft forces due to the rotor hub reactions are $Q = c^T F$, where c is given in section above and

$$F^T = \left[\gamma \frac{\partial C_H}{\partial a} \quad \gamma \frac{\partial C_H}{\partial a} \quad \delta \frac{\partial G}{\partial a} \quad \delta \frac{\partial C_{Mx}}{\partial a} \quad \delta \frac{\partial C_{My}}{\partial a} \quad -\gamma \frac{\partial C_Q}{\partial a} \right]$$

From the results of section above, the required hub reactions are as follows.

$$\gamma \frac{ZC_x}{\sigma_a} = \frac{1}{N} \sum_{m=1}^N (2 \sin \psi_m \gamma \frac{C_{fx}}{\sigma_a} + 2 \cos \psi_m \gamma \frac{C_{fr}}{\sigma_a})_{aero} + \sum_i I_{q,i}^* \cdot \vec{k}_B \left[\sum_{n=pN} e^{in\psi} i n^2 (\beta_{n-1}^{(i)} - \beta_{n+1}^{(i)}) \right]$$

$$\gamma \frac{ZC_y}{\sigma_a} = \frac{1}{N} \sum_{m=1}^N (-2 \cos \psi_m \gamma \frac{C_{fx}}{\sigma_a} + 2 \sin \psi_m \gamma \frac{C_{fr}}{\sigma_a})_{aero} + \sum_i I_{q,i}^* \cdot \vec{k}_B \left[\sum_{n=pN} e^{in\psi} i n^2 (\beta_{n-1}^{(i)} + \beta_{n+1}^{(i)}) \right]$$

$$\gamma \frac{ZC_T}{\sigma_a} = \frac{1}{N} \sum_{m=1}^N (2 \gamma \frac{C_{Tz}}{\sigma_a})_{aero} + 2 \sum_i I_{q,i}^* \cdot \vec{k}_B \left[\sum_{n=pN} e^{in\psi} i n^2 \beta_n^{(i)} \right]$$

$$\begin{aligned} \gamma \frac{ZC_{Mx}}{\sigma_a} &= \frac{1}{N} \sum_{m=1}^N (2 \sin \psi_m \gamma \frac{C_{Mx}}{\sigma_a})_{aero} \\ &- I_0^* \left[(\ddot{\alpha}_x + 2 \dot{\alpha}_y) \frac{2}{N} \sum_{m=1}^N \sin^2 \psi_m \right. \\ &\quad \left. - (\ddot{\alpha}_y - 2 \dot{\alpha}_x) \frac{2}{N} \sum_{m=1}^N \sin^2 \psi_m \cos^2 \psi_m \right] \\ &- I_0^* \left[\sum_{n=pN} e^{in\psi} i ((n^2 - 2n) \beta_{G,n-1} - (n^2 + 2n) \beta_{G,n+1}) \right] \\ &- \sum_i I_{q,i}^* \cdot \vec{k}_B \left[\sum_{n=pN} e^{in\psi} i ((n^2 - 2n) \beta_{n-1}^{(i)} - (n^2 + 2n) \beta_{n+1}^{(i)}) \right] \\ &- 2 \sum_i (I_{q,i}^* + \sum_j I_{q,qj}^* q_j \vec{q}_j) \cdot \vec{k}_B \left[\sum_{n=pN} e^{in\psi} ((n-1) \beta_{n-1}^{(i)} \right. \\ &\quad \left. - (n+1) \beta_{n+1}^{(i)}) \right] \end{aligned}$$

$$\begin{aligned}
\gamma \frac{\partial C_{Mg}}{\partial \alpha} = & +2 \sum_{m=1}^2 (-2 \cos \psi_m \gamma \frac{\partial \beta_m}{\partial \alpha})_{\text{aer}} \\
& - H_0^* \left[-(\ddot{\alpha}_x + 2 \dot{\alpha}_y) \sum_{m=1}^2 \sin \psi_m \cos \psi_m \right. \\
& \quad \left. + (\ddot{\alpha}_y - 2 \dot{\alpha}_x) \sum_{m=1}^2 \cos^2 \psi_m \right] \\
& - H_0^* \left[\sum_{n=pN} e^{in\psi} ((n^2 - 2n) \beta_{n-1} + (n^2 + 2n) \beta_{n+1}) \right] \\
& - H_0^* \vec{I}_{q:\alpha} \cdot \vec{t}_{KB} \left[\sum_{n=pN} e^{in\psi} ((n^2 - 2n) \beta_{n-1}^{(i)} + (n^2 + 2n) \beta_{n+1}^{(i)}) \right] \\
& + 2 \sum_i (I_{q_0 q_i}^* + \sum_j I_{q_0 q_i q_j q_j}^*) \cdot \vec{t}_{KB} \left[\sum_{n=pN} e^{in\psi} i ((n-1) \beta_{n-1}^{(i)} \right. \\
& \quad \left. + (n+1) \beta_{n+1}^{(i)}) \right]
\end{aligned}$$

$$\begin{aligned}
\gamma \frac{\partial C_Q}{\partial \alpha} = & +2 \sum_{m=1}^2 (2 \gamma \frac{\partial \beta_m}{\partial \alpha})_{\text{aero}} \\
& + 2 H_0^* (\ddot{\alpha}_x + \ddot{\alpha}_y) \\
& - 2 \sum_i I_{q:\alpha}^* \cdot \vec{t}_{KB} \left[\sum_{n=pN} e^{in\psi} n^2 \beta_n^{(i)} \right] \\
& + 4 \sum_i (I_{q_0 q_i}^* + \sum_j I_{q_0 q_i q_j q_j}^*) \cdot \vec{t}_{KB} \left[\sum_{n=pN} e^{in\psi} i n \beta_n^{(i)} \right]
\end{aligned}$$

where

$$\frac{2}{N} \sum_{m=1}^N \cos^2 \psi_m = \begin{cases} 1 & N \geq 3 \\ 1 + \cos 2\psi & N = 2 \end{cases}$$

$$\frac{2}{N} \sum_{m=1}^N \sin^2 \psi_m = \begin{cases} 1 & N \geq 3 \\ 1 - \cos 2\psi & N = 2 \end{cases}$$

$$\frac{2}{N} \sum_{m=1}^N \cos \psi_m \sin \psi_m = \begin{cases} 0 & N \geq 3 \\ \sin 2\psi & N = 2 \end{cases}$$

These hub reactions are harmonically analyzed in the evaluation of the vibratory airframe motion. The effect of the summation over all N blades then is to suppress the harmonics not at multiples of N/rev . An equivalent approach therefore is to omit the summation operator and only evaluate the pN/rev harmonics. Hence the aerodynamic forces are only evaluated for one blade at azimuth angle ψ .

The mean hub reactions, required in the solution for the steady state or slowly varying aircraft motion (section 5.3), are obtained by averaging the above results over one period. Note that only the aerodynamic terms contribute to the mean values of the hub forces and torque.

The hub forces due to the linear acceleration of the rotor mass

$$\Delta \begin{pmatrix} \gamma \frac{\partial C_H}{\partial \alpha} \\ \gamma \frac{\partial C_Y}{\partial \alpha} \\ \gamma \frac{\partial C_R}{\partial \alpha} \end{pmatrix} = -2M_b^* \begin{pmatrix} \ddot{x}_H \\ \ddot{y}_H \\ \ddot{z}_H \end{pmatrix}$$

have not been included here, since the airframe inertias include the rotor mass. For the static elastic airframe deflection, evaluated from the

mean hub reactions, the "static" hub acceleration must be included:

$$\Delta F = -2M_b^* \ddot{\alpha}_{\text{static}}$$

which consists of the gravitational force, and the centrifugal force due to the angular velocity of the body axes.

To solve the equations of motion for the engine and drive train, the rotor torque is required in the following form:

$$\begin{aligned} \gamma \frac{\tilde{C}_Q}{g_0} &= \frac{1}{N} \sum_{m=1}^N \left(\gamma \frac{C_m z}{\sigma a} \right)_{\text{aero}} \\ &\quad + I_o^* \ddot{\alpha}_z - \sum_i I_{q_i \alpha}^* \cdot \vec{k}_B \left[\sum_{n=pN} e^{in\psi} n^2 \beta_n^{(i)} \right] \\ &\quad + 2 \sum_i (I_{q_i q_j} + \sum_j I_{q_i q_j q_j \dot{\theta}_j}) \cdot \vec{k}_B \left[\sum_{n=pN} e^{in\psi} i n \beta_n^{(i)} \right] \\ &\quad - \gamma [Q_E \dot{\psi}_s + Q_\theta \Delta \theta_{\text{govr}}] \end{aligned}$$

(see section 5.1.9).

5.1.8 Aircraft equations.- The differential equations of motion for the aircraft degrees of freedom are given in section 4.2.4. For the n-th harmonics of the rigid body motion, these equations take the form

$$H_n \begin{pmatrix} \phi_F \\ \partial F \\ \psi_F \\ x_F \\ y_F \\ z_F \end{pmatrix}_n = F_n$$

The forcing function is due to the rotor hub reactions

$$F = \{Q_k^*\}_{\text{rotor } \#1} + \{Q_k^*\}_{\text{rotor } \#2}$$

From the equations of section 4.2.4, the transfer matrix H_n is as follows.

$$H_n = \begin{bmatrix} -R_e^T I^* R_e n^2 & 0 \\ -M^*(\vec{V} \times) R_e i_n + G & -M^* n^2 \end{bmatrix}$$

For the n -th harmonics of the aircraft elastic motion, the equation of motion is

$$[-M_k^* n^2 + \{M_k^* g_s \omega_k + \frac{2\delta}{\sigma_a} \frac{q}{A} V F_{q_k i_k}\} i_n + M_k^* \omega_k^2] \phi_n^{(k)} = (Q_k^*)_n$$

where Q_k^* is the generalized force due to the rotor hub reactions ($k \geq 7$). The only aircraft aerodynamic forces included in the high frequency response are the damping coefficients of the elastic modes (see section 4.2.7).

Only the harmonics of N/rev are excited in the nonrotating frame. The aircraft response to each of the two rotors is evaluated separately. For the response to the rotor #1 hub reactions, the harmonics at $n = N_1, 2N_1, 3N_1$, etc., are required. The time scale of the aircraft equations is the rotational speed of rotor #1, so the harmonics of motion due to rotor #2 are at $n = (\Omega_2/\Omega_1)n_2$. For the response to rotor #2 hub reactions the harmonics at $n = (\Omega_2/\Omega_1)N_2, (\Omega_2/\Omega_1)2N_2, (\Omega_2/\Omega_1)3N_2$, etc., are required. The equations of the airframe motion are not solved here for the static response ($n = 0$). The hub reactions of rotor #2 are evaluated as a function of its azimuth angle, ψ_2 ; to obtain the response of the airframe these hub reactions must be used at $\psi = \psi_2 - \Delta\psi_{21}$.

The hub reactions are evaluated at azimuth stations ψ_j as the rotor equations are being solved. Then the airframe vibration motion is obtained from

$$\{\phi_n^{(k)}\} = H_n^{-1} \{Q_k^*\}_n = H_n^{-1} C^T F_n$$

for n a nonzero multiple of N ; where

$$F_n = \sum_{j=1}^J F_j \frac{k_n e^{-in\psi_j}}{j}$$

are the harmonics of the rotor hub reaction. The motion $\phi_n^{(k)}$ is evaluated for excitation from rotor #1 and for excitation from rotor #2. For rotor #2 the harmonics must be multiplied by

$$e^{in\Delta\psi_{21}}$$

since for the airframe motion at ψ , the hub reactions at $\psi + \Delta\psi_{21}$ are required (only if $\Omega_1 = \Omega_2$).

5.1.9 *Transmission and engine equations.* - The differential equations of motion for the rotor and engine speed perturbations are given in section 4.3.2. The equations for the n-th harmonics are

$$H_n \begin{pmatrix} \psi_3 \\ \psi_I \\ \psi_e \\ \theta_{govr_3} \\ \theta_{govr_1} \\ \theta_{govr_2} \end{pmatrix}_n = F_n$$

with the forcing function and transfer function matrix as follows.

$$F = C_D_1 \left(\gamma \frac{\tilde{C}_D}{\sigma_a} \right)_1 + C_D_2 \left(\gamma \frac{\tilde{C}_D}{\sigma_a} \right)_2$$

with

$$\begin{bmatrix} C_D_1 & C_D_2 \end{bmatrix} = \begin{bmatrix} -1 & -f_3 \\ K_{MI_1} & -f_2 \\ 0 & 0 \\ 0 & 0 \\ 0 & 0 \\ 0 & 0 \end{bmatrix}$$

$$H_n = -Mn^2 + C_{in} + K$$

with

$$M = \begin{bmatrix} r_E^2 I_E^* + I_{\alpha_1}^* + f_2 I_{\alpha_2}^* & f_1 I_{\alpha_2}^* & r_E^2 I_E^* & 0 & 0 & 0 \\ -k_M I_1 I_{\alpha_1}^* + f_1 I_{\alpha_2}^* & f_0 I_{\alpha_2}^* + k_M r_E^2 I_E^* & 0 & 0 & 0 & 0 \\ r_E^2 I_E^* & 0 & r_E^2 I_E^* & 0 & 0 & 0 \\ 0 & 0 & 0 & \tau_{zz} & 0 & 0 \\ 0 & 0 & 0 & 0 & \tau_{z_1} & 0 \\ 0 & 0 & 0 & 0 & 0 & \tau_{z_2} \end{bmatrix}$$

$$C = \begin{bmatrix} r_E^2 Q_{\alpha_1}^* + \gamma_1 Q_{\beta_1}^* + f_3 \gamma_2 Q_{\beta_2}^* & f_2 \gamma_2 Q_{\beta_2}^* & r_E^2 Q_{\alpha_2}^* & 0 & 0 & 0 \\ -k_M I_1 Q_{\beta_1}^* + f_2 \gamma_2 Q_{\beta_2}^* & f_1 \gamma_2 Q_{\beta_2}^* + k_M r_E^2 Q_{\alpha_2}^* & 0 & 0 & 0 & 0 \\ r_E^2 Q_{\alpha_2}^* & r_E^2 Q_{\alpha_2}^* + \sqrt{M_{zz} K_{zz}} g_s & 0 & 0 & 0 & 0 \\ k_{P_E} & 0 & 0 & \tau_{z_1} & 0 & 0 \\ -k_{P_1} & 0 & 0 & 0 & \tau_{z_1} & 0 \\ -k_{P_2} & 0 & 0 & 0 & 0 & \tau_{z_2} \end{bmatrix}$$

$$K = \begin{bmatrix} 0 & 0 & 0 & -r_E Q_t^* & \gamma_1 Q_{\alpha_1} & f_3 \gamma_2 Q_{\beta_2} \\ 0 & \frac{k^*}{I_{\alpha_1} I_{\alpha_2}} & 0 & 0 & -k_M \gamma_1 Q_{\alpha_1} & f_2 \gamma_2 Q_{\beta_2} \\ 0 & -k_{ME_2}^* & k_{ME_1}^* & -r_E Q_t^* & 0 & 0 \\ K_{IE} & 0 & 0 & 1 & 0 & 0 \\ -K_{I_1} & 0 & 0 & 0 & -1 & 0 \\ -K_{I_2} & 0 & 0 & 0 & 0 & -1 \end{bmatrix}$$

where

$$f_n = \frac{(N I_b \Sigma^n)_2}{(N I_b \Sigma^n)_1}$$

The torque \tilde{C}_Q is defined in section 5.1.7. In summing over all N blades, all the harmonics of the torque cancel except those at N/rev. Hence the drive train equations are only solved for the $n = N, 2N, 3N, \dots$, harmonics.

The rotor torque ($\gamma \tilde{C}_Q/\sigma_a$) is evaluated at the azimuth stations ψ_j as the rotor equations are being solved. Then the transmission vibratory motion is obtained from

$$\begin{pmatrix} N_s \\ \psi_I \\ \psi_e \\ \theta_{govr} \\ \theta_{govr_1} \\ \theta_{govr_2} \end{pmatrix}_n = H_n^{-1} C_D \left(\gamma \frac{\tilde{C}_Q}{\sigma_a} \right)_n$$

for n a nonzero multiple of N ; where

$$\left(\gamma \frac{\tilde{C}_Q}{\sigma_a} \right)_n = \sum_{j=1}^J \left(\gamma \frac{\tilde{C}_Q}{\sigma_a} \right)_j \frac{k_n e^{-in\psi_j}}{J}$$

are the harmonics of the torque. For rotor #2 the harmonics are multiplied by

$$e^{in\Delta\psi_2}$$

The transmission motion is evaluated for excitation from rotor #1 and for excitation from rotor #2.

5.1.10 *Static elastic deflection*. - The equations of motion for the static elastic deflection of the airframe and drive train are

$$M_k^* \omega_k^2 q_{sk} = (Q_k^*)_{\text{rotors}} + \frac{2\delta}{\sigma a} \frac{q}{A} [F_{qk\delta} \begin{pmatrix} \delta_y \\ \delta_e \\ \delta_a \\ \delta_r \end{pmatrix}]$$

$$-K_{MI_1} (\delta \frac{C_Q}{\sigma a})_1 + \frac{(N I_b \Sigma^2)_z}{(N I_b \Sigma^2)_1} (\delta \frac{C_Q}{\sigma a})_2 + K_{MI_2}^* \Psi_I = 0$$

$$K_{ME_1}^* \Psi_e - K_{ME_2}^* \Psi_I = (\delta \frac{C_Q}{\sigma a})_1 + \frac{(N I_b \Sigma^3)_z}{(N I_b \Sigma^3)_1} (\delta \frac{C_Q}{\sigma a})_2$$

(from sections 4.2.4 and 4.3.2). Here Q_k^* is the mean generalized force due to the two rotors, and C_Q is the mean rotor torque.

Hence the solution for the static elastic airframe motion ($k \geq 7$) is

$$(q_{sk})_{\text{static}} = \frac{1}{M_k^* \omega_k^2} \left[(c_k^T F_o)_{\text{rotor } \#1} + (c_k^T F_o)_{\text{rotor } \#2} + \frac{2\delta}{\sigma a A} q F_{qk\delta} \begin{pmatrix} \delta_y \\ \delta_e \\ \delta_a \\ \delta_r \end{pmatrix} \right]$$

where c_k^T is the k-th row of c^T ; and

$$F_o = \frac{1}{J} \sum_{j=1}^J F_j - 2M_b^* \ddot{\alpha}_{\text{static}}$$

is the mean hub reaction including the rotor mass inertial reaction. The static elastic drive train motion is

$$\begin{pmatrix} \psi_I \\ \psi_e \end{pmatrix}_{\text{static}} = H_o^{-1} \begin{pmatrix} (\delta \frac{C_Q}{\sigma_a})_1 \\ (\delta \frac{C_Q}{\sigma_a})_2 \end{pmatrix}$$

where

$$H_o^{-1} = \begin{bmatrix} \frac{K_{Mz_1}}{K_{Mz_2}^*} & -\frac{(NI_b \sigma_z^2)_2}{(NI_b \sigma_z^2)_1} \frac{1}{K_{Mz_2}^*} \\ \frac{K_{Mz_2}^* + K_{ME_2}^* K_{Mz_1}}{K_{ME_1}^* K_{Mz_2}^*} & \frac{(NI_b \sigma_z^2)_2}{(NI_b \sigma_z^2)_1} \frac{\frac{K_{Mz_2}^* r_{z_1}/r_{zz} - K_{ME_2}^*}{K_{ME_1}^* K_{Mz_2}^*}} \end{bmatrix}$$

and $\gamma C_Q/\sigma_a$ is the mean torque.

5.1.11 Two-rotor aircraft.- In the present model, the two rotors of a helicopter can influence each other through excitation of vibratory airframe motion. The analysis proceeds as follows (see fig. 27). The rotor analysis calculates the hub reactions of each of the two rotors. From these hub reactions, the aircraft equations of motion are solved for the harmonics of the airframe rigid body and elastic motion. Then the hub motion can be evaluated at each rotor, due to the forces of each rotor. The motion at each hub due to the two rotors is summed. Then the rotor equations are solved for the rotor motion and for the hub reactions again.

It is useful to be able to suppress the feedback of the nonrotating frame vibration to either or both rotors. The coupling can be suppressed by omitting the summation of the two hub motion components at one or both hubs (the dotted line in fig. 27). The entire vibratory hub motion can be suppressed by setting it to zero at one or both hubs (the static or low frequency hub motion and the acceleration due to gravity should be retained however). Suppressing the entire vibratory hub motion is equivalent to dropping the

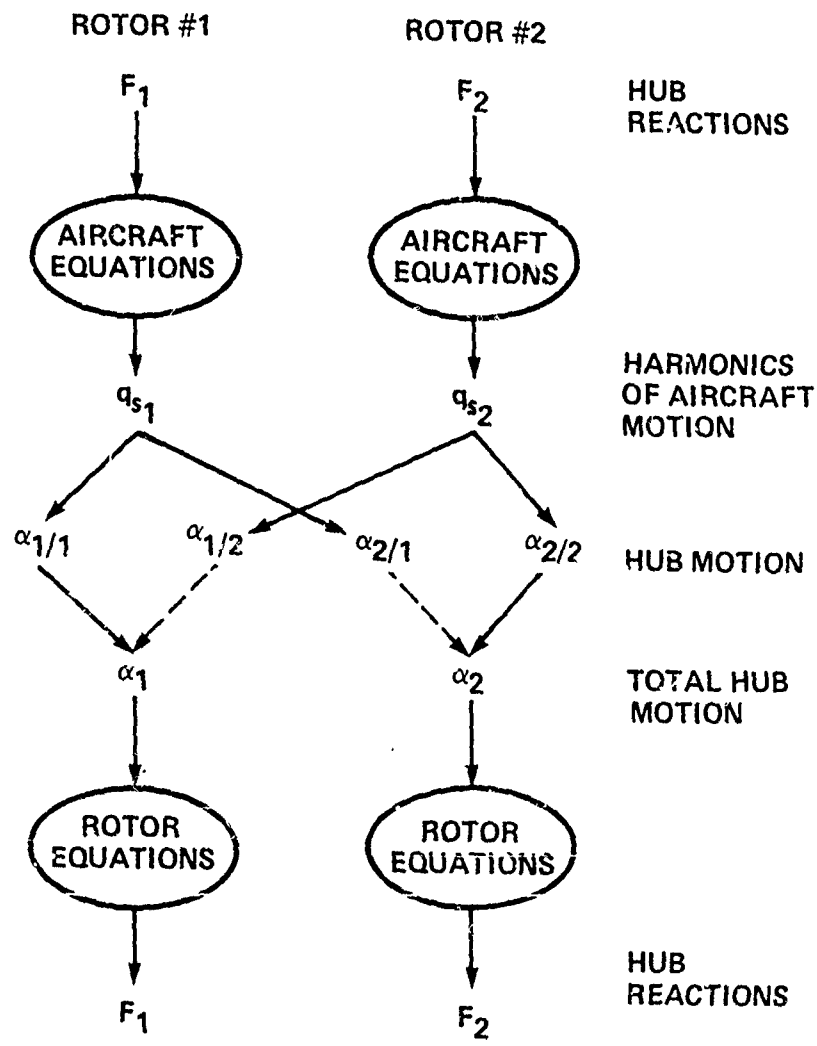


Figure 27. Outline of dynamic interaction of the two rotors.

aircraft degrees of freedom as far as the rotor analysis is concerned, but it still may be useful to evaluate the aircraft vibration due to the hub reactions.

It should also be possible in a similar fashion to suppress the hub motion due to the static elastic deflection of the airframe and drive train.

The procedure described above is based on the assumption that the entire system is periodic, which in fact is true only if both rotors have the same rotational speed ($\Omega_2/\Omega_1 = 1$). When the two rotors do not turn at the same speed, the motion in the nonrotating frame is not periodic even in steady flight. The most important example is the single main-rotor and the tail-rotor configuration. In order to analyze a periodic system still, it is necessary to neglect the mutual interference of the two rotors. The analysis proceeds as described above, except that the hub motion of one rotor due to the vibratory airframe motion produced by the other rotor is always suppressed (the dotted line in fig. 27). Effectively the helicopter is then being analyzed as two single rotor systems, except for the coupling through the aircraft "static" motion (steady state of slowly varying, including the airframe static elastic deflection).

5.1.12 *Circulation convergence.*— The blade motion will be calculated for a given induced velocity distribution over the rotor disk, uniform or nonuniform. When the converged solution for the blade motion is obtained, the rotor loading (C_T or bound circulation) is re-evaluated. Then the induced velocity estimate can be updated, and the blade motion solution repeated. This procedure continues until the root-mean-squared change in the bound circulation from one iteration to the next is less than a specified tolerance level:

$$\frac{1}{J} \sum_{j=1}^J (\Delta \Gamma_j)^2 < \left(\epsilon \frac{2\pi\sigma}{N} \right)^2$$

where Γ_j is the maximum bound circulation and the summation is over the azimuth. When uniform inflow is used, the criterion is

$$(\Delta C_T)^2 + \delta (\Delta C_{M_y}^2 + \Delta C_{M_x}^2) < (\epsilon \sigma)^2$$

To improve the convergence of the iterative calculation of the rotor loading and wake induced velocity, a lag is introduced in the thrust coefficient and used to calculate λ_i :

$$C_T = f C_{T_{\text{new}}} + (1-f) C_{T_{\text{old}}}$$

where $C_{T_{\text{old}}}$ is the thrust used to calculate λ_i in the last iteration, and $C_{T_{\text{new}}}$ is the thrust calculated using that value of λ_i . The factor f should have a value equal to the thrust lift deficiency function

$$f = \frac{1}{1 + \frac{\sigma_a}{4} \frac{\partial \lambda}{\partial T}}$$

(see section 6.1.5). Similarly, for a nonuniform inflow calculation a lag is introduced in the blade bound circulation used to evaluate the induced velocity.

5.1.13 Calculation procedure.— In summary, the calculation of the rotor motion and airframe vibration proceeds as follows. The input quantities are the linear and angular velocity perturbations of the rigid body motion; the rotational speed perturbation; the collective and cyclic pitch control angles of the two rotors; the aircraft aerodynamic control positions; and the gust velocity components at the two rotors. The output quantities are the generalized forces due to the mean hub reactions of the two rotors; and the converged solution for the blade motion and aircraft vibration.

The outermost loop is an iteration on the rotor induced velocity and bound circulation evaluation. The next loop is an iteration on the rotor and aircraft motion calculation.

One cycle of the blade and aircraft motion calculation consists of the following steps. First the transfer matrices H_n^{-1} are evaluated. Then there are a number of cycles of successive evaluation of the rotor and airframe motion by the following procedure. First the hub motion harmonics are evaluated. Next there is an azimuth loop for the rotor. At each azimuth step the rotor blade motion harmonics and the aerodynamic hub reactions are updated. Next the total hub reactions are evaluated; the aircraft vibration and drive train vibration harmonics are updated from the hub reactions; and the static elastic deflection is evaluated.

Within the azimuth loop of the rotor motion calculation there are the following steps. First the hub motion and blade motion are evaluated from the harmonics. Then there is an integration over the radial station. Within the radial station loop the blade section pitch, velocity, angle-of-attack, and Mach number are evaluated; the lift, drag, and moment coefficients are evaluated; and the section aerodynamic forces are evaluated. The generalized aerodynamic forces of the blade modes are evaluated by integrating the section forces over the blade radius, and then the blade motion harmonics are updated. The aerodynamic hub forces and moments are also updated.

After each cycle of the blade motion calculation, the convergence is tested by comparing the blade and airframe motion harmonics with the values at the beginning of the cycle.

Finally, after the converged blade motion is obtained, the induced velocity and circulation convergence is tested by comparing the rotor bound circulation with the values at the beginning of the iteration.

5.2 Rotor Performance, Loads, and Noise

Once the solution for the periodic motion of the helicopter has been obtained, the performance, loads, and noise of the rotor can be evaluated. The rotor loads of interest include the tension and shear forces, bending moments, and torsion moment at various blade radial stations; the control

loads; the blade root forces and moments; and the net rotor hub reactions. The rotor-induced vibration can be evaluated at various points in the aircraft. From the rotor aerodynamic loading the rotational noise can be calculated. The rotor loads at radial station r will be calculated by integrating the aerodynamic and inertial forces acting on the blade outboard of r .

5.2.1 *Rotor performance.* - To evaluate the rotor performance, the mean rotor hub reactions are required:

$$\left(\begin{array}{c} \frac{C_F}{q} \\ \frac{C_M}{q} \\ \frac{C_T}{q} \\ \frac{C_{Mx}}{q} \\ \frac{C_{My}}{q} \\ -\frac{C_Q}{q} \end{array} \right) = \frac{1}{J} \sum_{j=1}^J \left(\begin{array}{c} \sin \psi_j \frac{C_{Fz}}{\sigma} + \cos \psi_j \frac{C_{Fr}}{\sigma} \\ -\cos \psi_j \frac{C_{Fz}}{\sigma} + \sin \psi_j \frac{C_{Fr}}{\sigma} \\ \frac{C_{Fg}}{\sigma} \\ \sin \psi_j \frac{C_{Mx}}{\sigma} \\ -\cos \psi_j \frac{C_{Mx}}{\sigma} \\ -\frac{C_{Mz}}{\sigma} \end{array} \right)$$

where the summation operator averages the forces and moments over the azimuth. These quantities are directly available from the rotor analysis (see section 5.1.7), where they are used also to calculate the generalized forces acting on the aircraft.

The rotor performance is determined in particular by the thrust and torque. The power delivered to the rotor through the shaft is $P = \Omega Q$. The propulsive force is the component of the net rotor force in the direction of the aircraft velocity:

$$PF = -X = \frac{-\mu_x H + \mu_y Y + \mu_z T}{\sqrt{\mu_x^2 + \mu_y^2 + \mu_z^2}}$$

and then the rotor lift, normal to the aircraft velocity, is

$$L = \sqrt{T^2 + H^2 + Y^2 - X^2}$$

So L and X are the wind axis components of the net aerodynamic force of the rotor.

The hub reactions relative to the tip-path plane are obtained by multiplying the force vector by the rotation matrix

$$R_{TS} = \begin{bmatrix} 1 & 0 & \beta_c \\ 0 & 1 & \beta_s \\ -\beta_c & -\beta_s & 1 \end{bmatrix}$$

where β_c and β_s are the tip-path plane tilt angles. Also of interest are the magnitude of the net force of the rotor, and its tilt angles relative to the reference plane: $\theta = \tan^{-1}(H/T)$ and $\phi = \tan^{-1}(Y/T)$.

It is useful to split the rotor power according to the type of energy loss. The induced, interference, profile, parasite, and climb power losses are obtained as follows.

$$C_{Pi} = \int \lambda_i dC_T = \int \lambda_i \omega a \left(\frac{F_z}{\rho C} \right) dT$$

$$C_{P_{int}} = \int \lambda_{int} dC_T = \int \lambda_{int} \omega a \left(\frac{F_z}{\rho C} \right) dT$$

$$C_{P_c} = V_c W / \rho A (\rho R)^3$$

$$\begin{aligned} C_{P_p} + C_{P_c} &= -VX / \rho A (\rho R)^3 = -C_x (V / \rho R) \\ &= -\mu_x C_H + \mu_y C_Y + \mu_z C_T \end{aligned}$$

$$C_{P_p} = (C_{P_p} + C_{P_c}) - C_{P_c}$$

$$C_{P_0} + C_{P_i} + C_{P_{int}} = C_P - (C_{P_p} + C_{P_c})$$

$$C_{P_0} = (C_{P_0} + C_{P_i} + C_{P_{int}}) - C_{P_i} - C_{P_{int}}$$

The induced and interference power losses are obtained by integrating the inflow velocities over the rotor disk.

The ideal power loss, consisting of the parasite, climb, and minimum induced losses, is defined as follows:

$$C_{P_{ideal}} = (\lambda_{ideal} + \mu_z) C_T - \mu_x C_H + \mu_y C_Y$$

where

$$\lambda_{ideal} = \frac{C_T}{2 \sqrt{\mu_x^2 + \mu_y^2 + (\lambda_{ideal} + \mu_z)^2}}$$

Then the nonideal power loss, consisting of the profile and excess induced losses, is defined as

$$\begin{aligned} C_{P_n} &= C_P - C_{P_{ideal}} \\ &= (C_{P_0} + C_{P_i} + C_{P_{int}}) - \lambda_{ideal} C_T \end{aligned}$$

A measure of the rotor efficiency is the figure of merit, defined for hover as

$$M = \frac{C_T^{3/2} / \sqrt{2}}{C_P}$$

This will be generalized for axial and forward flight to

$$M = \frac{C_{P\text{ideal}}}{C_f} = 1 - \frac{C_{P_n}}{C_f}$$

The ratios C_{P_i}/C_T and $C_{P\text{int}}/C_T$ may be considered equivalent induced velocities. A measure of the excess induced losses is the ratio

$$\kappa = \frac{C_{P_i}}{\lambda_{\text{ideal}} C_T}$$

and the profile losses can be expressed in terms of an equivalent section drag coefficient:

$$C_{d_0} = 8 \frac{C_f}{\sigma}$$

$$C_{d_n} = 8 \frac{C_{f_n}}{\sigma}$$

In forward flight, the rotor drag is defined by

$$D_r = \frac{P}{V} + X = \frac{P_o + P_i + P_{\text{int}}}{V}$$

or in terms of an equivalent drag area $\delta = D_r / 2\rho V^2$. A measure of the rotor efficiency in forward flight is the rotor lift to drag ratio, L/D_r . Similarly the total drag is defined as

$$D_{\text{total}} = \frac{P}{V}$$

and the total lift to drag ratio is L/D_{total} .

The section power loading can be split into components in a similar fashion:

$$\frac{dC_p/\sigma}{dr} = r \frac{f_x}{c}$$

$$\frac{dC_p/\sigma}{dr} = \lambda_i \frac{f_z}{c}$$

$$\frac{dC_{p,i}/\sigma}{dr} = \lambda_{int} \frac{f_z}{c}$$

$$\frac{dC_p/\sigma}{dr} = u_T \frac{f_{x_0}}{c} + u_R \frac{f_{r_0}}{c} = \frac{1}{2} U (U^2 C_d + U_R^2 C_{d,radial}) \frac{c}{c_m}$$

5.2.2 Section force.- The total tension and shear forces on the blade section at radial station r are $\vec{F}(r) = \vec{F}_A - \vec{F}_I$, where

$$\vec{F}_I = \int_r \vec{a} \, d\vec{r}$$

$$\vec{F}_A = \int_r (f_x \vec{i}_B + f_r \vec{j}_B + f_z \vec{k}_B) \, d\vec{r}$$

(see section 2.2.10; here \vec{a} includes the gravitational acceleration). Hence

$$\begin{aligned} F_{shear} &= \frac{\vec{F}}{I_b S c^2 / R} \\ &= \gamma \left(\frac{C_{fx}}{\sigma_a} \vec{i}_B + \frac{C_{fr}}{\sigma_a} \vec{j}_B + \frac{C_{fz}}{\sigma_a} \vec{k}_B \right) \\ &= \gamma \int_r \left(\frac{f_x}{ac} \vec{i}_B + \frac{f_r}{ac} \vec{j}_B + \frac{f_z}{ac} \vec{k}_B \right) d\vec{r} - \frac{1}{I_b} \int_r \vec{a} \, d\vec{r} \end{aligned}$$

Substituting for \vec{a} from section 2.2.4, the inertial term becomes

$$-\int_C^I \vec{a} \cdot d\vec{q} = \vec{\tau}_B \left[\begin{array}{l} - \int_C^I m \vec{d}q (\ddot{x}_B \sin \psi - \ddot{y}_B \cos \psi) \\ + \int_C^I g \vec{m} \vec{d}q (\dot{\alpha}_z + \dot{\psi}_s - \psi_s) \\ + \sum_i T_B \cdot \int_C^I \vec{\eta}_i \cdot \vec{m} \vec{d}q (\ddot{q}_i - \dot{q}_i) \\ + \int_C^I (x_{FA} \cos \theta - x_{FA} + (g - c_{FA}) \delta_{FA} z) \vec{m} \vec{d}q \end{array} \right]$$

$$+ \vec{J}_B \left[\begin{array}{l} - \int_C^I m \vec{d}q (\ddot{x}_B \cos \psi + \ddot{y}_B \sin \psi) \\ + 2 \int_C^I g \vec{m} \vec{d}q (\dot{\alpha}_z + \dot{\psi}_s) \\ + \sum_i 2 T_B \cdot \int_C^I \vec{\eta}_i \cdot \vec{m} \vec{d}q \ddot{q}_i \\ + \int_C^I g \vec{m} \vec{d}q \end{array} \right]$$

$$+ k_B \left[\begin{array}{l} - \int_C^I m \vec{d}q \ddot{z}_B \\ - \int_C^I g \vec{m} \vec{d}q ((\ddot{\alpha}_x + 2\ddot{\alpha}_y) \sin \psi \\ \quad - (\ddot{\alpha}_y - 2\ddot{\alpha}_x) \cos \psi) \\ - \sum_i T_B \cdot \int_C^I \vec{\eta}_i \cdot \vec{m} \vec{d}q \ddot{q}_i \\ - \int_C^I g \vec{m} \vec{d}q \ddot{\beta}_C \end{array} \right]$$

or

$$-\frac{1}{I_b} \int_r^l \vec{a}_m dq = \vec{\tau}_B \begin{bmatrix} -M_b^* (\ddot{x}_n \sin \psi - \ddot{y}_n \cos \psi) \\ + S_b^* (\ddot{\alpha}_z + \dot{\psi}_s - \psi_s) \\ + \sum_i T_B \cdot S_{q_i}^* (\ddot{q}_i - q_i) \\ + I_{\epsilon_{x_0}}^* \end{bmatrix}$$

$$+ \vec{\delta}_B \begin{bmatrix} -M_b^* (\ddot{x}_n \cos \psi + \ddot{y}_n \sin \psi) \\ + 2S_b^* (\ddot{\alpha}_z + \dot{\psi}_s) \\ + \sum_i 2T_B \cdot S_{q_i}^* \dot{q}_i \\ + S_L^* \end{bmatrix}$$

$$+ \vec{k}_B \begin{bmatrix} -M_b^* \ddot{z}_n \\ -S_b^* ((\ddot{\alpha}_x + z\ddot{\alpha}_y) \sin \psi \\ \quad - (\ddot{\alpha}_y - z\ddot{\alpha}_x) \cos \psi) \\ - \sum_i T_B \cdot S_{q_i}^* \ddot{q}_i \\ - S_b^* \ddot{\beta}_G \end{bmatrix}$$

The components of the tension and shear forces in the local blade axes are obtained by multiplying \vec{F}_{shear} by the rotation matrix R_{xs} :

$$R_{xs} = \begin{bmatrix} 1 & \vec{k}_B \cdot \vec{\phi} & 0 \\ -\vec{k}_B \cdot \vec{\phi} & 1 & \vec{i}_B \cdot \vec{\phi} \\ 0 & -\vec{i}_B \cdot \vec{\phi} & 1 \end{bmatrix}$$

where

$$\vec{\phi} = \vec{i}_B (\beta_G + \delta_{FA_1} - \delta_{FA_2}) + \vec{k}_B (\psi_s - \delta_{FA_3}) + (z_o \vec{i} - x_o \vec{k})'$$

The force is multiplied by R_B to obtain the components in the section principal axes, where

$$R_B = \begin{bmatrix} \cos\theta & 0 & -\sin\theta \\ 0 & 1 & 0 \\ \sin\theta & 0 & \cos\theta \end{bmatrix}$$

The integrals of the aerodynamic forces will be evaluated as follows:

$$\int_r^i f(\rho) d\rho = \int_r^{r_i + \frac{1}{2}\Delta r_i} f d\rho + \sum_{i=I+1}^M \int_{r_i - \frac{1}{2}\Delta r_i}^{r_i + \frac{1}{2}\Delta r_i} f d\rho$$

$$= f_x (r_x + \frac{1}{2} \Delta r_x - r) + \sum_{i=x+1}^M f_i \Delta r_i$$

$$= \sum_{i=x}^M f(r_i) h_i$$

where I is the maximum index (over $i = 1$ to M) such that

$r_I - \frac{1}{2} \Delta r_I < r$ ($I = 1$ if $r_1 - \frac{1}{2} \Delta r_1 \geq r$); and $h_i = \Delta r_i$ for $i = I + 1$ to M , except

$$h_x = r_x + \frac{1}{2} \Delta r_x - r \quad \text{if } r_x - \frac{1}{2} \Delta r_x < r$$

$$= \Delta r_x + \min (r_x - \frac{1}{2} \Delta r_x - r, 0)$$

The inertia constants are evaluated by trapezoidal integration over the blade properties defined at $r = (j - 1) \Delta r$ ($j = 1$ to $M + 1$, $\Delta r = 1/M$):

$$\int_r^I f(g) dg = \int_r^{r_x} f(g) dg + \sum_{i=x}^M \int_{r_i}^{r_{i+1}} f(g) dg$$

$$= f_{x-1} \frac{(r_x - r)^2}{2 \Delta r} + f_x \left[\frac{(r_x - r)(r + 2\Delta r - r_x)}{2 \Delta r} + \frac{\Delta r}{2} \right]$$

$$+ \sum_{i=x+1}^M f_i \Delta r + f_{M+1} \frac{\Delta r}{2}$$

$$= \sum_{i=x-1}^{M+1} f(r_i) h_i$$

where I is the index ($i = 2$ to $M + 1$) such that $r_{I-1} \leq r < r_I$; and $h_1 = \Delta r$, except

$$h_{x-1} = \frac{(r_x - r)^2}{2\Delta r}$$

$$h_x = \frac{(r_x - r)(r + 2\Delta r - r_x)}{2\Delta r} + \frac{\Delta r}{2}$$

$$h_{x+1} = h_{x+1} - \frac{\Delta r}{2}$$

Similarly

$$\begin{aligned} \int_0^r f(g) dg &= \sum_{i=1}^{I-2} \int_{r_i}^{r_{i+1}} f(g) dg + \int_{r_{x-1}}^r f(g) dg \\ &= f_1 \frac{\Delta r}{2} + \sum_{i=2}^{I-2} f_i \Delta r + f_{x-1} \frac{\Delta r}{2} \\ &\quad + \left[f_{x-1} + \underbrace{\frac{f_{x-1}(r_x - r) + f_x(r - r_{x-1})}{\Delta r}}_{\Delta r} \right] \frac{r - r_{x-1}}{2} \\ &= \sum_{i=1}^I f(r_i) h_i \end{aligned}$$

with I as defined above; and $h_1 = \Delta r$, except

$$h_x = \frac{(r - r_x + \Delta r)^2}{2\Delta r}$$

$$h_{x-1} = \frac{\Delta r}{2} + \frac{(r_x - r + \Delta r)(r - r_x + \Delta r)}{2\Delta r}$$

$$h_1 = h_1 - \frac{\Delta r}{2}$$

5.2.3 Section bending moment.- The bending moment on the blade section at radial station r is

$$\vec{M}_{\text{bend}}^* = \frac{\vec{M}^{(2)}}{I_b \Omega^2} = \gamma \frac{\vec{M}_A^{(2)}}{\dot{a}c} - \frac{\vec{M}_I^{(2)}}{I_b}$$

where $\vec{M}^{(2)} = M_x \vec{i} + M_z \vec{k} = (\vec{i} i_{xs} + \vec{k} k_{xs}) \vec{M}$. As in section 2.2.7, the aerodynamic and inertial moments are as follows.

$$\begin{aligned}\frac{\vec{M}_A^{(2)}}{\dot{a}c} &= \int_r^l (g - r) \left(\frac{\vec{r}_z}{\dot{a}c} \vec{i}_x - \frac{\vec{r}_x}{\dot{a}c} \vec{i}_z \right) dm \\ \frac{\vec{M}_I^{(2)}}{I_b} &= \frac{1}{I_b} (\tau \vec{r}_{xs} + \vec{R} \vec{E}_{xs}) \int_r^l \int \left(\vec{r} \Big|_{g \times z} - \vec{r} \Big|_{\infty} \right) x \vec{a} dm dr \\ &\approx \frac{1}{I_b} (\tau \vec{r} + \vec{R} \vec{E}) \int_r^l \left[\begin{array}{c} (g - r) \vec{z} + (x_s + x_i) \vec{r} + z_0 \vec{k} \\ -(x_0 \vec{r} + z_0 \vec{k}) \end{array} \right] x \vec{a} dm dr \\ &= \frac{1}{I_b} \left\{ \begin{array}{l} \int_r^l (g - r) \vec{z} \times \vec{a} dm dr \\ + \int_r^l \left[\begin{array}{c} - (z_0 \vec{r} - x_0 \vec{k} - x_i \vec{k}) \\ + (z_0 \vec{r} - x_0 \vec{k}) \end{array} \right] \left[\begin{array}{c} -g - 2g \dot{\psi}_s \\ -2 \vec{E}_g \cdot (z_0 \vec{r} - x_0 \vec{k}) \end{array} \right] dm dr \\ - \int_r^l \sum p_k \left(\vec{r} \times \vec{X}_k(r) - \vec{r} \times \vec{X}_k(\infty) \right. \\ \quad \left. + \vec{x}_k x_z \vec{r} \right) dm dr \end{array} \right\}\end{aligned}$$

Substituting for the acceleration from section 2.2.4, the inertial moment becomes:

$$\begin{aligned}
\vec{M}_I^{(2)} = & \sum_i \ddot{q}_i \int_r^l (\rho - r) \vec{\eta}_i \cdot d\vec{r} \\
& + \sum_i \ddot{q}_i \int_r^l [g(\vec{\eta}_i - \vec{\eta}_i(r)) - \vec{k}_B \vec{k}_B \cdot \vec{\eta}_i(r)] d\vec{r} \\
& + \sum_i \dot{q}_i \left[\begin{array}{l} (\delta_{FA_1} - \delta_{FA_2}) \int_r^l (\rho - r) (\vec{\eta} \times \vec{\eta}_i) d\vec{r} \\
+ \int_r^l [(z_0 \vec{r} - x_0 \vec{k} - x_I \vec{k}) \\
- (z_0 \vec{r} - x_0 \vec{k})] I_r] \vec{k}_B \cdot \vec{\eta}_i d\vec{r} \\
- \vec{k}_B (\vec{\eta}' \cdot \vec{k} \times \vec{\eta}) \Big|_{r=0} \int_r^l (\rho - r) d\vec{r} \\
+ \vec{k}_B \int_0^r \vec{\eta}'' \cdot (z_0 \vec{r} - x_0 \vec{k} - x_I \vec{k}) d\vec{r} \int_r^l (\rho - r) d\vec{r} \\
+ \vec{k}_B \int_r^l (z_0 \vec{r} - x_0 \vec{k} - x_I \vec{k}) \cdot \{ \vec{\eta}'' \int_0^r (\rho' - r) d\vec{r} \\
- \vec{\eta}' (\rho - r) m \} d\vec{r} \\
+ ((\beta_G + \beta_C) \vec{k}_B + \vec{\psi}_s \vec{E}_B) \int_r^l (\rho - r) g m d\vec{r} \\
+ (\theta_G - \theta_C + z \dot{\beta}_G) \vec{k}_B \int_r^l (\rho - r) [z_{FA} - g \delta_{FA_1} \\
+ (z - z_{FA_2}) \delta_{FA_2} - \vec{k}_B \cdot (z_0 \vec{r} - x_0 \vec{k} - x_I \vec{k})] m d\vec{r} \\
+ 2 \dot{\psi}_s \left[\begin{array}{l} \int_r^l (\rho - r) [g(\delta_{FA_1} - \delta_{FA_2}) \vec{k}_B \\
- (x_{FA} + \vec{k}_{FA} \delta_{FA_2}) \vec{E}_B] m d\vec{r} \\
+ \int_r^l \{ \vec{k}_B g \vec{k}_B \cdot (z_0 \vec{r} - x_0 \vec{k} - x_I \vec{k}) \\
+ \vec{k}_B \cdot \vec{k}_B \cdot (z_0 \vec{r} - x_0 \vec{k} - x_I \vec{k}) \\
- g(z_0 \vec{r} - x_0 \vec{k}) \} I_r \} m d\vec{r} \end{array} \right] \end{array} \right] \end{aligned}$$

$$\begin{aligned}
& - \sum_i p_i \int_r^l (g-r) \vec{r} \times \vec{X}_i \, m \, dg \\
& - \sum_i p_i \left\{ \vec{k}_B \vec{r}_e \cdot \vec{X}_i (g-r) + g \vec{z}_k \times \vec{z}_i \right\}_r \\
& \quad + g \vec{r} \times (\vec{X}_i - \vec{X}_i|_r) \} \, m \, dg \\
& + [\vec{r}_B \ddot{z}_B - \vec{k}_B (\ddot{x}_B \sin \psi - \ddot{y}_B \cos \psi)] \int_r^l (g-r) \, m \, dg \\
& + [\vec{r}_B ((\ddot{a}_x + 2\dot{a}_y) \sin \psi - (\ddot{a}_y - 2\dot{a}_x) \cos \psi) \\
& \quad + \vec{k}_B \ddot{a}_z] \int_r^l (g-r) \, g \, m \, dg \\
& + \int_r^l (g-r) [\vec{r}_B (\delta_{FA_1} - \delta_{FA_2}) g + \vec{k}_B (x_2 \cos \theta - x_{FA} - f_{FA} \delta_{FA_3})] \, m \, dg \\
& \quad - \int_r^l g \times \vec{k} \, m \, dg
\end{aligned}$$

or

$$\begin{aligned}
\frac{\vec{M}_E^{(2)}}{\vec{I}_{\vec{q}_0}} &= \sum_i (I_{q_i \alpha}^* - r S_{q_i}^*) \ddot{q}_i \\
& + \sum_i (\vec{r}_B \vec{r}_e \cdot I_{q_i \alpha}^* + r \vec{k}_B \vec{r}_B \cdot S_{q_i}^* - \vec{\eta}_i (r) S_{q_i}^*) \ddot{q}_i \\
& + \sum_i 2 I_{q_i \dot{q}_i}^* \dot{q}_i \\
& + (I_0^* - r S_b^*) (\vec{r}_B (\ddot{\beta}_G + \beta_G) + \vec{k}_B \dot{\beta}_G) \\
& + I_{q_i \dot{\beta}_G}^* \vec{k}_B (\ddot{\theta}_G - \theta_G + 2\dot{\beta}_G) \\
& + 2 I_{q_i \dot{\psi}_S}^* \dot{\psi}_S
\end{aligned}$$

$$\begin{aligned}
& - \sum_i S_{q_{op}}^* \ddot{\rho}_i \\
& - \sum_i S_{q_{op}}^* \dot{\rho}_i \\
& + (S_b^* - rM_b^*) (\ddot{x}_B \ddot{z}_B - \ddot{k}_B (\ddot{x}_B \sin \psi - \ddot{y}_B \cos \psi)) \\
& + (I_o^* - rS_b^*) (\ddot{k}_B ((\ddot{\alpha}_x + z\ddot{\alpha}_y) \sin \psi \\
& \quad - (\ddot{\alpha}_y - z\ddot{\alpha}_x) \cos \psi) + \ddot{k}_B \ddot{\alpha}_z) \\
& + I_{m_x}^*
\end{aligned}$$

The components of the bending moment in the principal axes of the section are then obtained by

$$\begin{pmatrix} M_x \\ M_z \end{pmatrix}_{xs} = \begin{bmatrix} \cos \theta & -\sin \theta \\ \sin \theta & \cos \theta \end{bmatrix} \begin{pmatrix} M_x \\ M_z \end{pmatrix}_B$$

The integrals are evaluated as described in section 5.2.2.

5.2.4 Section torsion moment.- The torsion moment on the blade section at radial station r is

$$M_{tors}^* = \frac{Mr}{I_b S^2} = \gamma \frac{Mr_A}{ac} - \frac{Mr_z}{I_b}$$

where $M_r = \vec{J}_{xs} \cdot \vec{M} = (\vec{j} + (x_0 \vec{i} + z_0 \vec{k})') \cdot \vec{M}$. As in section 2.2.8, the aerodynamic and inertial moments are as follows.

$$\begin{aligned}\frac{M_{rA}}{ac} &= \int_r^l \frac{Ma}{ac} \vec{J} \\ &\quad + \vec{J}_{xs} \cdot \int_r^l [(\beta - r) \vec{j} + (x_0 \vec{i} + z_0 \vec{k}) \\ &\quad - (x_0 \vec{i} + z_0 \vec{k})|_r] \times \left(\frac{F_x}{ac} \vec{i}_s + \frac{F_z}{ac} \vec{k}_s \right) \vec{J} \\ &= \int_r^l \frac{Ma}{ac} \vec{J} \\ &\quad + \int_r^l \left(\frac{F_x}{ac} \vec{i}_s + \frac{F_z}{ac} \vec{k}_s \right) \cdot [(z_0 \vec{i} - x_0 \vec{k}) \\ &\quad - (z_0 \vec{i} - x_0 \vec{k})|_r - (\beta - r) (z_0 \vec{i} - x_0 \vec{k})'|_r] \vec{J} \\ \frac{M_{rI}}{I_{\theta}} &= \frac{1}{I_{\theta}} \vec{J}_{xs} \cdot \int_r^l [(\beta - r) \vec{j} + (x_0 + x) \vec{i} + (z_0 + z) \vec{k} \\ &\quad - (x_0 \vec{i} + z_0 \vec{k})|_r] \times \vec{a} \ dm \vec{J} \\ &= \frac{1}{I_{\theta}} \left[\int_r^l [(z_0 \vec{i} - x_0 \vec{k} - x_I \vec{k}) - (z_0 \vec{i} - x_0 \vec{k})|_r \\ &\quad - (\beta - r) (z_0 \vec{i} - x_0 \vec{k})'|_r] \cdot \vec{a} \ dm \vec{J} \right. \\ &\quad + \int_r^l \ddot{\theta} \vec{a} \vec{J} + \int_r^l I_{\theta} \cos \sin \theta \vec{J} \\ &\quad + \int_r^l I_{\theta} \tilde{\theta} (\cos^2 \theta - \sin^2 \theta) \vec{J} \\ &\quad \left. + (x_0 \vec{i} + z_0 \vec{k})' \cdot \int_r^l [(z_0 \vec{i} - x_0 \vec{k} - x_I \vec{k}) \\ &\quad - (z_0 \vec{i} - x_0 \vec{k})|_r] \vec{a} \ dm \vec{J} \right]\end{aligned}$$

Then substituting for the acceleration from section 3.2.4 gives for the inertial term:

$$\begin{aligned}
 M_{r\perp} = & \sum_i \ddot{p}_i \int_r^l \dot{\xi}_i I_{\theta} d\xi \\
 & + \sum_i p_i \int_r^l I_{\theta} \dot{\xi}_i (\omega^2 \theta - \sin^2 \theta) d\xi \\
 & + ((\ddot{\beta}_G + \beta_G) \vec{k}_B - \ddot{\psi}_S \vec{t}_B) \cdot \int_r^l \vec{X} g_m d\xi \\
 & + \sum_i \ddot{q}_i \int_r^l \vec{X} \cdot (-\vec{j} \times \vec{\eta}_i) m d\xi \\
 & + \sum_i q_i \left[\int_r^l \left[\begin{array}{l} [\vec{\eta}_i - \vec{\eta}_i(r) - (g-r)\vec{\eta}'_i(r)] \cdot \\ [\vec{t}_B(x_{FA} + t_{FA} \delta_{FA} z - x_I \cos \theta) \\ + \vec{k}_B g (\delta_{FA}, -\delta_{FA} z)] \end{array} \right] m d\xi \right. \\
 & \quad + \int_r^l x_z [-\vec{\eta}'_i(r) \cdot \vec{t}_B g - \vec{\eta}_i \cdot \vec{k}_B \sin \theta] m d\xi \\
 & \quad + \frac{1}{2} \int_r^l \left\{ \begin{array}{l} [\vec{\eta}_i - \vec{\eta}_i(r) \\ - (g-r)\vec{\eta}'_i(r)] \cdot \vec{t}_B \vec{k}_B \cdot (z_0 \vec{t} - x_0 \vec{k}) \\ + [(z_0 \vec{t} - x_0 \vec{k}) - (z_0 \vec{t} - x_0 \vec{k})' |_r \\ - (g-r)(z_0 \vec{t} - x_0 \vec{k})' |_r] \cdot \vec{t}_B \vec{k}_B \cdot \vec{\eta}_i \\ - \vec{j} \times \vec{\eta}'_i(r) \cdot [(z_0 \vec{t} - x_0 \vec{k}) \\ - (z_0 \vec{t} - x_0 \vec{k})' |_r] \end{array} \right\} g \\
 & \quad \left. - \vec{\eta}_i(r) \right] g \quad \left. \right\} m d\xi
 \end{aligned}$$

$$\begin{aligned}
& + [\vec{k}_B \ddot{z}_B + \vec{i}_B (\ddot{x}_B \sin \psi - \ddot{y}_B \cos \psi)] \cdot \int_r^l \vec{X} g \, dy \\
& + [\vec{k}_B ((\ddot{\alpha}_x + 2\ddot{\alpha}_y) \sin \psi - (\ddot{\alpha}_y - 2\ddot{\alpha}_x) \cos \psi) \\
& \quad - \vec{i}_B \ddot{\alpha}_z] \cdot \int_r^l \vec{X} g \, dy \\
& + \int_r^l [I_\theta \cos \theta \sin \theta - \cos \theta g (\delta_{FA_1} - \delta_{FA_2}) x_{Im}] \, dy
\end{aligned}$$

where

$$\begin{aligned}
\vec{X} = & (z_B^2 - x_B^2 - x_B^2) - (z_B^2 - x_B^2) \Big|_r \\
& - (g - r)(z_B^2 - x_B^2)' \Big|_r
\end{aligned}$$

or

$$\begin{aligned}
\frac{M_{Fz}}{I_B} = & \sum_i I_{p,q}^* \ddot{p}_i + \sum_i I_{p,q}^* \dot{p}_i \\
& + I_{p,\alpha}^* \cdot (\vec{k}_B (\beta_G + \beta_g) - \vec{i}_B \ddot{\psi}_s) \\
& + \sum_i S_{p,q}^* \ddot{q}_i + \sum_i S_{p,q}^* \dot{q}_i \\
& + S_{p,\alpha}^* \cdot (\vec{k}_B \ddot{z}_B + \vec{i}_B (\ddot{x}_B \sin \psi - \ddot{y}_B \cos \psi)) \\
& + I_{p,\alpha}^* \cdot (\vec{k}_B ((\ddot{\alpha}_x + 2\ddot{\alpha}_y) \sin \psi - (\ddot{\alpha}_y - 2\ddot{\alpha}_x) \cos \psi) - \vec{i}_B \ddot{\alpha}_z) \\
& + I_{p,\alpha}^*
\end{aligned}$$

The integrals are evaluated as described in section 5.2.2.

5.2.5 Control load.- The control load at the blade root is given by the moment about the feathering axis:

$$M_{con} = \frac{M_{FA}}{I_b \omega^2} = \gamma \frac{M_{FA_A}}{ac} - \frac{M_{FA_I}}{I_b}$$

where $M_{FA} = \hat{e}_{FA} \cdot \vec{M}$. From section 2.2.9, the equation of motion for rigid pitch is

$$M_{FA_A} - M_{FA_I} = \left(\sum_i I_{\rho, \dot{\rho}_i} \ddot{\rho}_i \right) [\omega_0^2 (\rho_0 - \rho_r) + g_s \omega_0 (\dot{\rho}_0 - \dot{\rho}_r)]$$

Hence the control load can be evaluated from

$$\begin{aligned} -M_{con} &= I_{\rho_0}^* \ddot{\rho}_0 + \sum_i I_{\rho, \dot{\rho}_i}^* \ddot{\rho}_i + \sum_i I_{\rho, \dot{\rho}_i}^* \rho_i \\ &\quad - \sum_i (S_{\rho, \dot{q}_i}^* + \sum_j S_{\rho, \dot{q}_j, q_j}^* q_j) \ddot{q}_i \\ &\quad - \sum_i (S_{\rho, q_i}^* + \sum_j S_{\rho, q_j, q_j}^* q_j) q_i \\ &\quad + (I_{\rho, \alpha}^* + \sum_j I_{\rho, \alpha, q_j}^* q_j) \cdot (T_B (\ddot{x}_s + \ddot{\alpha}_x) - T_B (\dot{\beta}_G + \beta_G) \\ &\quad - T_B ((\ddot{\alpha}_x + 2\ddot{\alpha}_y) \sin \psi - (\ddot{\alpha}_y - 2\ddot{\alpha}_x) \cos \psi)) \\ &\quad + (S_{\rho, 0}^* + \sum_j S_{\rho, q_j}^* q_j) \cdot (-T_B \ddot{z}_B - T_B (\ddot{x}_B \sin \psi - \ddot{y}_B \cos \psi)) \\ &\quad - I_{\rho, 0}^* - \gamma \frac{M_{po, max}}{ac} \end{aligned}$$

The inertial constants are defined in section 2.2.19.

5.2.6 Root forces and moments. - Following section 2.2.18, the forces and moments at the blade root are

$$\begin{aligned}\vec{F}_{\text{root}} &= \frac{\vec{F}}{I_b S^2/R} = \gamma \left(\frac{C_{fx}}{\sigma_a} \vec{t}_B + \frac{C_{fr}}{\sigma_a} \vec{j}_B + \frac{C_{fz}}{\sigma_a} \vec{k}_B \right) \\ &= \gamma \int_0^1 \left(\frac{f_x}{\sigma_a} \vec{t}_B + \frac{f_z}{\sigma_a} \vec{j}_B + \frac{f_z}{\sigma_a} \vec{k}_B \right) dr - \frac{1}{I_b} \int_0^1 \vec{a} m dr\end{aligned}$$

$$\begin{aligned}\vec{M}_{\text{root}} &= \frac{\vec{M}}{I_b S^2} = \gamma \left(\frac{C_{mx}}{\sigma_a} \vec{t}_B - \frac{C_{mz}}{\sigma_a} \vec{k}_B \right) \\ &= \gamma \int_0^1 \left(\frac{f_z}{\sigma_a} \vec{t}_B - \frac{f_x}{\sigma_a} \vec{k}_B \right) r dr - \frac{1}{I_b} \int_0^1 \vec{r} \times \vec{a} m dr\end{aligned}$$

Substituting for the acceleration from section 2.2.4 gives the components of the blade root force and moment in the rotating frame:

$$\begin{aligned}\gamma \frac{C_{fx}}{\sigma_a} &= \left(\gamma \frac{C_{fx}}{\sigma_a} \right)_{\text{aero}} - M_b^* (\ddot{x}_a \sin \psi_m - \ddot{y}_a \cos \psi_m) \\ &\quad + S_b^* (\dot{\alpha}_z + \dot{\psi}_s) - S_b^* \dot{\psi}_s \\ &\quad + \sum_i S_{q_i}^* \cdot \vec{k}_B (\ddot{q}_i - q_i) \\ &\quad + I_{fx}^*\end{aligned}$$

$$\begin{aligned}\gamma \frac{C_{fr}}{\sigma_a} &= \left(\gamma \frac{C_{fr}}{\sigma_a} \right)_{\text{aero}} - M_b^* (\ddot{x}_a \cos \psi_m + \ddot{y}_a \sin \psi_m) \\ &\quad + 2 S_b^* (\dot{\alpha}_z + \dot{\psi}_s) \\ &\quad + \sum_i 2 S_{q_i}^* \cdot \vec{k}_B \dot{q}_i \\ &\quad + S_b^*\end{aligned}$$

$$\gamma \frac{C_{xz}}{\sigma_a} = \left(\gamma \frac{C_{xz}}{\sigma_a} \right)_{aero} - M_b^* \ddot{z}_b$$

$$- S_b^* ((\ddot{\alpha}_x + 2\dot{\alpha}_y) \sin \psi_m - (\ddot{\alpha}_y - 2\dot{\alpha}_x) \cos \psi_m)$$

$$- S_b^* \beta_G - \sum_i S_i^* \cdot \vec{l}_i \ddot{q}_i$$

$$\gamma \frac{C_{mx}}{\sigma_a} = \left(\gamma \frac{C_{mx}}{\sigma_a} \right)_{aero} - S_b^* \ddot{z}_b$$

$$- I_o^* ((\ddot{\alpha}_x + 2\dot{\alpha}_y) \sin \psi_m - (\ddot{\alpha}_y - 2\dot{\alpha}_x) \cos \psi_m)$$

$$- I_o^* (\beta_G + \dot{\beta}_G)$$

$$- \sum_i I_{q_i \alpha}^* \vec{l}_i (\ddot{q}_i + \dot{q}_i)$$

$$- 2 \sum_i (I_{q_i \dot{q}_i}^* + \sum_j I_{q_i \dot{q}_j}^* q_j \dot{q}_j) \cdot \vec{l}_i \dot{q}_i$$

$$- 2 (I_{q_i \dot{\psi}}^* + \sum_j I_{q_i \dot{\psi} q_j}^* \dot{q}_j) (\dot{\psi}_i + \dot{\alpha}_x)$$

$$- I_{m_{x0}}^*$$

$$\begin{aligned}
\ddot{\gamma}_{\frac{\partial \alpha}{\partial q}}^{C_{m2}} = & \left(\ddot{\gamma}_{\frac{\partial \alpha}{\partial q}}^{C_{m2}} \right)_{aero} - S_b^* (\ddot{x}_b \sin \psi_m - \ddot{y}_b \cos \psi_m) \\
& + I_0^* (\ddot{\omega}_z + \dot{\psi}_S) + \sum_i I_{q,a}^* \cdot \vec{k}_B \cdot \ddot{q}_i \\
& + 2 \sum_i (I_{q,\dot{q},q_i}^* + \sum_j I_{q,\dot{q},q_i, q_j}^* \ddot{q}_j) \cdot \vec{k}_B \cdot \ddot{q}_i \\
& - (I_{q,\dot{q},\dot{q}}^* + \sum_j I_{q,\dot{q},q_j}^* \ddot{q}_j) (\ddot{\theta}_G - \theta_C + 2\dot{\beta}_G)
\end{aligned}$$

The inertial constants are defined in section 2.2.19. Here the gravitational forces is included in the linear acceleration terms, and the root reaction forces due to the blade mass and weight are retained.

To be consistent with the Fourier analysis used in the equations of motion, the aerodynamic forces must be operated on as follows. Let F_j be the aerodynamic force evaluated at $\psi_j = j\Delta\psi$ ($j = 1$ to J , $\Delta\psi = 2\pi/J$). The function F is harmonically analyzed as in section 2.1.4, and then the function is re-evaluated (at $\psi_k = k\Delta\psi$) using those harmonics:

$$\begin{aligned}
\tilde{F}_k &= \sum_n F_n e^{in\psi_k} \\
&= \sum_n \left(\frac{1}{J} K_n \sum_{j=1}^J F_j e^{-int\psi_j} \right) e^{in\psi_k} \\
&= \sum_{j=1}^J F_j \left(\frac{1}{J} \sum_n K_n e^{in(\psi_k - \psi_j)} \right) \\
&= \sum_{j=1}^J F_j S_{kj}
\end{aligned}$$

where

$$S_{kj} = \frac{1}{4} \sum_n K_n e^{in(k-j)\Delta\theta}$$

This operation is applied to the aerodynamic load used to evaluate the section force, the section bending moment, the section torsion moment, the control load, and the root forces and moments.

5.2.7 Hub reactions.- Following section 2.2.18, the total force and moment acting on the rotor hub, resolved in the nonrotating frame (the S system) are

$$\vec{F}_{hub} = \frac{\vec{F}}{NI_b S^2 / R} = \gamma \left(\frac{C_H}{\sigma_a} \vec{T}_S + \frac{C_Y}{\sigma_a} \vec{J}_S + \frac{C_T}{\sigma_a} \vec{R}_S \right)$$

$$\vec{M}_{hub} = \frac{\vec{M}}{NI_b S^2} = \gamma \left(\frac{C_{Mx}}{\sigma_a} \vec{T}_S + \frac{C_{My}}{\sigma_a} \vec{J}_S - \frac{C_Q}{\sigma_a} \vec{R}_S \right)$$

The hub reactions are obtained from the root forces and moments by resolving the rotating components into the nonrotating frame and summing over all the blades:

$$\begin{array}{c|c} \begin{pmatrix} \delta \frac{C_H}{\sigma_a} \\ \delta \frac{C_Y}{\sigma_a} \\ \delta \frac{C_T}{\sigma_a} \\ \delta \frac{C_{Mx}}{\sigma_a} \\ \delta \frac{C_{My}}{\sigma_a} \\ -\delta \frac{C_Q}{\sigma_a} \end{pmatrix} & = \frac{1}{N} \sum_{m=1}^N \begin{pmatrix} \sin \psi_m \delta \frac{C_{fx}}{\sigma_a} + \cos \psi_m \delta \frac{C_{fr}}{\sigma_a} \\ -\cos \psi_m \delta \frac{C_{fx}}{\sigma_a} + \sin \psi_m \delta \frac{C_{fr}}{\sigma_a} \\ \gamma \frac{C_{fz}}{\sigma_a} \\ \sin \psi_m \delta \frac{C_{mx}}{\sigma_a} \\ -\cos \psi_m \delta \frac{C_{mx}}{\sigma_a} \\ -\gamma \frac{C_{mq}}{\sigma_a} \end{pmatrix} \end{array}$$

Applying the summation operator gives directly the hub reactions in the time domain, over a period $2\pi/N$. Alternatively, the rotating frame forces and moments can be harmonically analyzed, and then the harmonics of the rotor hub reactions obtained from the harmonics of the root forces and moments, by

$$\begin{pmatrix} C_H \\ C_Y \\ C_Z \\ C_{M_X} \\ C_{M_Y} \\ -C_Q \end{pmatrix} = \sum_{n=pN}^{\infty} e^{int_n} \begin{pmatrix} \frac{1}{2}((C_{fr})_{n-1} + (C_{fr})_{n+1}) - \frac{i}{2}((C_{fx})_{n-1} - (C_{fx})_{n+1}) \\ -\frac{i}{2}((C_{fr})_{n-1} - (C_{fr})_{n+1}) - \frac{1}{2}((C_{fx})_{n-1} + (C_{fx})_{n+1}) \\ (C_{fz})_n \\ -\frac{i}{2}((C_{mx})_{n-1} - (C_{mx})_{n+1}) \\ -\frac{1}{2}((C_{mx})_{n-1} + (C_{mx})_{n+1}) \\ -(C_{mz})_n \end{pmatrix}$$

Only harmonics at multiples of N/rev are transmitted by the hub to the non-rotating frame. It is useful however to evaluate all harmonics of the root forces and moments in the nonrotating frame, according to the above relations, since a real rotor will not accomplish this filtering exactly.

5.2.8 *Vibration*.- Following the evaluation of the hub motion in the section 4.2.2, the linear acceleration in the aircraft at an arbitrary point \vec{r} is

$$\begin{pmatrix} \alpha_x \\ \alpha_y \\ \alpha_z \end{pmatrix} = [(-\vec{r}_x) \hat{R}_e \quad I \quad \dots \vec{r}_x \dots] \{ \dot{\vec{q}}_{fk} \} + [-(\vec{v}_x) \hat{R}_e] \begin{pmatrix} \dot{\varphi}_F \\ \dot{\theta}_F \\ \dot{\psi}_F \end{pmatrix}$$

(inertial acceleration in the F coordinate frame). The harmonics of the vibration are thus

$$\vec{\alpha}_{pN} = [(-\vec{r} \times) R_e \quad I \quad -\vec{s}_e \cdot] \{ -(\rho N)^2 \phi_{pN}^{(x)} \} \\ + [(-\vec{v} \times) R_e \quad 0 \quad 0] \{ i \rho N \phi_{pN}^{(x)} \}$$

Dividing by the dimensionless acceleration due to gravity ($g/\Omega^2 R$) gives the vibration in g's.

5.2.9 *Fatigue damage assessment.* - The fatigue damage due to the blade bending loads, torsion loads, and control loads is determined principally by the mean and 1/2 peak-to-peak values. An improved estimate of the fatigue damage can be obtained by using Miner's rule, with the method of reference 29 for counting the loading cycles.

The counting method applied to periodic loading consists of the following steps. First all the relative minima and maxima in one revolution are identified. The absolute maximum and absolute minimum give one loading cycle:

$$S_0 = \frac{1}{2} (P_{max} - P_{min}) = \frac{1}{2} \text{ peak-to-peak}$$

The absolute maximum and absolute minimum are discarded then, leaving a set of L peaks.

Consider the first group of K peaks ($K = 3$ or 4 usually, unless there is a lot of high frequency variation in the loading). The 1/2 peak-to-peak value within this subset of K peaks gives the amplitude of one loading cycle:

$$S_1 = \frac{1}{2} (P_{max} - P_{min}) = \frac{1}{2} \text{ peak-to-peak}$$

Consider the next group of K peaks, using the last peak of the previous group as the first peak of this group, to identify the loading cycle amplitude S_2 . The counting procedure continues in this fashion, taking K peaks at a time to identify loading cycles.

Each group uses $K-1$ new peaks to obtain one loading cycle, so in $K-1$ revolutions of L peaks each, L cycles will be identified. This means that each loading cycle identified occurs $1/(K-1)$ times per revolution. For periodic data, it is equivalent to consider the L groups of K peaks, starting at each of the peaks in the set over one revolution.

Then for one revolution of the rotor, there has been identified the loading cycle

$$S_0 = \frac{1}{2} \text{ peak-to-peak}$$

occurring one time per rev; and the loading cycles

$$S_\lambda, \quad \lambda = 1 \text{ to } L$$

each occurring $1/(K-1)$ times per rev.

Miner's rule for the damage fraction is

$$DF = \sum \frac{n}{N}$$

where n is the number of applied cycles at level S , and N is the allowable number of cycles at level S . The $S-N$ curve will be approximated by

$$N = \frac{C}{(S/S_E - 1)^M}$$

where S_E is the endurance limit; and C and M are constants depending on the material. Hence

$$DF = \frac{1}{CS_E^M} \sum n(S - S_E)^M$$

Using the loading cycles amplitude and frequency determined above, gives the damage fraction

$$DF = \frac{1}{CS_E^M} \left[(S_0 - S_E)^M + \frac{1}{K-1} \sum_{k=1}^L (S_k - S_E)^M \right]$$

for one revolution.

The damage fraction is required for an analysis of an actual rotor design, but for more general investigations a parameter emphasizing the applied loading would be useful. Often in fact the loading will be below the endurance limit of the specific design considered, but still an assessment of the influence of the loading waveform and amplitude on the relative fatigue damage is required. Such an assessment can be obtained by considering the damage fraction obtained from Miner's rule for small endurance limit. In that case, the damage is proportional to

$$DN = \sum n S^M = S_0^M + \frac{1}{K-1} \sum_{k=1}^L S_k^M$$

A more useful representative of the fatigue characteristic of the rotor loading is

$$S_{eq} = (DN)^{\frac{1}{M}}$$

which is the equivalent 1/2 peak-to-peak loading amplitude which would alone give the same damage number as the actual loading.

5.2.10 *Rotational noise*. - The rotational noise due to the blade aerodynamic loads and thickness will be calculated using the following equations for the far field harmonics of the sound pressure disturbance. Consider a rotor moving through the air with velocity components

$$(V_x, V_y, V_z) = (M_x, M_y, M_z) c_s$$

Using a tip-path plane coordinate frame, these velocity components are

$$V_x = (M_x - \beta_c M_z) S R$$

$$V_y = (M_y + \beta_s M_z) S R$$

$$V_z = (M_z + \beta_c M_x - \beta_s M_y) S R$$

An observer position relative to the hub, moving with the rotor, is defined by the components x_o , y_o , and z_o (positive aft, to the right, and upward); or in terms of a range s_o , an elevation angle θ_o (positive above the tip-path plane), and an azimuth angle ψ_o (defined as for the rotor azimuth):

$$x_o = s_o \cos \theta_o \cos \psi_o$$

$$y_o = s_o \cos \theta_o \sin \psi_o$$

$$z_o = s_o \sin \theta_o$$

Write the blade section forces as

$$\Delta F_z = f_{z_{\text{TPP}}} l_z(x)$$

$$\Delta F_x = f_{x_{\text{TPP}}} l_x(x)$$

$$\Delta F_r = f_{r_{\text{TPP}}} l_r(x)$$

where F_{zTPP} , F_{xTPP} , and F_{rTPP} are the section aerodynamic forces; and ℓ_z , ℓ_x , and ℓ_r are chordwise loading distribution functions. The section forces relative to the tip-path plane are obtained from the forces relative to the shaft axes as follows:

$$F_{zTPP} = F_z - \tilde{F}_r (\beta_c \cos \psi + \beta_s \sin \psi) + F_x (\beta_s \cos \psi - \beta_c \sin \psi)$$

$$F_{xTPP} = F_x - F_z (\beta_s \cos \psi - \beta_c \sin \psi)$$

$$F_{rTPP} = \tilde{F}_r + F_z (\beta_c \cos \psi + \beta_s \sin \psi)$$

This loading can be written as Fourier series:

$$F_{zTPP} = \sum_{n=-\infty}^{\infty} F_{zn}(r) e^{inSt}$$

$$F_{xTPP} = \sum_{n=-\infty}^{\infty} F_{xn}(r) e^{inSt}$$

$$F_{rTPP} = \sum_{n=-\infty}^{\infty} F_{rn}(r) e^{inSt}$$

The blade thickness distribution is written as

$$t(x) = A_{xs} a(x)$$

where A_{xs} is the section area, and $a(x)$ is a chordwise distribution function. The velocity normal to the section, $V_T = \Omega r + V_x \sin \Omega t$, can also be expanded as a Fourier series

$$V_T = 5\zeta r \sum_{n=-1}^1 V_n(r) e^{in\Omega t}$$

where $V_0 = 1$, $V_1 = (V_y - iV_x)/(2\Omega r)$, and $V_{-1} = (V_y + iV_x)/(2\Omega r)$.

The sound pressure at the observer has a periodic component, which is the rotor rotational noise:

$$P = \sum_{m=-\infty}^{\infty} P_m e^{imN\Omega t}$$

for $t = 0$ to $2\pi/N\Omega$. Then the harmonics of the far field rotational noise due to the rotor blade lift, drag, and thickness are:

$$P_m = -\frac{(mN\Omega)^2 N g}{4\pi c_s (1-M\cos\delta_r)^2} e^{-imN\Omega\tau_0/c_s} \sum_{n=-1}^1 \left[e^{-i(mN-n)(4r-\frac{\pi}{2})} \right.$$

$$\left. (1-\frac{n}{mN}) \int_0^R A_{xs} a_{mn-n} V_n J_{mn-n} dr \right]$$

$$-\frac{imN^2 \Omega^2 \sin\delta_r}{4\pi c_s^2 (1-M\cos\delta_r)^2} e^{-imN\Omega\tau_0/c_s} \sum_{n=-\infty}^{\infty} \left[e^{-i(mN-n)(4r-\frac{\pi}{2})} \right.$$

$$\left. \int_0^R d_{mn-n} F_{zn} J_{mn-n} dr \right]$$

$$+ \frac{imN^2}{4\pi c_s r_0 (1-M\cos\delta_r)} e^{-imN\Omega r_0/c_s} \sum_{n=-\infty}^{\infty} \left[e^{-i(mN-n)(4r-\frac{\pi}{2})} \right. \\ \left. (1-\frac{n}{mN}) \int_0^R l_{mN-n} \frac{f_{xn}}{r} J_{mN-n} dr \right]$$

$$- \frac{mN^2 \Omega^2 \cos\Omega r}{4\pi c_s r_0 (1-M\cos\delta_r)^2} e^{-imN\Omega r_0/c_s} \sum_{n=-\infty}^{\infty} \left[e^{-i(mN-n)(4r-\frac{\pi}{2})} \right. \\ \left. \int_0^R l_{mN-n} f_{xn} J'_{mN-n} dr \right]$$

where the argument of the Bessel function J_{mN-n} is

$$\frac{mN\Omega r}{c_s} \quad \frac{\cos\Omega r}{1-M\cos\delta_r}$$

and

$$\Omega_r = \tan^{-1} \frac{y_0 - M_y r_0}{x_0 - M_x r_0}$$

$$\vec{r}_0 = \frac{1}{\beta^2} (\vec{r}_0 - M_x x_0 + M_y y_0 + M_z z_0)$$

$$\vec{r}_0^2 = \beta^2 (x_0^2 + y_0^2 + z_0^2) + (M_x x_0 - M_y y_0 - M_z z_0)^2$$

$$\beta^2 = 1 - M_x^2 - M_y^2 - M_z^2$$

$$\frac{\cos \theta_r}{1 - M \cos \delta_r} = \frac{1}{S_0} \sqrt{(x_0 - M_x \sigma_0)^2 + (y_0 + M_y \sigma_0)^2}$$

$$\sigma_0 (1 - M \cos \delta_r)^2 = \frac{S_0^2}{\sigma_0}$$

$$\sigma_0 (1 - M \cos \delta_r) = S_0$$

$$\frac{\sin \theta_r}{\sigma_0 (1 - M \cos \delta_r)^2} = \frac{z_0 + M_z \sigma_0}{S_0^2}$$

The sound pressure harmonics can be presented in dB:

$$SPL_m = 10 \log \frac{2 |P_m|^2}{P_{ref}^2}$$

for a single sided spectrum ($P_{ref} = .00002 \text{ N/m}^2$). The overall sound pressure level is

$$OSPL = 10 \log \left(\frac{P_{rms}}{P_{ref}} \right)^2 = 10 \log \sum_{m=1}^{\infty} \frac{2 |P_m|^2}{P_{ref}^2}$$

The time history is also of interest for rotational noise.

The chordwise distribution functions for lift and thickness give

$$l_n = \int_{x_{se}}^{x_{te}} l(x) e^{-inx/c} dx$$

$$a_n = \int_{x_{se}}^{x_{te}} a(x) e^{-inx/c} dx$$

A simple and generally conservative approximation is impulsive lift and thickness, for which $l_n = a_n = 1$. Thin airfoil type loading

$$l(x) = \frac{2}{\pi c} \sqrt{\frac{1-\zeta}{1+\zeta}}$$

gives

$$l_n = e^{-in\frac{x_m}{c}} [J_0\left(\frac{nc}{2r}\right) + i J_1\left(\frac{nc}{2r}\right)]$$

where x_m is the midchord distance from the spanwise axis of the blade. For NACA 4- and 5-digit airfoil series, $A_{xs} = .685\tau c^2$ where τ is the thickness to chord ratio. For these airfoils

$$a_n = e^{-in\left(\frac{x_m}{c} - \frac{1}{2}\right)\frac{\pi}{\tau}} \int_0^1 ca e^{-in\frac{\zeta}{\tau}} d\zeta$$

where

$$ac = \frac{tc}{A_{xs}} = 14.597 \left[.2969\sqrt{\zeta} - .1260\zeta - .3516\zeta^2 + .2843\zeta^3 - .1015\zeta^4 \right]$$

A rectangular loading distribution gives

$$l_n = e^{-inx_m/c} \frac{2r}{cn} \sin \frac{cn}{2r}$$

which might be appropriate for the drag.

5.3 Steady State or Slowly Varying Aircraft Motion

The linearized equations of motion for the rotorcraft rigid body degrees of freedom are

$$\left[R_e^T I^* R_e + 2 I_{01}^* \vec{\xi}_1 \vec{g}_1^T + 2 I_{02}^* (\frac{\Omega_1}{\Omega_2})^2 \vec{\xi}_2 \vec{g}_2^T \right] \begin{pmatrix} \dot{\phi}_F \\ \dot{\theta}_F \\ \dot{\psi}_F \end{pmatrix} = \vec{Q}_{\text{moment}}^{\text{rotor } \#1} + \vec{Q}_{\text{moment}}^{\text{rotor } \#2} + \vec{Q}_{\text{moment}}^{\text{aero}}$$

$$M^* \begin{pmatrix} \dot{x}_F \\ \dot{y}_F \\ \dot{z}_F \end{pmatrix} - M^* (\vec{v}_x) R_e \begin{pmatrix} \dot{\phi}_F \\ \dot{\theta}_F \\ \dot{\psi}_F \end{pmatrix} = \vec{Q}_{\text{force}}^{\text{rotor } \#1} + \vec{Q}_{\text{force}}^{\text{rotor } \#2} + \vec{Q}_{\text{force}}^{\text{aero}} + M^* g \vec{k}_E - G \begin{pmatrix} \dot{\phi}_F \\ \dot{\theta}_F \\ \dot{\psi}_F \end{pmatrix}$$

from section 4.2.4. Here

$$\vec{g}^T = \text{first 3 elements of 6th row of } c$$

$$\vec{f} = \text{first 3 elements of 6th column of } c^T$$

with the matrices c and c^T defined in section 4.2. The terms involving I_{01}^* and I_{02}^* account for the rotational moments of inertia of the two rotors. The rotor mass is included in the aircraft gross weight and moments of inertia. Note that $M^*g = \gamma 2C_W/\sigma a$. Hence if these equations are divided by $2\gamma/a$ (rotor #1 parameters), they will be in the form of rotor coefficient to solidity ratio, with the components in the body axes (F system). When the rotor speed perturbation is included, the equations of motion become

$$\begin{bmatrix} \dot{\phi}_F \\ \dot{\alpha}_F \\ \dot{\psi}_F \\ \dot{x}_F \\ \dot{y}_F \\ \dot{z}_F \\ \dot{\psi}_S \end{bmatrix} = \begin{bmatrix} \vec{Q}_{\text{moment}}^{\text{rotor } \#1} + \vec{Q}_{\text{moment}}^{\text{rotor } \#2} + \vec{Q}_{\text{moment}}^{\text{aero}} \\ \vec{Q}_{\text{force}}^{\text{rotor } \#1} + \vec{Q}_{\text{force}}^{\text{rotor } \#2} + \vec{Q}_{\text{force}}^{\text{aero}} \\ -(\delta \frac{C_Q}{\sigma_a})_1 - \frac{(N I_b S^3)_2}{(N I_b S^3)_1} (\delta \frac{C_Q}{\sigma_a})_2 \end{bmatrix}$$

$$+ \begin{bmatrix} 0 \\ M^* (\vec{v}_x) \vec{k}_e \begin{pmatrix} \dot{\phi}_F \\ \dot{\alpha}_F \\ \dot{\psi}_F \end{pmatrix} + M^* g \vec{k}_e - G \begin{pmatrix} \dot{\phi}_F \\ \dot{\alpha}_F \\ \dot{\psi}_F \end{pmatrix} \\ - r_E^2 Q_{\Sigma}^* \dot{\psi}_S + r_E Q_t^* \theta_t + (\delta \frac{C_{P_E}}{\sigma_a})_{\text{trim}} \end{bmatrix}$$

(see section 4.3.2). The inertia matrix is as follows:

$$\begin{bmatrix} R_e^T I^* R_e & 0 & 2 I_{\alpha_1}^* \vec{j}_1 \\ + 2 I_{\alpha_1}^* \vec{j}_1 \vec{j}_1^T & 0 & + 2 I_{\alpha_2}^* \frac{S_{\alpha_1}}{S_{\alpha_2}} \vec{j}_2 \\ + 2 I_{\alpha_2}^* \left(\frac{S_{\alpha_1}}{S_{\alpha_2}}\right)^2 \vec{j}_2 \vec{j}_2^T & M^* & 0 \\ 0 & 0 & H^* \\ I_{\alpha_1}^* \vec{j}_1^T & 0 & H^* \\ + \frac{(N I_b S^3)_2}{(N I_b S^3)_1} I_{\alpha_2}^* \vec{j}_2^T & & \end{bmatrix}$$

where I_R^* includes the rotational moments of inertia of the two rotors:

$$\begin{aligned} I_R^* &= \frac{1}{N^2} I_E \left(C_E^2 I_E + I_{\omega_1} + \left(\frac{I_{\omega_1}}{C_E}\right)^2 I_{\omega_2} \right) \\ &= C_E^2 I_E^* + I_{\omega_1}^* + \frac{(NI_b \Omega^2)_2}{(NI_b \Omega^2)_1} I_{\omega_2}^* \end{aligned}$$

The solution for the generalized forces due to the airframe aerodynamics is described in section 4.2.6. The solution for the generalized forces due to the two rotors is described in section 4.2.5.

In the trim analysis, these equations are solved for the case of steady state flight. The controls are adjusted until the desired operating condition is achieved.

In the transient analysis, these equations are numerically integrated in time. A non-equilibrium flight path is produced by a prescribed control or gust input.

In the flight dynamics analysis, the stability derivatives in a linear expansion of the rotor and airframe aerodynamic generalized forces are obtained by prescribed perturbations of the body motion and controls.

5.3.1 Trim analysis. - The helicopter trim calculation determines the control positions and aircraft orientation for the specified flight condition. For steady state flight the perturbation rigid body motion is zero, so the net force and moment on the aircraft must be zero. Thus the rigid body equations of motion give six equations to be solved for the six trim variables, consisting of the four pilot's controls (δ_o , δ_c , δ_s , and δ_p) and the two trim Euler angles (θ_{FT} and ϕ_{FT}). The controls are adjusted until equilibrium flight is achieved for the specified flight condition. For level flight ($\theta_{FP} = 0$) or a specified climb velocity, it is assumed that the engine can supply whatever power is required to maintain the rotor rotational speed. Alternatively, the aircraft power available can be specified (such as for power-off descent). Then there is an additional trim variable (the flight path angle θ_{FP}) and an additional equation to be solved (the power required equals the power available).

The helicopter can also be trimmed in a steady turn by prescribing the turn rate $\dot{\psi}_F$. A coordinated turn is obtained if zero sideslip ($\psi_{FP} = 0$) is specified. In forward flight the resultant bank angle should be

$$\tan \phi_{FT} = \sqrt{n^2 - 1} = \dot{\psi}_F V / g$$

where n is the normal load factor.

Hence the trim analysis solves the equations of motion for a specified steady flight speed and rotor speed (and possibly a specified turn rate). Setting the perturbation rigid body motion and rotational speed to zero gives the following equations:

$$\begin{aligned} \frac{\alpha}{2\sigma} \left(\vec{Q}_{\text{moment}}_{\text{rotor } \#1} + \vec{Q}_{\text{moment}}_{\text{rotor } \#2} + \vec{Q}_{\text{moment}}_{\text{aero}} \right) &= 0 \\ \frac{C_w}{\sigma} \vec{k}_E + \frac{1}{g} \frac{C_w}{\sigma} (\vec{V} \times) R \vec{k}_F \dot{\psi}_F \\ + \frac{\alpha}{2\gamma} \left(\vec{Q}_{\text{force}}_{\text{rotor } \#1} + \vec{Q}_{\text{force}}_{\text{rotor } \#2} + \vec{Q}_{\text{force}}_{\text{aero}} \right) &= 0 \\ \left(\frac{C_Q}{\sigma} \right)_{\text{rotor } \#1} + \frac{(\gamma N I_b \Delta \ell^3)_2}{(\gamma N I_b \Delta \ell^3)_1} \left(\frac{C_Q}{\sigma} \right)_{\text{rotor } \#2} &= \left(\frac{C_P}{\sigma} \right)_{\substack{\text{rotor power} \\ \text{available}}} \end{aligned}$$

The contributions to the force and moment are from the hub reactions of the two rotors, the airframe aerodynamics, the acceleration due to the turn rate, and the aircraft weight.

The pilot's controls are collective stick δ_o , lateral cyclic stick δ_c , longitudinal cyclic stick δ_s , pedal δ_p , and throttle δ_t . The controls of the two rotors and aircraft are related to the pilot's controls by

$$\vec{v} = T_{CFE} \vec{v}_p + \vec{v}_o$$

where \vec{v}_o is the control input with all sticks centered (see section 4.1.6). The throttle control variables (δ_t and θ_t) are not used for the trim analysis.

For some rotorcraft configurations the pilot's collective stick (δ_o) does not control the rotor collective pitch, rotor trim being handled by a rotor speed governor using collective pitch feedback. In such a case the static component of the blade pitch governor, $(\Delta\theta_{govr})_{static}$ for either or both rotors, can be used as the trim variable in place of δ_o . Hence $\Delta\theta_{govr}$ is added to the rotor collective pitch θ_{75} obtained from \vec{v}_p and \vec{v}_o .

The table below summarizes the options considered for the trim analysis. For each case there are a number of trim variables, which are adjusted to achieve the target values of an equal number of trimmed quantities. In the free flight cases, the helicopter is trimmed to force and moment equilibrium. In the wind tunnel cases rotor #1 is trimmed to a prescribed operating condition. The trim option and the degrees of freedom representing the aircraft can be specified independently; hence it is possible to use a free flight trim option with an analysis of a helicopter in a wind tunnel. The options called wind tunnel cases are however more typical of wind tunnel test configurations, particularly with only one rotor rather than the complete aircraft. The trim variables consist of the four pilot's controls, aircraft orientation parameters, and wind tunnel orientation parameters. The aircraft orientation parameters consist of the trim Euler angles, flight path angles, and turn rate; they are used only for the free flight cases. The wind tunnel orientation parameters consist of the test module yaw and pitch angles.

The free flight cases include the following options. In the level flight case the pilots controls and the aircraft Euler angles are used to trim the six components of the net force and moment on the aircraft to zero. In the climb or descent case, the flight path angle is used in addition to trim the power required to a specified value. (In vertical flight $\theta_{FP} = \pm 90^\circ$ however, so the parameter which would have to be varied to achieve the specified power

Helicopter Trim Options

	trim variables									
	δ_o	δ_c	δ_s	δ_p	α_{FT}	ϕ_{FT}	ψ_{FP}	$\dot{\psi}_F$	ψ_T	δ_T
Free Flight Cases										
No trim										
\vec{F}, \vec{M}	T	T	T	T	T	T			Z	Z
\vec{F}, \vec{M}	T	T	T	T	T		T			
$\vec{F}, \vec{M}, C_P/\sigma$	T	T	T	T	T	T		T		
$\vec{F}, \vec{M}, C_P/\sigma$	T	T	T	T	T		T	T		
F_x, F_z, M_y	T		T		T					
$F_x, F_z, M_y, C_P/\sigma$	T		T		T			T		
Wind Tunnel Cases										
No trim										
C_T/σ	T				Z	Z	Z	Z	Z	
C_T/σ										T
C_P/σ	T									
β_c, β_s			T	T						
$C_T/\sigma, \beta_c, \beta_s$	T	T	T							
$C_L/\sigma, C_X/\sigma, C_Y/\sigma$	T	T	T							
$C_L/\sigma, C_X/\sigma, C_Y/\sigma$	T	T								T
$C_L/\sigma, C_X/\sigma, \beta_c, \beta_s$	T	T	T							T
β_c				T						
$C_T/\sigma, \beta_c$	T		T							
$C_L/\sigma, C_X/\sigma$	T		T							
$C_L/\sigma, C_X/\sigma$	T									T
$C_L/\sigma, C_X/\sigma, \beta_c$	T		T							T

T = trim variable

Z = zero

aircraft velocity and rotor
rotational speed fixed

requirements is the helicopter vertical speed.) Optionally the sideslip angle ψ_{FP} can replace the roll angle ϕ_{FT} as a trim variable. A useful alternative is to trim the longitudinal variables only. The net vertical and horizontal forces and pitch moment are trimmed to zero using collective and longitudinal cyclic stick controls and aircraft pitch attitude. This longitudinal trim is exact for the case of a laterally symmetric aircraft in a symmetric flight condition. It is also a useful approximation which may converge better than a full six degree of freedom trim analysis; and when neglecting the tail rotor in the analysis.

The wind tunnel cases include the following options. The rotor thrust or power can be trimmed with collective pitch. The rotor tip-path plane tilt can be trimmed with lateral and longitudinal cyclic pitch. The tip-path plane is defined as the first harmonics of the tip deflection z_{tip} :

$$z_{tip} = \beta_0 + \sum_i \gamma_i \vec{t}_B \cdot \vec{\eta}_i (1)$$

The rotor lift and drag (in wind axes) and the side force can be trimmed using collective and cyclic control. Either the drag coefficient to solidity ratio C_X/σ can be specified, or the equivalent drag area X/q (so $C_X/\sigma = (X/q)^{1/2} (V/\Omega R)^2 / A_b$). As an alternative, the shaft angle of attack can be used in place of longitudinal cyclic or collective pitch as a control variable. It is also possible to trim only the longitudinal variables.

The trim iteration can also be omitted. In this case the helicopter or rotor performance is evaluated for a specified control setting.

In the free flight cases, the criterion for convergence of the trim iteration is that the net force and moment be less than a certain tolerance level as specified by the parameter ϵ :

$$\frac{[(C_{F_x}/\sigma)^2 + (C_{F_y}/\sigma)^2 + (C_{F_z}/\sigma)^2]^{1/2}}{C_w/\sigma} < \epsilon$$

$$\frac{[(C_{Mx}/\sigma)^2 + (C_{My}/\sigma)^2 + (C_{Mz}/\sigma)^2]^{\frac{1}{2}}}{.05 C_w/\sigma} < \epsilon$$

and

$$\frac{|C_p/\sigma - (C_p/\sigma)_{target}|}{\max((C_p/\sigma)_{target}, .001)} < \epsilon$$

when the power is trimmed as well. For the wind tunnel cases, the following criterion is used:

$$\frac{|f - f_{target}|}{\max(|f_{target}|, f_{min})} < \epsilon$$

where $f = C_T/\sigma, C_p/\sigma, C_L/\sigma, C_X/\sigma$, or C_Y/σ as appropriate (with $f_{min} = .01, .001, .01, .001$, or $.001$ respectively). The criterion for the flapping is

$$|\beta_c - (\beta_c)_{target}| < \epsilon$$

$$|\beta_s - (\beta_s)_{target}| < \epsilon$$

(with β_c and β_s in radians).

The trim problem is to find the values of the control variables (\vec{v}) such that the target values of certain trim quantities (\vec{M}) are achieved. The complex, nonlinear equations involved require an iterative solution procedure. A first order expansion of $\vec{M}(\vec{v})$ gives

$$\vec{M}_{target} = \vec{M}_{n+1} \cong \vec{M}_n + \frac{\partial \vec{M}}{\partial v} (\vec{v}_{n+1} - \vec{v}_n)$$

or

$$\vec{v}_{n+1} = \vec{v}_n + D^{-1} (\vec{M}_{\text{target}} - \vec{M}_n) F$$

The partial derivative matrix required is

$$D = \frac{\partial M}{\partial v} = \left[\cdots \frac{\partial \vec{M}}{\partial v_i} \cdots \right] = \left[\cdots \frac{\vec{M}(v_i) - \vec{M}(v_i - \Delta v_i)}{\Delta v_i} \cdots \right]$$

The factor $F \leq 1$ is included to avoid overshoot oscillations in the trim iteration by reducing the step size.

The matrix D^{-1} is constructed as follows. First \vec{M}_{old} is calculated using the initial values of \vec{v} . Then each control v_i is decreased by the increment Δv_i , and \vec{M}_{new} is calculated; then the i-th column of D is given by

$$(\vec{M}_{\text{new}} - \vec{M}_{\text{old}}) / \Delta v_i$$

and the control is restored to its initial value. Finally the matrix D is inverted, and all elements multiplied by the factor F . The partial derivative matrix can be recalculated occasionally as the iteration proceeds, to improve the convergence. Generally a step size of about $\Delta = 1$ degree is satisfactory for all control variables.

5.3.2 Transient analysis. - The helicopter transient analysis involves numerically integrating the equations of motion for the rigid body and rotor speed degrees of freedom. A non-equilibrium flight path is produced by a prescribed control or gust input as a function of time. The assumptions of this analysis are that the aircraft motion is slow compared to the rotor speed, and that the perturbed rigid body motion is small. The assumption of

quasistatic body motion allows the periodic rotor motion solution to be used with the transient analysis. The small motion assumption arises because it was assumed that the perturbation rotor hub motion is small; it is consistent therefore to integrate the linearized equations for the rigid body motion.

The degrees of freedom considered are the six linear and angular rigid body motions (x_F , y_F , z_F , ϕ_F , θ_F , ψ_F) and the rotor speed perturbation ($\dot{\psi}_s$). The input parameters are the aircraft controls (δ_o , δ_c , δ_s , δ_p , δ_t) and aerodynamic gusts. Optionally any of these degrees of freedom can be held constant. The transient analysis with all seven degrees of freedom fixed produces the rotor response to control and gust inputs. The equations to be integrated are:

$$\bar{J} \begin{pmatrix} \dot{\phi}_F \\ \dot{\theta}_F \\ \dot{\psi}_F \\ \dot{x}_F \\ \dot{y}_F \\ \dot{z}_F \\ \dot{\psi}_s \end{pmatrix} = \begin{pmatrix} \vec{\Delta Q}_{\text{moment}} \\ \vec{\Delta Q}_{\text{force}} \\ -\Delta \left(\delta \frac{C_Q}{\sigma a} \right)_1 - \frac{(N I_b S^3)}{(N I_b S^3)}_1 \Delta \left(\delta \frac{C_Q}{\sigma a} \right)_2 \\ + \begin{pmatrix} 0 \\ M^*(\vec{V}_x) R e \begin{pmatrix} \dot{\phi}_F \\ \dot{\theta}_F \\ \dot{\psi}_F \end{pmatrix} - G \begin{pmatrix} \dot{\phi}_F \\ \dot{\theta}_F \\ \dot{\psi}_F \end{pmatrix} \\ - \tilde{r}_E^2 Q_{SL}^* \dot{\psi}_s + \tilde{r}_E Q_E^* \theta_T \end{pmatrix} \end{pmatrix}$$

where $\vec{\Delta Q}$ is the rotor and aerodynamic generalized force, less the trim value; and ΔC_Q is the rotor torque, less the trim value. The initial conditions are zero (except for $\dot{\psi}_F$ when the helicopter is trimmed in a steady turn).

The transient rotor speed perturbations will produce throttle and rotor collective pitch increments due to the governor:

$$\Delta\theta_t = -k_{P_e}\dot{\psi}_s - k_{I_e}\psi_s$$

and

$$(\Delta\theta_{gover})_{\text{static}} = (\Delta\theta_{gover})_{\text{trim}} + k_P\dot{\psi}_s + k_I\psi_s$$

for rotor #1 and rotor #2. The rotor azimuth perturbation ψ_s will also produce cyclic pitch increments due to the trim swash-plate tilt:

$$\begin{pmatrix} \Delta\theta_{1c} \\ \Delta\theta_{2c} \end{pmatrix} = \psi_s \begin{pmatrix} \theta_{1s} \\ -\theta_{2s} \end{pmatrix}_{\text{trim}}$$

For rotor #2 these cyclic pitch increments must be multiplied by Ω_2/Ω_1 . An autopilot is also included, since the transient rigid body motions can be divergent in some flight conditions:

$$\Delta\delta_s = k_s (\tau_s \dot{\theta}_F + \theta_F)$$

$$\Delta\delta_c = -k_c (\tau_c \dot{\phi}_F + \phi_F)$$

Hence the pilot's control positions consist of the trim setting, the transient term, and the autopilot term; and the individual control positions are obtained from

$$\vec{v} = T_{CFE} (\vec{v}_{P_{\text{trim}}} + \vec{v}_{P_{\text{transient}}} + \vec{v}_{P_{\text{autopilot}}}) + \vec{v}_o$$

with the governor contributions added to the elements of \vec{v} as required.

The transient calculation begins with the trim solution, at time $t = 0$. The pilot's controls or gust input are specified as a function of t . The equations of motion above are in the form

$$\ddot{y} = f(t, y, \dot{y})$$

A fourth order Runge-Kutta method will be used to numerically integrate these equations from time t_n to time $t_{n+1} = t_n + h$:

$$k_1 = f(t_n, y_n, \dot{y}_n)$$

$$k_2 = f\left(t_n + \frac{h}{2}, y_n + \frac{h}{2}\dot{y}_n + \frac{h^2}{8}k_1, \dot{y}_n + \frac{h}{2}k_1\right)$$

$$k_3 = f\left(t_n + \frac{h}{2}, y_n + \frac{h}{2}\dot{y}_n + \frac{h^2}{8}k_1, \dot{y}_n + \frac{h}{2}k_2\right)$$

$$k_4 = f(t_n + h, y_n + h\dot{y}_n + \frac{h^2}{2}k_3, \dot{y}_n + h k_3)$$

$$y_{n+1} = y_n + h\dot{y}_n + \frac{h^2}{6}(k_1 + 2k_2 + 2k_3) + O(h^5)$$

$$\dot{y}_{n+1} = \dot{y}_n + \frac{h}{6}(k_1 + 2k_2 + 2k_3 + k_4)$$

Note that it is necessary to solve for the periodic rotor motion four times per integration step.

5.3.3 Flight dynamics analysis. - The flight dynamics analysis here consists of a calculation of the helicopter stability derivatives and an analysis of the resulting linear differential equations. As for the transient analysis it is assumed that the body motion will be slow (compared to the rotor rotational speed), so the quasistatic rotor solution can be used. The assumption that the perturbation body motion has small magnitude is here consistent with the stability derivative representation of the rotor.

The equations of motion are the same as considered for the transient analysis (section 5.3.2). Here the rotor hub forces and the aircraft aerodynamic forces are expanded in terms of the stability derivatives. By making successive perturbations to the inputs for the rotor and aircraft analysis, the generalized forces can be expanded as follows:

$$\vec{\Delta Q} = a_2 \ddot{z}_F + a_1 \begin{pmatrix} \dot{\phi}_F \\ \dot{\theta}_F \\ \dot{\psi}_F \\ \dot{x}_F \\ \dot{y}_F \\ \dot{z}_F \\ \dot{\psi}_S \end{pmatrix} + b_1 \begin{pmatrix} \overset{\text{con}}{\theta}_{\text{rotor \#1}} \\ \overset{\text{con}}{\theta}_{\text{rotor \#2}} \\ \delta_g \\ \delta_e \\ \delta_a \\ \delta_r \end{pmatrix} + b_G \begin{pmatrix} u_G \\ v_G \\ w_G \end{pmatrix}$$

The coefficients of the matrices are the aircraft stability derivatives. There are contributions from each rotor, and from the wing/body, horizontal tail, and vertical tail. The airframe terms include the effects of the rotor-induced interference velocities. The result for ΔC_Q is similar (rotor contributions only). The gust velocity here is uniform throughout space.

The rotor speed governor, defined by the following control laws

$$\begin{aligned} \Delta \theta_t &= -k_{P_e} \dot{\psi}_S - k_{I_e} \psi_S \\ (\Delta \theta_{gover})_1 &= k_{P_1} \dot{\psi}_S + k_{I_1} \psi_S \\ (\Delta \theta_{gover})_2 &= k_{P_2} \dot{\psi}_S + k_{I_2} \psi_S \end{aligned}$$

will be directly included in the stability derivatives. It is also necessary to account for the cyclic pitch perturbations due to the rotor azimuth perturbation:

$$\begin{pmatrix} \Delta\theta_{1c} \\ \Delta\theta_{1s} \end{pmatrix} = \Psi_s \begin{pmatrix} \theta_{1s} \\ -\theta_c \end{pmatrix}_{\text{trim}}$$

For rotor #2 these cyclic pitch increments must be multiplied by Ω_2/Ω_1 .

The result is a set of linear differential equations of the form

$$A_2 \ddot{x} + A_1 \dot{x} + A_0 x = Bv + B_p v_p + B_G g$$

describing the flight dynamics of the aircraft. The state vector x consists of the rigid body and rotor speed degrees of freedom:

$$x = [\phi_f \ \theta_f \ \psi_f \ x_f \ y_f \ z_f \ \psi_s]^T$$

The control and gust vectors are defined as follows

$$\begin{aligned} v &= [(\bar{\theta}_0 \ \bar{\theta}_{1c} \ \bar{\theta}_{1s})_{\text{rotor } \#1} \ (\bar{\theta}_0 \ \bar{\theta}_{1c} \ \bar{\theta}_{1s})_{\text{rotor } \#2} \ \delta_f \ \delta_e \ \delta_a \ \delta_r \ \bar{\theta}_c]^T \\ &= T_{CFE} v_p \end{aligned}$$

$$v_p = [\delta_a \ \delta_c \ \delta_s \ \delta_p \ \delta_t]^T$$

$$g = [u_g \ v_g \ w_g]^T$$

(the gust components are in wind axes). Optionally any of the degrees of freedom can be omitted from the analysis. Using these equations the helicopter flying qualities can be examined, in terms of the eigenvalues and eigenvectors. The transfer function (pole-zero set or frequency response) or the transient response to a prescribed control or gust input can also be obtained. The transient response can be calculated by numerically integrating the equations

$$\ddot{x} = -A_z^{-1} A_1 \dot{x} - A_z^{-1} A_2 x + A_z^{-1} B_p v_p + A_z^{-1} B_G g$$

in a manner similar to the transient analysis (see section 5.3.2). In this case only a gust that is uniform throughout space can be considered.

The stability derivatives are obtained in body axes (the F system) relative to the aircraft center of gravity. There are contributions from each of the rotors, and the aircraft aerodynamic components (wing/body, horizontal tail, and vertical tail). The following notation is used for the stability derivatives.

<u>Equation</u>	<u>Notation</u>	<u>Variable</u>	<u>Subscript</u>
roll moment	$I_x^* L$	$\dot{\phi}_F$	p
pitch moment	$I_y^* M$	$\dot{\theta}_F$	q
yaw moment	$I_z^* N$	$\dot{\psi}_F$	r
longitudinal force	$M^* X$	\dot{x}_F	u
lateral force	$M^* Y$	\dot{y}_F	v
vertical force	$M^* Z$	\dot{z}_F	w
torque	$I_R^* Q$	$\dot{\psi}_s$	Ω

The aircraft inertias are introduced so that the coefficient of the highest time derivative in an equation is unity. The derivatives are defined with positive signs on the right-hand side of the equation of motion.

Application of this procedure to the wind tunnel case will give the wind or shaft axis derivatives of a single rotor alone.

5.3.4 *Transient gust and control*.— Transient gust and control inputs are required when the equations of motion are integrated for the transient or flight dynamics analysis. The pilot's control increment $\Delta \vec{v}_p$ is required at time t . A simple form is

$$\Delta \vec{v}_p = \vec{v}_{p_0} C(t)$$

where \vec{v}_{p_0} is a constant vector and C is a scalar function of time. More generally, the control input can be a function of the aircraft motion as well.

The gust velocity $\vec{g} = (u_g \ v_g \ w_g)^T$ (in wind axes) is required at the time t , at the location of both rotors and the airframe aerodynamic components. Consider a convected gust field, defined by a function $G(x_g, y_g, z_g)$. The gust coordinates have origin at the center of gravity when $t = 0$. The aircraft velocity is v_a , in the x (wind axis) direction. The gust field has velocity v_g in the negative x_g direction; the gust is coming from azimuth angle ψ_g relative to the aircraft (see fig. 28). Hence given the position r (in wind axes), the location in the gust field is

$$\begin{pmatrix} x_g \\ y_g \\ z_g \end{pmatrix} = \begin{pmatrix} -x \cos \psi_g + y \sin \psi_g + (v_g - v_a \cos \psi_g)t \\ -x \sin \psi_g - y \cos \psi_g - (v_a \sin \psi_g)t \\ z \end{pmatrix}$$

The position vector for the wind/body is

$$\vec{r} = R_{FV}^T \vec{r}_{WB}$$

with \vec{r}_{WB} in the F frame, relative to the aircraft center of gravity; the position vectors for the horizontal tail, vertical tail, and rotor hub are obtained in a similar manner. The positions on the rotor disk are

$$\vec{r} = \vec{R}_{FV}^T (\vec{r}_{hub} + \vec{R}_{SF}^T (r \cos \psi \vec{\tau}_s + r \sin \psi \vec{\delta}_s))$$

(neglecting the tilt of the tip-path plane relative to the hub; the sign of the $\vec{\delta}_s$ component is changed for a clockwise rotating rotor). A one-dimensional convected gust field is defined by

$$\vec{g} = \vec{g}_0 G(x_g)$$

Note that the gust is convected at the rate V_g relative to the aircraft if V_a is not used, and at a rate V_g relative to the fixed frame if V_a is used. With $V_g = 0$ the gust field is stationary (relative to the aircraft or the earth if V_a is not or is used).

Alternatively, a uniform gust field can be used, which is a function of time only. A simple form is

$$\vec{g} = \vec{g}_0 G(t)$$

where \vec{g}_0 is a constant vector and G is a scalar function of time.

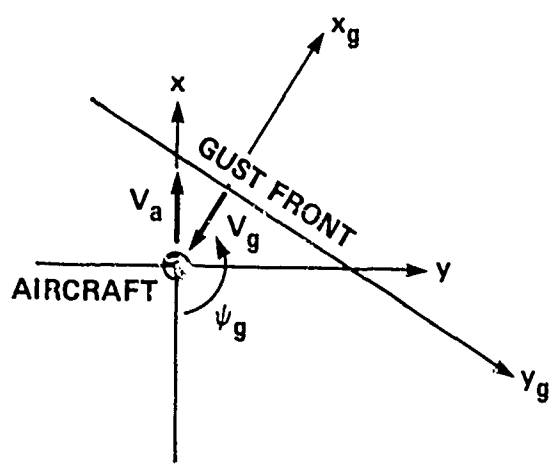


Figure 28. Convected gust description.

5.3.5 Calculation procedure.-- The solution for the rotorcraft aerodynamics and dynamics proceeds as follows. The job begins with data input and initial calculations. Next the trim solution is obtained. Then the aeroelastic stability analysis, flight dynamics analysis, or transient analysis is performed as required. An old job can be restarted in any of these four tasks (trim, flutter, flight dynamics, or transient).

In the trim analysis the controls are iterated until the required operating state is achieved. Since the nonuniform inflow influence coefficients depend on the rotor thrust (through the wake geometry) it is necessary to iterate between the influence coefficient calculation and the trimmed motion and forces calculation (unless the rotor thrust is specified as part of the definition of the required operating state). The trim analysis is performed first for uniform inflow, then for nonuniform inflow with a prescribed wake, and finally for nonuniform inflow with a free wake geometry. After obtaining the trim solution, the aircraft performance and loads can be calculated (this is the trim restart entry point for an old job).

In the transient analysis, the rigid body equations of motion are numerically integrated. At each time step there is an iteration between the non-uniform inflow influence coefficient calculation, and the calculation of the rotor and airframe motion and forces.

In the flight dynamics analysis, the stability derivatives are calculated and the matrices are constructed that describe the linear differential equations of motion. At each motion or control increment in the stability derivative calculation there is an iteration between the influence coefficient calculation and the calculation of the motion and forces. Finally the system of linear differential equations is analyzed (optionally including a numerical integration as for the transient analysis).

In the flutter analysis the matrices are constructed that describe the linear differential equations of motion, and the constant coefficient or periodic coefficient equations are analyzed. Optionally the equations are reduced to just the aircraft rigid body degrees of freedom by assuming quasi-static response of the other degrees of freedom, and the equations are analyzed as for the flight dynamics task.

6. AEROELASTIC STABILITY

The objective of the aeroelastic analysis is to derive a set of linear differential equations describing the perturbed motion of the helicopter from the trim flight condition. The stability of the system is defined by the eigenvalues of these equations.

6.1 Rotor Model

The differential equations of motion for the rotor blade have been derived in section 2.2.18. Here it is necessary to linearize the inertial and aerodynamic forces in these equations.

6.1.1 *Rotor degrees of freedom.* - The rotor blade motion is described by coupled flap/lag bending, rigid pitch and elastic torsion, and optionally the gimbal pitch and roll motion (or teeter motion for the two-bladed rotor case). The blade degrees of freedom are written as the sum of trim terms and perturbation terms. The trim solution is described in section 5.1; the perturbation motions are the degrees of freedom for the aeroelastic analysis. In particular, the generalized coordinate of the i -th blade bending mode is written

$$q_i = q_{i\text{trim}} + \delta q_i$$

or for the bending deflection

$$(\vec{z}_0 - \vec{x}_0) = (\vec{z}_0 - \vec{x}_0)_{\text{trim}} + \sum_{i=1}^{\infty} \delta f_i \vec{v}_i$$

After substituting for q_i , the delta notation indicating the perturbed motion can be omitted.

The rotor equations of motion have been obtained in the rotating frame, with degrees of freedom describing the motion of each blade separately. In fact, however, the rotor responds as a whole to excitation from the nonrotating frame -- shaft motion, aerodynamic gusts, or control inputs. It is desirable to work with degrees of freedom that reflect this behavior. Such a

representation of the rotor motion simplifies both the analysis and the understanding of the behavior.

The appropriate transformation to obtain the degrees of freedom and equations of motion in the nonrotating frame is of the Fourier type. There are many similarities between this coordinate change and Fourier series, discrete Fourier transforms, and Fourier interpolation; the common factor is the periodic nature of the system. A Fourier series representation of the blade motion is appropriate for dealing with the steady-state solution (section 5.1.1). Here we are considering the general dynamic behavior, including transient motions; hence the Fourier coordinate transformation is required. This coordinate transformation has been widely used in the classical literature, although often with only a heuristic basis. For example, it has been used in ground resonance analyses to represent the rotor lag motion (ref. 30) and in helicopter stability and control analyses for the rotor flap motion (ref. 31). More recently, there have been applications of the Fourier coordinate transformation with a sounder mathematical basis (e.g., ref. 32).

Consider a rotor with N blades equally spaced around the azimuth, at $\psi_m = \psi + m\Delta\psi$ (where $\Delta\psi = 2\pi/N$ and the blade index m ranges from 1 to N). Hence $\psi = At$ is the dimensionless time variable. Let $q^{(m)}$ be the degree of freedom in the rotating frame for the m -th blade, $m = 1$ to N . The Fourier coordinate transformation is a linear transform of the degrees of freedom from the rotating to the nonrotating frame. Thus the following new degrees of freedom are introduced:

$$\beta_0 = \frac{1}{N} \sum_{m=1}^N q^{(m)}$$

$$\beta_{nc} = \frac{1}{N} \sum_{m=1}^N q^{(m)} \cos m\psi_m$$

$$\beta_{ns} = \frac{1}{N} \sum_{m=1}^N q^{(m)} \sin m\psi_m$$

$$\beta_{N/2} = \frac{1}{N} \sum_{m=1}^N q^{(m)} (-1)^m$$

Here β_o is a collective mode, β_{1C} and β_{1S} are cyclic modes, and $\beta_{N/2}$ is the reactionless mode. For example, for the rotor flap motion, β_o is the coning degree of freedom, while β_{1C} and β_{1S} are the tip-path plane tilt degrees of freedom. The inverse transformation is

$$q^{(m)} = \beta_o + \sum_n (\beta_{nc} \cos n\psi_m + \beta_{ns} \sin n\psi_m) + \beta_{N/2} (-1)^m$$

which gives the motion of the individual blades again. The summation over n goes from 1 to $(N-1)/2$ for N odd and from 1 to $(N-2)/2$ for N even.

The $\beta_{N/2}$ degree of freedom appears in the transformation only if N is even. The corresponding transformation for the velocity and acceleration are

$$\dot{q}^{(m)} = \dot{\beta}_o + \sum_n [(\dot{\beta}_{nc} + n\beta_{ns}) \cos n\psi_m + (\dot{\beta}_{ns} - n\beta_{nc}) \sin n\psi_m] + \dot{\beta}_{N/2} (-1)^m$$

$$\ddot{q}^{(m)} = \ddot{\beta}_o + \sum_n [(\ddot{\beta}_{nc} + 2n\dot{\beta}_{ns} - \beta_{nc}) \cos n\psi_m + (\ddot{\beta}_{ns} - 2n\dot{\beta}_{nc} - \beta_{ns}) \sin n\psi_m] + \ddot{\beta}_{N/2} (-1)^m$$

Note that transformation to the nonrotating frame introduces Coriolis and centrifugal terms.

The variables β_o , β_{nc} , β_{ns} , and $\beta_{N/2}$ are degrees of freedom, that is, functions of time, just as the variables $q^{(m)}$ are. These degrees of freedom describe the rotor motion as a whole, in the nonrotating frame, while $q^{(m)}$ describes the motion of an individual blade in the rotating frame. Thus we have a linear, reversible transformation between the N degrees of freedom $q^{(m)}$ in the rotating frame ($m = 1, \dots, N$) and the N degrees of freedom $(\beta_o, \beta_{nc}, \beta_{ns}, \beta_{N/2})$ in the nonrotating frame. Compare this

coordinate transformation with a Fourier series representation of the steady-state solution. In that case, $q^{(m)}$ is a periodic function of ψ_m , so the motions of all the blades are identical. It follows that the motion in the rotating frame may be represented by a Fourier series, the coefficients of which are steady in time but infinite in number. Thus there are similarities between the Fourier coordinate transformation and the Fourier series, but they are by no means identical.

This coordinate transform must be accompanied by a conversion of the equations of motion for $q^{(m)}$ from the rotating to the nonrotating frame. This conversion is accomplished by operating on the equations of motion with the following summation operations:

$$\frac{1}{N} \sum_m (\dots) \quad \frac{2}{N} \sum_m (\dots) \cos \psi_m \quad \frac{2}{N} \sum_m (\dots) \sin \psi_m \quad \frac{1}{N} \sum_m (\dots) (-1)^m$$

The result is equations for the β_o , β_{nc} , β_{ns} , and $\beta_{N/2}$ degrees of freedom, respectively. Note that these are the same operations as are involved in transforming the degrees of freedom from the rotating to the nonrotating frame. Since the operators are linear, constants may be factored out. Thus with constant coefficients in the equations of motion, the operators act only on the degrees of freedom. By making use of the definition of the degrees of freedom in the nonrotating frame, and the corresponding results for the time derivatives, the conversion of the equations of motion is then straightforward. Complexities arise when it is necessary to consider periodic coefficients, such as due to the aerodynamics of the rotor in nonaxial flow.

The total force and moment on the hub have been obtained by summing the contributions from the individual blades. The result is operators exactly of the form above, for obtaining the total hub reaction in the nonrotating frame from the root reaction of the individual blades in the rotating frame. The origin of the summation operation is clear, and the $\sin \psi_m$ or $\cos \psi_m$ factors arise when the rotating forces are resolved into the nonrotating frame. In fact, the equation conversion operators in general may be viewed as simply resolving the moments on the individual blades into the nonrotating frame.

The Fourier coordinate transformation is often associated in rotor dynamics with the generalized Floquet analysis. The latter is a stability analysis for linear differential equations with periodic coefficients. Indeed, there is a fundamental link between these topics because both are associated with the rotation of the system. They are, however, truly separate subjects -- either can be required in the rotor analysis without the other. For example, a rotor in axial flow on a flexible support (or with some other relation to the nonrotating frame) requires the Fourier coordinate transformation to represent the blade motion, but is then a constant coefficient system. Alternatively, for the shaft-fixed dynamics of a rotor in forward flight, a single-blade representation in the rotating frame is appropriate, but there are periodic coefficients due to the forward flight aerodynamics which require the Floquet analysis to determine the system stability.

For the present investigation, the degrees of freedom to be transformed to the nonrotating frame are blade bending, blade pitch, and gimbal motion. The nomenclature for the corresponding degrees of freedom in the rotating and nonrotating frames are as follows:

	<u>rotating</u>	<u>nonrotating</u>			
bending	$\tilde{q}_i^{(m)}$	$\beta_i^{(1)}$	$\beta_{nc}^{(1)}$	$\beta_{ns}^{(1)}$	$\beta_{N/2}^{(1)}$
torsion	$\tilde{\rho}_i^{(m)}$	$\theta_i^{(1)}$	$\theta_{nc}^{(1)}$	$\theta_{ns}^{(1)}$	$\theta_{N/2}^{(1)}$
gimbal	β_a θ_a	β_{Gc}	β_{Gs}		

The notation $\beta^{(i)}$ is used for the i -th bending mode in the nonrotating frame. With the modes ordered according to frequency, $\beta^{(1)}$ is thus usually the fundamental lag mode, and $\beta^{(2)}$ the fundamental flap mode. Similarly, $\theta^{(1)}$ is the i -th torsion mode, with $\theta^{(0)}$ rigid pitch and the remaining modes elastic torsion. The collective and cyclic modes (0, 1C, 1S) are particularly important because of their fundamental role in the coupled motion of the rotor and the nonrotating system. When the transformation of

the equations and degrees of freedom is accomplished, for axial flow there is a complete decoupling of the variables into the following sets:

- (a) the collective and cyclic (0, 1C, 1S) rotor degrees of freedom together with the gimbal tilt and rotor speed degrees of freedom and the rotor shaft motion
- (b) the 2C, 2S, ..., nc, ns, and N/2 rotor degrees of freedom (as present)

Thus the rotor motion in the first set is coupled with the fixed system, while the second set consists of purely internal rotor motion. Nonaxial flow couples to some extent, all the rotor degrees of freedom and the fixed system variables, primarily due to the aerodynamic terms; still above separation of the degrees of freedom remains a dominant feature of the rotor dynamic behavior.

For a two-bladed rotor, the blade bending degrees of freedom are coning and teetering type modes:

$$\beta_0 = \frac{1}{N} \sum_{m=1}^2 q^{(m)} = \frac{1}{2} (q^{(2)} + q^{(1)})$$

$$\beta_1 = \frac{1}{N} \sum_{m=1}^2 q^{(m)} (-1)^m = \frac{1}{2} (q^{(2)} - q^{(1)})$$

The pitch/torsion degrees of freedom θ_0 and θ_1 are similarly defined. The teetering degree of freedom β_T is also included for the two-bladed rotor (in place of the gimbal degrees of freedom). The teetering motion is defined in the rotating frame, hence

$$\beta_0 = \beta_T (-1)^m$$

$$\theta_G = 0$$

The special characteristics of the two-bladed rotor dynamics are reflected in the appearance of the teetering-type degrees of freedom (β_1 , θ_1 , and β_T), rather than the cyclic motions (1C and 1S) as for $N \geq 3$. The coning and

teetering equations of motion are obtained by applying to the rotating frame equations the following operators:

$$+ \sum_{\infty} (\dots) \quad \frac{1}{n} \sum_{\infty} (\dots) (-1)^m$$

6.1.2 *Rotor equations and hub reactions.* - The equations of motion for the coupled flap/lag bending and for elastic torsion/rigid pitch motion of the blade in the rotating frame (section 2.2.18) are linearized for the aeroelastic analysis. The result is:

$$\begin{aligned}
 & \overset{*}{I}_{q_k} (\ddot{\theta}_k + \dot{\gamma}_s \dot{\theta}_k + \dot{\gamma}_k^2 \dot{\theta}_k) + 2 \sum_i \overset{*}{I}_{q_k q_i} \dot{\theta}_k \dot{q}_i \\
 & - \sum_i S_{q_k p_i}^* \ddot{p}_i - \sum_i S_{q_k p_i}^* p_i \\
 & + \overset{*}{I}_{q_k \alpha} \cdot \vec{k}_B (\ddot{\psi}_s + \ddot{\alpha}_z) + \overset{*}{I}_{q_k \alpha} \cdot \vec{l}_B (\ddot{\beta}_G + \ddot{\beta}_C) \\
 & + 2 \overset{*}{I}_{q_k \dot{\alpha}} (\dot{\psi}_s + \dot{\alpha}_z) - \overset{*}{I}_{q_k \dot{\beta}} (\ddot{\theta}_G - \dot{\theta}_G + 2\dot{\beta}_G) \\
 & + S_{q_k}^* \vec{l}_B \ddot{z}_m - S_{q_k}^* \vec{k}_B (\ddot{x}_m \sin \psi_m - \ddot{y}_m \cos \psi_m) \\
 & + \overset{*}{I}_{q_k \alpha} \cdot \vec{l}_B ((\ddot{\alpha}_x + 2\dot{\alpha}_y) \sin \psi_m - (\ddot{\alpha}_y - 2\dot{\alpha}_x) \cos \psi_m) \\
 & = \gamma \frac{M_{q_k \text{aero}}}{ac}
 \end{aligned}$$

$$\begin{aligned}
& \overline{I}_{pk}^* (\ddot{p}_k + g_s \omega_k \dot{p}_k + \omega_k^2 p_k) \\
& + \sum_i \overline{I}_{pk\ddot{p}_i}^* \ddot{p}_i + \sum_i \overline{I}_{pkp_i}^* p_i \\
& - \sum_i S_{pkq_i}^* \ddot{q}_i - \sum_i S_{pkq_i}^* q_i \\
& + \overline{I}_{pk\alpha}^* \cdot \vec{k}_e (\ddot{\psi}_s + \ddot{\alpha}_z) - \overline{I}_{pk\alpha}^* \cdot \vec{k}_g (\ddot{\beta}_g + \ddot{\beta}_g) \\
& - S_{pk}^* \cdot \vec{k}_g \ddot{\psi}_e - S_{pk}^* \cdot \vec{k}_e (\ddot{x}_e \sin \psi_m - \ddot{y}_e \cos \psi_m) \\
& - \overline{I}_{pk\alpha}^* \cdot \vec{k}_g ((\ddot{\alpha}_x + 2\ddot{\alpha}_y) \sin \psi_m - (\ddot{\alpha}_y - 2\ddot{\alpha}_x) \cos \psi_m) \\
& = \gamma \frac{M_{pk\text{cent}}}{\omega} + S_{pk}^* p_r
\end{aligned}$$

where

$$\begin{aligned}
p_r = & \Theta_{ik} \cos \psi_m + \Theta_{is} \sin \psi_m + \Delta \theta_{gmr} + \Delta \theta_{m\text{end}} \\
& - \sum_i K_{t_i} q_i - k_{pg} \beta_g + (\Theta_{is} \cos \psi_m - \Theta_{ik} \sin \psi_m) \psi_s
\end{aligned}$$

The inertia constants are defined in section 6.1.3. Only linear lag damping has been considered here, and for convenience the lag damper term is included in the coefficient $I_{q_k \dot{q}_i}^*$. Introducing the Fourier coordinate transformation for the blade degrees of freedom, the rotor hub forces and moments derived in section 2.2.18 become:

$$\delta \frac{2C_H}{\sigma_a} = \delta \left(\frac{2C_H}{\sigma_a} \right)_{\text{new}} - 2M_b^* \ddot{\gamma}_b + \sum_i S_q^* \cdot \vec{k}_B \beta_{is}^{(i)}$$

$$\delta \frac{2C_Y}{\sigma_a} = \delta \left(\frac{2C_Y}{\sigma_a} \right)_{\text{new}} - 2M_b^* \ddot{\gamma}_b - \sum_i S_q^* \cdot \vec{k}_B \beta_x^{(i)}$$

$$\delta \frac{2C_T}{\sigma_a} = \delta \left(\frac{2C_T}{\sigma_a} \right)_{\text{new}} - 2M_b^* \ddot{\gamma}_b - \sum_i S_q^* \cdot \vec{k}_B \beta_o^{(i)}$$

$$\begin{aligned} \delta \frac{2C_{Mx}}{\sigma_a} = \delta \left(\frac{2C_{Mx}}{\sigma_a} \right)_{\text{new}} & - I_o^* (\ddot{\alpha}_x + 2\dot{\alpha}_y) - I_o^* (\beta_{Gx} - 2\dot{\beta}_{Gx}) \\ & - \sum_i I_{q,\alpha}^* \cdot \vec{k}_B (\beta_{is}^{(i)} - 2\dot{\beta}_x^{(i)}) \\ & + \sum_i S_{q,\alpha}^* \cdot \vec{k}_B (\dot{\theta}_{is}^{(i)} - 2\dot{\theta}_{ic}^{(i)}) \\ & - \sum_i 2I_{q,qi}^* \cdot \vec{k}_B (\dot{\beta}_{is}^{(i)} - \beta_{ic}^{(i)}) \end{aligned}$$

$$\begin{aligned} \delta \frac{2C_{My}}{\sigma_a} = \delta \left(\frac{2C_{My}}{\sigma_a} \right)_{\text{new}} & - I_o^* (\ddot{\alpha}_y - 2\dot{\alpha}_x) + I_o^* (\beta_{Gx} + 2\dot{\beta}_{Gx}) \\ & + \sum_i I_{q,\alpha}^* \cdot \vec{k}_B (\beta_{ic}^{(i)} + 2\dot{\beta}_{is}^{(i)}) \\ & - \sum_i S_{q,\alpha}^* \cdot \vec{k}_B (\dot{\theta}_{ic}^{(i)} + 2\dot{\theta}_{is}^{(i)}) \\ & + \sum_i 2I_{q,qi}^* \cdot \vec{k}_B (\dot{\beta}_{ic}^{(i)} + \beta_{is}^{(i)}) \end{aligned}$$

$$\begin{aligned} \delta \frac{2C_Q}{\sigma_a} = \delta \left(\frac{2C_Q}{\sigma_a} \right)_{\text{new}} & + I_o^* (\ddot{\gamma}_S + \ddot{\alpha}_Z) \\ & + \sum_i I_{q,\alpha}^* \cdot \vec{k}_B \beta_o^{(i)} \\ & - \sum_i S_{q,\alpha}^* \cdot \vec{k}_B \theta_o^{(i)} \\ & + \sum_i 2I_{q,qi}^* \cdot \vec{k}_B \beta_o^{(i)} \end{aligned}$$

The equations of motion for gimbal tilt and roll, or for the teeter motion of a two-bladed rotor, are obtained from

$$\gamma \frac{ZC_My}{\sigma_a} + I_0^* c_{GC}^* \dot{\beta}_{GC} + I_0^* (\dot{\beta}_{GC}^2 - 1) \beta_{GC} = 0$$

$$- \gamma \frac{ZC_Mx}{\sigma_a} + I_0^* c_{GS}^* \dot{\beta}_{GS} + I_0^* (\dot{\beta}_{GS}^2 - 1) \beta_{GS} = 0$$

or

$$- \gamma \frac{C_{MT}}{\sigma_a} + I_0^* c_T^* \dot{\beta}_T + I_0^* (\dot{\beta}_T^2 - 1) \beta_T = 0$$

where

$$\begin{aligned} \gamma \frac{C_{MT}}{\sigma_a} &= \frac{1}{2} \sum_{m=1}^2 (-1)^m \gamma \frac{C_{Mx}}{\sigma_a} \\ &= \gamma \left(\frac{C_{MT}}{\sigma_a} \right)_{aero} \\ &\quad - I_0^* ((\ddot{\alpha}_x + 2\dot{\alpha}_y) \sin \psi - (\ddot{\alpha}_y - 2\dot{\alpha}_x) \cos \psi) \\ &\quad - I_0^* (\dot{\beta}_T + \beta_T) \\ &\quad - \sum_i I_{qia}^* \vec{t}_{iB} (\ddot{\beta}_i^{(i)} + \dot{\beta}_i^{(i)}) \\ &\quad + \sum_i S_{q,p,i}^* \vec{t}_{iB} (\ddot{\theta}_i^{(i)} + \dot{\theta}_i^{(i)}) \\ &\quad - 2 \sum_i I_{q,q,i}^* \vec{t}_{iB} \dot{\beta}_i^{(i)} \end{aligned}$$

(section 2.2.18). Also, for a two-bladed rotor, the hub reactions take a somewhat different form:

$$\begin{aligned} \gamma \frac{ZC_H}{\sigma_a} &= \gamma \left(\frac{ZC_H}{\sigma_a} \right)_{aero} - ZM_b^* \ddot{x}_h \\ &\quad + \sum_i S_{q,p,i}^* \vec{t}_{iB} (2 \sin \psi \ddot{\beta}_i^{(i)} + 4 \cos \psi \dot{\beta}_i^{(i)} - 2 \sin \psi \dot{\beta}_i^{(i)}) \end{aligned}$$

$$\gamma \frac{ZC_Y}{\sigma a} = \gamma \left(\frac{ZC_Y}{\sigma a} \right)_{aero} - ZM_L^* \ddot{\gamma}_B - \sum_i S_{q,i}^* \vec{k}_B \left(2 \cos \psi \beta_1^{(ii)} - 4 \sin \psi \dot{\beta}_1^{(i)} - 2 \cos \psi \beta_1^{(i)} \right)$$

$$\gamma \frac{ZC_{Mx}}{\sigma a} = 2 \sin \psi \left(\gamma \frac{C_M}{\sigma a} \right)$$

$$\gamma \frac{ZC_{My}}{\sigma a} = -2 \cos \psi \left(\gamma \frac{C_M}{\sigma a} \right)$$

The aerodynamic forces required are

$$\frac{ZC_H}{\sigma a} = \frac{N}{2} \sum_m \left(\sin \psi_m \int_0^1 \frac{F_x}{\sigma C} dr + \cos \psi_m \int_0^1 \frac{F_r}{\sigma C} dr \right)$$

$$\frac{ZC_Y}{\sigma a} = \frac{N}{2} \sum_m \left(-\cos \psi_m \int_0^1 \frac{F_x}{\sigma C} dr + \sin \psi_m \int_0^1 \frac{F_r}{\sigma C} dr \right)$$

$$\frac{C_r}{\sigma a} = \frac{1}{2} \sum_m \int_0^1 \frac{F_r}{\sigma C} dr$$

$$\frac{ZC_{Mx}}{\sigma a} = \frac{N}{2} \sum_m \sin \psi_m \int_0^1 \frac{F_r}{\sigma C} r dr$$

$$\frac{ZC_{My}}{\sigma a} = \frac{N}{2} \sum_m (-\cos \psi_m) \int_0^1 \frac{F_r}{\sigma C} r dr$$

$$\frac{C_r}{\sigma a} = \frac{1}{2} \sum_m \int_0^1 \frac{F_x}{\sigma C} dr$$

$$\frac{M_{aero}}{\sigma C} = \int_0^1 \vec{r}_B \cdot \left(\frac{F_r}{\sigma C} \vec{r}_B - \frac{F_x}{\sigma C} \vec{r}_B \right) dr$$

$$\frac{M_{px}^{new}}{ac} = \int_{r_{FA}}^r \sum_k \frac{M_k}{ac} - \int_{r_{FA}}^r \left(\frac{f_x}{ac} \dot{q}_k + \frac{f_z}{ac} \ddot{q}_k \right) \cdot \vec{x}_{Ak} dr$$

and

$$\frac{C_m}{a} = \frac{1}{N} \sum (-1)^m \int_0^r \frac{f_z}{ac} r dr$$

6.1.3 *Inertial constants.*— The inertial constants for these linearized equations of motion are obtained from the constants defined in section 2.2.19 as follows:

$$(I_{q_k}^*)_{eqs} = I_{q_k}^*$$

$$(I_{q_k q_i}^*)_{eqs} = I_{q_k q_i}^* + \sum_j I_{q_k q_i q_j}^* \ddot{q}_j + \frac{1}{2} g e n g \vec{r}_B \cdot \vec{\gamma}_k'(e) \vec{r}_B \cdot \vec{\gamma}_i'(e)$$

$$(S_{q_k p_i}^*)_{eqs} = S_{q_k p_i}^* + \sum_j S_{q_k p_i q_j}^* \ddot{q}_j + \ddot{r}_i$$

$$(S_{q_k p_i}^*)_{eqs} = S_{q_k p_i}^* + \sum_j S_{q_k p_i q_j}^* \ddot{q}_j + \ddot{r}_i$$

$$(I_{q_k \alpha}^*)_{eqs} = I_{q_k \alpha}^*$$

$$(I_{q_k \dot{\alpha}}^*)_{eqs} = I_{q_k \dot{\alpha}}^* + \sum_j I_{q_k \dot{\alpha} q_j}^* \ddot{q}_j + \ddot{r}_i$$

$$(I_{q_k \beta}^*)_{eqs} = I_{q_k \beta}^* + \sum_j I_{q_k \beta q_j}^* \ddot{q}_j + \ddot{r}_i$$

$$(S_{q_k}^*)_{eqs} = S_{q_k}^*$$

$$(\overline{I}_{pk}^*)_{eqs} = I_{pk}^*$$

$$(\overline{I}_{pk\dot{p}_i}^*)_{eqs} = \overline{I}_{pk\dot{p}_i}^*$$

$$(\overline{I}_{pk\dot{p}_i}^*)_{eqs} = I_{pk\dot{p}_i}^*$$

$$(S_{pk\ddot{q}_i}^*)_{eqs} = S_{pk\ddot{q}_i}^* + \sum_j S_{pk\ddot{q}_i q_j}^* q_{j+rim}$$

$$(S_{pk\ddot{q}_i}^*)_{eqs} = S_{pk\ddot{q}_i}^* + \sum_j (S_{pk\ddot{q}_i q_j}^* + S_{pk\ddot{q}_i q_0}^*) q_{j+rim}$$

$$(\overline{I}_{pk\alpha}^*)_{eqs} = I_{pk\alpha}^* + \sum_j I_{pk\alpha q_j}^* q_{j+rim}$$

$$(S_{pk}^*)_{eqs} = S_{pk}^* + \sum_j S_{pkq_j}^* q_{j+rim}$$

$$(M_b^*)_{eqs} = M_b^*$$

$$(\overline{I}_0^*)_{eqs} = I_0^*$$

$$(S_{q_0\ddot{p}_i}^*)_{eqs} = S_{q_0\ddot{p}_i}^* + \sum_j S_{q_0\ddot{p}_i q_j}^* q_{j+rim}$$

$$(\overline{I}_{q_0\dot{q}_i}^*)_{eqs} = \overline{I}_{q_0\dot{q}_i}^* + \sum_j \overline{I}_{q_0\dot{q}_i q_j}^* q_{j+rim}$$

$$(S_{pk^0})_{eqs} = I_{pk^0}^* \omega_0^z \tilde{\beta}_k(r_F)$$

6.1.4 Aerodynamic forces.- The blade section forces and pitch moment as derived in section 2.4.1 are:

$$\frac{F_z}{ac} = U(u_r \frac{c_s}{2a} - u_p \frac{c_d}{2a}) \frac{c}{cm}$$

$$\frac{F_x}{ac} = U(u_p \frac{c_s}{2a} + u_r \frac{c_d}{2a}) \frac{c}{cm}$$

$$\frac{F_r}{ac} = (u u_r \frac{c_s}{2a}) \frac{c}{cm}$$

$$\frac{M_a}{ac} = (-x_A U^2 \frac{c_s}{2a} + U^2 c \frac{c_m}{2a} + \frac{M_{us}}{ac}) \frac{c}{cm}$$

Each component of the velocity seen by the blade has a trim term and a small perturbation term, so we write

$$\theta \Rightarrow \theta + \delta\theta$$

$$u_r \Rightarrow u_r + \delta u_r$$

$$u_p \Rightarrow u_p + \delta u_p$$

$$u_R \Rightarrow u_R + \delta u_R$$

It follows that the perturbation of angle of attack, resultant velocity, and Mach number are:

$$\delta\theta = \delta\theta - (u_r \delta u_p - u_p \delta u_r) / U^2$$

$$\delta u = (u_r \delta u_r + u_p \delta u_p) / U$$

$$\delta M = M_{tip} \delta u$$

and the perturbations of the aerodynamic coefficients are

$$Sc_d = \frac{\partial c_d}{\partial \alpha} \delta \alpha + \frac{\partial c_d}{\partial M} \delta M = c_{d\alpha} \delta \alpha + c_{dM} \delta M$$

with similar results for c_m and c_d . The perturbations of the section aerodynamic forces may then be obtained by carrying out the differential operation on the expressions for F_z , F_x , F_r , and M_a , using the above results to express the perturbations in terms of $\delta \theta$, δu_T , δu_p , and δu_R . The coefficients of the perturbation quantities are evaluated at the trim state. The results for the perturbation forces are:

$$\begin{aligned} \delta \frac{F_z}{ac} &= \left(u_T \frac{c_{d\alpha}}{za} - u_p \frac{c_{d\alpha}}{za} \right) \underset{cm}{\equiv} \delta \theta \\ &\quad + \left[- \frac{u_T}{u} \left(u_T \frac{c_{d\alpha}}{za} - u_p \frac{c_{d\alpha}}{za} \right) + \left(\frac{c_d}{za} + M \frac{c_{dM}}{za} \right) \frac{u_T u_p}{u} \right. \\ &\quad \left. - \left(\frac{c_d}{za} + M \frac{c_{dM}}{za} \right) \frac{u_p^2}{u} - \frac{c_d}{za} u \right] \underset{cm}{\equiv} \delta u_p \\ &\quad + \left[\frac{u_p}{u} \left(u_T \frac{c_{d\alpha}}{za} - u_p \frac{c_{d\alpha}}{za} \right) + \left(\frac{c_d}{za} + M \frac{c_{dM}}{za} \right) \frac{u_T^2}{u} \right. \\ &\quad \left. + \frac{c_d}{za} u - \left(\frac{c_d}{za} + M \frac{c_{dM}}{za} \right) \frac{u_T u_p}{u} \right] \underset{cm}{\equiv} \delta u_T \\ &= F_{z\theta} \delta \theta + F_{zp} \delta u_p + F_{zT} \delta u_T \end{aligned}$$

$$\begin{aligned}
\delta \frac{F_x}{ac} &= \left(u_{up} \frac{c_{xu}}{za} + u_{ur} \frac{c_{du}}{za} \right) \frac{c}{cm} \delta\theta \\
&+ \left[-\frac{u_r}{u} \left(u_p \frac{c_{xu}}{za} + u_r \frac{c_{du}}{za} \right) + \left(\frac{c_x}{za} + M \frac{c_{dm}}{za} \right) \frac{u_p^2}{u} \right. \\
&\quad \left. + \frac{c_x}{za} u + \left(\frac{c_d}{za} + M \frac{c_{dm}}{za} \right) \frac{u_r u_p}{u^2} \right] \frac{c}{cm} \delta u_p \\
&+ \left[\frac{u_p}{u} \left(u_p \frac{c_{du}}{za} + u_r \frac{c_{dx}}{za} \right) + \left(\frac{c_d}{za} + M \frac{c_{dm}}{za} \right) \frac{u_p u_r}{u} \right. \\
&\quad \left. + \left(\frac{c_d}{za} + M \frac{c_{dm}}{za} \right) \frac{u_r^2}{u} + \frac{c_d}{za} u \right] \frac{c}{cm} \delta u_r \\
&= F_{x_\theta} \delta\theta + F_{x_p} \delta u_p + f_{x_r} \delta u_r
\end{aligned}$$

$$\begin{aligned}
\delta \frac{M_a}{ac} &= \left[u^2 \left(-x_A \frac{c_{xu}}{za} + c \frac{c_{du}}{za} \right) \right] \frac{c}{cm} \delta\theta \\
&+ \left[u_p \left(-x_A \frac{c_{xu}}{za} + c \frac{c_{du}}{za} \right) - x_A u_r \left(2 \frac{c_x}{za} + M \frac{c_{dm}}{za} \right) \right. \\
&\quad \left. + c_{ur} \left(2 \frac{c_m}{za} + M \frac{c_{dm}}{za} \right) \right] \frac{c}{cm} \delta u_p \\
&+ \left[-u_r \left(-x_A \frac{c_{du}}{za} + c \frac{c_{dx}}{za} \right) - x_A u_p \left(2 \frac{c_d}{za} + M \frac{c_{dm}}{za} \right) \right. \\
&\quad \left. + c_{up} \left(2 \frac{c_m}{za} + M \frac{c_{dm}}{za} \right) \right] \frac{c}{cm} \delta u_r \\
&+ \frac{Mus}{ac} \frac{c}{cm} \\
&= M_{a\theta} \delta\theta + M_{ap} \delta u_p + M_{ar} \delta u_r + \frac{Mus}{ac} \frac{c}{cm}
\end{aligned}$$

$$\begin{aligned}
\delta \frac{F_r}{a_c} &= \left(u_{UR} \frac{c_d}{2a} \right) \frac{\epsilon}{cm} \delta \theta \\
&+ \left[-\frac{u_{UR}}{U} \frac{c_d}{2a} + \left(\frac{c_d}{2a} + M \frac{c_m}{2a} \right) \frac{u_{UR}}{U} \right] \frac{\epsilon}{cm} \delta u_p \\
&+ \left[\frac{u_p u_R}{U} \frac{c_d}{2a} + \left(\frac{c_d}{2a} + M \frac{c_m}{2a} \right) \frac{u_R u_T}{U} \right] \frac{\epsilon}{cm} \delta u_T \\
&+ \left(U \frac{c_d}{2a} \right) \frac{\epsilon}{cm} \delta u_R \\
&= F_{r\theta} \delta \theta + F_{rp} \delta u_p + F_{rt} \delta u_T + F_{rR} \delta u_R
\end{aligned}$$

The blade trim velocity components are defined in section 2.4.2. The perturbation velocity components are due to the blade degrees of freedom, the shaft motion, and the aerodynamic gust velocity:

$$\begin{aligned}
\delta u_T &= (\mu_x \alpha_x + i \dot{\gamma}_B + v_G) \cos \psi_m + (\mu_z \alpha_y - \dot{x}_B + u_G) \sin \psi_m \\
&+ (\mu_x \cos \psi_m - \mu_y \sin \psi_m) (\alpha_z + \dot{\psi}_S) + r (\dot{\alpha}_z + \dot{\psi}_S) \\
&+ \sum_i \dot{q}_i \vec{k}_B \cdot \vec{\eta}_i + u_R \sum_i \dot{q}_i \vec{k}_B \cdot \vec{\eta}'_i
\end{aligned}$$

$$\begin{aligned}
\delta u_R &= -(\mu_x \alpha_x + i \dot{\gamma}_B + v_G) \sin \psi_m + (\mu_z \alpha_y - \dot{x}_B + u_G) \cos \psi_m \\
&- (\mu_x \sin \psi_m + \mu_y \cos \psi_m) (\alpha_z + \dot{\psi}_S) - \mu_z \beta_G \\
&+ \sum_i \dot{q}_i [\vec{k}_B \cdot (\vec{\eta}_i - u_T \vec{\eta}'_i) - \mu_z \vec{k}_B \cdot \vec{\eta}'_i]
\end{aligned}$$

$$\begin{aligned}\delta u_p = & (\dot{\alpha}_x - \mu_x \alpha_y - \mu_y \alpha_x - w_0 + \lambda_u) + u_R \beta_G \\ & + r (\dot{\beta}_G + \dot{\alpha}_x \sin \psi_m - \dot{\alpha}_y \cos \psi_m + \lambda_x \cos \psi_m + \lambda_y \sin \psi_m) \\ & + \sum_i \dot{q}_i \vec{T}_B \cdot \vec{\gamma}_i + u_R \sum_i q_i \vec{T}_B \cdot \vec{\gamma}'_i \\ \delta \theta = & \sum_i p_i \vec{\beta}_i\end{aligned}$$

The gust velocity components are here assumed to be uniform throughout space. Perturbation inflow components λ_u , λ_x , and λ_y have been included in δu_p (see section 6.1.5). Recall that the body Euler angle contributions are not included in the evaluation of α_x , α_y , and α_z here. The perturbation quantities required for the unsteady pitch moment are

$$\begin{aligned}B = & \sum_i \dot{p}_i \vec{\beta}_i + u_R \sum_i p_i \vec{\beta}'_i + \beta_G + \sum_i q_i \vec{T}_B \cdot \vec{\gamma}'_i \\ \ddot{w} + u_R w' = & V \sum_i \dot{p}_i \vec{\beta}_i + u_R V \sum_i p_i \vec{\beta}'_i \\ & - 2u_R \cos \theta \dot{\beta}_G - u_R \cos \theta \beta_G \\ & + 2u_R \sin \theta (\dot{\alpha}_z + \dot{\psi}_s) + u_R \sin \theta (\alpha_z + \psi_s) \\ & - 2u_R \sum_i \dot{q}_i \vec{\tau} \cdot \vec{\gamma}'_i \\ & + \sum_i q_i (-u_R \vec{\tau} \cdot \vec{\gamma}'_i - u_R^2 \vec{\tau} \cdot \vec{\gamma}''_i)\end{aligned}$$

(see section 2.4.8). The derivatives of the blade section aerodynamic coefficients with respect to angle of attack and Mach number are obtained from steady, two-dimensional airfoil characteristics with corrections for tip flow, yawed flow, and dynamic stall effects, as described in sections 2.4.4 and 2.4.7.

Combining the expansion for the section forces and moment in terms of the velocity perturbations, and the velocity in terms of the motion of the rotor and shaft, the perturbation aerodynamic blade forces expanded linearly in the degrees of freedom are obtained. Giving names to the aerodynamic coefficients at this point in the analysis, the results for the required aerodynamic forces on the rotating blade are as follows. The aerodynamic force for flap/lag bending is:

$$\begin{aligned}
 & \int_0^1 \vec{\eta}_k \cdot \left(\frac{\vec{F}_z}{ac} \vec{t}_k - \frac{\vec{F}_x}{ac} \vec{k}_k \right) dr \\
 &= M_{q_k \mu} [(\mu_z \alpha_x + i_{\mu} + v_G) \cos \psi_m \\
 &\quad + (\mu_z \alpha_y - i_{\mu} + u_G) \sin \psi_m] \\
 &+ M_{q_k \xi} (\dot{\alpha}_z + \dot{\psi}_s) + M_{q_k \zeta} (\alpha_z + \psi_s) \\
 &+ M_{q_k \lambda} (\dot{z}_n - \mu_x \alpha_y - \mu_y \alpha_x - w_G + \lambda_n) \\
 &+ M_{q_k \dot{\beta}} (\dot{\beta}_G + \dot{\alpha}_x \sin \psi_m - \dot{\alpha}_y \cos \psi_m + \lambda_x \cos \psi_m + \lambda_y \sin \psi_m) \\
 &+ M_{q_k \beta} \beta_G + \sum_i M_{q_k q_i} \dot{q}_i + \sum_i M_{q_k \gamma_i} \dot{\gamma}_i \\
 &+ \sum_i M_{q_k p_i} p_i
 \end{aligned}$$

The radial force is

$$\begin{aligned}
 \int_0^1 \frac{\tilde{F}_r}{ac} dr &= R_\mu [-(\mu_z \alpha_x + i_{\mu} + v_G) \sin \psi_m + (\mu_z \alpha_y - i_{\mu} + u_G) \cos \psi_m] \\
 &+ R_r [(\mu_z \alpha_x + i_{\mu} + v_G) \cos \psi_m + (\mu_z \alpha_y - i_{\mu} + u_G) \sin \psi_m] \\
 &+ R_\xi (\dot{\alpha}_z + \dot{\psi}_s) + R_\zeta (\alpha_z + \psi_s) \\
 &+ R_\lambda (\dot{z}_n - \mu_x \alpha_y - \mu_y \alpha_x - w_G + \lambda_n) \\
 &+ R_{\dot{\beta}} (\dot{\beta}_G + \dot{\alpha}_x \sin \psi_m - \dot{\alpha}_y \cos \psi_m + \lambda_x \cos \psi_m + \lambda_y \sin \psi_m) \\
 &+ R_\beta \beta_G + \sum_i R_{q_i} \dot{q}_i + \sum_i R_{\gamma_i} \dot{\gamma}_i + \sum_i R_{p_i} \dot{p}_i
 \end{aligned}$$

The aerodynamic force for blade torsion and pitch is:

$$\begin{aligned}
 \int_0^l \vec{g}_k \frac{M_k}{a_c} dr - \int_0^l (\frac{\dot{x}}{a_c} \vec{T}_k + \frac{\dot{F}_z}{a_c} \vec{T}_k) \cdot \vec{X}_{A_k} dr \\
 = M_{pk\mu} [(\mu_z \alpha_x + i_m + v_G) \cos \psi_m + (\mu_z \alpha_y - i_n + u_G) \sin \psi_m] \\
 + M_{pk\delta} (\dot{\alpha}_z + \dot{i}_s) + M_{pk\lambda} (\alpha_z + i_s) \\
 + M_{pk\lambda} (\dot{i}_n - \mu_x \alpha_y - \mu_y \alpha_x - w_G + \lambda_n) \\
 + M_{pk\beta} (\dot{\beta}_G + \dot{\alpha}_x \sin \psi_m - \dot{\alpha}_y \cos \psi_m + \lambda_x \cos \psi_m + \lambda_y \sin \psi_m) \\
 + M_{pk\beta} \beta_G + \sum_i M_{pk} \dot{q}_i \dot{q}_i + \sum_i M_{pk} q_i \dot{q}_i \\
 + \sum_i M_{pk} \dot{p}_i \dot{p}_i + \sum_i M_{pk} p_i p_i
 \end{aligned}$$

Finally, the aerodynamic hub forces and moments are similar to the result for the blade bending, but with the following changes in the integrands and notation:

	<u>Integrand</u>	<u>Coefficient Notation</u>
Flap moment	$r F_z$	M
Torque	$r F_x$	Q
Blade drag force	F_x	H
Thrust	F_z	T

Combining the results for the expansion of the aerodynamic forces and the expansions of the velocities, the aerodynamic coefficients can be evaluated. The aerodynamic coefficients are constant for axial flow, but for nonaxial flow they are periodic functions of ψ_m . The coefficients for flap/lag bending are:

$$M_{q_k \mu} = \int_0^l \vec{\eta}_k \cdot (\vec{F}_{z_T} \vec{t}_B - \vec{F}_{x_T} \vec{k}_B) dr$$

$$M_{q_k \dot{\gamma}} = \int_0^l \vec{\eta}_k \cdot (\vec{F}_{z_T} \vec{t}_B - \vec{F}_{x_T} \vec{k}_B) r dr$$

$$M_{q_k \dot{\gamma}} = (\mu_x \cos \psi_m - \mu_y \sin \psi_m) M_{q_k \mu}$$

$$M_{q_k \lambda} = \int_0^l \vec{\eta}_k \cdot (\vec{F}_{z_P} \vec{t}_B - \vec{F}_{x_P} \vec{k}_B) dr$$

$$M_{q_k \dot{\beta}} = \int_0^l \vec{\eta}_k \cdot (\vec{F}_{z_P} \vec{t}_B - \vec{F}_{x_P} \vec{k}_B) r dr$$

$$M_{q_k \beta} = u_R M_{q_k \lambda}$$

$$M_{q_k \dot{\gamma}_i} = \int_0^l \vec{\eta}_k \cdot (\vec{F}_{z_T} \vec{t}_B - \vec{F}_{x_T} \vec{k}_B) \vec{k}_B \cdot \vec{\gamma}_i dr + \int_0^l \vec{\eta}_k \cdot (\vec{F}_{z_P} \vec{t}_B - \vec{F}_{x_P} \vec{k}_B) \vec{t}_B \cdot \vec{\gamma}_i dr$$

$$M_{q_k \dot{\gamma}_i} = u_R \int_0^l \vec{\eta}_k \cdot (\vec{F}_{z_T} \vec{t}_B - \vec{F}_{x_T} \vec{k}_B) \vec{k}_B \cdot \vec{\gamma}'_i dr + u_R \int_0^l \vec{\eta}_k \cdot (\vec{F}_{z_P} \vec{t}_B - \vec{F}_{x_P} \vec{k}_B) \vec{t}_B \cdot \vec{\gamma}'_i dr$$

$$M_{q_k \dot{\beta}_i} = \int_0^l \vec{\eta}_k \cdot (\vec{F}_{z_\theta} \vec{t}_B - \vec{F}_{x_\theta} \vec{k}_B) \vec{s}_i dr$$

The aerodynamic coefficients for the flap moment are

$$\begin{aligned}
 M_{\mu} &= \int_0^1 F_{z_T} r dr \\
 M_{\dot{\beta}} &= \int_0^1 F_{z_T} r^2 dr \\
 M_{\beta} &= (\mu_x \cos \Phi_m - \mu_y \sin \Phi_m) M_{\mu} \\
 M_x &= \int_0^1 F_{z_P} r dr \\
 M_{\dot{\beta}} &= \int_0^1 F_{z_P} r^2 dr \\
 M_{\beta} &= u_R M_x \\
 M_{q_i} &= \int_0^1 (F_{z_T} \vec{k}_B \cdot \vec{\eta}_i + F_{z_P} \vec{k}_B \cdot \vec{\eta}'_i) r dr \\
 M_{\dot{q}_i} &= u_R \int_0^1 (F_{z_T} \vec{k}_B \cdot \vec{\eta}'_i + F_{z_P} \vec{k}_B \cdot \vec{\eta}''_i) r dr \\
 M_{p_i} &= \int_0^1 F_{z_B} \vec{\beta}_i r dr
 \end{aligned}$$

The aerodynamic coefficients for the other hub forces and moments follow the pattern of the flap moment, with the following changes in the notation and integrands:

	<u>Integrand</u>	<u>Coefficient</u>
Flap moment	$r F_z$	M
Torque	$r F_x$	Q
Blade drag force	F_x	H
Thrust	F_z	T

The radial force coefficients are

$$R_x = \int_0^1 F_{Rx} dr$$

$$R_r = \int_0^1 \tilde{F}_{rT} dr$$

$$R_{\dot{r}} = \int_0^1 \tilde{F}_{rT} r dr$$

$$R_S = (\mu_x \cos \psi_m - \mu_y \sin \psi_m) R_r - (\mu_x \sin \psi_m + \mu_y \cos \psi_m) R_x - \int_0^1 \frac{f_x}{ac} dr$$

$$R_{\dot{x}} = \int_0^1 \tilde{F}_{rP} dr$$

$$R_{\dot{r}P} = \int_0^1 \tilde{F}_{rP} r dr$$

$$R_{\dot{z}} = u_R R_r - \mu_z R_x - \int_0^1 \frac{f_z}{ac} dr$$

$$R_{\dot{\eta}_i} = \int_0^1 (\tilde{F}_{rT} \vec{k}_B \cdot \vec{\eta}_i + \tilde{F}_{rP} \vec{v}_B \cdot \vec{\eta}_i) dr$$

$$\begin{aligned} R_{\dot{\eta}'_i} &= u_R \int_0^1 (\tilde{F}_{rT} \vec{k}_B \cdot \vec{\eta}'_i + \tilde{F}_{rP} \vec{v}_B \cdot \vec{\eta}'_i) dr \\ &\quad + \int_0^1 F_{rK} [\vec{k}_B \cdot (\vec{\eta}'_i - u_T \vec{\eta}_i) - \mu_z \vec{v}_B \cdot \vec{\eta}'_i] dr \\ &\quad - \int_0^1 \left(\frac{f_z}{ac} \vec{k}_B \cdot \vec{\eta}'_i + \frac{f_x}{ac} \vec{v}_B \cdot \vec{\eta}'_i \right) dr \end{aligned}$$

$$R_{\dot{\xi}_i} = \int_0^1 \tilde{F}_{r\theta} \vec{\xi}_i dr$$

where

$$\begin{aligned}\tilde{F}_{r_T} &= F_{r_T} - F_{z_T} [\beta_G + \delta_{M_1} - \delta_{FA_2} + \vec{k}_B \cdot (\lambda_0 \vec{t} + z_0 \vec{R})'] \\ &\quad - F_{x_T} [\delta_{FA_3} + \vec{k}_B \cdot (\lambda_0 \vec{t} + z_0 \vec{R})']\end{aligned}$$

and \tilde{F}_{r_p} and \tilde{F}_{r_θ} are similarly defined. Finally, the aerodynamic coefficients for the blade pitch and torsion are

$$M_{Ax\mu} = \int_{C_{FA}}^l [\tilde{\beta}_k M_{a_T} - (F_{x_T} \vec{t}_B + F_{z_T} \vec{k}_B) \cdot \vec{X}_{A_k}] dr$$

$$\begin{aligned}M_{Ak\dot{\beta}} &= \int_{C_{FA}}^l [\tilde{\beta}_k M_{a_T} - (F_{x_T} \vec{t}_B + F_{z_T} \vec{k}_B) \cdot \vec{X}_{A_k}] r dr \\ &\quad - \int_{C_{FA}}^l \tilde{\beta}_k \frac{c^2}{32} (1 + 4 \frac{x_{Ae}}{c}) 2 u_R \sin \theta \operatorname{sign} V \frac{c}{cm} dr\end{aligned}$$

$$\begin{aligned}M_{Ak\dot{\beta}} &= (\mu_x \cos \psi_m - \mu_y \sin \psi_m) M_{Ak\mu} \\ &\quad - \int_{C_{FA}}^l \tilde{\beta}_k \frac{c^2}{32} (1 + 4 \frac{x_{Ae}}{c}) u_R \sin \theta \operatorname{sign} V \frac{c}{cm} dr\end{aligned}$$

$$M_{Ax\lambda} = \int_{C_{FA}}^l [\tilde{\beta}_k M_{a_p} - (F_{x_p} \vec{t}_B + F_{z_p} \vec{k}_B) \cdot \vec{X}_{A_k}] dr$$

$$\begin{aligned}M_{Ak\dot{\beta}} &= \int_{C_{FA}}^l [\tilde{\beta}_k M_{a_p} - (F_{x_p} \vec{t}_B + F_{z_p} \vec{k}_B) \cdot \vec{X}_{A_k}] r dr \\ &\quad + \int_{C_{FA}}^l \tilde{\beta}_k \frac{c^2}{32} (1 + 4 \frac{x_{Ae}}{c}) 2 u_R \cos \theta \operatorname{sign} V \frac{c}{cm} dr\end{aligned}$$

$$\begin{aligned}M_{Ax\beta} &= u_R M_{Ak\lambda} \\ &\quad - \int_{C_{FA}}^l \tilde{\beta}_k \frac{c^2}{32} |V| (1 + 4 \frac{x_{Ae}}{c})^2 \frac{c}{cm} dr \\ &\quad + \int_{C_{FA}}^l \tilde{\beta}_k \frac{c^2}{32} (1 + 4 \frac{x_{Ae}}{c}) u_R \cos \theta \operatorname{sign} V \frac{c}{cm} dr\end{aligned}$$

$$M_{q_k q_i} = \int_{r_{FA}}^r [\bar{\zeta}_k M_{a_T} - (F_{x_T} \vec{t}_B + F_{z_T} \vec{k}_B) \cdot \vec{X}_{A_k}] \vec{k}_B \cdot \vec{\eta}_i dr \\ + \int_{r_{FA}}^r [\bar{\zeta}_k M_{a_P} - (F_{x_P} \vec{t}_B + F_{z_P} \vec{k}_B) \cdot \vec{X}_{A_k}] \vec{t}_B \cdot \vec{\eta}_i dr \\ + \int_{r_{FA}}^r \bar{\zeta}_k \frac{c^2}{32} (1 + 4 \frac{x_{Ac}}{c}) 2 u_R \vec{t} \cdot \vec{\eta}_i' \text{ sign} \sqrt{\frac{c}{cm}} dr$$

$$M_{q_k q_i} = u_R \int_{r_{FA}}^r [\bar{\zeta}_k M_{a_T} - (F_{x_T} \vec{t}_B + F_{z_T} \vec{k}_B) \cdot \vec{X}_{A_k}] \vec{k}_B \cdot \vec{\eta}_i' dr \\ + u_R \int_{r_{FA}}^r [\bar{\zeta}_k M_{a_P} - (F_{x_P} \vec{t}_B + F_{z_P} \vec{k}_B) \cdot \vec{X}_{A_k}] \vec{t}_B \cdot \vec{\eta}_i' dr \\ - \int_{r_{FA}}^r (\frac{F_x}{ac} \vec{t}_B + \frac{F_z}{ac} \vec{k}_B) \cdot \vec{X}_{A_k q_i} dr \\ - \int_{r_{FA}}^r \bar{\zeta}_k \frac{c^2}{32} |V| (1 + 4 \frac{x_{Ac}}{c})^2 \vec{t}_B \cdot \vec{\eta}_i' \frac{c}{cm} dr \\ + \int_{r_{FA}}^r \bar{\zeta}_k \frac{c^2}{32} (1 + 4 \frac{x_{Ac}}{c}) [u_R \vec{t} \cdot \vec{\eta}_i' + u_R^2 \vec{t} \cdot \vec{\eta}_i''] \text{ sign} \sqrt{\frac{c}{cm}} dr$$

$$M_{p_k p_i} = \int_{r_{FA}}^r [\bar{\zeta}_k M_{a_B} - (F_{x_B} \vec{t}_B + F_{z_B} \vec{k}_B) \cdot \vec{X}_{A_k}] \bar{\zeta}_i dr \\ - \int_{r_{FA}}^r \bar{\zeta}_k \frac{c^2}{16} u_R \bar{\zeta}_i' |V| (1 + 4 \frac{x_{Ac}}{c}) (1 + 2 \frac{x_{Ac}}{c}) \frac{c}{cm} dr$$

$$M_{p_k \dot{p}_i} = - \int_{r_{FA}}^r \bar{\zeta}_k \bar{\zeta}_i \frac{c^2}{16} |V| (1 + 4 \frac{x_{Ac}}{c}) (1 + 2 \frac{x_{Ac}}{c}) \frac{c}{cm} dr$$

where

$$\vec{X}_{A_k q_i} = - \int_{r_{FA}}^r \bar{\zeta}_k \vec{\eta}_i'' (r-g) dg$$

$$\vec{X}_{A_k q_0} = - \vec{\eta}_i + \vec{\eta}_i(r_{FA}) + \vec{\eta}_i'(r_{FA})(r-r_{FA})$$

6.1.5 *Inflow dynamics.* - The aerodynamic forces on the rotor result in wake-induced inflow velocities at the disk, for both the trim and transient loadings. The wake-induced velocity perturbations can be a significant factor in the rotor aeroelastic behavior; an extreme case is the influence of the shed wake on rotor blade flutter. The rotor inflow dynamics should therefore be included in the aeroelastic analysis. However, the relationship between the inflow perturbations and the transient loading is likely more complex even than for the steady problem (nonuniform wake-induced inflow calculation), and models for the perturbation inflow dynamics are still under development. In the present analysis, an elementary representation of the inflow dynamics is used. The basic assumption is that the rotor total forces vary slowly enough (compared to the wake response) that the classical actuator disk results are applicable to the perturbation as well as the trim velocities.

A contribution to the velocity normal to the rotor disk of the following form has been included in δu_p :

$$\delta u_p = \lambda_u + \lambda_x r \cos \psi_m + \lambda_y r \sin \psi_m$$

where λ_u is the inflow perturbation component uniform over the disk, while the λ_x and λ_y components vary linearly over the disk. The inflow dynamics model must relate these inflow components to the transient aerodynamic forces on the rotor, specifically to the thrust, pitch moment, and roll moment; and to the transient rotor velocity perturbations δu_x , δu_y , and δu_z . Following reference 33 we use:

$$\begin{pmatrix} \lambda_u \\ \lambda_x \\ \lambda_y \end{pmatrix} = \begin{bmatrix} \frac{\partial \lambda}{\partial T} & 0 & 0 \\ K_x \frac{\partial \lambda}{\partial T} & \frac{\partial \lambda}{\partial M} & 0 \\ K_y \frac{\partial \lambda}{\partial T} & 0 & \frac{\partial \lambda}{\partial M} \end{bmatrix} \begin{pmatrix} \tilde{G} \\ -C_{Mxy} \\ C_{Mx} \end{pmatrix}$$

where

$$\tilde{C}_T = C_T - \frac{C_{T,trim}}{\mu^2/k_f^2 + \lambda^2/k_m^4} \left(\frac{\kappa_x}{k_f^2} \delta M_x + \frac{\kappa_y}{k_f^2} \delta M_y + \frac{\lambda}{k_m^2} \delta M_z \right)$$

and

$$\frac{\partial \lambda}{\partial T} = \frac{1}{2 \sqrt{\mu^2/k_f^2 + \lambda^2/k_m^4} + \frac{C_T \lambda / k_m^4}{\mu^2/k_f^2 + \lambda^2/k_m^4}}$$

$$\frac{\delta \lambda}{\delta M} = \frac{\delta m}{\sqrt{\mu^2/k_f^2 + \lambda^2/k_m^4}}$$

Here we have included linear velocity perturbations due to the thrust, consistent with the trim inflow model of section 2.4.3, which gives expressions for the constants κ_x and κ_y . These relations for the inflow perturbations imply the following lift deficiency functions:

$$C = \begin{cases} \frac{1}{1 + \frac{\sigma a}{16} \frac{\partial \lambda}{\partial M}} & \text{for moments} \\ \frac{1}{1 + \frac{\sigma a}{4} \frac{\partial \lambda}{\partial T}} & \text{for thrust} \end{cases}$$

$$C = \begin{cases} \frac{1}{1 + \frac{\sigma a}{8\mu}} & \text{forward flight} \\ \frac{1}{1 + \frac{\sigma a}{8\lambda}} & \text{moments in hover} \\ \frac{1}{1 + \frac{\sigma a}{16\lambda}} & \text{thrust in hover} \end{cases}$$

(see ref. 33). A time lag in the inflow response to loading changes will also be included:

$$\begin{pmatrix} \tau_T \dot{\lambda}_u \\ \tau_M \dot{\lambda}_x \\ \tau_M \dot{\lambda}_y \end{pmatrix} + \begin{pmatrix} \lambda_u \\ \lambda_x \\ \lambda_y \end{pmatrix} = L \begin{pmatrix} \tilde{c}_T \\ -c_{My} \\ c_{Mx} \end{pmatrix}$$

using $\tau_T = \kappa_T \delta\lambda/\delta T$ and $\tau_M = \kappa_M \delta\lambda/\delta M$, with the constants $\kappa_T = .85$ and $\kappa_M = .11$ (refs. 34 to 36). These relations give a dimensional time lag of $\tau \approx .22/\lambda\Omega$ in hover, and in forward flight $\tau_T = .42/\mu\Omega$ and $\tau_M = .22/\mu\Omega$.

The effect of the ground on the inflow dynamics is to add a perturbation due to changes in the rotor height above the ground:

$$\delta\lambda = \frac{\partial\lambda}{\partial z} \delta z$$

As for the trim inflow analysis, the result of reference 4 for the ratio of the induced velocity in and out of ground effect is used:

$$\frac{v_\infty}{v} = \frac{T}{T_\infty} = \frac{1}{1 - \left(\frac{\cos\epsilon}{4z}\right)^2}$$

which gives

$$\frac{\partial\lambda}{\partial z} = \frac{\lambda_i \cos^2\epsilon}{8z^3}$$

Expressions for $\cos\epsilon$ and z are derived in section 2.4.3. Since $\delta\lambda/\delta z > 0$, ground effect introduces a positive spring to the rotorcraft flight dynamics. A decrease in the rotor height above the ground produces a decrease in the induced velocity, hence a rotor thrust increase that acts as a spring against the vertical height change.

For the side-by-side helicopter configuration, the antisymmetric dynamics exhibit an unstable roll oscillation due to interaction of the rotor wake

and ground. Such behavior can be included in the ground effect model derived here by using a negative value for $\delta\lambda/\delta z$ (a negative roll spring), which must be obtained from experimental data. In this case the inflow perturbations of the two rotors are related to the symmetric and antisymmetric height perturbations:

$$\begin{aligned}\delta\lambda_1 &= \frac{\partial\lambda}{\partial z_s} \delta z_s + \frac{\partial\lambda}{\partial z_A} \delta z_A \\ &= \frac{1}{2} \left(\frac{\partial\lambda}{\partial z_s} + \frac{\partial\lambda}{\partial z_A} \right) \delta z_1 + \frac{1}{2} \left(\frac{\partial\lambda}{\partial z_s} - \frac{\partial\lambda}{\partial z_A} \right) \delta z_2 \\ \delta\lambda_2 &= \frac{\partial\lambda}{\partial z_s} \delta z_s - \frac{\partial\lambda}{\partial z_A} \delta z_A \\ &= \frac{1}{2} \left(\frac{\partial\lambda}{\partial z_s} - \frac{\partial\lambda}{\partial z_A} \right) \delta z_1 + \frac{1}{2} \left(\frac{\partial\lambda}{\partial z_s} - \frac{\partial\lambda}{\partial z_A} \right) \delta z_2\end{aligned}$$

where δz_1 and δz_2 are the height perturbations at the two rotor hubs. A form applicable in general is

$$\begin{aligned}\delta\lambda_1 &= \frac{\partial\lambda}{\partial z_1} \delta z_1 + \frac{\partial\lambda}{\partial z_{12}} \delta z_2 \\ \delta\lambda_2 &= \frac{\partial\lambda}{\partial z_{21}} \frac{R_1}{R_2} \delta z_1 + \frac{\partial\lambda}{\partial z_2} \frac{R_1}{R_2} \delta z_2\end{aligned}$$

including the factor R_1/R_2 since the hub motion is normalized using R_1 .

Finally, the rotor/rotor interference is included in the inflow dynamics model, using the same interference factors κ_{12} and κ_{21} as for the trim induced velocity model (see section 2.4.3).

In summary, the differential equations for the inflow perturbations λ_x and λ_y are:

$$k_M \frac{\partial \lambda}{\partial M} \begin{pmatrix} \dot{\lambda}_x \\ \dot{\lambda}_y \end{pmatrix} + \begin{pmatrix} \lambda_x \\ \lambda_y \end{pmatrix} - \frac{\sigma a}{2\gamma} \begin{bmatrix} k_x \frac{\partial \lambda}{\partial T} & \frac{\partial \lambda}{\partial M} & 0 \\ k_y \frac{\partial \lambda}{\partial T} & 0 & \frac{\partial \lambda}{\partial M} \end{bmatrix} \begin{pmatrix} \gamma \frac{2C_T}{\sigma a} \\ -\gamma \frac{2C_{M_y}}{\sigma a} \\ \gamma \frac{2C_{M_x}}{\sigma a} \end{pmatrix}_{\text{zero}} = 0$$

for rotor #1 and for rotor #2. The coupled equations for the uniform inflow perturbations of the two rotors are:

$$\begin{aligned} & \left(\left(k_T \frac{\partial \lambda}{\partial T} \right)_1 \dot{\lambda}_{u_1}, \dot{\lambda}_{u_1} \right) + \left(\lambda_{u_1} \right. \\ & \quad \left. \left(k_T \frac{\partial \lambda}{\partial T} \right)_2 \dot{\lambda}_{u_2} \right) \\ & - \begin{bmatrix} 1 & k_{12} \frac{(SQR)_2}{(SQR)_1} \\ k_{21} \frac{(SQR)_1}{(SQR)_2} & 1 \end{bmatrix} \left\{ \begin{array}{l} \left(\frac{\sigma a}{2\gamma} \frac{\partial \lambda}{\partial T} \right)_1 \left(\gamma \frac{2C_T}{\sigma a} \right)_{\substack{\text{rotor \#1} \\ \text{zero}}} \\ \left(\frac{\sigma a}{2\gamma} \frac{\partial \lambda}{\partial T} \right)_2 \left(\gamma \frac{2C_T}{\sigma a} \right)_{\substack{\text{rotor \#2} \\ \text{zero}}} \end{array} \right\} \\ & + \begin{bmatrix} \frac{\partial \lambda}{\partial z_1} & \frac{\partial \lambda}{\partial z_{1,2}} \\ \frac{\partial \lambda}{\partial z_1} \frac{R_1}{R_2} & \frac{\partial \lambda}{\partial z_2} \frac{R_1}{R_2} \end{bmatrix} \left\{ \begin{array}{l} \delta z_{\text{hub\#1}} \\ \delta z_{\text{hub\#2}} \end{array} \right\} = 0 \end{aligned}$$

The velocity perturbations δu_x , δu_y , and δu_z are required for

$$\gamma \frac{2C_T}{\sigma a} = \gamma \frac{2C_T}{\sigma a} - \frac{(\gamma 2C_T/\sigma a)_{\text{trim}}}{(\mu^2/k_f^2 + \lambda^2/k_a^2)} \left(\frac{\mu_x}{k_f^2} \delta u_x + \frac{k_y}{k_f^2} \delta u_y + \frac{\lambda}{k_a^2} \delta u_z \right)$$

In shaft axes, the shaft motion and gusts give

$$\delta u_x = -\dot{x}_h + u_g$$

$$\delta u_y = \dot{y}_h + v_g$$

$$\delta u_z = \dot{z}_h - w_g$$

The rotor height perturbation δ_z is obtained from the vertical component of the displacement at the rotor hub:

$$\begin{aligned}\delta z &= -\vec{k}_E \cdot (\vec{x}_h \vec{i}_s + \vec{y}_h \vec{j}_s + \vec{z}_h \vec{k}_s) \\ &= -\vec{k}_E \cdot \left(\sum_k \tilde{\vec{\xi}}_k(\vec{r}_{hub}) q_{sk} \right)\end{aligned}$$

expressing the hub motion in terms of airframe degrees of freedom. For the rigid body degrees of freedom the mode shapes are:

$$[\tilde{\vec{\xi}}_1 \dots \tilde{\vec{\xi}}_6] = [(-\vec{r}_{hub} x) \vec{r}_E \quad I]$$

(section 4.2.1). Hence

$$\begin{aligned}-\delta z &= (-\vec{z}_{hub} \cos \theta_{FT} \sin \phi_{FT} + \vec{y}_{hub} \cos \theta_{FT} \cos \phi_{FT}) \phi_F \\ &\quad + (-\vec{z}_{hub} \sin \theta_{FT} \cos \phi_{FT} - \vec{y}_{hub} \sin \theta_{FT} \sin \phi_{FT} \\ &\quad \quad \quad - \vec{x}_{hub} \cos \theta_{FT}) \theta_F \\ &\quad + (-\sin \theta_{FT}) x_F + (\cos \theta_{FT} \sin \phi_{FT}) y_F \\ &\quad + (\cos \theta_{FT} \cos \phi_{FT}) z_F \\ &\quad + \sum_{k=1}^{\infty} \vec{k}_E \cdot \tilde{\vec{\xi}}_k(\vec{r}_{hub}) q_{sk}\end{aligned}$$

Note that a spring is introduced into the z_F equation (if $\cos\theta_{FT}\cos\phi_{FT} \neq 0$), and also possibly into the y_F and x_F equations.

The time lag is often not an important factor, so a quasistatic model for the inflow dynamics is generally sufficient. Dropping the time lag terms, the equations for λ_u , λ_x , and λ_y reduce to linear algebraic equations. Hence in the quasistatic case the inflow perturbations do not increase the order of the system. The wake influence reduces to an algebraic substitution relation, which if incorporated analytically would lead to lift deficiency functions; with large-order systems, it is more practical to accomplish the substitution numerically.

6.1.6 Rotor equations of motion.- The linear differential equations of motion for the rotor model can be constructed now. The equations of motion are in the nonrotating frame, that is the Fourier coordinate transformation has been applied to the bending and torsion degrees of freedom of the blade. For now only a three-bladed rotor is considered; the equations are extended to an arbitrary number of blades below. The equations of motion for the rotor, and the hub reactions, take the following form:

$$A_2 \ddot{x}_R + A_1 \dot{x}_R + A_0 x_R + \tilde{A}_2 \ddot{\alpha} + \tilde{A}_1 \dot{\alpha} = B v_R + M_{aero}$$

$$F = C_2 \ddot{x}_R + C_1 \dot{x}_R + C_0 x_R + \tilde{C}_2 \ddot{\alpha} + \tilde{C}_1 \dot{\alpha} + F_{aero}$$

The coefficient matrices are constructed from the results of section 6.1.2. Here the matrices only include the structural and inertial terms; M_{aero} and F_{aero} are the aerodynamic forces. The vectors of the rotor degrees of freedom (x_R), shaft motion (α), rotor blade pitch input (v_R), aerodynamic gust (g_s , in shaft axes), and the hub forces and moments (F) are defined as:

$$x_R = [\beta_0^{(k)} \beta_{IC}^{(k)} \beta_{IS}^{(k)} \theta_0^{(k)} \theta_{IC}^{(k)} \theta_{IS}^{(k)} \beta_{SC} \beta_{SS} \psi_s \lambda_i \lambda_x \lambda_y]^T$$

$$v_R = [\theta_0^{\text{con}} \theta_{IC}^{\text{con}} \theta_{IS}^{\text{con}}]^T$$

$$g_s = [u_s \ v_g \ w_g]^T$$

$$\omega = [x_R \ y_R \ z_R \ \alpha_x \ \alpha_y \ \alpha_z]^T$$

$$F = \left[\gamma \frac{2C_y}{\omega} \quad \gamma \frac{2C_y}{\omega} \quad \gamma \frac{2C_T}{\omega} \quad \gamma \frac{2C_{Mx}}{\omega} \quad \gamma \frac{2C_{My}}{\omega} \quad -\gamma \frac{2C_M}{\omega} \right]^T$$

Note that in the rotor degrees of freedom x_R , the notation $\beta^{(k)}$ and $\theta^{(k)}$ is intended to cover as many bending and torsion modes as the analysis requires. Also, the degrees of freedom used for the inflow dynamics model are Λ_u , Λ_x , and Λ_y defined by $\dot{\Lambda} = \lambda$ (in order that the highest order derivatives will be $\ddot{\Lambda}$, in the acceleration matrix). The inertial matrices are defined in section 6.4.1.

The aerodynamic terms M_{aero} and F_{aero} are required to complete the differential equations of the rotor model. They are obtained by summing over all N blades the aerodynamic forces in the rotating frame (section 6.1.4) and introducing the Fourier coordinate transformation for the blade bending and torsion degrees of freedom as required. The result for the required aerodynamic forces is

$$-M_{aero} = A_1 \dot{x}_R + A_0 x_R + \tilde{A}_1 \dot{\alpha} + \tilde{A}_0 \alpha - B_6 q_s$$

$$F_{aero} = C_1 \dot{x}_R + C_0 x_R + \tilde{C}_1 \dot{\alpha} + \tilde{C}_0 \alpha + D_6 q_s$$

For the case of a rotor operating in axial flow ($\mu = 0$) the aerodynamic coefficients for the blade forces in the rotating frame are constants, independent of the blade azimuth angle ψ_m . The coefficients are also then entirely independent of the blade index (m); hence the summation over the N blades operates only on the system degrees of freedom, not on the aerodynamic coefficients themselves (which factor out of the summation). The resulting coefficient matrices, which are constant for axial flow, are defined in section 6.4.2.

For the case of a rotor operating in nonaxial flow ($\mu > 0$) the aerodynamic coefficients of the rotating blade forces are periodic functions of ψ_m because of the periodically varying aerodynamics of the edgewise moving rotor.

It follows that the rotor in nonaxial flight is described by a system of differential equations with periodic coefficients. It is possible to express the aerodynamic coefficient of the rotating blade forces as Fourier series, and then to obtain the coefficients of the nonrotating equations in terms of these harmonics. However, the simplest approach for numerical work with large-order systems is to leave the coefficients of the nonrotating equations in terms of the summation over the N blades of the rotor. The summation is easily performed numerically, and it is found that this form is also appropriate for a constant coefficient approximation to the system. For nonaxial flow, the coefficient matrices are periodic functions of the blade azimuth angle $\psi_m = \psi + m\Delta\psi$, $\Delta\psi = 2\pi/N$. The period is $\Delta\psi = (2/3)\pi = 120^\circ$ for the $N = 3$ case considered here. The coefficient matrices for nonaxial flow are defined in section 6.4.3.

The rotor equations as constructed here are not entirely complete. First, the rotor aerodynamic thrust and hub moments:

$$-\gamma \frac{\partial \tilde{C}_T}{\partial \alpha} = -(\gamma \frac{\partial C_T}{\partial \alpha})_{aero} + \frac{\partial \lambda}{\partial \mu} \left[\frac{\mu_n}{k_f^2} (-\dot{x}_n + u_G) + \frac{\mu_n}{k_f^2} (v_n + v_G) + \frac{\lambda}{k_n^4} (\dot{z}_n - w_G) \right]$$

$$(\gamma \frac{\partial C_{Th}}{\partial \alpha})_{aero}$$

$$(\gamma \frac{\partial C_{Mx}}{\partial \alpha})_{aero}$$

where

$$\frac{\partial \lambda}{\partial \mu} = \frac{(\gamma \frac{\partial C_T}{\partial \alpha})_{aero}}{\mu^2/k_f^2 + \lambda^2/k_n^4}$$

have been put in place for the λ_u , λ_x , and λ_y equations. Because of the rotor/rotor interference and ground effect, it is appropriate to finish the construction of these equations at a later stage (section 6.3.1).

Secondly, we have substituted in the equation of motion for rigid pitch:

$$\dot{\theta}_{con} = \sum_i K_{pi} q_i - k_{pg} \beta_g + (\theta_{1c} \cos \psi_m - \theta_{1c} \sin \psi_m) \psi_s$$

However, the rotor pitch control θ_{con} here still includes the governor and mast bending terms, as well as external control inputs.

Thirdly, the rotor torque $\gamma C_Q / \sigma a$ has been put in place as the equations of motion for the rotational speed perturbation ψ_s . The drive train couples the rotational speed perturbations of the two rotors, so it is necessary to construct these equations at a later stage (section 6.3.1).

Consider now the case of a rotor with four or more blades. Each rotating degree of freedom of the blade (bending or torsion motion) must result in N degrees of freedom for the rotor as a whole. Thus increasing the number of blades adds degrees of freedom and equations of motion to the rotor description. In axial flow these additional degrees of freedom do not couple with the collective and cyclic degrees of freedom of the rotor. Hence the equations given above remain valid for rotors with $N > 3$ also, and we need be concerned here only with the equations of motion for the additional degrees of freedom. These additional degrees of freedom are not coupled inertially with the shaft or gimbal motion. The additional equations of motion for bending and torsion of a rotor blade with four or more blades are then:

$$A_2 \ddot{x}_R + A_1 \dot{x}_R + A_0 x_R = B v_R + M_{aero}$$

with the vectors of the degrees of freedom and blade pitch control here defined as follows:

$$x_R = [\beta_{nc}^{(k)} \beta_{ns}^{(k)} \beta_{n/2}^{(k)} \theta_{nc}^{(k)} \theta_{ns}^{(k)} \theta_{n/2}^{(k)}]^T$$

$$v_R = [\theta_{nc}^{con} \theta_{ns}^{con} \theta_{n/2}^{con}]^T$$

The inertial coefficient matrices are given in section 6.1.4.

The aerodynamic forces are required to complete the equations of motion. In axial flow the aerodynamic forces still do not couple the additional degrees of freedom for $N \geq 4$ with the shaft or gimbal motion. Hence the aerodynamic forces for axial flow take the form

$$-M_{aero} = A_1 \dot{x}_R + A_0 x_R$$

with the coefficient matrices defined in section 6.1.5.

The aerodynamic forces in nonaxial flow ($\mu > 0$) couple all degrees of freedom of the rotor with each other and with the shaft and gimbal motion. Then not only are additional degrees of freedom and equations of motion involved if $N > 3$, but the number of blades also influences the equations and the hub reactions given above. Rather than directly presenting the aerodynamic matrices for the general case of three or more blades in nonaxial flow, the analysis is extended by means of an observed pattern in the coefficients. In the nonaxial flow equations (section 6.4.3), note the repeated occurrence of the following submatrices:

$$P = \begin{bmatrix} 1 & C_1 & S_1 \\ 2C_1 & 2C_1^2 & 2C_1S_1 \\ 2S_1 & 2C_1S_1 & 2S_1^2 \end{bmatrix} = \begin{pmatrix} 1 \\ 2C_1 \\ 2S_1 \end{pmatrix} (1 \ C_1 \ S_1)$$

$$DP = \begin{bmatrix} 0 & -S_1 & C_1 \\ 0 & -2C_1S_1 & 2C_1^2 \\ 0 & -2S_1^2 & 2C_1S_1 \end{bmatrix} = \begin{pmatrix} 1 \\ 2C_1 \\ 2S_1 \end{pmatrix} (0 \ -S_1 \ C_1)$$

(using the notation $S_n = \sin n\psi_m$ and $C_n = \cos n\psi_m$). These matrices are a direct result of the introduction of the Fourier coordinate transformation (columns) and the application of the summation operators to obtain the non-rotating equations (rows). The matrix DP arises from application of the

Fourier transformation to the time derivatives (\dot{q}_i or \dot{p}_i). In the B_G and \tilde{A} matrices, only some columns of P and DP appear, while in the C matrices only some rows appear. The extension to an arbitrary number of blades ($N \geq 3$) is then simply

$$P = \begin{pmatrix} 1 \\ 2C_1 \\ 2S_1 \\ \vdots \\ 2C_n \\ 2S_n \\ (-1)^m \end{pmatrix} (1 \ C_1 \ S_1 \ \dots \ C_n \ S_n \ (-1)^m)$$

$$DP = \begin{pmatrix} 1 \\ 2C_1 \\ 2S_1 \\ \vdots \\ 2C_n \\ 2S_n \\ (-1)^m \end{pmatrix} (0 \ -S_1 \ C_1 \ \dots \ -nS_n \ nC_n \ 0)$$

Rotors with three or more blades may be analyzed within the same general framework, but the two-bladed rotor is a special case. The rotor with $N \geq 3$ has axi-symmetric inertial and structural properties and hence the nonrotating frame equations have constant coefficients in axial flow.

In contrast, the lack of axi-symmetry with two blades leads to periodic coefficient differential equations, even in the inertial terms and in axial flow. Only in special cases are the dynamics of a two-bladed rotor described by constant coefficient equations. The equations of motion again take the form

$$\ddot{A}_2 \ddot{x}_R + A_1 \dot{x}_R + A_0 x_R + \tilde{\ddot{A}}_2 \ddot{\alpha} + \tilde{\ddot{A}}_1 \dot{\alpha} = B v_R + M_{aero}$$

$$F = C_2 \ddot{x}_R + C_1 \dot{x}_R + C_0 x_R + \tilde{\ddot{C}}_2 \ddot{\alpha} + \tilde{\ddot{C}}_1 \dot{\alpha} + F_{aero}$$

with now for $N = 2$ the rotor degrees of freedom and pitch input defined as follows:

$$x_R = [\beta_0^{(k)} \quad \beta_1^{(k)} \quad \theta_0^{(k)} \quad \theta_1^{(k)} \quad \beta_T \quad \eta_s \quad \lambda_u \quad \lambda_x \quad \lambda_y]^T$$

$$v_R = [\theta_0^{\text{con}} \quad \theta_1^{\text{con}}]^T$$

The inertial coefficient matrices are defined in section 6.4.6. Note that there are periodic coefficients in the matrices coupling the rotor and shaft motion (\tilde{A} , C , \tilde{C}).

The required aerodynamic forces for the two-bladed rotor case again take the form

$$-M_{aero} = A_1 \dot{x}_R + A_0 x_R + \tilde{\ddot{A}}_1 \dot{\alpha} + \tilde{\ddot{A}}_0 \alpha - B_G g_s$$

$$F_{aero} = C_1 \dot{x}_R + C_0 x_R + \tilde{\ddot{C}}_1 \dot{\alpha} + \tilde{\ddot{C}}_0 \alpha + D_G g_s$$

The aerodynamic coefficient matrices are defined in section 6.4.7.

An independent blade analysis is useful for problems not involving the shaft motion or other excitation from the nonrotating frame. The only rotor blade degrees of freedom involved are the bending and torsion motion. The shaft motion, gimbal motion, and the rotor speed perturbation are dropped

from the system. Only a single blade need be analyzed, in the rotating frame. The equations of motion for the bending and torsion modes are then:

$$\begin{aligned} I_{q_k}^* (\ddot{q}_k + g_s \omega_k \dot{q}_k + \omega_k^2 q_k) + 2 \sum_i I_{q_k \dot{q}_i}^* \dot{q}_i \\ - \sum_i S_{q_k \dot{p}_i}^* \ddot{p}_i - \sum_i S_{q_k p_i}^* p_i \\ - \sum_i \delta M_{q_k \dot{q}_i} \dot{q}_i - \sum_i \delta M_{q_k q_i} q_i - \sum_i \delta M_{q_k p_i} p_i = 0 \end{aligned}$$

$$\begin{aligned} I_{p_k}^* (\ddot{p}_k + g_s \omega_k \dot{p}_k + \omega_k^2 p_k) + \sum_i I_{p_k \dot{p}_i}^* \ddot{p}_i + \sum_i I_{p_k p_i}^* p_i \\ - \sum_i S_{p_k \dot{q}_i}^* \ddot{q}_i - \sum_i (S_{p_k q_i}^* - k_{p_i} S_{p_k 0}^*) q_i \\ - \sum_i \delta M_{p_k \dot{q}_i} \dot{q}_i - \sum_i \delta M_{p_k q_i} q_i \\ - \sum_i \delta M_{p_k p_i} p_i - \sum_i \delta M_{p_k \dot{p}_i} \dot{p}_i = S_{p_k 0}^* \theta_{con} \end{aligned}$$

or

$$A_2 \ddot{x}_R + A_1 \dot{x}_R + A_0 x_R = B v_R$$

with $x_R = (q_k \ p_k)^T$ and $v_R = \theta_{con}$. These equations can also be obtained by dropping all degrees of freedom except the collective modes from the analysis above; a separate construction for the independent blade case is more efficient however.

6.1.7 Constant coefficient approximation. - The rotor dynamics in non-axial flow are described by a set of linear differential equations with periodic coefficients. A constant coefficient approximation for nonaxial flow is desirable (if it is demonstrated to be accurate enough) because the calculation required to analyze the dynamic behavior is reduced considerably compared to that for the periodic coefficient equations, and because the powerful techniques for analyzing time-invariant linear differential equations are then applicable. However, such a model is only an approximation to the

correct aeroelastic behavior. The accuracy of the approximation must be determined by comparison with the correct periodic coefficient solutions. The constant coefficient approximation derived here uses the mean values of the periodic coefficients of the differential equations in the nonrotating frame.

To find the mean value of the coefficients, the operator

$$\frac{1}{2\pi} \int_0^{2\pi} (\dots) d\psi$$

is applied to the periodic aerodynamic coefficients (given in section 6.4.3), resulting in terms of the following form for the $N = 3$ case:

$$\begin{aligned} & \frac{1}{2\pi} \int_0^{2\pi} \frac{1}{N} \sum_m \begin{pmatrix} 1 \\ \cos \psi_m \\ \sin \psi_m \\ 2 \cos^2 \psi_m \\ 2 \sin^2 \psi_m \\ 2 \sin \psi_m \cos \psi_m \end{pmatrix} M(\psi_m) d\psi \\ &= \frac{1}{N} \sum_m \frac{1}{2\pi} \int_0^{2\pi} \begin{pmatrix} 1 \\ \cos \psi_m \\ \sin \psi_m \\ 2 \cos^2 \psi_m \\ 2 \sin^2 \psi_m \\ 2 \sin \psi_m \cos \psi_m \end{pmatrix} M(\psi_m) d\psi_m = \begin{pmatrix} M^0 \\ \frac{1}{2} M^{1c} \\ \frac{1}{2} M^{1s} \\ M^0 + \frac{1}{2} M^{2c} \\ M^0 - \frac{1}{2} M^{2s} \\ \frac{1}{2} M^{2s} \end{pmatrix} \end{aligned}$$

Here M^{nc} and M^{ns} are the harmonics of a Fourier series representation of the rotating blade aerodynamic coefficient M :

$$M(\psi_m) = M^0 + \sum_{n=1}^{\infty} M^{nc} \cos n\psi_m + M^{ns} \sin n\psi_m$$

In the present case, these harmonics must be evaluated numerically. The aerodynamic coefficient M is calculated at J points, equally spaced around the azimuth. Then the harmonics are calculated using the Fourier interpolation formulas:

$$M^o = \frac{1}{J} \sum_j M(\psi_j)$$

$$M^{nc} = \frac{1}{J} \sum_j M(\psi_j) \cos n\psi_j$$

$$M^{ns} = \frac{1}{J} \sum_j M(\psi_j) \sin n\psi_j$$

where $\psi_j = j\Delta\psi = j(2\pi/J)$ ($j = 1, \dots, J$). The number of harmonics required is $n = N-1$ for N odd and $n = N-2$ for N even (N is the number of blades). Good accuracy from the Fourier interpolation requires at least that $J = 6n$. Using these Fourier interpolation expressions, the required harmonics are

$$\begin{vmatrix} M^o \\ \frac{1}{2}M^{nc} \\ \frac{1}{2}M^{ns} \\ M^o + \frac{1}{2}M^{2c} \\ M^o - \frac{1}{2}M^{2c} \\ \frac{1}{2}M^{2s} \end{vmatrix} = \frac{1}{J} \sum_j \begin{vmatrix} 1 \\ \cos \psi_j \\ \sin \psi_j \\ 2\cos^2 \psi_j \\ 2\sin^2 \psi_j \\ 2\sin \psi_j \cos \psi_j \end{vmatrix} M(\psi_j)$$

It follows then that the constant coefficient approximation is obtained from the periodic coefficient expressions by the simple transformation:

$$\frac{1}{N} \sum_{m=1}^N (\dots) M(\psi_m) \Rightarrow \frac{1}{J} \sum_{j=1}^J (\dots) M(\psi_j)$$

The summation over N blades ($m = 1, \dots, N$; $\Delta\psi = 2\pi/N$) for a periodic coefficient is replaced by a summation over the rotor azimuth ($j = 1, \dots, J$; $\Delta\psi = 2\pi/J$) for the constant coefficient approximation. This is quite convenient since the same procedure may be used to evaluate the coefficients for the two cases, with simply a change in the azimuth increment. The periodic

coefficients must be evaluated throughout the period of $\psi = 0$ to $2\pi/N$; the constant coefficient approximation (mean values only) is evaluated only once.

With the substitution $(1/N) \sum_m \rightarrow (1/J) \sum_j$, the results given in section 6.4.3 for the periodic coefficient matrices are directly applicable to the constant coefficient approximation as well.

For the case of a rotor with four or more blades, the constant coefficient approximation involves the transformation of higher order harmonics:

$$\frac{1}{N} \sum_{m=1}^N \begin{pmatrix} 1 \\ C_n \\ S_n \\ C_n C_\alpha \\ C_n S_\alpha \\ S_n S_\alpha \\ (-1)^m \\ C_n (-1)^m \\ S_n (-1)^m \end{pmatrix} M(\psi_m) \Rightarrow \frac{1}{J} \sum_{j=1}^J \begin{pmatrix} 1 \\ C_n \\ S_n \\ C_n C_\alpha \\ C_n S_\alpha \\ S_n S_\alpha \\ 0 \\ 0 \\ 0 \end{pmatrix} M(\psi_j)$$

So the periodic coefficient results are still applicable to the constant coefficient approximation if the summation over the N blades is replaced by a summation around the rotor azimuth.

This transformation is also applicable to the case of a two-bladed rotor, but the constant coefficient approximation is not as useful or as accurate for $N = 2$ as for $N \geq 3$. With three or more blades, the source of the periodic coefficients is nonaxial flow, hence the periodicity is order μ or smaller. At low advance ratio then, the constant coefficient approximation may be expected to be a good representation of the correct dynamics. The two-bladed rotor has also periodic coefficients due to the inherent lack of axi-symmetry of the rotor. This periodicity is large even for axial flow, and neglecting it in the constant coefficient approximation may be a poor representation of the dynamics. In particular, it is not possible to use the constant coefficient approximation as formulated here for the flight dynamics.

analysis of a two-bladed rotor helicopter, since this averaging eliminates the coupling between the rotor and the shaft motion.

6.2 Aircraft Model

6.2.1 *Aircraft degrees of freedom.* - The aircraft motion is described by the rigid body and elastic airframe degrees of freedom:

$$x_s = \{q_{sk}\} = [\phi_f \psi_f \chi_f \eta_f z_f q_{sk} (k \geq 7)]^T$$

as defined in section 4.2.1. The aircraft controls consist of flaperon, elevator, aileron, and rudder deflections:

$$v_s = [\delta_f \delta_e \delta_a \delta_r]^T$$

The rotor hub motion is obtained from

$$\dot{\alpha} = c x_s$$

where c is defined in section 4.2.2, including the sign changes for a clockwise rotating rotor and scaling for rotor #2. Recall that the Euler angles do not contribute to α_x , α_y , and α_z however. In addition there is a linear acceleration due to the rotation of the velocity vector in body axes by the Euler angular velocities, written

$$\ddot{\alpha} = \bar{c} \dot{x}_s$$

(see section 4.2.2).

The feedback of the airframe elastic motion to the rotor cyclic pitch is

$$\Delta\theta_{\text{west}} = - \sum_{i=7}^{\infty} q_{si} [k_{mc_i} \cos \Psi_m + k_{ms_i} \sin \Psi_m]$$

as defined in section 4.2.3.

6.2.2 Aircraft equations of motion.- The linearized equations of motion for the aircraft rigid body and elastic motion are:

$$\begin{bmatrix} R_e^T I^* R_e & 0 & 0 \\ 0 & M^* & 0 \\ 0 & 0 & M_k^* \end{bmatrix} \ddot{x}_s + \begin{bmatrix} 0 & 0 & 0 \\ -M^*(\vec{v}_x)R_e & 0 & 0 \\ 0 & 0 & M_k^* g_s w_k \end{bmatrix} \dot{x}_s \\ + \begin{bmatrix} 0 & 0 & 0 \\ G & 0 & 0 \\ 0 & 0 & M_k^* w_k^2 \end{bmatrix} x_s = \{ Q_k^* \}$$

(see section 4.2.4). The generalized forces due to the rotor hub reactions are

$$\{ Q_k^* \}_{\text{rotor}} = c^T F$$

where c^T is defined in section 4.2.5, including the sign changes for a clockwise rotating rotor and the scaling for rotor #2.

The generalized forces due to the aircraft aerodynamics can be linearized by successively perturbing the inputs to the analysis described in section 4.2.6. Hence for the rigid body degrees of freedom we obtain:

$$\{ Q_k^* \}_{\text{aero}} = a_2 \ddot{z}_F + a_1 \begin{pmatrix} \dot{\phi}_F \\ \dot{\theta}_F \\ \dot{\psi}_F \\ \dot{x}_F \\ \dot{y}_F \\ \dot{z}_F \end{pmatrix} + b \begin{pmatrix} \delta_F \\ \delta_e \\ \delta_a \\ \delta_r \end{pmatrix} + b_{1S} \begin{pmatrix} u_G \\ v_G \\ w_G \end{pmatrix} + b_{12} \begin{pmatrix} \lambda_{u_1} \\ \lambda_{u_2} \end{pmatrix}$$

(The coefficients of the matrices are the aircraft stability derivatives, due to the wing/body, horizontal tail, and vertical tail.) A gust velocity uniform throughout space is considered; hence the gust velocity components are the same at the wing/body and tail. The mean inflow perturbations influence the airframe through the rotor-induced aerodynamic interference, which is modelled as described in section 4.2.6. So the interference velocities at the wing and tail are obtained from

$$\begin{pmatrix} \vec{\lambda}_W \\ \vec{\lambda}_H \\ \vec{\lambda}_V \end{pmatrix} = \begin{bmatrix} K_{W1} C_{W1} R_{SF}^T (-\vec{k}_S) & K_{W2} C_{W2} R_{SF}^T (-\vec{k}_S) \\ K_{H1} C_{H1} R_{SF}^T (-\vec{k}_S) & K_{H2} C_{H2} R_{SF}^T (-\vec{k}_S) \\ K_{V1} C_{V1} R_{SF}^T (-\vec{k}_S) & K_{V2} C_{V2} R_{SF}^T (-\vec{k}_S) \end{bmatrix} \begin{pmatrix} \lambda_{u_1} \\ \lambda_{u_2} \end{pmatrix}$$

From section 4.2.7, the generalized forces for the airframe elastic degrees of freedom ($k \geq 7$) are:

$$(Q_k^*)_{aero} = \frac{2\gamma}{\sigma_a} \frac{q}{A} \left[-\frac{F_{q_k q_k}}{V} \dot{q}_k + F_{q_k \delta} \begin{pmatrix} \delta_f \\ \delta_e \\ \delta_a \\ \delta_r \end{pmatrix} \right]$$

Hence the aeroelastic motion of the helicopter airframe is described by a set of linear, constant coefficient differential equations of the form

$$a_2 \ddot{x}_S + a_1 \dot{x}_S + a_0 x_S = b v_S + b_G g + b_\lambda \begin{pmatrix} \lambda_{u_1} \\ \lambda_{u_2} \end{pmatrix} + c_1^T F_1 + c_2^T F_2$$

where x_s is the vector of aircraft degrees of freedom, v_s is the vector of aircraft control variables, g is the vector of gust velocity components (in wind axes), and F_1 and F_2 are the hub reactions of the two rotors.

6.2.3 *Drive train equations of motion.* - A model for the transmission and engine dynamics was derived in section 4.3.2. The degrees of freedom involved are the rotational speed perturbations of the two rotors ($\dot{\psi}_{s1}$ and $\dot{\psi}_{s2}$) and the engine speed perturbation (degree of freedom ψ_e , defined relative to the rotation of rotor #1). With the coupling of the rotors by the drive train, it is more appropriate to use the degrees of freedom defined by

$$\dot{\psi}_{s1} = \dot{\psi}_s, \quad \dot{\psi}_{s2} = (r_i / r_{i2}) \dot{\psi}_s + \dot{\psi}_I$$

or

$$\dot{\psi}_s = \dot{\psi}_{s1}, \quad \dot{\psi}_I = \dot{\psi}_{s2} - (r_i / r_{i2}) \dot{\psi}_{s1}$$

where $r_{i1} / r_{i2} = \Omega_2 / \Omega_1$ is the ratio of the trim rotational speeds of the two rotors. So $\dot{\psi}_s$ is the rotational speed perturbation of the rotors and drive train as a whole, while $\dot{\psi}_I$ represents differential rotation of the two rotors. The degrees of freedom ψ_I and ψ_e therefore involve elastic deflection of the drive train. The engine model introduces the throttle control variable θ_t . The linearized equations of motion for the drive train are then:

$$\begin{aligned} & \left(\frac{\partial C_Q}{\partial \alpha} \right)_1 + \frac{(N I_b \Sigma^3)_2}{(N I_b \Sigma^3)_1} \left(\frac{\partial C_Q}{\partial \alpha} \right)_2 \\ & + r_i^2 I_E^* (\ddot{\psi}_s + \ddot{\psi}_e) + r_i^2 Q_{\Sigma}^* (\dot{\psi}_s + \dot{\psi}_e) = r_i \omega_t^* \theta_t \\ \\ & - k_{M\psi_I} \left(\frac{\partial C_Q}{\partial \alpha} \right)_1 + \frac{(N I_b \Sigma^2)_2}{(N I_b \Sigma^2)_1} \left(\frac{\partial C_Q}{\partial \alpha} \right)_2 \\ & + k_{M\psi_I} (r_i^2 I_E^* \ddot{\psi}_I + r_i^2 Q_{\Sigma}^* \dot{\psi}_I) + k_{M\psi_I}^* \dot{\psi}_I = 0 \end{aligned}$$

$$c_E^2 I_E^* (\ddot{\psi}_s + \ddot{\psi}_e) + c_E^2 Q_{st}^* (\dot{\psi}_s + \dot{\psi}_e) \\ + K_{ME_1}^* \psi_e - K_{ME_2}^* \psi_x = c_E Q_t^* \theta_t$$

The constants appearing in these equations are defined in section 4.3.2 for several drive train configurations.

For the autorotation case the ψ_e degree of freedom is dropped, and the Q_Ω , Q_t , and I_E engine terms in the ψ_s and ψ_I equations are omitted. For the engine out case, with the engine and rotors still connected, the engine terms Q_Ω and Q_t are omitted. The case of constant rotor speed is treated by dropping the ψ_s and ψ_I degrees of freedom from the system.

The rotor speed governor, consisting of $\dot{\psi}_s$ and ψ_s feedback to the engine throttle and to the collective pitch of each rotor, is described by the following equations:

$$\tau_{ze} \ddot{\Delta\theta}_t + \tau_{1e} \Delta\dot{\theta}_t + \Delta\theta_t = -k_{pe} \dot{\psi}_s - k_{Ie} \psi_s \\ \tau_{z1} \ddot{\Delta\theta}_{govr_1} + \tau_{11} \Delta\dot{\theta}_{govr_1} + \Delta\theta_{govr_1} = k_{p1} \dot{\psi}_s + k_{I1} \psi_s \\ \tau_{z2} \ddot{\Delta\theta}_{govr_2} + \tau_{12} \Delta\dot{\theta}_{govr_2} + \Delta\theta_{govr_2} = k_{p2} \dot{\psi}_s + k_{I2} \psi_s$$

(see section 4.3.3). For the tilting proprotor configuration, the variable ψ_s is replaced by the symmetric variable $\psi_{sym} = \psi_s + 1/2 \psi_I$.

6.3 Coupled Rotor and Aircraft

6.3.1 Coupled equations of motion. - The equations of motion have been derived for the two rotors and the aircraft body. The rotor equations of motion take the form

$$A_2 \ddot{x}_R + A_1 \dot{x}_R + A_0 x_R + \tilde{A}_2 \ddot{\alpha} + \tilde{A}_1 \dot{\alpha} + \tilde{A}_0 \alpha = B v_R + B_G g_s$$

$$f = C_2 \ddot{x}_R + G \dot{x}_R + C_0 x_R + \tilde{C}_2 \ddot{\alpha} + \tilde{G} \dot{\alpha} + \tilde{C}_0 \alpha + D_G g_s$$

(see section 6.1.6). The rotor degrees of freedom vector x_R consists of flap/lag bending, rigid pitch and elastic torsion, gimbal or teeter motion, rotational speed, and inflow perturbations. The rotor control vector v_R consists of the blade pitch control. The gust vector in shaft axes is related to the gust vector in velocity axes by

$$g_s = R_G g$$

(section 4.1.4). The hub motion is related to the aircraft degrees of freedom by

$$\alpha = c x_s$$

$$\dot{\alpha} = c \dot{x}_s$$

$$\ddot{\alpha} = c \ddot{x}_s + \bar{c} \dot{x}_s$$

(section 4.2.2; only the 3×3 submatrix in the upper left corner of \bar{c} is nonzero). For rotor #2 it is necessary to change the time scale to the rotational speed of rotor #1.

$$\frac{\partial}{\partial \bar{\tau}_2 t} = \frac{\bar{\tau}_1}{\bar{\tau}_2} \frac{\partial}{\partial \tau_1 t}$$

So the matrices A_1 , \tilde{A}_1 , C_1 , and \tilde{C}_1 are multiplied by (Ω_1/Ω_2) ; and the matrices A_2 , \tilde{A}_2 , C_2 , \tilde{C}_2 are multiplied by $(\Omega_1/\Omega_2)^2$.

The aircraft equations of motion take the form

$$\begin{aligned} a_2 \ddot{x}_s + a_1 \dot{x}_s + a_0 x_s &= b v_s + b_G g + b_\lambda \begin{pmatrix} \dot{\lambda}_{u_1} \\ (\bar{\tau}_1/\bar{\tau}_2) \dot{\lambda}_{u_2} \end{pmatrix} \\ &\quad + C_{R1}^T F_{R1} + C_{R2}^T F_{R2} \end{aligned}$$

(see section 6.2.2). The vector x_s consists of the aircraft rigid body and elastic airframe degrees of freedom. The vector v_s consists of the aircraft controls.

The equations for the rotor and aircraft can now be combined to construct the set of linear differential equations that describes the dynamics of the complete system. These equations take the following form:

$$A_2 \ddot{x} + A_1 \dot{x} + A_0 x = Bv + B_p v_p + B_g g$$

The state vector x , control vectors v and v_p , and the gust vector g are defined as:

$$x = \begin{bmatrix} (\beta^{(k)} \theta^{(k)} \beta_{GC} \beta_{GS})_{\text{rotor}\#1} \psi_s \lambda_u, \lambda_x, \lambda_y, \\ (\beta^{(k)} \theta^{(k)} \beta_{GC} \beta_{GS})_{\text{rotor}\#2} \psi_I \lambda_{u2} \lambda_{x2} \lambda_{y2} \\ \psi_F \theta_F \lambda_F x_F y_F z_F q_{sx}^{(k \geq 7)} \psi_e \Delta\theta_t \Delta\theta_{gov1}, \Delta\theta_{gov2} \end{bmatrix}^T$$

$$v = \begin{bmatrix} \theta_{\text{rotor}\#1}^{\text{con}} \theta_{\text{rotor}\#2}^{\text{con}} \delta_f \delta_c \delta_a \delta_r \theta_t \end{bmatrix}^T$$

$$v_p = \begin{bmatrix} \delta_a \delta_c \delta_s \delta_r \delta_t \end{bmatrix}^T$$

$$g = \begin{bmatrix} u_g v_g w_g \end{bmatrix}^T$$

The vector of the degrees of freedom for the entire system (x) consists of the degrees of freedom of the two rotors and the aircraft. The rotational speed degrees of freedom of the two rotors are replaced by the coupled degrees of freedom ψ_s and ψ_I ; and the engine speed degree of freedom ψ_e is added. The governor dynamics introduce the degrees of freedom $\Delta\theta_t$, $\Delta\theta_{gov1}$, $\Delta\theta_{gov2}$. The vector of control variables for the entire system (v) consists of the blade pitch of the two rotors, the aircraft controls, and the engine throttle. The vector of the pilot's controls (v_p) is related to the individual control inputs by the linear transformation

$$v = T_{CFE} v_p$$

where T_{CFE} is defined in section 4.1.6. The aerodynamic gust vector (g) is in velocity axes.

The coupled equations of motion are obtained by substituting the hub motion into the rotor equations and hub reactions, and then the hub reactions into the body equations of motion. The resulting coefficient matrices for the coupled system are:

A_{2R1}		$\tilde{A}_{2R1} C_{R1}$
$A_2 =$	$\left(\frac{S_{L1}}{S_{L2}}\right)^2 A_{2R2}$	$\left(\frac{S_{L1}}{S_{L2}}\right)^2 \tilde{A}_{2R2} C_{R2}$
	$-C_{R1}^T C_{2R1} - \left(\frac{S_{L1}}{S_{L2}}\right)^2 C_{R2}^T C_{2R2}$	$a_2 - C_{R1}^T \tilde{C}_{2R1} C_{R1} - \left(\frac{S_{L1}}{S_{L2}}\right)^2 C_{R2}^T \tilde{C}_{2R2} C_{R2}$
A_{1R1}		$\tilde{A}_{1R1} C_{R1} + \tilde{A}_{2R1} \bar{C}_{R1}$
$A_1 =$	$\left(\frac{S_{L1}}{S_{L2}}\right) A_{1R2}$	$\left(\frac{S_{L1}}{S_{L2}}\right) \tilde{A}_{1R2} C_{R2} + \left(\frac{S_{L1}}{S_{L2}}\right)^2 \tilde{A}_{2R2} \bar{C}_{R2}$
	$-C_{R1}^T C_{1R1} - \left(\frac{S_{L1}}{S_{L2}}\right)^2 C_{R2}^T C_{1R2}$	$a_1 - C_{R1}^T \tilde{C}_{1R1} C_{R1} - \left(\frac{S_{L1}}{S_{L2}}\right)^2 C_{R2}^T \tilde{C}_{1R2} C_{R2}$ $-C_{R1}^T \tilde{C}_{2R1} \bar{C}_{R1} - \left(\frac{S_{L1}}{S_{L2}}\right)^2 C_{R2}^T \tilde{C}_{2R2} \bar{C}_{R2}$
A_{0R1}		$\tilde{A}_{0R1} C_{R1}$
$A_0 =$	A_{0R2}	$\tilde{A}_{0R2} C_{R2}$
	$-C_{R1}^T C_{0R1} - C_{R2}^T C_{0R2}$	$a_0 - C_{R1}^T \tilde{C}_{0R1} C_{R1} - C_{R2}^T \tilde{C}_{0R2} C_{R2}$

B_{R1}			
	B_{R2}		
		k_s	

$B_{GR1} R_{GR1}$
$B_{GR2} R_{GR2}$
$b_G + \bar{c}_{R1}^T D_{GR1} R_{GR1} + \bar{c}_{R2}^T D_{GR2} R_{GR2}$

Recall that the Euler angle contributions are not to be included in α_x , α_y , and α_z . Hence in constructing A_o it is necessary to skip the angular hub motion (α_x , α_y , α_z) columns of \tilde{A}_o and \tilde{C}_o for the Euler angle (ϕ_F , θ_F , ψ_F) columns of c (and A_o) when evaluating $\tilde{A}_o c$ and $\tilde{C}_o c$.

The rotor mass will be included in the helicopter gross weight. Hence in constructing A_2 it is necessary to skip the linear hub motion (x_h , y_h , z_h) columns of \tilde{C}_2 for the rigid body (ϕ_F , θ_F , ψ_F , x_F , y_F , z_F) columns of c (and A_2) when evaluating $\tilde{C}_2 c$. Also the rotor mass is included in the generalized mass of the airframe free vibration modes; so the linear hub motion columns of \tilde{C}_2 will be skipped for all the body degrees of freedom columns of c when evaluating $\tilde{C}_2 c$. This approach is also required for the $c^T \tilde{C}_2 c$ term in A_1 . Since the term involving \tilde{c} is the linear hub acceleration due to Euler angle velocities, which has already been included in a_1 if the gross weight includes the rotor mass, it follows that the entire $c^T \tilde{C}_2 \tilde{c}$ term is to be dropped.

The construction of the coupled equations of motion is still incomplete. The matrices defined above basically account for the coupling of the rotors and aircraft through the rotor hubs. It remains to account for the coupling which occurs through other paths.

Frequently the rotor is modelled as having a rigid control system. This option requires some restructuring of the equations of motion, since the rotor equations have been derived assuming that the blade rigid pitch degrees of freedom are present in the model and that the blade pitch control inputs enter through these degrees of freedom. In the limit of infinite control system stiffness, the solution of the rigid pitch equation of motion reduces to

$$\ddot{\theta}_0 = \ddot{\theta}_r = \dot{\theta}_{con} - \sum_i k_{p_i} q_i - k_{p_G} \beta_G + (\theta_{1S} \cos \psi_m - \theta_{1C} \sin \psi_m) \psi_s$$

or in the nonrotating frame

$$\begin{pmatrix} \theta_0 \\ \theta_{1C} \\ \theta_{1S} \\ \theta_{nC} \\ \theta_{nS} \\ \theta_{N/2} \end{pmatrix}_0 = \begin{pmatrix} \theta_0 \\ \theta_K \\ \theta_{1S} \\ \theta_{nC} \\ \theta_{nS} \\ \theta_{N/2} \end{pmatrix}_{con} - \sum_i k_{p_i} \begin{pmatrix} \beta_0 \\ \beta_{1C} \\ \beta_{1S} \\ \beta_{nC} \\ \beta_{nS} \\ \beta_{N/2} \end{pmatrix}_i - k_{p_G} \begin{pmatrix} 0 \\ \beta_{G,C} \\ \beta_{G,S} \\ 0 \\ 0 \\ 0 \end{pmatrix} + \begin{pmatrix} 0 \\ \theta_{1S} \\ -\theta_{1C} \\ 0 \\ 0 \\ 0 \end{pmatrix} \psi_s$$

for $N \geq 3$; and

$$\begin{pmatrix} \theta_0 \\ \theta_1 \end{pmatrix}_0 = \begin{pmatrix} \theta_0 \\ \theta_1 \end{pmatrix}_{con} - \sum_i k_{p_i} \begin{pmatrix} \beta_0 \\ \beta_1 \end{pmatrix}_i - k_{p_G} \begin{pmatrix} \beta_T \\ 0 \end{pmatrix} + (\theta_{1S} \cos \psi - \theta_{1C} \sin \psi) \psi_s$$

for $N = 2$. The blade rigid pitch motion in this limit consists of the commanded control input, feedback of the bending and gimbal motion due to the kinematic coupling, and a pitch change due to the azimuth perturbation with a fixed swashplate. Substituting for p_o , the pitch/bending, pitch/gimbal, and pitch/azimuth coupling requires operations on the columns of A_o , as defined by the above equations. Next the rotor terms in the control matrix B are reconstructed from the rigid pitch columns of A_o since the blade pitch motion becomes a control variable rather than a degree of freedom. Then the equations of motion for the rigid pitch degrees of freedom are dropped from the system.

So far the aerodynamic hub forces have been put in place for the λ_u , λ_x , and λ_y equations of the two rotors; $\alpha = cx_s$ has been substituted for the hub motion; and the time scale for rotor #2 has been changed to Ω_1 . Completion of the equations of motion for the inflow dynamics requires the following steps.

- a. Multiply the thrust by $(\sigma a / 2\gamma) \partial \lambda / \partial T$ and the moments by $(\sigma a / 2\gamma) \partial \lambda / \partial M$.
- b. Add κ_x times the λ_u equation to the λ_x equation, and κ_y times the λ_u equation to the λ_y equation.
- c. Construct the ground effect terms (body motion contributions to $-(\partial \lambda / \partial z) \zeta z$) in the λ_{u1} and λ_{u2} equations.
- d. Account for the coupling of the λ_{u1} and λ_{u2} equations due to rotor/rotor interference.
- e. Construct the diagonal terms: 1 in A_1 and $\tau = K_M \partial \lambda / \partial M$ or $K_T \partial \lambda / \partial T$ in A_2 (times (Ω_1 / Ω_2) and $(\Omega_1 / \Omega_2)^2$ for rotor #2).
- f. Construct the aerodynamic interference terms

$$b_\lambda \left(\frac{\dot{\lambda}_{u1}}{(s\tau_1 / s\tau_2) \dot{\lambda}_{u2}} \right)$$

in the aircraft equations.

So far the torque has been put in place for the rotational speed equations of the two rotors; $\alpha = cx_s$ has been substituted for the hub motion; and the

time scale for rotor #2 has been changed to Ω_1 . Completion of the equations of motion for the drive train dynamics requires the following steps.

- Transform the ψ_{s1} and ψ_{s2} columns of the matrices according to

$$\psi_{s1} = \psi_s$$

$$\psi_{s2} = \frac{r_{x1}}{r_{x2}} \psi_s + \psi_x$$

to convert from ψ_{s1} and ψ_{s2} degrees of freedom to ψ_s and ψ_I degrees of freedom.

- Combine C_{Q1} and C_{Q2} as required for the ψ_s and ψ_I equations.
- Construct the equation of motion for ψ_e and complete construction of the ψ_s and ψ_I equation by adding inertial, damping, and spring terms. Construct throttle control terms in ψ_s and ψ_e equations.
- Construct the governor equations, and the governor degree of freedom terms in the other equations of motion.

It is still necessary to account for the mast bending and governor feedback terms in the pitch control θ_{con} . The pitch/mast bending coupling is (for each rotor)

$$\begin{pmatrix} \Delta\theta_{1c} \\ \Delta\theta_{1s} \end{pmatrix} = - \sum_{i=1}^{\infty} \begin{pmatrix} K_{Mc;i} \\ k_{MS;i} \end{pmatrix} q_{Si}$$

for $N \geq 3$, and

$$\Delta\theta_1 = - \sum_{i=1}^{\infty} (K_{Mc;i} \cos \psi + k_{MS;i} \sin \psi) q_{Si}$$

for $N = 2$.

For a two-bladed rotor the pitch control degrees of freedom are θ_0 and θ_1 . It is also useful to consider conventional cyclic control, which gives

$$\Delta\theta_1 = \theta_{1c} \cos \psi + \theta_{1s} \sin \psi$$

The Θ_{1c} and Θ_{1s} columns of the control matrix can be constructed from the θ_1 column according to this equation.

Next, the pilot's control matrix is constructed from the individual control matrix by the linear transformation $B_p = BT_{CFE}$.

Finally, the unused equations of motion and degrees of freedom are eliminated from the model by deleting the appropriate rows and columns from the coefficient matrices. Note that a number of the degrees of freedom are first order (no spring terms): all the inflow perturbation variables, the rigid body degrees of freedom ψ_F , x_F , y_F , and z_F (except possibly in ground effect), and perhaps the rotational speed degree of freedom (in axial flow with no integral governor).

6.3.2 Quasistatic approximation. - It is frequently possible to reduce the order of the system of equations describing the rotorcraft dynamics by considering a quasistatic approximation for certain of the degrees of freedom. Assume that the equations of motion have been reordered so that the quasistatic variables (x_0) appear last in the state vector:

$$x = \begin{pmatrix} x_1 \\ x_0 \end{pmatrix}$$

The quasistatic approximation consists of neglecting the acceleration and velocity terms of the quasistatic variables. Thus the equations of motion take the form:

$$\begin{bmatrix} A''_2 & 0 \\ A''_2 & 0 \end{bmatrix} \begin{pmatrix} x_1 \\ x_0 \end{pmatrix} + \begin{bmatrix} A''_1 & 0 \\ A''_1 & 0 \end{bmatrix} \begin{pmatrix} x_1 \\ x_0 \end{pmatrix} + \begin{bmatrix} A''_0 & A''_0 \\ A''_0 & A''_0 \end{bmatrix} \begin{pmatrix} x_1 \\ x_0 \end{pmatrix} = \begin{pmatrix} B' \\ B'' \end{pmatrix} v$$

The quasistatic variables now are not described by differential equations but rather by linear algebraic equations. The solution for x_0 then is simply

$$x_0 = (A''_0)^{-1} [B'' v - A''_2 \ddot{x}_1 - A''_1 \dot{x}_1 - A''_0 x_1]$$

Substituting for x_0 in the x_1 equations of motion gives then the reduced-order equations for the quasistatic approximation:

$$[A''_2 - A''_0 (A''_0)^{-1} A''_2] \ddot{x}_1 + [A''_1 - A''_0 (A''_0)^{-1} A''_1] \dot{x}_1 + [A''_0 - A''_0 (A''_0)^{-1} A''_0] x_1 = [B' - A''_0 (A''_0)^{-1} B'] v$$

In the present analysis, the quasistatic approximation can be applied to the inflow dynamics of either or both rotors, to the rigid pitch/elastic torsion degrees of freedom of either or both rotors, to all the degrees of freedom for either or both rotors, or even to all the degrees of freedom except the rigid-body motions of the aircraft.

The quasistatic approximation retains the low-frequency dynamics of the eliminated degrees of freedom. Whether that is a satisfactory representation of the elastic behavior must be established by comparison with the results of the higher order model.

The quasistatic approximation as implemented here does not give the low frequency response when applied to a two-bladed rotor. The source of this difficulty is the fact that the teetering equations of motion ($\beta_j^{(k)}, \theta_1^{(k)}, \beta_T$) are really still in the rotating frame, so the response of the teetering modes to low frequency inputs from the nonrotating frame is not at low frequency also, but rather at frequencies around 1/rev.

6.3.3 Symmetric aircraft. - With lateral symmetry of both the aircraft and flight state, the symmetric and antisymmetric motions are completely decoupled. Hence it is possible to analyze the dynamics by considering two sets of equations, each of half the order as the whole system. This case is applicable to side-by-side or tilting proprotor aircraft configuration in a trim flight condition with no sideward velocity or turn rate.

The equations of motion must be restructured in terms of symmetric and antisymmetric degrees of freedom. The motions of the right and left sides of the aircraft are given by respectively the sum and difference of the symmetric and antisymmetric degrees of freedom:

$$\begin{aligned} \dot{q}_{\text{rotor } \#1} &= q_{\text{sym}} + q_{\text{anti}} \\ \dot{q}_{\text{rotor } \#2} &= q_{\text{sym}} - q_{\text{anti}} \end{aligned}$$

These conversions apply to the rotor bending, torsion, gimbal, and inflow degrees of freedom, and to the rotor pitch control variables. The columns of the coefficient matrices are reconstructed according to these definitions of the symmetric and antisymmetric degrees of freedom. The symmetric and antisymmetric equations of motion are obtained by operating on the rows of the matrices as follows:

$$\begin{aligned} (\text{sym eq}) &= \frac{1}{2}(\text{rotor } \#1 \text{ eq}) + \frac{1}{2}(\text{rotor } \#2 \text{ eq}) \\ (\text{antisym eq}) &= \frac{1}{2}(\text{rotor } \#1 \text{ eq}) - \frac{1}{2}(\text{rotor } \#2 \text{ eq}) \end{aligned}$$

Finally, the symmetric and antisymmetric drive train motions are obtained from

$$\begin{aligned} \psi_s &= \psi_{\text{sym}} + \psi_{\text{anti}} \\ \psi_a &= -2\psi_{\text{anti}} \\ \psi_e &= \psi_{\text{eng}} - \psi_{\text{anti}} \end{aligned}$$

(from section 4.3.3); the columns of the matrices are reconstructed according to these equations. Now the symmetric and antisymmetric degrees of freedom are completely decoupled, and may be analyzed separately. The state vector, control vectors, and gust vector for the symmetric system are:

$$x = [\beta^{(k)} \theta^{(k)} \beta_{6c} \beta_{6s} \psi_s \lambda_n \lambda_x \lambda_y \theta_F x_F z_F q_{ex} \psi_e \Delta\theta_t \Delta\theta_{gmr}]^T$$

$$v = [\theta^{\text{con}} \delta_i \delta_e \theta_t]^T$$

$$v_p = [\delta_0 \ \delta_s \ \delta_t]^T$$

$$g = [w_G \ w_G]^T$$

The state vector, control vectors, and gust vector for the antisymmetric system are:

$$x = [\beta^{(k)} \ \theta^{(k)} \ \beta_{Gc} \ \beta_{Gs} \ \psi_i \ \lambda_u \ \lambda_v \ \lambda_y \ \phi_f \ \psi_f \ \gamma_f \ \eta_{sk}]^T$$

$$v = [\theta^{\text{con}} \ \delta_a \ \delta_r]^T$$

$$v_p = [\delta_c \ \delta_p]^T$$

$$g = [v_G]^T$$

Note that it is necessary to designate symmetric and antisymmetric elastic airframe vibration modes.

6.4 Matrices of Rotor Equations of Motion

6.4.1 *Inertial matrices for rotor equations.* - The inertial matrices for the rotor equations of motion in the nonrotating frame are given below. For clarity, the superscript * denoting the normalization of the inertial coefficients has been omitted.

I_{q_k}		$-S_{q_k \ddot{p}_1}$			$I_{q_k^\alpha} \cdot \vec{k}_B$		
	I_{q_k}		$-S_{q_k \ddot{p}_1}$	$I_{q_k^\alpha} \cdot \vec{k}_B$	$-I_{q_k} \cdot \vec{k}_B$		
		I_{q_k}		$-S_{q_k \ddot{p}_1}$	$I_{q_k} \cdot \vec{k}_B$	$I_{q_k^\alpha} \cdot \vec{k}_B$	
$-S_{p_k \ddot{q}_1}$		I_{p_k} $+I_{p_k \ddot{p}_1}$				$I_{p_k^\alpha} \cdot \vec{k}_B$	
	$-S_{p_k \ddot{q}_1}$		I_{p_k} $+I_{p_k \ddot{p}_1}$		$-I_{p_k^\alpha} \cdot \vec{k}_B$		
	$-S_{p_k \ddot{q}_1}$			I_{p_k} $+I_{p_k \ddot{p}_1}$		$-I_{p_k^\alpha} \cdot \vec{k}_B$	
$I_{q_1^\alpha} \cdot \vec{k}_B$			$-S_{q_0 \ddot{p}_1} \cdot \vec{k}_B$	I_o			
		$I_{q_1^\alpha} \cdot \vec{k}_B$		$-S_{q_0 \ddot{p}_1} \cdot \vec{k}_B$	I_o		
$I_{q_1^\alpha} \cdot \vec{k}_B$		$-S_{q_0 \ddot{p}_1} \cdot \vec{k}_B$			I_o		

	$S_{q_k} \cdot \vec{i}_B$			$I_{q_k \alpha} \cdot \vec{k}_B$
	$S_{q_k} \cdot \vec{k}_B$			$-I_{q_k \alpha} \cdot \vec{i}_B$
$-S_{q_k} \cdot \vec{k}_B$			$I_{q_k \alpha} \cdot \vec{i}_B$	
		$-S_{p_k} \cdot \vec{k}_B$		$I_{p_k \alpha} \cdot \vec{i}_B$
	$S_{p_k} \cdot \vec{i}_B$			$I_{p_k \alpha} \cdot \vec{k}_B$
$-S_{p_k} \cdot \vec{i}_B$			$-I_{p_k \alpha} \cdot \vec{k}_B$	
				$-I_o$
			I_o	
				I_o

$\tilde{A}_2 =$

				$2I_{q_k} \psi$
			$2I_{q_k^\alpha} \cdot \vec{i}_B$	
			$2I_{q_k^\alpha} \cdot \vec{i}_B$	
			$-2I_{p_k^\alpha} \cdot \vec{k}_B$	
			$-2I_{p_k^\alpha} \cdot \vec{k}_B$	
$\tilde{\chi}_1 =$			$2I_o$	
			$2I_o$	

B =

	$S_{q_1} \cdot \vec{k}_B$						
	$-S_{q_1} \cdot \vec{k}_B$						
$-2S_{q_1} \cdot \vec{I}_B$		$-I_{q_1 \alpha} \cdot \vec{I}_B$		$S_{q_0 \vec{p}_1} \cdot \vec{I}_B$	I_0		
						I_0	
				$-S_{q_0 \vec{p}_1} \cdot \vec{I}_B$			
					I_0		
				$I_{q_1 \alpha} \cdot \vec{I}_B$			
					$2S_{q_0 \vec{p}_1} \cdot \vec{k}_B$		
				$-2I_{q_1 \alpha} \cdot \vec{k}_B$			

$C_2 =$

$2I_{q_i \alpha} \cdot \vec{I}_B$	$-2I_{q_o \dot{q}_i} \cdot \vec{I}_B$	$-2S_{q_o \ddot{p}_i} \cdot \vec{I}_B$	$2I_o$
$2I_{q_o \dot{q}_i} \cdot \vec{I}_B$	$2I_{q_i \alpha} \cdot \vec{I}_B$	$-2S_{q_o \dot{q}_i} \cdot \vec{I}_B$	$2I_o$
$2I_{q_o \ddot{p}_i} \cdot \vec{I}_B$	$-2I_{q_i \alpha} \cdot \vec{I}_B$	$-2I_{q_o \dot{q}_i} \cdot \vec{k}_B$	$-4I_{q_o \dot{q}_i} \cdot \vec{k}_B$
$-2I_{q_i \alpha} \cdot \vec{k}_B$	$2I_{q_o \dot{q}_i} \cdot \vec{k}_B$	$2I_{q_o \ddot{p}_i} \cdot \vec{k}_B$	$-4I_{q_o \dot{q}_i} \cdot \vec{k}_B$

५

$c_o =$	$2I_{q_0 \cdot i_B}$	$2I_{q_0 \cdot i_B^t}$
---------	----------------------	------------------------

$$\tilde{c}_2 = \begin{bmatrix} -2M_b & & & & & \\ & -2M_b & & & & \\ & & -2M_b & & & \\ & & & -I_o & & \\ & & & & -I_o & \\ & & & & & -2I_o \end{bmatrix}$$

$$\tilde{c}_1 = \begin{bmatrix} & & & & & \\ & & & & & \\ & & & & & \\ & & & & & \\ & & & & & -2I_o \\ & & & & 2I_o & \\ & & & & & \\ & & & & & \\ & & & & & \end{bmatrix}$$

6.4.2 Aerodynamic matrices for rotor equations in axial flow.- The aerodynamic matrices for the rotor equations of motion in axial flow are given below.

$$A_1 = \begin{bmatrix} -\gamma M_c q_k \dot{q}_i & & & & & -\gamma M_{q_k} \dot{\zeta} & -\gamma M_{q_k} \lambda \\ & -\gamma M_{q_k} \dot{q}_i & & & -\gamma M_{q_k} \dot{\beta} & & -\gamma M_{q_k} \dot{\beta} \\ & & -\gamma M_{q_k} \dot{q}_i & & -\gamma M_{q_k} \dot{\beta} & & -\gamma M_{q_k} \dot{\beta} \\ -\gamma M_{p_k} \dot{q}_i & & -\gamma M_{p_k} \dot{p}_i & & -\gamma M_{p_k} \dot{\zeta} & -\gamma M_{p_k} \lambda & \\ -\gamma M_{p_k} \dot{q}_i & & -\gamma M_{p_k} \dot{p}_i & -\gamma M_{p_k} \dot{\beta} & & & -\gamma M_{p_k} \dot{\beta} \\ & -\gamma M_{p_k} \dot{q}_i & & -\gamma M_{p_k} \dot{p}_i & -\gamma M_{p_k} \dot{\beta} & & -\gamma M_{p_k} \dot{\beta} \\ & & -\gamma M_{p_k} \dot{q}_i & & -\gamma M_{p_k} \dot{\beta} & & -\gamma M_{p_k} \dot{\beta} \\ A_1 = & & -\gamma M_{q_i} & & -\gamma M_{\beta} & & -\gamma M_{\beta} \\ & & -\gamma M_{q_i} & & -\gamma M_{\beta} & & -\gamma M_{\beta} \\ \gamma Q_{p_i} & & & & \gamma Q_{\zeta} & \gamma Q_{\lambda} & \\ -2\gamma T_{q_i} & & & & -2\gamma T_{\zeta} & -2\gamma T_{\lambda} & \\ & -\gamma M_{q_i} & & -\gamma M_{\beta} & & & -\gamma M_{\beta} \\ & & -\gamma M_{q_i} & & -\gamma M_{\beta} & & -\gamma M_{\beta} \end{bmatrix}$$

$$A_0 = \begin{bmatrix} -\gamma M_{q_k q_i} & -\gamma M_{q_k p_i} & -\gamma M_{q_k \zeta} \\ -\gamma M_{q_k q_i} & -\gamma M_{q_k \dot{q}_i} & -\gamma M_{q_k \dot{p}_i} \\ \gamma M_{q_k \dot{q}_i} & -\gamma M_{q_k q_i} & -\gamma M_{q_k \dot{p}_i} \\ -\gamma M_{p_k q_i} & -\gamma M_{p_k \dot{q}_i} & -\gamma M_{p_k p_i} \\ -\gamma M_{p_k q_i} & -\gamma M_{p_k \dot{q}_i} & -\gamma M_{p_k \dot{p}_i} \\ \gamma M_{p_k \dot{q}_i} & -\gamma M_{p_k q_i} & \gamma M_{p_k \dot{p}_i} \\ -\gamma M_{q_i} & -\gamma M_{q_i} & -\gamma M_{p_i} \\ \gamma M_{q_i} & -\gamma M_{q_i} & -\gamma M_{p_i} \\ \gamma Q_{q_i} & \gamma Q_{p_i} & \gamma Q_\zeta \\ -2\gamma T_{q_i} & -2\gamma T_{p_i} & -2\gamma T_\zeta \\ -\gamma M_{q_i} & -\gamma M_{q_i} & -\gamma M_\beta \\ \gamma M_{q_i} & -\gamma M_{q_i} & -M_p \\ \end{bmatrix}$$

		$-\gamma M_{q_k \lambda}$		$-\gamma M_{q_k \dot{\zeta}}$
	$-\gamma M_{q_k \mu}$			$\gamma M_{q_k \dot{\beta}}$
$\gamma M_{q_k \mu}$			$-\gamma M_{q_k \dot{\beta}}$	
		$-\gamma M_{p_k \lambda}$		$-\gamma M_{p_k \dot{\zeta}}$
	$-\gamma M_{p_k \mu}$			$\gamma M_{p_k \dot{\beta}}$
$\gamma M_{p_k \mu}$			$-\gamma M_{p_k \dot{\beta}}$	
	$-\gamma M_\mu$			γM_β
γM_μ			$-\gamma M_\beta$	
		γQ_λ		γQ_ζ
$-\frac{\mu_x}{\kappa_f^2} \frac{\partial \lambda}{\partial \mu}$	$+\frac{\mu_y}{\kappa_f^2} \frac{\partial \lambda}{\partial \mu}$	$-\frac{2\gamma T_\lambda}{\kappa_h^4} \frac{\partial \lambda}{\partial \mu}$		$-2\gamma T_\zeta$
	$-\gamma M_\mu$			γM_β
γM_μ			$-\gamma M_\beta$	

$$\tilde{A}_o = \begin{bmatrix} & & & \gamma\mu_y^M q_k^\lambda & \gamma\mu_x^M q_k^\lambda & -\gamma M_{q_k^\zeta} \\ & & & -\gamma\mu_z^M q_k^\lambda & & \\ & & & & -\gamma\mu_z^M q_k^\mu & \\ & & & & -\gamma\mu_y^M p_k^\lambda & -\gamma\mu_x^M p_k^\lambda & -\gamma M_{p_k^\zeta} \\ & & & & -\gamma\mu_z^M p_k^\mu & & \\ & & & & & -\gamma\mu_z^M p_k^\mu & \\ & & & & & -\gamma\mu_z^M \mu & \\ & & & & & & -\gamma\mu_z^M \mu \\ & & & & & & \\ & & & -\gamma\mu_y^Q \lambda & -\gamma\mu_x^Q \lambda & \gamma Q_\zeta \\ & & & 2\gamma\mu_y^T \lambda & 2\gamma\mu_x^T \lambda & -2\gamma T_\zeta \\ & & & -\gamma\mu_z^M \mu & & \\ & & & & -\gamma\mu_z^M \mu & \end{bmatrix}$$

		$-\gamma^M q_k^\lambda$
	$\gamma^M q_k^\mu$	
$\gamma^M q_k^\mu$		
		$-\gamma^M p_k^\lambda$
	$\gamma^M p_k^\mu$	
$\gamma^M p_k^\mu$		
		γ^M_μ
γ^M_μ		
		γQ_λ
$-\frac{\mu_x}{\kappa_f^2} \frac{\partial \lambda}{\partial \mu}$	$-\frac{\mu_y}{\kappa_f^2} \frac{\partial \lambda}{\partial \mu}$	$-2\gamma T_\lambda + \frac{\lambda}{\kappa_h^4} \frac{\partial \lambda}{\partial \mu}$
	γ^M_μ	
γ^M_μ		

$$C_1 = \begin{bmatrix} & & & & & \gamma H_{\dot{\beta}}^* \\ & & & & & \gamma R_{\dot{\beta}} \\ & & & & & \gamma H_{\dot{\beta}} \\ & & & & & \gamma R_{\dot{\beta}} \\ & & & & & -\gamma H_{\dot{\beta}} \\ & & & & & \gamma R_{\dot{\beta}} \\ & & & & & -\gamma H_{\dot{\beta}} \\ & & & & & \gamma R_{\dot{\beta}} \\ & & & & & \gamma M_{\dot{\beta}} \\ & & & & & \gamma T_{\zeta}^* \\ & & & & & 2\gamma T_{\lambda} \\ & & & & & \gamma M_{\dot{\beta}} \\ & & & & & -\gamma M_{\dot{\beta}} \\ & & & & & \gamma M_{\dot{\beta}} \\ & & & & & -2\gamma Q_{\zeta} \\ & & & & & -2\gamma Q_{\lambda} \end{bmatrix}$$

	γR_{q_i}	γH_{q_i}	γR_{p_i}	γH_{q_i}	γR_{β}	γH_{β}
	$-\gamma H_{*q_i}$	$+\gamma R_{*q_i}$			$-\gamma H_{\dot{\beta}}$	$+\gamma R_{\dot{\beta}}$
	$-\gamma H_{q_i}$	γR_{q_i}	$-\gamma H_{p_i}$	γR_{p_i}	$-\gamma H_{\beta}$	γR_{β}
	$-\gamma R_{q_i}$	$-\gamma H_{*q_i}$			$-\gamma R_{\dot{\beta}}$	$-\gamma H_{\dot{\beta}}$
$2\gamma T_{q_i}$		$2\gamma T_{p_i}$			$2\gamma T_{\zeta}$	
	$-\gamma M_{q_i}$	γM_{q_i}		γM_{p_i}	$-\gamma M_{\dot{\beta}}$	γM_{β}
	$-\gamma M_{q_i}$	$-\gamma M_{\zeta_i}$	$-\gamma M_{p_i}$		$-\gamma M_{\beta}$	$-\gamma M_{\dot{\beta}}$
	$-2\gamma Q_{q_i}$		$-2\gamma Q_{p_i}$			$-2\gamma Q_{\zeta}$

$C_0 =$

$$\tilde{C}_1 = \begin{bmatrix} -\gamma(H_\mu + R_\mu) & \gamma R_r & & \gamma H_\beta^* & -\gamma R_\beta & \\ -\gamma R_r & -\gamma(H_\mu + R_\mu) & & \gamma R_\beta^* & \gamma H_\beta^* & \\ & & 2\gamma T_\lambda & & & 2\gamma T_\zeta \\ -\gamma M_\mu & & & \gamma M_\beta^* & & \\ & -\gamma M_\mu & & & \gamma M_\beta^* & \\ & & -2\gamma Q_\lambda & & & -2\gamma Q_\zeta \end{bmatrix}$$

$$\tilde{C}_0 = \begin{bmatrix} & & & \gamma u_z R_r & -\gamma u_z (H_\mu + R_\mu) \\ & & & -\gamma u_z (H_\mu + R_\mu) & \gamma u_z R_r \\ & & & -2\gamma u_y T_\lambda & -2\gamma u_x T_\lambda & 2\gamma T_\zeta \\ & & & & \gamma u_z M_\mu & \\ & & & & -\gamma u_z M_\mu & \\ & & & & 2\gamma u_y Q_\lambda & 2\gamma u_x Q_\lambda & -2\gamma Q_\zeta \end{bmatrix}$$

$$D_G = \begin{bmatrix} \gamma (H_\mu + R_\mu) & \gamma R_r \\ \gamma R_r & -\gamma (H_\mu + R_\mu) \\ & -2\gamma T_\lambda \\ \gamma M_\mu & \\ & -\gamma M_\mu \\ & & 2\gamma Q_\lambda \end{bmatrix}$$

6.4.3 Aerodynamic matrices for rotor equations in nonaxial flow.- The aerodynamic matrices for the rotor equations of motion in nonaxial flow are given below. Note that each matrix is a summation over all the blades, that is, $m = 1, \dots, N$. The notation $C = \cos\psi_m$ and $S = \sin\psi_m$ is used in these matrices.

11

$-H_{q_k q_l}$	$H_{q_k \dot{q}_l} S$ $-H_{q_k \dot{q}_l} C$ $-H_{q_k q_l}$	$-H_{q_k \dot{q}_l} C$ $-H_{q_k q_l}$	$-H_{q_k p_l}$	$-H_{q_k p_l} \epsilon$	$-H_{q_k p_l} S$ $-H_{q_k p_l} \epsilon'$	$-H_{q_k \dot{p}_l} S$ $-H_{q_k \dot{p}_l} \epsilon'$	$-H_{q_k \dot{p}_l} \zeta$
$-H_{q_k q_l} 2C$	$H_{q_k \dot{q}_l} 2CS$ $-H_{q_k \dot{q}_l} 2C^2$ $-H_{q_k q_l}$	$-H_{q_k \dot{q}_l} 2C$ $-H_{q_k q_l}$	$-H_{q_k p_l} 2C$ $-H_{q_k p_l} 2CS$	$-H_{q_k p_l} 2C^2$ $-H_{q_k p_l} 2S^2$	$-H_{q_k p_l} 2CS$ $-H_{q_k p_l} 2S^2$	$-H_{q_k \dot{p}_l} 2CS$ $-H_{q_k \dot{p}_l} 2C^2$	$-H_{q_k \dot{p}_l} 2C$ $-H_{q_k \dot{p}_l} 2S$
$-H_{q_k q_l} 2S$	$H_{q_k \dot{q}_l} 2S^*$ $-H_{q_k q_l}$	$-H_{q_k \dot{q}_l} 2CS$ $-H_{q_k q_l}$	$-H_{q_k p_l} 2S$ $-H_{q_k p_l} 2S^*$	$-H_{q_k p_l} 2CS$ $-H_{q_k p_l} 2S^*$	$-H_{q_k \dot{p}_l} 2S^2$ $-H_{q_k \dot{p}_l} 2S^*$	$-H_{q_k \dot{p}_l} 2CS$ $-H_{q_k \dot{p}_l} 2S^2$	$-H_{q_k \dot{p}_l} 2S$ $-H_{q_k \dot{p}_l} 2S^2$
$-H_{p_k q_l}$	$+H_{p_k \dot{q}_l} S$ $-H_{p_k \dot{q}_l} C$ $-H_{p_k q_l}$	$-H_{p_k \dot{q}_l} C$ $-H_{p_k q_l}$	$-H_{p_k p_l}$	$-H_{p_k p_l}$	$-H_{p_k \dot{p}_l} S$ $-H_{p_k \dot{p}_l} C$ $-H_{p_k \dot{p}_l}$	$-H_{p_k \dot{p}_l} S$ $-H_{p_k \dot{p}_l} C$ $-H_{p_k \dot{p}_l}$	$-H_{p_k \dot{p}_l} \zeta$
$-H_{p_k q_l} 2C$	$+H_{p_k \dot{q}_l} 2CS$ $-H_{p_k \dot{q}_l} 2C^2$ $-H_{p_k q_l}$	$-H_{p_k \dot{q}_l} 2C$ $-H_{p_k q_l}$	$-H_{p_k p_l} 2C$ $-H_{p_k p_l} 2CS$	$-H_{p_k p_l} 2C^2$ $-H_{p_k p_l} 2CS$	$-H_{p_k \dot{p}_l} 2CS$ $-H_{p_k \dot{p}_l} 2C^2$	$+H_{p_k \dot{p}_l} 2CS$ $-H_{p_k \dot{p}_l} 2C^2$	$-H_{p_k \dot{p}_l} 2C$ $-H_{p_k \dot{p}_l} 2S$
$-H_{p_k q_l} 2S$	$+H_{p_k \dot{q}_l} 2S^2$ $-H_{p_k \dot{q}_l} 2CS$ $-H_{p_k q_l}$	$-H_{p_k \dot{q}_l} 2CS$ $-H_{p_k p_l} 2S^2$ $-H_{p_k p_l}$	$-H_{p_k p_l} 2S$ $-H_{p_k p_l} 2S^2$	$-H_{p_k p_l} 2CS$ $-H_{p_k p_l} 2S^2$	$-H_{p_k \dot{p}_l} 2S^2$ $-H_{p_k \dot{p}_l} 2CS$	$-H_{p_k \dot{p}_l} 2CS$ $-H_{p_k \dot{p}_l} 2S^2$	$-H_{p_k \dot{p}_l} 2S$ $-H_{p_k \dot{p}_l} 2S^2$
\sum_{\square}	$-H_{q_k 2CS}$ $-H_{q_k 2C^2}$ $-H_{q_k q_l}$	$-H_{q_k 2C^2}$ $-H_{q_k 2CS}$ $-H_{q_k q_l}$	$-H_{p_k 2C}$ $-H_{p_k 2CS}$ $-H_{p_k p_l}$	$-H_{p_k 2C^2}$ $-H_{p_k 2CS}$ $-H_{p_k p_l}$	$-H_{p_k \dot{p}_l} 2CS$ $-H_{p_k \dot{p}_l} 2C^2$	$+H_{p_k \dot{p}_l} 2CS$ $-H_{p_k \dot{p}_l} 2C^2$	$-H_{p_k \dot{p}_l} 2C$ $-H_{p_k \dot{p}_l} 2S$
$-H_{q_k 2S}$	$+M_{q_k 2S^2}$ $-H_{q_k 2CS}$ $-H_{q_k q_l}$	$-M_{q_k 2S^2}$ $-M_{q_k 2S^*}$ $-M_{q_k q_l}$	$-M_{q_k p_l} 2S$ $-M_{q_k p_l} 2S^*$ $-M_{q_k p_l}$	$-M_{q_k p_l} 2CS$ $-M_{q_k p_l} 2S^2$ $-M_{q_k p_l}$	$-M_{p_k \dot{p}_l} 2S^2$ $-M_{p_k \dot{p}_l} 2CS$	$+M_{p_k \dot{p}_l} 2S^2$ $-M_{p_k \dot{p}_l} 2CS$	$-M_{p_k \dot{p}_l} 2C$ $-M_{p_k \dot{p}_l} 2S$
$-H_{q_k q_l}$	$-M_{q_k 2S^*}$ $-H_{q_k 2CS}$ $-H_{q_k q_l}$	$-M_{q_k 2S^*}$ $-M_{q_k 2S^*}$ $-M_{q_k q_l}$	$-M_{q_k p_l} 2S$ $-M_{q_k p_l} 2S^*$ $-M_{q_k p_l}$	$-M_{q_k p_l} 2CS$ $-M_{q_k p_l} 2S^2$ $-M_{q_k p_l}$	$-M_{q_k \dot{p}_l} 2S^2$ $-M_{q_k \dot{p}_l} 2CS$	$+M_{q_k \dot{p}_l} 2S^2$ $-M_{q_k \dot{p}_l} 2CS$	$-M_{q_k \dot{p}_l} 2C$ $-M_{q_k \dot{p}_l} 2S$
Q_{q_k}	$Q_{q_k} C$ $-Q_{q_k} S$ $-Q_{q_k} q_l$	$Q_{q_k} S$ $Q_{q_k} C$ $Q_{q_k} q_l$	$Q_{p_k} C$ $Q_{p_k} C$ $Q_{p_k} q_l$	$Q_{p_k} S$ $Q_{p_k} C$ $Q_{p_k} q_l$	$-Q_{p_k} S$ $Q_{p_k} C$ $Q_{p_k} q_l$	$Q_{p_k} S$ $Q_{p_k} C$ $Q_{p_k} q_l$	$Q_{p_k} \zeta$
$-2T_{q_k}$	$-2T_{q_k} C$ $-2T_{q_k} S$ $-2T_{q_k} q_l$	$-2T_{q_k} S$ $-2T_{q_k} C$ $-2T_{q_k} q_l$	$-2T_{p_k} C$ $-2T_{p_k} q_l$	$-2T_{p_k} S$ $-2T_{p_k} q_l$	$-2T_{p_k} C$ $-2T_{p_k} q_l$	$-2T_{p_k} S$ $-2T_{p_k} q_l$	$-2T_{p_k} \zeta$
$-H_{q_k q_l}$	$-H_{q_k 2C^2}$ $-H_{q_k 2CS}$ $-H_{q_k q_l}$	$-H_{q_k 2C}$ $-H_{q_k 2C^2}$ $-H_{q_k q_l}$	$-H_{p_k 2C}$ $-H_{p_k 2CS}$ $-H_{p_k q_l}$	$-H_{p_k 2C^2}$ $-H_{p_k 2CS}$ $-H_{p_k q_l}$	$-H_{p_k 2CS}$ $-H_{p_k 2C^2}$ $-H_{p_k q_l}$	$H_{p_k 2S}$ $-H_{p_k 2C^2}$ $-H_{p_k q_l}$	$-H_{p_k 2C}$ $-H_{p_k 2S}$
$-H_{q_k q_l} 2S$	$-M_{q_k 2CS}$ $-H_{q_k 2S^*}$ $-H_{q_k q_l}$	$-M_{q_k 2C^2}$ $-H_{q_k 2S^*}$ $-H_{q_k q_l}$	$-M_{q_k 2S}$ $-M_{q_k 2S^*}$ $-M_{q_k q_l}$	$-M_{q_k 2S^2}$ $-M_{q_k 2S^*}$ $-M_{q_k q_l}$	$-M_{p_k 2S^2}$ $-M_{p_k 2S^*}$ $-M_{p_k q_l}$	$H_{p_k 2S}$ $-H_{p_k 2C^2}$ $-H_{p_k q_l}$	$-H_{p_k 2C}$ $-H_{p_k 2S}$

$$A_0 = \gamma \frac{1}{N} \sum_{\square}$$

$M_{q_k \mu} S$	$-M_{q_k \mu} C$	$-M_{q_k \lambda} \dot{\lambda}$	$-M_{q_k \beta} \dot{\beta} S$	$M_{q_k \beta} \dot{\beta} C$	$-M_{q_k \zeta} \dot{\zeta}$
$M_{q_k \mu} 2CS$	$-M_{q_k \mu} 2C^2$	$-M_{q_k \lambda} 2C$	$-M_{q_k \beta} 2CS$	$M_{q_k \beta} 2C^2$	$-M_{q_k \zeta} 2C$
$M_{q_k \mu} 2S^2$	$-M_{q_k \mu} 2CS$	$-M_{q_k \lambda} 2S$	$-M_{q_k \beta} 2S^2$	$M_{q_k \beta} 2CS$	$-M_{q_k \zeta} 2S$
$M_{p_k \mu} S$	$-M_{p_k \mu} C$	$-M_{p_k \lambda} \dot{\lambda}$	$-M_{p_k \beta} \dot{\beta} S$	$M_{p_k \beta} \dot{\beta} C$	$-M_{p_k \zeta} \dot{\zeta}$
$M_{p_k \mu} 2CS$	$-M_{p_k \mu} 2C^2$	$-M_{p_k \lambda} 2C$	$-M_{p_k \beta} 2CS$	$M_{p_k \beta} 2C^2$	$-M_{p_k \zeta} 2C$
$M_{p_k \mu} 2S^2$	$-M_{p_k \mu} 2CS$	$-M_{p_k \lambda} 2S$	$-M_{p_k \beta} 2S^2$	$M_{p_k \beta} 2CS$	$-M_{p_k \zeta} 2S$
$M_{\mu} 2CS$	$-M_{\mu} 2C^2$	$-M_{\lambda} 2C$	$-M_{\beta} 2CS$	$M_{\beta} 2C^2$	$-M_{\zeta} 2C$
$M_{\mu} 2S^2$	$-M_{\mu} 2CS$	$-M_{\lambda} 2S$	$-M_{\beta} 2S^2$	$M_{\beta} 2CS$	$-M_{\zeta} 2S$
$-Q_{\mu} S$	$Q_{\mu} C$	Q_{λ}	$Q_{\beta} \dot{\beta} S$	$-Q_{\beta} \dot{\beta} C$	$Q_{\zeta} \dot{\zeta}$
$2T_{\mu} S$ $-\frac{\mu_x}{\kappa_f^2} \frac{\partial \lambda}{\partial \mu}$	$-2T_{\mu} C$ $+\frac{\mu_y}{\kappa_f^2} \frac{\partial \lambda}{\partial \mu}$	$-2T_{\lambda}$ $+\frac{\lambda}{\kappa_h^4} \frac{\partial \lambda}{\partial \mu}$	$-2T_{\beta} \dot{\beta} S$	$2T_{\beta} \dot{\beta} C$	$-2T_{\zeta} \dot{\zeta}$
$M_{\mu} 2CS$	$-M_{\mu} 2C^2$	$-M_{\lambda} 2C$	$-M_{\beta} 2CS$	$M_{\beta} 2C^2$	$-M_{\zeta} 2C$
$M_{\mu} 2S^2$	$-M_{\mu} 2CS$	$-M_{\lambda} 2S$	$-M_{\beta} 2S^2$	$M_{\beta} 2CS$	$-M_{\zeta} 2S$

$$\tilde{A}_1 = \gamma \frac{1}{N} \sum_m$$

$$\tilde{A}_o = \gamma \frac{1}{N} \sum_m$$

		$\mu_y^M q_k \lambda$ $-\mu_z^M q_k u^C$	$\mu_x^M q_k \lambda$ $-\mu_z^M q_k u^S$	$-M_{q_k} \zeta$
		$\mu_y^M q_k \lambda^{2C}$ $-\mu_z^M q_k u^{2C^2}$	$\mu_x^M q_k \lambda^{2C}$ $-\mu_z^M q_k u^{2CS}$	$-M_{q_k} \zeta^{2C}$
		$\mu_y^M q_k \lambda^{2S}$ $-\mu_z^M q_k u^{2CS}$	$\mu_x^M q_k \lambda^{2S}$ $-\mu_z^M q_k u^{2S^2}$	$-M_{q_k} \zeta^{2S}$
		$\mu_y^M p_k \lambda$ $-\mu_z^M p_k u^C$	$\mu_x^M p_k \lambda$ $-\mu_z^M p_k u^S$	$-M_{p_k} \zeta$
		$\mu_y^M p_k \lambda^{2C}$ $-\mu_z^M p_k u^{2C^2}$	$\mu_x^M p_k \lambda^{2C}$ $-\mu_z^M p_k u^{2CS}$	$-M_{p_k} \zeta^{2C}$
		$\mu_y^M p_k \lambda^{2S}$ $-\mu_z^M p_k u^{2CS}$	$\mu_x^M p_k \lambda^{2S}$ $-\mu_z^M p_k u^{2S^2}$	$-M_{p_k} \zeta^{2S}$
		$\mu_y^M \lambda^{2C}$ $-\mu_z^M \mu^{2C^2}$	$\mu_x^M \lambda^{2C}$ $-\mu_z^M \mu^{2CS}$	$-M_\zeta^{2C}$
		$\mu_y^M \lambda^{2S}$ $-\mu_z^M \mu^{2CS}$	$\mu_x^M \lambda^{2S}$ $-\mu_z^M \mu^{2S^2}$	$-M_\zeta^{2S}$
		$-\mu_y^Q \lambda$ $\mu_z^Q u^C$	$-\mu_x^Q \lambda$ $\mu_z^Q u^S$	Q_ζ
		$2\mu_y^T \lambda$ $-2\mu_z^T u^C$	$2\mu_x^T \lambda$ $-2\mu_z^T u^S$	$-2T_\zeta$
		$\mu_y^M \lambda^{2C}$ $-\mu_z^M \mu^{2C^2}$	$\mu_x^M \lambda^{2C}$ $-\mu_z^M \mu^{2CS}$	$-M_\zeta^{2C}$
		$\mu_y^M \lambda^{2S}$ $-\mu_z^M \mu^{2CS}$	$\mu_x^M \lambda^{2S}$ $-\mu_z^M \mu^{2S^2}$	$-M_\zeta^{2S}$

$$B_G = \gamma \frac{1}{N} \sum_m$$

$M_{q_k^\mu} S$	$M_{q_k^\mu} C$	$-M_{q_k^\lambda} \lambda$
$M_{q_k^\mu} 2CS$	$M_{q_k^\mu} 2C^2$	$-M_{q_k^\lambda} 2C$
$M_{q_k^\mu} 2S^2$	$M_{q_k^\mu} 2CS$	$-M_{q_k^\lambda} 2S$
$M_{p_k^\nu} S$	$M_{p_k^\mu} C$	$-M_{p_k^\lambda} \lambda$
$M_{p_k^\mu} 2CS$	$M_{p_k^\mu} 2C^2$	$-M_{p_k^\lambda} 2C$
$M_{p_k^\mu} 2S^2$	$M_{p_k^\mu} 2CS$	$-M_{p_k^\lambda} 2S$
$M_\mu 2CS$	$M_\mu 2C^2$	$-M_\lambda 2C$
$M_\mu 2S^2$	$M_\mu 2CS$	$-M_\lambda 2S$
$-Q_\mu S$	$-Q_\mu C$	Q_λ
$2T_\mu S$ $-\frac{\mu_x}{\kappa_f^2} \frac{\partial \lambda}{\partial \mu}$	$2T_\mu C$ $-\frac{\mu_y}{\kappa_f^2} \frac{\partial \lambda}{\partial \mu}$	$-2T_\lambda \lambda$ $+\frac{\lambda}{\kappa_h^4} \frac{\partial \lambda}{\partial \mu}$
$M_\mu 2CS$	$M_\mu 2C^2$	$-M_\lambda 2C$
$M_\mu 2S^2$	$M_\mu 2CS$	$-M_\lambda 2S$

$$C_1 = \begin{bmatrix} H_{q_i}^* 2S & H_{q_i}^* 2CS & H_{q_i}^* 2S^2 & H_{\beta}^* 2CS^2 & H_{\beta}^* 2CS \\ R_{q_i}^* 2C & R_{q_i}^* 2C^2 & R_{q_i}^* 2CS & R_{\beta}^* 2CS & R_{\beta}^* 2CS \\ -H_{q_i}^* 2C & -H_{q_i}^* 2C^2 & -H_{q_i}^* 2CS & -H_{\beta}^* 2CS & -H_{\beta}^* 2CS \\ +R_{q_i}^* 2S & +R_{q_i}^* 2CS & +R_{q_i}^* 2S^2 & +R_{\beta}^* 2CS & +R_{\beta}^* 2S^2 \\ 2T_{q_i} & 2T_{q_i}^* C & 2T_{q_i}^* S & 2T_{\beta}^* C & 2T_{\beta}^* S \\ M_{q_i}^* 2S & M_{q_i}^* 2CS & M_{q_i}^* 2S^2 & M_{\beta}^* 2CS & M_{\beta}^* 2S^2 \\ -M_{q_i}^* 2C & -M_{q_i}^* 2C^2 & -M_{q_i}^* 2CS & -M_{\beta}^* 2CS & -M_{\beta}^* 2CS \\ -2Q_{q_i}^* & -2Q_{q_i}^* C & -2Q_{q_i}^* S & -2Q_{\beta}^* C & -2Q_{\beta}^* S \end{bmatrix}$$

$$C_0 = \frac{1}{N} \sum_n$$

$H_{q_i} 2S$	$-H_{q_i} 2S^2$	$H_{q_i} 2CS$	$H_{p_i} 2S$	$H_{p_i} 2CS$	$H_{p_i} 2S^2$	$-H_B 2S^2$	$H_B 2CS$	$H_\zeta 2S$		
$R_{q_i} 2C$	$H_{q_i} 2CS$	$H_{q_i} 2S^2$	$R_{q_i} 2C^2$	$R_{p_i} 2C$	$R_{p_i} 2C^2$	$R_{p_i} 2CS$	$H_B 2CS$	$H_B 2S^2$	$R_B 2C^2$	
$R_{q_i} 2CS$	$-R_{q_i} 2CS$	$R_{q_i} 2C^2$	$R_{q_i} 2CS$	$R_{p_i} 2C$	$R_{p_i} 2C^2$	$R_{p_i} 2CS$	$-R_B 2CS$	$R_B 2CS$	$R_\zeta 2C$	
$R_{q_i} 2C^2$	$R_{q_i} 2CS$	$R_{q_i} 2CS$				$R_B 2C^2$	$R_B 2CS$			
$+R_{q_i} 2S$	$-H_{q_i} 2C^2$	$-H_{q_i} 2CS$	$-H_{p_i} 2C$	$-H_{p_i} 2C^2$	$-H_{p_i} 2CS$	$H_B 2CS$	$-H_B 2C^2$	$-H_\zeta 2C$		
$+R_{q_i} 2S^2$	$+R_{q_i} 2CS$	$+R_{q_i} 2CS$	$+R_{p_i} 2S$	$+R_{p_i} 2CS$	$+R_{p_i} 2S^2$	$-R_B 2S^2$	$+R_B 2CS$	$+R_\zeta 2S$		
$2T_{q_i}$	$-2T_{q_i} S$	$2T_{q_i} C$	$2T_{p_i}$	$2T_{p_i} C$	$2T_{p_i} S$	$-2T_B S$	$2T_B C$	$2T_\zeta$		
$2T_{q_i} C$	$2T_{q_i} S$					$2T_B C$	$2T_B S$			
$M_{q_i} 2S$	$-M_{q_i} 2S^2$	$M_{q_i} 2CS$	$M_{p_i} 2S$	$M_{p_i} 2CS$	$M_{p_i} 2S^2$	$-M_B 2S^2$	$M_B 2CS$	$M_\zeta 2S$		
$+M_{q_i} 2CS$	$+M_{q_i} 2S^2$					$+M_B 2CS$	$+M_B 2S^2$			
$-M_{q_i} 2C$	$M_{q_i} 2CS$	$-M_{q_i} 2C^2$	$-M_{p_i} 2C$	$-M_{p_i} 2C^2$	$-M_{p_i} 2CS$	$M_B 2CS$	$-M_B 2C^2$	$-M_\zeta 2C$		
$-M_{q_i} 2C^2$	$-M_{q_i} 2CS$	$-M_{q_i} 2CS$				$-M_B 2C^2$	$-M_B 2CS$			
$-2Q_{q_i}$	$2Q_{q_i} S$	$-2Q_{q_i} C$	$-2Q_{p_i}$	$-2Q_{p_i} C$	$-2Q_{p_i} S$	$2Q_B S$	$-2Q_B C$	$-2Q_\zeta$		
$-2Q_{q_i} C$	$-2Q_{q_i} S$	$-2Q_{q_i} S$				$-2Q_B C$	$-2Q_B S$			

$$\tilde{c}_1 = \gamma \frac{1}{N} \sum_m$$

$-H_\mu 2S^2$	$H_\mu 2CS$	$H_\lambda 2S$	$-H_\zeta 2C$	$-H_\beta 2CS$	$H_\zeta 2S$
$-R_\mu 2C^2$	$-R_\mu 2CS$	$R_\lambda 2C$	$+R_\zeta 2S$	$-R_\beta 2C^2$	$R_\zeta 2C$
$-R_r 2CS$	$R_r 2C^2$				
$H_\mu 2CS$	$-H_\mu 2C^2$	$-H_\lambda 2C$	$-H_\beta 2CS$	$H_\beta 2C^2$	$H_\beta 2S^2$
$-R_\mu 2CS$	$-R_\mu 2S^2$	$+R_\lambda 2S$	$+R_\beta 2S^2$	$-R_\beta 2CS$	$R_\beta 2CS$
$-R_r 2S^2$	$+R_r 2CS$				
$-2T_\mu S$	$2T_\mu C$	$2T_\lambda$	$2T_\beta S$	$-2T_\beta C$	$2T_\zeta$
$-M_\mu 2S^2$	$M_\mu 2CS$	$M_\lambda 2S$	$M_\beta 2S^2$	$-M_\beta 2CS$	$M_\zeta 2S$
$M_\mu 2CS$	$+M_\beta 2C^2$	$-M_\lambda 2C$	$-M_\beta 2CS$	$-M_\mu 2C^2$	$-M_\zeta 2C$
$2Q_\mu S$	$-2Q_\mu C$	$-2Q_\lambda$	$-2Q_\beta S$	$2Q_\beta C$	$-2Q_\zeta$

$$\tilde{C}_o = \gamma \frac{1}{N} \sum_m$$

		$\mu_z H_\mu 2CS$ $-\mu_y H_\lambda 2S$ $-\mu_z R_\mu 2CS$ $-\mu_y R_\lambda 2C$ $\mu_z R_r 2C^2$	$\mu_z R_\mu 2C^2$ $-\mu_x H_\lambda 2S$ $\mu_z H_\mu 2S^2$ $-\mu_x R_\lambda 2C$ $\mu_z R_r 2CS$	$H_\zeta 2S$ $R_\zeta 2C$
		$-\mu_z H_\mu 2C^2$ $+\mu_y H_\lambda 2C$ $-\mu_z R_\mu 2S^2$ $-\mu_y R_\lambda 2S$ $+\mu_z R_r 2CS$	$\mu_z R_\mu 2CS$ $+\mu_x H_\lambda 2C$ $-\mu_z H_\mu 2CS$ $-\mu_x R_\lambda 2S$ $+\mu_z R_r 2S^2$	$-H_\zeta 2C$ $+R_\zeta 2S$
		$-2\mu_y T_\lambda$ $2\mu_z T_\mu C$	$-2\mu_x T_\lambda$ $2\mu_z T_\mu S$	$2T_\zeta$
		$-\mu_y M_\lambda 2S$ $+\mu_z M_\mu 2CS$	$-\mu_x M_\lambda 2S$ $+\mu_z M_\mu 2S^2$	$M_\zeta 2S$
		$\mu_y M_\lambda 2C$ $-\mu_z M_\mu 2C^2$	$\mu_x M_\lambda 2C$ $-\mu_z M_\mu 2CS$	$-M_\zeta 2C$
		$2\mu_y Q_\lambda$ $-2\mu_z Q_\mu C$	$2\mu_x Q_\lambda$ $-2\mu_z Q_\mu S$	$-2Q_\zeta$

$$D_G = \gamma \frac{1}{N} \sum_m$$

$H_\mu^{2S^2}$	H_μ^{2CS}	$-H_\lambda^{2S}$
$+R_\mu^{2C^2}$	$-R_\mu^{2CS}$	$-R_\lambda^{2C}$
$+R_r^{2CS}$	$+R_r^{2C^2}$	
$-H_\mu^{2CS}$	$-H_\mu^{2C^2}$	H_λ^{2C}
$+R_\mu^{2CS}$	$-R_\mu^{2S^2}$	$-R_\lambda^{2S}$
$+R_r^{2S^2}$	$+R_r^{2CS}$	
$2T_\mu^S$	$2T_\mu^C$	$-2T_\lambda$
$M_\mu^{2S^2}$	M_μ^{2CS}	$-M_\lambda^{2S}$
$-M_\mu^{2CS}$	$-M_\mu^{2C^2}$	M_λ^{2C}
$-2Q_\mu^S$	$-2Q_\mu^C$	$2Q_\lambda$

6.4.4 *Inertial matrices for rotor with four or more blades.* - The inertial matrices for the equations of motion of a rotor with four or more blades are given below.

$$A_2 = \begin{bmatrix} I_{q_k} & & & -S_{q_k \ddot{p}_i} & \\ & I_{q_k} & & -S_{q_k \ddot{p}_i} & \\ & & I_{q_k} & & -S_{q_k \ddot{p}_i} \\ -S_{p_k \dot{q}_i} & & & I_{p_k} \\ & & & +I_{p_k \ddot{p}_i} & \\ -S_{p_k \dot{q}_i} & & & I_{p_k} \\ & & & +I_{p_k \ddot{p}_i} & \\ & -S_{p_k \dot{q}_i} & & & I_{p_k} \\ & & & & +I_{p_k \ddot{p}_i} \end{bmatrix}$$

$$A_1 = \begin{bmatrix} I_{q_k} g_s v_k \\ +2I_{q_k \dot{q}_i} & 2nI_{q_k} & & & -2nS_{q_k \ddot{p}_i} \\ -2nI_{q_k} & I_{q_k} g_s v_k \\ +2I_{q_k \dot{q}_i} & & 2nS_{q_k \ddot{p}_i} & & \\ & & I_{q_k} g_s v_k \\ & & +2I_{q_k \dot{q}_i} & & \\ & -2nS_{p_k \dot{q}_i} & & I_{p_k} g_s \omega_k & 2nI_{p_k} \\ & & & +2nI_{p_k \ddot{p}_i} & \\ 2nS_{p_k \ddot{q}_i} & & & -2nI_{p_k} \\ & & & -2nI_{p_k \ddot{p}_i} & I_{p_k} g_s \omega_k \\ & & & & I_{p_k} g_s \omega_k \end{bmatrix}$$

$I_{q_k} (v_k^2 - n^2)$	$nI_{q_k} g_s v_k$ $+n^2 I_{q_k \dot{q}_i}$		$-S_{q_k p_i}$ $+n^2 S_{q_k \ddot{p}_i}$		
$-nI_{q_k} g_s v_k$ $-n^2 I_{q_k \dot{q}_i}$	$I_{q_k} (v_k^2 - n^2)$		$-S_{q_k p_i}$ $+n^2 S_{q_k \ddot{p}_i}$		
		$I_{q_k} v_k^2$			$-S_{q_k p_i}$
$-S_{p_k q_i}$ $+n S_{p_k \dot{q}_i}$ $+S_{p_k o^K p_i}$			$I_{p_k} (\omega_k^2 - n^2)$ $+I_{p_k p_i}$ $-n^2 I_{p_k \ddot{p}_i}$	$nI_{p_k} g_s \omega_k$	
	$-S_{p_k q_i}$ $+n S_{p_k \dot{q}_i}$ $+S_{p_k o^K p_i}$		$-nI_{p_k} g_s \omega_k$	$I_{p_k} (\omega_k^2 - n^2)$ $+I_{p_k p_i}$ $-n^2 I_{p_k \ddot{p}_i}$	
		$-S_{p_k q_i}$ $+S_{p_k o^K p_i}$			$I_{p_k} \omega_k^2$ $+I_{p_k p_i}$

$$B = \begin{bmatrix} & & \\ & & \\ & & \\ s_{p_k o} & & \\ & s_{p_k o} & \\ & & s_{p_k o} \end{bmatrix}$$

6.4.5 Aerodynamic matrices for rotor with four or more blades in axial flow.- The aerodynamic matrices for the equations of motion of a rotor with four or more blades in axial flow are given below.

$$A_1 = \begin{bmatrix} -\gamma M_{q_k \dot{q}_i} & & & & \\ & -\gamma M_{q_k \dot{q}_i} & & & \\ & & -\gamma M_{q_i \dot{q}_i} & & \\ & -\gamma M_{p_k \dot{q}_i} & & -\gamma M_{p_k \dot{p}_i} & \\ & -\gamma M_{p_k \dot{q}_i} & & -\gamma M_{p_k \dot{p}_i} & \\ & & -\gamma M_{p_k \dot{q}_i} & & -\gamma M_{p_k \dot{p}_i} \end{bmatrix}$$

$$A_0 = \begin{bmatrix} -\gamma M_{q_k q_i} & -n\gamma M_{q_k \dot{q}_i} & & -\gamma M_{q_k p_i} & & \\ n\gamma M_{q_k \dot{q}_i} & -\gamma M_{q_k q_i} & & & -\gamma M_{q_i p_i} & \\ & & -\gamma M_{q_k q_i} & & & -\gamma M_{q_k p_i} \\ -\gamma M_{p_k q_i} & -n\gamma M_{p_k \dot{q}_i} & & -\gamma M_{p_k p_i} & -n\gamma M_{p_k \dot{p}_i} & \\ n\gamma M_{p_k \dot{q}_i} & -\gamma M_{p_k q_i} & & n\gamma M_{p_k \dot{p}_i} & -\gamma M_{p_k p_i} & \\ & & -\gamma M_{p_k q_i} & & & -\gamma M_{p_k p_i} \end{bmatrix}$$

6.4.6 *Inertial matrices for two-bladed rotor.*- The inertial matrices for the two-bladed rotor equations of motion are given below. The notation $C = \cos\psi_m$ and $S = \sin\psi_m$ is used, where $\psi_m = \psi + m\pi$.

I_{q_k}	$-S_{q_k \dot{p}_i}$		$I_{q_k^\alpha \cdot \vec{k}_B}$
I_{c_k}	$-S_{q_k \dot{p}_i}$	$I_{q_k^\alpha \cdot \vec{I}_B}$	
$-S_{p_k \dot{q}_i}$	I_{p_k} $+ I_{p_k \dot{p}_i}$		$I_{p_k^\alpha \cdot \vec{I}_B}$
$-S_{p_k \dot{q}_i}$	I_{p_k} $+ I_{p_k \dot{p}_i}$	I_{p_k} $-I_{p_k^\alpha \cdot \vec{k}_B}$	
$I_{q_i^\alpha \cdot \vec{I}_B}$		$-S_{q_o \dot{p}_i}$	I_o
$I_{q_i^\alpha \cdot \vec{k}_B}$		$-S_{q_o \dot{p}_i}$	

$$A_2 = \frac{1}{N} \sum_m$$

$I_{q_k} g_s v_k$	$2I_{q_k} \dot{\psi}$
$+2I_{q_k} \dot{q}_1$	
$I_{q_k} g_s v_k$	$-2I_{q_k} \dot{\beta}$
$+2I_{c_k} \dot{q}_1$	
$I_{p_k} g_s \omega_k$	$I_{p_k} g_s \omega_k$
	$I_{p_k} g_s \omega_k$
	$I_{p_k} g_s \omega_k$
$2I_{q_o} \dot{q}_1 \cdot \vec{I}_B$	$I_{oT} C_T$
$2I_{q_o} \dot{q}_1 \cdot \vec{k}_B$	

$$A_1 = \frac{1}{N} \sum$$

$I_{q_k} v_k^2$	$-S_{q_k p_i}$						
$I_{q_k} v_k^2$	$-S_{q_k p_i}$	$I_{q_k \alpha} \cdot \vec{I}_B$					
$-S_{p_k q_i}$ $+S_{p_k^\alpha p_i}$	$I_{p_k} \omega_k^2$ $+I_{p_k} p_i$						
$-S_{p_k q_i}$ $+S_{p_k^\alpha p_i}$	$I_{p_k} \omega_k^2$ $+I_{p_k} p_i$	$I_{p_k} \omega_k^2$ $+I_{p_k} p_i$	$S_{p_k^\alpha p_T}$ $-I_{p_k \alpha} \cdot \vec{k}_B$	$S_{p_k^\alpha} (\theta_{1C} S_{p_k^\alpha p_T} - \theta_{1S} C) (-1)^m$			
$I_{q_i \alpha} \cdot \vec{I}_B$		$-S_{q_o \ddot{p}_i}$	$I_o v_T^2$				
$A_o = \frac{1}{N} \sum$							

$S_{q_k} \cdot \vec{i}_B$	$I_{q_k \alpha} \cdot \vec{k}_B$	$I_{q_k \alpha} \cdot \vec{i}_B$
$-S_{q_k} \cdot \vec{k}_B S(-1)^m$	$I_{q_k \alpha} \cdot \vec{i}_B S(-1)^m$	$-I_{q_k \alpha} \cdot \vec{i}_B C(-1)^m$
	$-S_{p_k} \cdot \vec{k}_B$	$I_{p_k \alpha} \cdot \vec{i}_B$
$-S_{p_k} \cdot \vec{i}_B S(-1)^m$	$-I_{p_k \alpha} \cdot \vec{k}_B S(-1)^m$	$I_{p_k \alpha} \cdot \vec{k}_B C(-1)^m$
	$I_0 S(-1)^m$	$-I_0 C(-1)^m$
		I_0

$$\tilde{A}_2 = \frac{1}{N} \sum_m$$

	$2I_{q_k} \dot{\psi}$		
	$2I_{q_k^\alpha} \cdot \vec{t}_B C(-1)^m$	$2I_{q_k^\alpha} \cdot \vec{t}_B S(-1)^m$	
	$-2I_{p_k^\alpha} \cdot k_B C(-1)^m$	$-2I_{p_k^\alpha} \cdot k_B S(-1)^m$	
	$2I_o C(-1)^m$	$2I_o S(-1)^m$	

$$\tilde{A}_1 = \frac{1}{N} \sum_m$$

$$B = \begin{bmatrix} & & \\ & & \\ & s_{p_k o} & \\ & & s_{p_k o} \\ & & \\ & & \\ & & \\ & & \\ & & \\ & & \end{bmatrix}$$

$$C_2 = \frac{1}{N} \sum_m \begin{bmatrix} S_{q_i} \cdot \vec{k}_B 2S(-1)^m & & \\ & -S_{q_i} \cdot \vec{k}_B 2C(-1)^m & \\ & & \\ -2I_{q_i} \cdot \vec{k}_B & & \\ & -I_{q_i \alpha} \cdot \vec{k}_B 2S(-1)^m & S_{q_o \vec{p}_i} \cdot I_2 2S(-1)^m & -2I_o S(-1)^m \\ & I_{q_i \alpha} \cdot \vec{k}_B 2C(-1)^m & -S_{q_o \vec{p}_i} \cdot I_B 2C(-1)^m & 2I_o C(-1)^m \\ & -2I_{q_i \alpha} \cdot \vec{k}_B & 2S_{q_o \vec{p}_i} \cdot \vec{k}_B & -2I_o \end{bmatrix}$$

$$C_1 = \frac{1}{N} \sum_m \begin{bmatrix} S_{q_i} \cdot \vec{k}_B 4C(-1)^m & & & \\ & S_{q_i} \cdot \vec{k}_B 4S(-1)^m & & \\ & & & \\ & -4I_{q_o \vec{p}_i} \cdot \vec{k}_B S(-1)^m & & \\ & 4I_{q_o \vec{p}_i} \cdot \vec{k}_B C(-1)^m & & \\ & -4I_{q_o \vec{p}_i} \cdot \vec{k}_B & & \end{bmatrix}$$

$-S_{q_1} \cdot \vec{k}_B 2S(-1)^m$			
$S_{q_1} \cdot \vec{k}_B 2C(-1)^m$			
$-I_{q_1^a} \cdot \vec{l}_B 2S(-1)^m$	$S_{q_0} \vec{p}_1 \cdot \vec{l}_B 2S(-1)^m$	$-2I_0 S(-1)^m$	
$I_{q_1^a} \cdot \vec{l}_B 2C(-1)^m$	$-S_{q_0} \vec{p}_1 \cdot \vec{l}_B 2C(-1)^m$	$2I_0 C(-1)^m$	

$$C_0 = \frac{1}{N_m} \sum$$

$$\tilde{C}_2 = \frac{1}{N} \sum_m \begin{bmatrix} -2M_b & & & & \\ & -2M_b & & & \\ & & -2M_b & & \\ & & & -I_o 2S^2 & I_o 2CS \\ & & & I_o 2CS & -I_o 2C^2 \\ & & & & -2I_o \end{bmatrix}$$

$$\tilde{C}_1 = \frac{1}{N} \sum_m \begin{bmatrix} & & & & & \\ & & & & & \\ & & & & & \\ & & & -I_o 4CS & -I_o 4S^2 & \\ & & & I_o 4C^2 & I_o 4CS & \\ & & & & & \end{bmatrix}$$

6.4.7 Aerodynamic matrices for two-bladed rotor.- The aerodynamic matrices for the two-bladed rotor equations of motion are given below. The notation $C = \cos\psi_m$ and $S = \sin\psi_m$ is used, where $\psi_m = \psi + m\pi$.

$-M_{q_k \dot{q}_i}$	$-M_{q_k \dot{q}_i} (-1)^m$	$-M_{q_k \dot{\beta}} (-1)^m$	$-M_{q_k \dot{\zeta}}$	$-M_{q_k \dot{\lambda}}$	$-M_{q_k \dot{\beta}^S}$
$-M_{q_k \dot{\beta}} (-1)^m$	$-M_{q_k \dot{q}_i}$	$-M_{q_k \dot{\beta}} (-1)^m$	$-M_{q_k \dot{\zeta}} (-1)^m$	$-M_{q_k \dot{\beta}^C} (-1)^m$	$-M_{q_k \dot{\beta}^S} (-1)^m$
$-M_{p_k \dot{q}_i}$	$-M_{p_k \dot{q}_i} (-1)^m$	$-M_{p_k \dot{\beta}} (-1)^m$	$-M_{p_k \dot{\zeta}} (-1)^m$	$-M_{p_k \dot{\beta}^C}$	$-M_{p_k \dot{\beta}^S}$
$-M_{p_k \dot{\beta}} (-1)^m$	$-M_{p_k \dot{q}_i}$	$-M_{p_k \dot{\beta}} (-1)^m$	$-M_{p_k \dot{\zeta}} (-1)^m$	$-M_{p_k \dot{\beta}^C} (-1)^m$	$-M_{p_k \dot{\beta}^S} (-1)^m$
$-M_{q_i \dot{q}_i}$	$-M_{p_k \dot{q}_i}$	$-M_{p_k \dot{\beta}} (-1)^m$	$-M_{p_k \dot{\beta}} (-1)^m$	$-M_{p_k \dot{\beta}^C} (-1)^m$	$-M_{p_k \dot{\beta}^S} (-1)^m$
$-M_{q_i \dot{\beta}} (-1)^m$	$-M_{q_i \dot{q}_i}$	$-M_{q_i \dot{\beta}} (-1)^m$	$-M_{q_i \dot{\beta}} (-1)^m$	$-M_{q_i \dot{\beta}^C} (-1)^m$	$-M_{q_i \dot{\beta}^S} (-1)^m$
$-M_{q_i \dot{\lambda}} (-1)^m$	$-M_{q_i \dot{q}_i}$	$-M_{q_i \dot{\beta}} (-1)^m$	$-M_{q_i \dot{\beta}} (-1)^m$	$-M_{q_i \dot{\beta}^C} (-1)^m$	$-M_{q_i \dot{\beta}^S} (-1)^m$
$M_{q_i \dot{\beta}^S}$	$M_{q_i \dot{q}_i} (-1)^m$	$M_{q_i \dot{\beta}} (-1)^m$	$M_{q_i \dot{\beta}} (-1)^m$	$M_{q_i \dot{\beta}^C} (-1)^m$	$M_{q_i \dot{\beta}^S} (-1)^m$
$-2T_{q_i}$	$-2T_{q_i} (-1)^m$	$-2T_{\beta} (-1)^m$	$-2T_{\beta} (-1)^m$	$-2T_{\beta} (-1)^m$	$-2T_{\beta} (-1)^m$
$-M_{q_i 2C}$	$-M_{q_i 2C} (-1)^m$	$-M_{\beta} 2C (-1)^m$	$-M_{\beta} 2C (-1)^m$	$-M_{\beta} 2C^2$	$-M_{\beta} 2CS$
$-M_{q_i 2S}$	$-M_{q_i 2S} (-1)^m$	$-M_{\beta} 2S (-1)^m$	$-M_{\beta} 2S (-1)^m$	$-M_{\beta} 2CS$	$-M_{\beta} 2S^2$

$$A_1 = \gamma \frac{1}{N} \sum_m$$

$$A_0 = \gamma \frac{1}{N} \sum_m \begin{bmatrix} -M_{q_k q_i} & -M_{q_k q_i} (-1)^m & -M_{q_k p_i} & -M_{q_k p_i} (-1)^m & -M_{q_k \beta} & -M_{q_k \beta} (-1)^m \\ -M_{q_k q_i} (-1)^m & -M_{q_k q_i} (-1)^m & -M_{q_k p_i} & -M_{q_k p_i} (-1)^m & -M_{q_k \beta} & -M_{q_k \beta} (-1)^m \\ -M_{p_k q_i} & -M_{p_k q_i} (-1)^m & -M_{p_k p_i} & -M_{p_k p_i} (-1)^m & -M_{p_k \beta} & -M_{p_k \beta} (-1)^m \\ -M_{p_k q_i} (-1)^m & -M_{p_k q_i} (-1)^m & -M_{p_k p_i} & -M_{p_k p_i} (-1)^m & -M_{p_k \beta} & -M_{p_k \beta} (-1)^m \\ -M_{q_i} (-1)^m & -M_{q_i} (-1)^m & -M_{p_i} (-1)^m & -M_{p_i} (-1)^m & -M_{\beta} & -M_{\beta} (-1)^m \\ Q_{\gamma_i} & Q_{\gamma_i} (-1)^m & Q_{p_i} & Q_{p_i} (-1)^m & Q_{\beta} & Q_{\beta} (-1)^m \\ -2T_{q_i} & -2T_{q_i} (-1)^m & -2T_{p_i} & -2T_{p_i} (-1)^m & -2T_{\beta} & -2T_{\beta} (-1)^m \\ -M_{q_i} 2C & -M_{q_i} 2C (-1)^m & -M_{p_i} 2C & -M_{p_i} 2C (-1)^m & -M_{\beta} 2C & -M_{\beta} 2C \\ -M_{q_i} 2S & -M_{q_i} 2S (-1)^m & -M_{p_i} 2S & -M_{p_i} 2S (-1)^m & -M_{\beta} 2S & -M_{\beta} 2S \end{bmatrix}$$

$$\tilde{A}_1 = \gamma \frac{1}{N} \sum_m$$

$M_{q_k^\mu} S$	$-M_{q_k^\mu} C$	$-M_{q_k^\lambda}$	$-M_{q_k^\beta} S$	$M_{q_k^\beta} C$	$-M_{q_k^\zeta}$
$M_{q_k^\mu} S(-1)^m$	$-M_{q_k^\mu} C(-1)^m$	$-M_{q_k^\lambda} (-1)^m$	$-M_{q_k^\beta} S(-1)^m$	$M_{q_k^\beta} C(-1)^m$	$-M_{q_k^\zeta} (-1)^m$
$M_{p_k^\mu} S$	$-M_{p_k^\mu} C$	$-M_{p_k^\lambda}$	$-M_{p_k^\beta} S$	$M_{p_k^\beta} C$	$-M_{p_k^\zeta}$
$M_{p_k^\mu} S(-1)^m$	$-M_{p_k^\mu} C(-1)^m$	$-M_{p_k^\lambda} (-1)^m$	$-M_{p_k^\beta} S(-1)^m$	$M_{p_k^\beta} C(-1)^m$	$-M_{p_k^\zeta} (-1)^m$
$M_\mu S(-1)^m$	$-M_\mu C(-1)^m$	$-M_\lambda (-1)^m$	$-M_\beta S(-1)^m$	$M_\beta C(-1)^m$	$-M_\zeta (-1)^m$
$-Q_\mu S$	$Q_\mu C$	Q_λ	$Q_\beta S$	$-Q_\beta C$	Q_ζ
$2T_\mu S$ $-\frac{\mu_x}{\kappa_f^2} \frac{\partial \lambda}{\partial \lambda}$	$-2T_\mu C$ $+\frac{\mu_y}{\kappa_f^2} \frac{\partial \lambda}{\partial \mu}$	$-2T_\lambda$ $+\frac{\lambda}{\kappa_h^4} \frac{\partial \lambda}{\partial \mu}$	$-2T_\beta S$	$2T_\beta C$	$-2T_\zeta$
$M_\mu 2CS$	$-M_\mu 2C^2$	$-M_\lambda 2C$	$-M_\beta 2CS$	$M_\beta 2C^2$	$-M_\zeta 2C$
$M_\mu 2S^2$	$-M_\mu 2CS$	$-M_\lambda 2S$	$-M_\beta 2S^2$	$M_\beta 2CS$	$-M_\zeta 2S$

$M_z 2S$	$-M_z 2S$	$M_x 2S$	$-M_x 2S$
$M_y 2S$	$-M_y 2S$	$M_z 2S$	$-M_z 2S$
$M_x 2C^2$	$-M_x 2C^2$	$M_y 2CS$	$-M_y 2CS$
$M_z 2C^2$	$-M_z 2C^2$	$M_x 2CS$	$-M_x 2CS$
$M_y 2C$	$-M_y 2C$	$M_z 2C$	$-M_z 2C$
$M_x 2C$	$-M_x 2C$	$M_y 2C$	$-M_y 2C$
$M_z T_z$	$-M_z T_z$	$M_x T_z$	$-M_x T_z$
$M_y T_y$	$-M_y T_y$	$M_z T_y$	$-M_z T_y$
$M_x T_x$	$-M_x T_x$	$M_y T_x$	$-M_y T_x$
$M_z Q_z$	$-M_z Q_z$	$M_x Q_z$	$-M_x Q_z$
$M_y Q_y$	$-M_y Q_y$	$M_z Q_y$	$-M_z Q_y$
$M_x Q_x$	$-M_x Q_x$	$M_y Q_x$	$-M_y Q_x$
$M_z (-1)^m$	$-M_z (-1)^m$	$M_x (-1)^m$	$-M_x (-1)^m$
$M_y (-1)^m$	$-M_y (-1)^m$	$M_z (-1)^m$	$-M_z (-1)^m$
$M_x (-1)^m$	$-M_x (-1)^m$	$M_y (-1)^m$	$-M_y (-1)^m$
$M_z p_z$	$-M_z p_z$	$M_x p_x$	$-M_x p_x$
$M_y p_y$	$-M_y p_y$	$M_z p_z$	$-M_z p_z$
$M_x p_x$	$-M_x p_x$	$M_y p_y$	$-M_y p_y$
$M_z q_z$	$-M_z q_z$	$M_x q_x$	$-M_x q_x$
$M_y q_y$	$-M_y q_y$	$M_z q_z$	$-M_z q_z$
$M_x q_x$	$-M_x q_x$	$M_y q_y$	$-M_y q_y$

$$\tilde{A}_0 = \gamma \frac{1}{N} \sum_m$$

$M_{q_k^\mu} S$	$M_{q_k^\mu} C$	$-M_{\zeta_\lambda} \lambda$
$M_{q_k^\mu} S(-1)^m$	$M_{q_k^\mu} C(-1)^m$	$-M_{q_k^\lambda} (-1)^m$
$M_{p_k^\mu} S$	$M_{p_k^\mu} C$	$-M_{p_k^\lambda} \lambda$
$M_{p_k^\mu} S(-1)^m$	$M_{p_k^\mu} C(-1)^m$	$-M_{p_k^\lambda} (-1)^m$
$M_\mu S(-1)^m$	$M_\mu C(-1)^m$	$-M_\lambda (-1)^m$
$-Q_\mu S$	$-Q_\mu C$	Q_λ
$2T_\mu S$ $-\frac{\mu_x}{\kappa_f^2} \frac{\partial \lambda}{\partial \mu}$	$2T_\mu C$ $-\frac{\mu_y}{\kappa_f^2} \frac{\partial \lambda}{\partial \mu}$	$-2T_\lambda$ $+\frac{\lambda}{\kappa_h^4} \frac{\partial \lambda}{\partial \mu}$
$M_\mu 2CS$	$M_\mu 2C^2$	$-M_\lambda 2C$
$M_\mu 2S^2$	$M_\mu 2CS$	$-M_\lambda ?S$

$H_{\beta}^* 2S$	$H_{\beta}^* 2S(-1)^m$	$H_{\beta}^* 2S$	$H_{\beta}^* 2CS$	$H_{\beta}^* 2S^2$
$R_{\beta}^* q_i$	$R_{\beta}^* 2C(-1)^m$	$R_{\beta}^* 2C$	$R_{\beta}^* 2C^2$	$R_{\beta}^* 2CS$
$-H_{\beta}^* 2C$	$-H_{\beta}^* 2C(-1)^m$	$-H_{\beta}^* 2C$	$-H_{\beta}^* 2C^2$	$-H_{\beta}^* 2CS$
$+R_{\beta}^* q_i$	$+R_{\beta}^* 2S(-1)^m$	$+R_{\beta}^* 2S$	$+R_{\beta}^* 2CS$	$+R_{\beta}^* 2S^2$
$2T_{\beta}^* q_i$	$2T_{\beta}^* (-1)^m$	$2T_{\beta}^*$	$2T_{\beta}^* C$	$2T_{\beta}^* S$
$M_{\beta}^* 2S$	$M_{\beta}^* 2S(-1)^m$	$M_{\beta}^* 2S$	$M_{\beta}^* 2CS$	$M_{\beta}^* 2S^2$
$-N_{\beta}^* 2C$	$-N_{\beta}^* 2C(-1)^m$	$-N_{\beta}^* 2C$	$-N_{\beta}^* 2C^2$	$-N_{\beta}^* 2CS$
$-2Q_{\beta}^* q_i$	$-2Q_{\beta}^* (-1)^m$	$-2Q_{\beta}^*$	$-2Q_{\beta}^* C$	$-2Q_{\beta}^* S$

$$c_1 = \gamma \frac{1}{N} \sum_m$$

$H_{q_i} 2S$	$H_{q_i} 2S(-1)^m$	$H_{p_i} 2S$	$H_{p_i} 2S(-1)^m$	$H_{\beta} 2S(-1)^m$
$R_{q_i} 2C$	$R_{q_i} 2C(-1)^m$	$R_{p_i} 2C$	$R_{p_i} 2C(-1)^m$	$R_{\beta} 2C(-1)^m$
$-H_{q_i} 2C$	$-H_{q_i} 2C(-1)^m$	$-H_{p_i} 2C$	$-H_{p_i} 2C(-1)^m$	$-H_{\beta} 2C(-1)^m$
$+R_{q_i} 2S$	$+R_{q_i} 2S(-1)^m$	$+R_{p_i} 2S$	$+R_{p_i} 2S(-1)^m$	$+R_{\beta} 2S(-1)^m$
$2T_{q_i}$	$2T_{q_i} (-1)^m$	$2T_{p_i}$	$2T_{p_i} (-1)^m$	$2T_{\beta} (-1)^m$
$M_{q_i} 2S$	$M_{q_i} 2S(-1)^m$	$M_{p_i} 2S$	$M_{p_i} 2S(-1)^m$	$M_{\beta} 2S(-1)^m$
$-M_{q_i} 2C$	$-M_{q_i} 2C(-1)^m$	$-M_{p_i} 2C$	$-M_{p_i} 2C(-1)^m$	$-M_{\beta} 2C(-1)^m$
$-2Q_{q_i}$	$-2Q_{q_i} (-1)^m$	$-2Q_{p_i}$	$-2Q_{p_i} (-1)^m$	$-2Q_{\beta} (-1)^m$

$$C_o = \gamma \frac{1}{N} \sum m$$

$$\tilde{C}_1 = \gamma \frac{1}{N} \sum_m$$

$-H_\mu 2S^2$	$H_\mu 2CS$	$H_\lambda 2S$	$H_\beta 2S^2$	$-H_\beta 2CS$	$H_\zeta 2S$
$-R_\mu 2C^2$	$-R_\mu 2CS$	$R_\lambda 2C$	$R_\beta 2CS$	$-R_\beta 2C^2$	$R_\zeta 2C$
$-R_r 2CS$	$R_r 2C^2$				
$H_\mu 2CS$	$-H_\mu 2C^2$	$-H_\lambda 2C$	$-H_\beta 2CS$	$H_\beta 2C^2$	$-H_\zeta 2C$
$-R_\mu 2CS$	$-R_\mu 2S^2$	$+R_\lambda 2S$	$+R_\beta 2S^2$	$-R_\beta 2CS$	$+R_\zeta 2S$
$-R_r 2S^2$	$+R_r 2CS$				
$-2T_\mu S$	$2T_\mu C$	$2T_\lambda$	$2T_\beta S$	$-2T_\beta C$	$2T_\zeta$
$-M_\mu 2S^2$	$M_\mu 2CS$	$M_\lambda 2S$	$M_\beta 2S^2$	$-M_\beta 2CS$	$M_\zeta 2S$
$M_\mu 2CS$	$-M_\mu 2C^2$	$-M_\lambda 2C$	$-M_\beta 2CS$	$M_\beta 2C^2$	$-M_\zeta 2C$
$2Q_\mu S$	$-2Q_\mu C$	$-2Q_\lambda$	$-2Q_\beta S$	$2Q_\mu C$	$-2Q_\zeta$

		$\mu_z H_\mu 2CS$ $-\mu_z R_\mu 2CS$ $\mu_z R_r 2C^2$ $-\mu_y H_\lambda 2S$ $-\mu_y R_\lambda 2C$	$\mu_z H_\mu 2S^2$ $\mu_z R_\mu 2C^2$ $\mu_z R_r 2CS$ $-\mu_x H_\lambda 2S$ $-\mu_x R_\lambda 2C$	$H_\zeta 2S$ $R_\zeta 2C$
		$-\mu_z H_\mu 2C^2$ $-\mu_z R_\mu 2S^2$ $+\mu_z R_r 2CS$ $+\mu_y H_\lambda 2C$ $+\mu_y R_\lambda 2S$	$-\mu_z H_\mu 2CS$ $+\mu_z R_\mu 2CS$ $+\mu_z R_r 2S^2$ $+\mu_x H_\lambda 2C$ $+\mu_x R_\lambda 2S$	$-H_\zeta 2C$ $+R_\zeta 2S$
			$2\mu_z T_\mu C$ $-2\mu_y T_\lambda$	$2\mu_z T_\mu S$ $-2\mu_x T_\lambda$
$\tilde{C}_o = \gamma \frac{1}{N} \sum_m$		$\mu_z M_\mu 2CS$ $-\mu_y M_\lambda 2S$	$\mu_z M_\mu 2S^2$ $-\mu_x M_\lambda 2S$	$M_\zeta 2S$
		$-\mu_z M_\mu 2C^2$ $\mu_y M_\lambda 2C$	$-\mu_z M_\mu 2CS$ $\mu_x M_\lambda 2C$	$-M_\zeta 2C$
		$-2\mu_z Q_\mu C$ $+2\mu_y Q_\lambda$	$-2\mu_z Q_\mu S$ $+2\mu_x Q_\lambda$	$-2Q_\zeta$

$H_\mu 2S^2$	$H_\mu 2CS$	$-H_\lambda 2S$
$+R_\mu 2C^2$	$-R_\mu 2CS$	$-R_\lambda 2C$
$+R_r 2CS$	$+R_r 2C^2$	
$-H_\mu 2CS$	$-H_\mu 2C^2$	$+H_\lambda 2C$
$+R_\mu 2CS$	$-R_\mu 2S^2$	$-R_\lambda 2S$
$+R_r 2C^2$	$+R_r 2CS$	
$2T_\mu S$	$2T_\mu C$	$-2T_\lambda$
$M_\mu 2S^2$	$M_\mu 2CS$	$-M_\lambda 2S$
$-M_\mu 2CS$	$-M_\mu 2C^2$	$M_\lambda 2C$
$-2Q_\mu S$	$-2Q_\mu C$	$2Q_\lambda$

$$D_G = \gamma \frac{1}{N} \sum_m$$

7. LINEAR SYSTEM ANALYSIS

The flight dynamics and aeroelastic stability analyses (sections 5.3.3 and 6) result in a set of linear differential equations describing the aircraft motion, of the form

$$A_2 \ddot{x} + A_1 \dot{x} + A_0 x = B_0 v$$

where x is the vector of degrees of freedom and v is the vector of control and gust inputs. The coefficient matrices (A_2 , A_1 , A_0 , and B_0) are either constant or periodic in time. The analysis of these linear equations proceeds as follows (see reference 37).

7.1 State Variable Form

It is convenient to transform the equations to a standard first order form. Let MX be the number of degrees of freedom and MV the number of controls (dimensions of x and v). Assume that MX_1 of the degrees of freedom are first order, that is have a zero column in the spring matrix A_0 . Reorder the degrees of freedom so these first states occur last in the vector x :

$$\begin{pmatrix} x_2 \\ x_1 \end{pmatrix}$$

where x_2 are the $MX-MX_1$ second order degrees of freedom and x_1 are the MX_1 first order degrees of freedom. Then

$$A_0 = [\tilde{A}_0 \quad 0]$$

where \tilde{A}_0 has dimensions $MX * (MX-MX_1)$. The equation of motion can now be written in the form

$$\dot{x} = Ax + Bv$$

where

$$A = \begin{bmatrix} -A_2^{-1} A_1 & -A_2^{-1} \tilde{A}_0 \\ H & 0 & 0 \end{bmatrix}$$

$$B = \begin{bmatrix} A_2^{-1} B_0 \\ 0 \end{bmatrix}$$

with the state vector:

$$x = \begin{pmatrix} \dot{x}_2 \\ \dot{x}_1 \\ x_2 \end{pmatrix}$$

There are $MX_2 = 2*MX-MX_1$ states; the top MX states are the velocities of the degrees of freedom, and the bottom $MX-MX_1$ states are the displacements of the second order degrees of freedom.

7.2 Constant Coefficient System

7.2.1 *Eigen-analysis*.- The transient solution of $\dot{x} = Ax$ is

$$x = \sum_i u_i e^{\lambda_i t} q_i(0) = M e^{\Lambda t} q(0)$$

where λ_i and u_i are the eigenvalues and eigenvectors of the matrix A , and $q_i(0)$ are constants determined by the initial conditions. Λ is the diagonal matrix of eigenvalues, and M is the model matrix with the eigenvectors as columns. The system is unstable if $\operatorname{Re} \lambda_i > 0$ for any mode.

The frequency of a mode is $\omega = |\operatorname{Im} \lambda|$, and the natural frequency is $\omega_n = |\lambda|$. The frequency in Hz is obtained by multiplying by $\Omega/2\pi$. The period is then $T = 1/\omega$ sec, with ω the frequency in Hz. The damping ratio is $\zeta = -\operatorname{Re} \lambda / |\lambda|$ (fraction of critical damping). The time constant is

$\tau = -1/(\Omega R \epsilon \lambda)$ sec. The time to half-amplitude is then $\tau_{1/2} = .693\tau$ (or time to double-amplitude for unstable modes).

7.2.2 *Static response.* - The static response, obtained by setting $\dot{x} = 0$ in $\dot{x} = Ax + Bv$, is

$$x = -A^{-1}Bv$$

7.2.3 *Frequency response.* - The frequency response, obtained by setting $x = x_0 e^{i\omega t}$ and $v = v_0 e^{i\omega t}$ in $\dot{x} = Ax + Bv$, is

$$x_0 = Hv_0$$

where

$$H = -(A - i\omega)^{-1}B = -(A + i\omega)(A^2 + \omega^2 I)^{-1}B$$

The frequency response can also be obtained from the poles and zeros by

$$\frac{x_i}{v_j} = K_i \frac{\prod(z - i\omega)}{\prod(p - i\omega)}$$

where p are the poles (eigenvalues of A) and z are the zeros.

7.2.4 *Zeros.* - In Laplace form the equation $\dot{x} = Ax + Bv$ becomes

$$x = -(A - s)^{-1}Bv$$

By Cramer's rule then

$$\frac{x_i}{v_j} = - \frac{\det A^*}{\det(A - s)}$$

where $A^* = (A - s)$ with the i -th column replaced by the j -th column of B . The poles are defined by $\det(A - s) = 0$, hence are the eigenvalues of the matrix A , as above. The zeros are defined by $\det(A^*) = 0$. In A^* the diagonal elements are all of the form $(a_{kk} - s)$, except for the i -th column.

By expanding the determinant of A^* it is possible to reduce it to a form with $(a_{kk} - s)$ for all the diagonal elements:

$$-\det A^* = k_1 \det(A_1 - s)$$

Then the zeros are the eigenvalues of the matrix A_1 . We have then

$$\frac{x_i}{v_j} = -\frac{\det A^*}{\det(A-s)} = k_1 \frac{\det(A_1 - s)}{\det(A - s)} = k_1 \frac{\pi(z-s)}{\pi(p-s)}$$

and the static response is $k_2 = k_1 \pi z / \pi p$.

7.2.5 Transient response.- The general solution of $\dot{x} = Ax + Bv$ is

$$x = M e^{\lambda(t-t_0)} M^{-1} x_0 + \int_{t_0}^t M e^{\lambda(t-\tau)} M^{-1} B v d\tau$$

Consider the case with zero initial conditions at $t_0 = 0$ and control with time variation of the form $v = v_0 f(\tau)$ ($f = 0$ for $\tau < 0$). Then

$$\begin{aligned} x &= M \left\{ \int_0^t e^{\lambda_i(t-\tau)} f_i d\tau \right\} M^{-1} B v_0 \\ &= M \{ F_i(t) \} M^{-1} B v_0 \end{aligned}$$

where $F = \{F_i\}$ is a diagonal matrix depending on the eigenvalues and on the input function f . The cases considered are

- a. step response, $f = 1$
- b. impulse response, $f = \delta(t)$
- c. cosine impulse, $f = 1/2(1-\cos \frac{2\pi t}{T})$, $0 < t < T$
- d. sine doublet, $f = \sin \frac{2\pi t}{T}$, $0 < t < T$
- e. square impulse, $f = 1$, $0 < t < T$

f. square doublet, $f = 1$ for $0 < t < \frac{T}{2}$, $f = -1$ for $\frac{T}{2} < t < T$

The function $F_1(t)$ is readily evaluated for these and other inputs.

7.2.6 RMS gust response.- Consider the RMS gust response of the system $\dot{x} = Ax + Bg$. Here the only input considered is the vector of gust components g . The gust is model as a Markov process:

$$\dot{g} = -\frac{1}{\tau_G} g + w$$

where w is stationary white gaussian noise, with zero mean and correlation

$$E [w(t) w^T(\tau)] = Q_G \delta(t-\tau)$$

For an RMS gust velocity of σ_G , we have $Q_G = 2\sigma_G^2/\tau_G$. In forward flight the correlation time is obtained from $\tau_G = L/2V$, where L is the gust correlation length and V is the aircraft velocity. The RMS acceleration can be obtained by including accelerometers in the model:

$$\tau_a \ddot{\alpha} + \alpha = C_1 \dot{x} + C_0 x = (C_1 A + C_0)x + C_1 B g$$

where τ_a is the accelerometer lag. For the acceleration of a particular state x_i we have

$$\tau_a \ddot{\alpha}_i + \alpha_i = (\dot{x}_i)^*$$

so the row of C_1 has a 1 in the \dot{x}_i column, with the rest of the elements and the entire row of C_0 equal zero. For body axis acceleration at the point \vec{r} we have

$$\tau_a \ddot{\alpha}_B + \alpha_B = \sum \tilde{\beta}_k \ddot{q}_{sk} + \tilde{\omega}_F \times \tilde{v} = C_1 \dot{x} + C_0 x$$

where the summation is over the rigid body and elastic modes (see section 4.2.2). The matrix C_1 is here zero except for the rigid body and elastic airframe acceleration elements, and the matrix C_0 is zero except for the Euler angle velocity elements.

The aircraft, gust model, and accelerometers are thus described by the set of equations

$$\begin{pmatrix} x \\ \alpha \\ g \end{pmatrix} = \begin{bmatrix} A & 0 & B \\ \frac{1}{\tau_a}(GA + C) & -\frac{1}{\tau_a} & \frac{1}{\tau_a}GB \\ 0 & 0 & -\frac{1}{\tau_G} \end{bmatrix} \begin{pmatrix} x \\ \alpha \\ g \end{pmatrix} + \begin{bmatrix} 0 \\ 0 \\ H \end{bmatrix} w$$

or

$$\dot{z} = Fz + Gw$$

The correlation matrix

$$Z = E(z z^T)$$

is then the solution of the equations

$$FZ + ZF^T + GQ_GG^T = 0$$

The solution is

$$Z = \sigma^2 \frac{1}{\tau_G} M \left\{ \frac{(-M^{-1} I_G M^{-T})_{ij}}{\lambda_i + \lambda_j} \right\} M^T$$

where M is the model matrix of F , and I_G is the diagonal matrix with 1 for the gust columns and zero elsewhere. Note that only the diagonal elements of the correlation matrix Z are of interest normally. Let

$$\{m_{ij}\} = M$$

$$\{n_{ij}\} = M^{-1}$$

Then with the summation k extending only over the gust columns of M^{-1} ,

$$\frac{z_{xi}}{\sigma_g^2} = -\frac{2}{T_0} m_{xi} \left(\frac{n_{ik} n_{jk}}{\lambda_i + \lambda_j} \right) m_{xj}$$

is the RMS gust response of the i -th state.

7.3 Periodic Coefficient System

Consider the system of equations $\dot{x} = Ax + Bv$, where A is periodic with period T , $A(t+T) = A(t)$. The transient solution can be written

$$x = \sum_i u_i(t) e^{\lambda_i t} q_i(v)$$

as for the constant coefficient system, but here the modes u_i are periodic functions of time. The eigenvalues λ_i are obtained as follows.

The state transition matrix ϕ is calculated by integrating $\dot{\phi} = A\phi$ over one period, $t = 0$ to T , with initial conditions $\phi(0) = I$. Let $C = \phi(T)$, and let λ_c and v be the eigenvalues and eigenvectors of the matrix C . Then the system roots are

$$\lambda = \frac{1}{T} \ln \lambda_c = \frac{1}{T} (\ln |\lambda_c| + i \angle \lambda_c)$$

(the principal part – a multiple of $2\pi/T$ can be added to the frequency) and the mode shapes can be obtained from

$$u_i = e^{-\lambda_i t} \phi(t)v_i$$

The system is unstable if $\operatorname{Re}\lambda > 0$ (or $|\lambda_c| > 1$) for any mode.

It is necessary to integrate the equations $\dot{\phi} = f(t, \phi) = A(t)\phi$ numerically from $t = 0$ to $t = T$. Two methods are considered. The first method is a modified trapezoidal rule:

$$\begin{aligned}
\phi_{n+1} &= \phi_n + \frac{h}{2} (\dot{\phi}_{n+1} + \dot{\phi}_n) + O(h^3) \\
&= \phi_n + \frac{h}{2} (A_{n+1} \phi_{n+1} + A_n \phi_n) \\
&= (1 - \frac{h}{2} A_{n+1})^{-1} (1 + \frac{h}{2} A_n) \phi_n \\
&\approx (1 + \frac{h}{2} A_{n+1} + \frac{h^2}{4} A_{n+1}^2) (1 + \frac{h}{2} A_n) \phi_n \\
&= \phi_n + \frac{h}{2} (1 + \frac{h}{2} A_{n+1}) (A_n + A_{n+1}) \phi_n
\end{aligned}$$

where $\phi_n = \phi(t_n)$, $\phi_{n+1} = \phi(t_{n+1})$, and $h = t_{n+1} - t_n$. The second method is the fourth order Runge-Kutta method:

$$\phi_{n+1} = \phi_n + \frac{h}{6} (k_1 + 2k_2 + 2k_3 + k_4) + O(h^5)$$

$$k_1 = A_n \phi_n$$

$$k_2 = A_{n+\frac{1}{2}} (\phi_n + \frac{h}{2} k_1)$$

$$k_3 = A_{n+\frac{1}{2}} (\phi_n + \frac{h}{2} k_2)$$

$$k_4 = A_{n+1} (\phi_n + h k_3)$$

REFERENCES

1. Houbolt, John C., and Brooks, George W., "Differential Equations of Motion for Combined Flapwise Bending, Chordwise Bending, and Torsion of Twisted Nonuniform Rotor Blades," NACA Report 1346, 1958.
2. Bisplinghoff, Raymond L., Mar, James W., and Pian, Theodore H. H., Statics of Deformable Solids, Addison-Wesley, Reading, Massachusetts, 1965.
3. Lang, K.-W., and Nemat Nasser, S., "An Approach for Estimating Vibration Characteristics of Nonuniform Rotor Blades," AIAA Journal, Vol. 17, No. 9, September 1979.
4. Cheeseman, I. C., and Bennett, W. E., "The Effect of the Ground on a Helicopter Rotor in Forward Flight," ARC R & M 3021, September 1955.
5. Coleman, Robert P., Feingold, Arnold M., and Stempin, Carl W., "Evaluation of the Induced-Velocity Field of an Idealized Helicopter Rotor," NACA ARR L5E10, June 1945.
6. Mangler, K. W., and Squire, H. B., "The Induced Velocity Field of a Rotor," ARC R & M 2642, May 1950.
7. Drees, J. M., "A Theory of Airflow Through Rotors and its Application to Some Helicopter Problems," Journal of the Helicopter Association of Great Britain, Volume 3, Number 2, July-September 1949.
8. Johnson, Wayne, "The Response and Airloading of Helicopter Rotor Blades Due to Dynamic Stall," Massachusetts Institute of Technology, ASRL TR 130-1, May 1970.
9. McCroskey, W. J., "Recent Developments in Dynamic Stall," Symposium on Unsteady Aerodynamics, Tucson, Arizona, March 1975.
10. Beddoes, T. S., "A Synthesis of Unsteady Aerodynamic Effects Including Stall Hysteresis," Vertica, Vol. 1 No. 2, 1976.
11. Ham, Norman D., and Garelick, Melvin S., "Dynamic Stall Considerations in Helicopter Rotors," Journal of the American Helicopter Society, Vol. 13, No. 2, April 1968.
12. Harris, Franklin D., Tarzanin, Frank J., Jr., and Fisher, Richard K., Jr., "Rotor High Speed Performance, Theory vs. Test," Journal of the American Helicopter Society, Vol. 15, No. 3, July 1970.
13. Tarzanin, F. J., Jr., "Prediction of Control Loads due to Blade Stall," Journal of the American Helicopter Society, Vol. 17, No. 2, April 1972.

14. Gormont, Ronald E., "A Mathematical Model of Unsteady Aerodynamics and Radial Flow for Application to Helicopter Rotors," USAAVLABS TR 72-67, May 1973.
15. Johnson, Wayne, "A Comparison Between Experimental Data and Helicopter Airloads Calculated Using a Lifting-Surface Theory," Massachusetts Institute of Technology, ASRL TR 157-1, July 1970.
16. Scully, M. P., "Computation of Helicopter Rotor Wake Geometry and its Influence on Rotor Harmonic Airloads," Massachusetts Institute of Technology, ASRL TR 178-1, March 1975.
17. Ham, Norman D., "Some Conclusions from an Investigation of Blade-Vortex Interaction," Journal of the American Helicopter Society, Vol. 20, No. 4, October 1975.
18. Piziali, R. A., "Method for the Solution of the Aeroelastic Response Problem for Rotary Wings," Journal of Sound and Vibration, Vol. 4, No. 3, 1966.
19. Miller, R. H., "Rotor Blade Harmonic Air Loading," AIAA Journal, Vol. 2, No. 7, July 1964.
20. Landgrebe, Anton J., "The Wake Geometry of a Hovering Helicopter Rotor and its Influence on Rotor Performance," Journal of the American Helicopter Society, Vol. 17, No. 4, October 1972.
21. Kocurek, J. David, and Tangler, James L., "A Prescribed Wake Lifting Surface Hover Performance Analysis," Journal of the American Helicopter Society, Vol. 22, No. 1, January 1977.
22. Landgrebe, Anton J., Moffitt, Robert C., and Clark, David R., "Aero-dynamic Technology for Advanced Rotorcraft," Journal of the American Helicopter Society, Vol. 22, No. 2, April 1977.
23. Johnson, Wayne, "A Lifting-Surface Solution for Vortex-Induced Airloads," AIAA Journal, Vol. 9, No. 4, April 1971.
24. Johnson, Wayne, "Application of a Lifting-Surface Theory to the Calculation of Helicopter Airloads," American Helicopter Society Annual Forum, Washington, D.C., May 1971.
25. Etkin, Bernard, Dynamics of Flight, John Wiley and Sons, Inc., New York, 1959.
26. Dommasch, Daniel O., Sherby, Sydney S., and Connally, Thomas F., Airplane Aerodynamics, Fourth Edition, Pitman Publishing Corp., New York, 1967.
27. Kerrebrock, Jack L., Aircraft Engines and Gas Turbines, The MIT Press, Cambridge, Massachusetts, 1977.

28. Nasar, S. A., Electromagnetic Energy Conversion Devices and Systems, Prentice-Hall, Inc., Englewood Cliffs, New Jersey, 1970.
29. Chappell, David P., "Monitoring of Fatigue Loading on Rotor Systems and Related Components," Journal of the American Helicopter Society, Vol. 24, No. 2, April 1979.
30. Coleman, Robert P., and Feingold, Arnold M., "Theory of Self-Excited Mechanical Oscillations of Helicopter Rotors with Hinged Blades," NACA Report 1351, 1958.
31. Miller, R. H., "Helicopter Control and Stability in Hovering Flight," Journal of the Aeronautical Sciences, Vol. 15, No. 8, August 1948.
32. Hohenemser, Kurt H., and Yin, Sheng-Kuang, "Some Applications of the Method of Multiblade Coordinates," Journal of the American Helicopter Society, Vol. 17, No. 3, July 1972.
33. Johnson, Wayne, "Aeroelastic Analysis for Rotorcraft in Flight or in a Wind Tunnel," NASA TN D-8515, July 1977.
34. Peters, David A., "Hingeless Rotor Frequency Response with Unsteady Inflow," NASA SP-352, February 1974.
35. Carpenter, Paul J., and Fridovich, Bernard, "Effect of a Rapid Blade-Pitch Increase on the Thrust and Induced-Velocity Response of a Full-Scale Helicopter Rotor," NACA TN 3044, November 1953.
36. Hohenemser, K. H., and Crews, S. T., "Unsteady Hovering Wake Parameters Identified from Dynamic Model Tests," NASA CR 152022, June 1977.
37. DeRusso, Paul M., Roy, Rob J., and Close, Charles M., State Variables for Engineers, John Wiley and Sons, Inc., New York, 1965.

(18) NASA, 202.47.77.111.COM/

TR-80-A-5-PT-1

1 Report No NASA TM-81182- <u>PT-1</u>	2 Government Accession No AD-A090 513	3 Recipient's Catalog No JUN 80	
4 Title and Subtitle A COMPREHENSIVE ANALYTICAL MODEL OF ROTORCRAFT AERODYNAMICS AND DYNAMICS Part I: Analysis Development	5 Report Date 12 JUN 80	6 Performing Organization Code 124410	
7 Author(s) Wayne Johnson	8 Performing Organization Report No GNSF	9 Work Unit No 505-42-21	
9 Performing Organization Name and Address Ames Research Center and Aeromechanics Laboratory, AVRADCOM Research and Technology Laboratories Moffett Field, Calif. 94035	10 Contract or Grant No	11 Type of Report and Period Covered Technical Memorandum	
12 Sponsoring Agency Name and Address National Aeronautics and Space Administration, Washington, D.C. 20546 and U.S. Army Aviation Research and Development Command, St. Louis, Mo. 93166	13 Sponsoring Agency Code 121	14 Sponsoring Agency Code 121	
15 Supplementary Notes	16 Abstract The development of a comprehensive analytical model of rotorcraft aerodynamics and dynamics is presented. This analysis is designed to calculate rotor performance, loads, and noise; helicopter vibration and gust response; flight dynamics and handling qualities; and system aeroelastic stability. The analysis is a combination of structural, inertial, and aerodynamic models that is applicable to a wide range of problems and a wide class of vehicles. The analysis is intended for use in the design, testing, and evaluation of rotors and rotorcraft, and to be a basis for further development of rotary wing theories. The analysis is implemented in a digital computer program.		
17 Key Words (Suggested by Author(s)) Helicopter analysis Rotor aerodynamics Rotor dynamics	18 Distribution Statement Unlimited STAR Category - 01		
19 Security Classif (of this report) Unclassified	20. Security Classif (of this page) Unclassified	21 No of Pages 442	22 Price* \$11.75